

ARBITRATION UNDER ANNEX VII OF THE UNITED NATIONS
CONVENTION ON THE LAW OF THE SEA

PEOPLE'S REPUBLIC OF BANGLADESH

v.

REPUBLIC OF INDIA

REJOINDER OF THE REPUBLIC OF INDIA

VOLUME II

31 JULY 2013

LIST OF ANNEXES

- Annex RJ-1** Letter from the Secretary to the Government of Pakistan to the Secretary to the Government of India, Ministry of External Affairs, No. 1(1).3/10/50, 7 February 1951.
- Annex RJ-2** Copy of Express Letter from Foreign, New Delhi to Foreign, Karachi, No. F. 20/50-Pak.III, 13 March 1951.
- Annex RJ-3** Commander R.H. Kennedy, “A Brief Geographical and Hydro Graphical Study of Bays and Estuaries the Coasts of which Belong to Different States”, Document A/CONF.13/15, 13 November 1957, *Extract from the Official Records of the United Nations Conference on the Law of the Sea*, Vol. I (Preparatory Documents), pp. 198-243.
- Annex RJ-4** F. Blasco, E. Janodet and M.F. Bellan, “Natural Hazards and Mangroves in the Bay of Bengal”, *Journal of Coastal Research Special Issue No. 12: Coastal Hazards*, 1994, pp. 277-288.
- Annex RJ-5** K. Furukawa, E. Wolanski, “Sedimentation in Mangrove Forests”, *Mangroves and Salt Marshes*, Vol. 1, 1996, pp. 3-10.
- Annex RJ-6** Y. Mazda, M. Magi, M. Kogo, P.N. Hong, “Mangrove as Coastal Protection from Waves in the Tong King Delta, Vietnam”, *Mangroves and Salt Marshes*, Vol. 1, 1997, pp. 127-135.
- Annex RJ-7** J.M. Smoak, S.R. Patchneelam, “Sediment Mixing and Accumulation in a Mangrove Ecosystem: Evidence from ²¹⁰Pb, ²³⁴Th and ⁷Be”, *Mangroves and Salt Marshes*, Vol. 3, 1999, pp. 17-27.
- Annex RJ-8** K. Harada, F. Imamura, T. Hiraishi, “Experimental Study on the Effect in Reducing Tsunami by the Coastal Permeable Structures”, *Proceedings of the Twelfth International Offshore and Polar Engineering Conference*, 2002, pp. 652-658.
- Annex RJ-9** M. Bhattacharya, *Charting the Deep, A History of the Indian Naval Hydrographic Department*, National Hydrographic Office, 2004, pp. 130-131.

- Annex RJ-10** U. Thampanya, J.E. Vermaat, S. Sinsakul, N. Panapitukkul, “Coastal Erosion and Mangrove Progradation of Southern Thailand”, *Estuarine, Coastal and Shelf Science*, Vol. 68, 2006, pp. 75-85.
- Annex RJ-11** Affidavits regarding the Custody of the Original Radcliffe Map, 15 July 2013.
- Annex RJ-12** Note Verbale PM/NY/443/1/2013 from the Permanent Mission of India to the United Nations to the Secretary-General of the United Nations, 16 July 2013.

Annex RJ-1

Letter from the Secretary to the Government of Pakistan to
the Secretary to the Government of India, Ministry of External Affairs, No. 1(1).3/10/50,
7 February 1951.

BY AIR MAIL

No. 1 (U). 3/10/50.

Dated, the 7th February, 1951.

To

The Secretary to the Government of
India, Ministry of External Affairs,
New Delhi.

Sub : Demarcation of undisputed boundary between East Bengal and West Bengal.

Sir,

With reference to correspondence relating with telegram from the Government of Pakistan, Ministry of Foreign Affairs and Commonwealth Relations, No. 60, dated the 5th January, 1951, I am directed to say that the Government of Pakistan have very carefully considered the question of river boundary between Khulna and 24 Parganas and they are of the opinion that the boundary in this section should be fluctuating. It is hoped that the Government of India will agree and issue necessary instructions to the authorities concerned.

Yours faithfully,

Sd/- A.A. Shah.

for Secretary to the Government of
Pakistan.

Enclo : Nil.

Copy to :-

1. The Secretary to the Government of East Bengal, Finance and Revenue (Revenue) Department, Dacca, with reference to his letter No. 7546 J.R. dated the 12th December, 1950.

2. The High Commissioner for Pakistan in India New Delhi, in continuation of endorsement from the Govt. of Pakistan, Ministry of F.A. & C.R. No. I.A. 3/10/50, dated the 29th July, 1950.

A copy of the minutes of the meeting held at Calcutta, between the Survey Officers of the Govts. of India and Pakistan on the 15th July, 1950, is also enclosed.

Sd/- A.A. Shah,
for Secretary to the Govt. of Pakistan.

Annex RJ-2

Copy of Express Letter from Foreign, New Delhi to Foreign, Karachi, No. F. 20/50-Pak.III,
13 March 1951.

Copy of Express letter No. P. 21-20/50-Pak. III, dated the 13th March, 1951 from Foreign, New Delhi to Foreign, Karachi.

....

Reference your letter No. 1(1).3/10/50, dated the 7th February, 1951 regarding demarcation of undisputed portion of West Bengal-East Bengal boundary.

2. We agree that the boundary between Khulna and 24 parganas running along the midstream of the rivers should be a fluid one and are issuing necessary instructions to the authorities concerned. Kindly issue instruction to East Bengal also.

.....

The issue of the above has been authorized.

Annex RJ-3

Commander R.H. Kennedy, “A Brief Geographical and Hydro Graphical Study of Bays and Estuaries the Coasts of which Belong to Different States”, Document A/CONF.13/15, 13 November 1957, *Extract from the Official Records of the United Nations Conference on the Law of the Sea*, Vol. I (Preparatory Documents), pp. 198-243.

United Nations Conference on the Law of the Sea

Geneva, Switzerland
24 February to 27 April 1958

Document:
A/CONF.13/15

**A Brief Geographical and Hydro Graphical Study of Bays and Estuaries the Coasts of
which Belong to Different States**

Extract from the *Official Records of the United Nations Conference on the Law of
the Sea, Volume I (Preparatory Documents)*

Document A/CONF.13/15

A BRIEF GEOGRAPHICAL AND HYDROGRAPHICAL STUDY OF BAYS AND ESTUARIES
THE COASTS OF WHICH BELONG TO DIFFERENT STATES

BY COMMANDER R. H. KENNEDY

(Preparatory document No. 12) *

[Original text : English]
[13 November 1957]

CONTENTS

	<i>Page</i>		<i>Page</i>
INTRODUCTION	198	2. Shatt al-Arab	209
I. AFRICA		3. Khor Abdullah	209
1. Waterway at 11° N. ; 15° W. (approx.) between French Guinea and Portuguese Guinea	199	4. The Sunderbans (Hariabhanga and Raimangal Rivers)	209
2. Estuary of the Kunene River	199	5. Sir Creek	210
3. Estuary of the Kolente or Great Skarcies River	200	6. Naaf River	210
4. The mouth of the Manna or Mano River	200	7. Estuary of the Pakchan River	210
5. Tana River	200	8. Sibuko Bay	211
6. Cavally River	200	IV. CHINA	
7. Estuary of the Rio Muni	200	1. The Hong Kong Area	212
8. Estuary of the Congo River	201	(a) Deep Bay	212
9. Mouth of the Orange River	201	(b) Mirs Bay	212
II. AMERICA		(c) The Macao Area	213
1. Passamaquoddy Bay	201	2. Yalu River	213
2. Gulf of Honduras	202	3. Mouth of the Tyumen River	214
3. Gulf of Fonseca	203	V. EUROPE	
4. Salinas Bay	203	1. Gulf of Trieste	214
5. Chetumal Bay	204	2. Ems and Dollart	214
6. San Juan River	204	3. Lough Carlingford	215
7. Mazanillo Bay	204	4. Lough Foyle	216
8. Gulf of Paria	205	5. Flensburg Fjord or Flensburger Förde	216
9. Bay of Ancón de Sardinias	205	6. Estuary of the Bidasoa River	217
10. Bay of Oyapok	206	7. The mouth of the River Mino	218
11. Estuary of the Maroni River	206	8. Idefjord and its approaches	218
12. Estuary of the Corentyn River	206	9. Head of Bottenviken	219
13. Boca de Capones	207	10. The Area of Viro Lacti	220
14. Rio de la Plata	207	11. Estuary of River Guadiana	220
15. Estuary of the Coco (Wanks) River	208	12. The mouths of the River Evros	220
16. Rio Grande	208	ANNEX :	
III. ASIA		Maps	222
1. Gulf of Aqaba	208		

INTRODUCTION

The International Law Commission, in paragraph 7 of its commentary to article 7 (Bays)¹ stated that it "felt bound to propose only rules applicable to bays the coasts of which belong to a single State". The Commission continued that, as to other bays, it "does not

have sufficient data at its disposal concerning the frequency of such cases or the regulations at present

* This paper was prepared at the request of the Secretariat of the United Nations but should not be considered as a statement of the views of the Secretariat.

¹ Official Records of the General Assembly, Eleventh Session, Supplement No. 9 (A/3159), p. 16.

applicable to them". A similar difficulty was experienced in drafting article 13 (Delimitation of the territorial sea at the mouth of a river) and, as the comment on paragraph 2 of that article makes clear, the rule contained in article 13 is, due to a similar lack of the necessary data, confined to cases where the coasts of an estuary belong to a single State.

The purpose of the present study is, therefore, to provide a brief geographical and hydrographical description, together with maps, of bays and estuaries the coasts of which belong to different States. It is hoped that, by so doing, the Conference might have sufficient data upon which to base a broader formulation of the relevant rules.

It will be apparent from the study that it does not pretend to comprehend all such bays and estuaries throughout the world; nor are those included necessarily suitable for navigation. However, within practical limits, each bay or estuary is described in its essential features and references are given to assist in a more detailed examination should it be required. The references are to Charts and Sailing Directions published by the Hydrographic Department of the British Admiralty; when using the Sailing Directions (Pilots), their latest supplements should also be consulted. Miles referred to in the descriptions are sea miles, each constituting one sixtieth of a degree of latitude at the place being described. Special regulations regarding navigation, etc. in the few places where they are known to exist have been included; in the others it has been assumed that the only rules which apply are those customary for "innocent passage".

The configuration of the coasts on the sides of certain bays or gulfs may affect the size of any area lying between the belts of territorial sea therein. The arcs of circles from the prominent points on the coast, or from certain features which dry between tides, control the limits of these belts. They may thus reduce the separation of the limits from a distance equal to the maximum width of the bay less the sum of the breadths of the belts of territorial sea.

Although these are primarily physical studies, the positions of international boundaries, either as terminations of the land boundaries or those through the sea, have been mentioned; these positions, where given, must, however, be considered as approximate only. No comments or suggestions have been offered regarding the continuation of the land boundaries to the high seas. These studies should prove useful examples for the consideration of wider problems of bays and estuaries in general if the existence of the state boundaries be neglected.

I. AFRICA

1. Waterway at 11°N. ; 15°W. (approx.) between French Guinea and Portuguese Guinea (Annex, map No 1)

References : Chart No. 600

Africa Pilot, Volume I, Eleventh Edition, 1953

The area in the vicinity of the position where the land boundary between Portuguese and French Guinea

meets the sea is low and swampy and, as it lies in the proximity of the deltas of several rivers, is liable to change in configuration; the chart is based on an old survey and the scale is small; exact present-day details are not available.

As charted, the terminus of the land boundary is on the north side of the River Tristao, a creek about three-quarters of a mile wide, running in a north-west, south-east direction. This creek joins the Kasset River to the mouth of the River Camponi and separates Aube Island from the mainland; it is about 8 miles long. The Kasset River, flowing past the northern end of Aube Island, is the southern end of the creek separating Katak Island from Aube Island and the mainland; it is nearly a mile wide.

Katak Island and the mainland northward and eastward of it are Portuguese territory; Aube Island is French.

The approach to Kasset River is eastward of Sene and Samba, two sandy islets joined by a drying bank, between 6½ and 3 miles south-westward of Katak Island, and westward of the breakers which extend up to 8 miles south-westward of Aube Island. Depths in this approach are charted between 1½ and 4½ fathoms, but no depths are shown in the Kasset or Tristao Rivers or in the south-eastern approach to the latter.

About 15 miles south of Sene Islet lie Alcatraz Islet and Reef; the islet is a small volcanic rock, 40 feet high. A little over a mile south-westward of this islet, Wreck Islet is charted; this was reported in 1904 to have disappeared and a depth of 2 fathoms was obtained in its position. The reefs and fould ground extend 7 miles south-westward from Alcatraz Islet and are known as Alcatraz Reef.

Conflict Reef, with numerous rocky and sandy dangers, some above water and others below, lies 19 miles south-eastward of Alcatraz Islet and about the same distance southward of the south-eastern end of Aube Island. No soundings are charted between.

There is no entry or anchorage for ships of any size in the River Tristao.

As no detailed survey has been made of the area, there may be many undiscovered dangers there.

2. Estuary of the Kunene River (Annex, map No 2)

References : Chart No. 1806

Africa Pilot, Part II, Tenth Edition 1951

The Kunene, or Cunene, River separates Angola from South West Africa. Near its mouth, it passes through a sandy desert region which is almost rainless, although at times there are heavy dews. It only reaches the sea during the inland rainy season, at other times it is effectually barred by a sandbank on which the sea breaks furiously. The coasts on both sides of the mouth are comparatively straight, but in its immediate vicinity there is a slight inward curvature over a distance less than 5 miles with a penetration from the general line of less than a mile. Roughly half the coastline of the indentation is Portuguese. The area is uninhabited and there are no navigable channels. Great caution is neces-

sary in navigating near the coast as the surveys are very imperfect.

3. Estuary of the Kolente or Great Skarcies River (Annex, map No 3)

References : Charts Nos. 601, 686
Africa Pilot, Part I, Eleventh Edition, 1953

This estuary may be considered to lie between Sallatuk Point in French West Africa and Ballo Point in Sierra Leone, about $15\frac{1}{2}$ miles south-south-eastward. The coast is low, fronted by trees and mangroves and is cut into by many creeks. The Great Skarcies and Little Skarcies, or Kabra, River enter the estuary at its south-eastern end. From the mouth of the latter, the coast trends $17\frac{1}{2}$ miles north-westward to Sallatuk Point and $7\frac{1}{4}$ miles westward to Ballo Point. The whole of the area is shoal and is cluttered with drying mudbanks, the natures of which are continually changing. There are many breakers in the area. Yelibuya Island, low and about 3 miles across, lies close offshore about 5 miles south east of Sallatuk Point; Kortimaw Island, with an extensive drying bank seaward of it, lies $3\frac{1}{2}$ miles further south-eastward, with an islet between it and the coast north-eastwards. In 1933 there was an above-water mudbank 3 miles south-westward of Kortimaw Island; the drying portion of this bank extended 2 miles westward and nearly 3 miles south-westward. The main entrance channel to the rivers allows access to small craft of 9-foot draught; it lies between Yelibuya and Kortimaw Islands and thence between the latter and the coast. Another channel leads between Kortimaw Island and Ballo Point, an extensive bar of shoals, shifting sand and mud, renders it difficult of access.

The boundary between Sierra Leone and French West Africa follows the Kolente River for a considerable way but, before reaching the estuary, branches westward to meet the coast about a mile south-eastward of Sallatuk Point.

4. The mouth of the Manna, or Mano, River (Annex, map No 4)

References : Charts, Nos. 1363, 2478
Africa Pilot, Volume I, Eleventh Edition, 1953

The boundary between Sierra Leone and Liberia reaches the sea at the mouth of the Manna, or Mano, River. The coast on both sides is comparatively straight, and runs in a general north-westerly and south-easterly direction for a number of miles. For the last $2\frac{1}{2}$ miles of its journey, the river flows north-westwards parallel to the coast and is separated from the sea by a narrow strip of tree-covered sand. The mouth of the river is, in effect, closed, and breakers extend around its mouth. The remains of an old factory can be seen near the mouth.

5. Tana River (Annex, map No 5)

References : Chart No. 1359
Africa Pilot, Volume I, Eleventh Edition, 1953

The boundary between Ghana and French West

Africa follows the Tana River to the Tana or Tendo Lagoon, the northern coast of which is French territory, and the eastern end of the southern coast is the territory of Ghana. The French boundary crosses the lagoon in a southerly direction to meet the land boundary which crosses the low spit, about $1\frac{1}{2}$ miles wide, separating the lagoon from the sea, in a southerly direction, to reach the coast close west of the village of Newtown.

The sea coast is comparatively straight for many miles. Access to the lagoon from the sea is about 7 miles west of Assini, situated $12\frac{1}{2}$ miles west of Newtown. Owing to the nature of the bar there, passage into the lagoon is only possible during the Harmattan season.

6. Cavally River (Annex, map No 6)

References : Charts, Nos. 1980, 1365
Africa Pilot, Volume I, Eleventh Edition, 1953

The "thalweg" of the Cavally River forms the boundary between Liberia on the west and French West Africa on the east. The river, about 100 yards wide only on its entrance to the sea, cuts at right angles through a straight length of coastline about 9 miles long, which at both ends bends away in a convex curve. The entrance to the river is between two sandbanks about 20 feet high. There are submerged rocks about a quarter of a mile offshore and three-quarters of a mile south-westward of the entrance.

It is reported that the river can be navigated by small power vessels for about 50 miles; the entrance channel, however, is constantly changing, and its bar has the reputation of being the most dangerous on the coast; surf boats are often capsized and many lives lost annually. Vessels can anchor in depths of 7 to 9 fathoms about a mile south of the entrance. There is a French customs house close to the entrance.

7. Estuary of the Rio Muni (Annex, map No 7)

References : Charts, Nos. 1356, 1887
Africa Pilot, Part II, Tenth Edition, 1951

The "thalweg" of the Rio Muni where it enters the sea forms the boundary between Spanish Guinea and French Equatorial Africa. The Rio Muni flows into the north-east corner of Corisco Bay, and the River Mondah into the south-east corner. This bay has an entrance 33 miles wide and a penetration inland of 17 miles. The coast at the north-east corner of the bay is roughly in the shape of a semi-circle with a diameter of $12\frac{3}{4}$ miles; the Rio Muni enters through the south-eastern side. The breadth across the mouth of the river is about a mile. Within about $5\frac{1}{2}$ miles south-westward of the mouth are the two Spanish islands of Elobey. Isla de Corisco lies midway between the entrance points of Corisco Bay.

Depths in the bay are for the most part shallow, with the exception of the approaches to the two rivers; the approach to Rio Muni has a least depth of about 4 fathoms and runs in a straight line, passing about $2\frac{1}{2}$ miles south of the southernmost point of the coast at the northern end of the bay; the approach to the

River Mondah passes north and east of Isla de Corisco ; both these channels are buoyed.

Other islets in the bay are : Leva, about a mile south of Isla de Corisco ; Conga, with a small drying rock half a mile south-westward, $3\frac{3}{4}$ miles south-south-eastward of Isla de Corisco ; Bane, with detached drying banks up to $1\frac{3}{4}$ miles eastward and $2\frac{3}{4}$ miles north-eastward, about $5\frac{1}{2}$ miles south-east of Isla de Corisco. Other drying banks are : Banc Acanda, $1\frac{1}{2}$ miles north of the western entrance point of River Mondah ; Recife Buyumba, about $1\frac{1}{2}$ miles offshore and about $10\frac{1}{2}$ miles east of Isolote Bane ; a bank and reefs extending $1\frac{1}{4}$ miles south of Isla Elobey Chica and about a mile east of Isla Elobey Grande ; and Piedra Ugoti, about $1\frac{1}{4}$ miles offshore westward of Punta Corona, at the north-western end of the bay.

Both the whole of Corisco Bay and the bay forming its north-eastern end formed between Punta Mosquitos and Pointe Elobey conform to the International Law Commission's definition of a "bay" in article 7 of the 1956 report. About a fifth of the coastline of this smaller bay is French ; about a third of the coastline of the whole of Corisco Bay (excluding that of the islands and islets) is Spanish.

There are no ports in the bay ; there are anchorages off the various settlements in the rivers.

8. Estuary of the Congo River (Annex, map No 8)

References : Charts, Nos. 604, 638

Africa Pilot, Part II, Tenth Edition, 1951

The river Congo flows in a westerly direction to its mouth ; the northern side is Belgian territory and the southern is Portuguese. For the purpose of this description the estuary will be considered as seaward of a line joining Pointe Bulabemba on the northern bank to the entrance to the Rio do Fuma-Fuma on the southern bank, about $2\frac{3}{4}$ miles southward. The northern side comprises the entrances to two creeks lying between Pointe Bulabemba and Pointe Française about $2\frac{3}{4}$ miles west-north-westward, thence the south-west coast of Presqu'île de Banana which continues in a north-westerly direction for 23 miles to Ponta N'gelo, near which is the boundary with the Portuguese territory of Cabinda. The southern side continues in a westerly direction from the mouth of the Rio do Fuma-Fuma for 8 miles, thence turns north-north-eastward for $2\frac{1}{2}$ miles to Ponta do Padrao, whence it turns abruptly south-westwards for $4\frac{1}{2}$ miles to Ponta da Moita Seca. Thus, the entrance to the estuary between Ponta N'gelo and Ponta da Moita Seca is 25 miles wide ; the width between Ponta do Padrao and the low-water line of Pointe Française is $5\frac{1}{4}$ miles, and the breadth southward of Pointe Française is $4\frac{1}{2}$ miles. The penetration inland from the line joining the entrance points is about $11\frac{1}{2}$ miles.

There are no islands in the estuary ; drying banks close to the low-water line of the coast are charted off the mouth of the Rio do Fuma-Fuma, and in the mouths of rivers $2\frac{3}{4}$ and 5 miles westward of that river ; their outer edges do not lie more than half a mile offshore. The low-water line of Pointe Française is situated nearly half a mile southward of that point.

Depths from the coast graduate to the 10-fathom contour, and then descend abruptly into a deep gully running eastward from ocean depths right into the entrance to the river ; depths in this gully, inside the estuary, exceed 300 fathoms in places.

Vessels approaching from north-westward should keep at least $5\frac{1}{2}$ miles off the shore north of the river entrance until within about 3 miles of Ponta do Padrao, when course may be shaped for the river mouth. Beyond a position south-eastward of Pointe Française, the River Congo is well buoyed.

On the northern side the principal port in the estuary is Banana, in the creek east of Presqu'île de Banana, where there is anchorage in 3 fathoms and a wharf ; there is a bar to cross with 18 feet of water over it ; tidal streams are very strong. It is a pilot station for the River Congo. Vessels bound to and from ports in the Belgian Congo must enter or clear there and pass the health officer. On the southern side is the Portuguese port of Santo Antonio do Zaire, the principal town of the district. It lies about three-quarters of a mile within a creek south-east of Ponta do Padrao. There is a bar with only 7 feet of water over it and the river current flows strongly across the entrance.

Vessels awaiting daylight to make the entrance can find good anchorage one to two miles off Ponta da Moita Seca, also half a mile off shore south-west of Ponta do Padrao and $2\frac{3}{4}$ miles west of Pointe Française.

9. Mouth of the Orange River (Annex, map No 9)

References : Charts Nos. 897, 632

Africa Pilot, Part II, Tenth Edition, 1951

The Orange River, near its mouth, separates South West Africa, on its western and northern sides, from the Union of South Africa. The river, within its mouth, is over a mile wide but is full of ready islets ; in the dry season shoals and sandbanks are everywhere visible in its channel. The river breaks through a long sandy spit to reach the sea ; its mouth is only about 175 yards wide, and the sea breaks right across it. For many miles north-westward of the entrance, the coast is comparatively straight and sandy. This nature continues south-eastward for about 2 miles when the coast is fronted by drying rocky ledges. About 7 miles from the mouth, the coast turns from its general south-easterly trend to a south-south-westerly direction for 2 miles to form Peacock Roadstead, where it is reported that some shelter from the swell and the prevailing south-south-westerly wind may be obtained. The boundary is the north and west bank of the River.

II. AMERICA

1. Passamaquoddy Bay (Annex, map No 10)

References : Chart No. 464

Nova Scotia and Bay of Fundy Pilot, Ninth Edition, 1947

The boundary between the United States of America and Canada passes through Passamaquoddy Bay to the sea. The entrance to the bay lies between West Quoddy

Head and Bliss Island, 13 miles north-north-eastward, and is obstructed by Campobello and Deer Islands, both large, and by numerous smaller islands and dangers. The penetration inland of the bay varies between about 10 and 18 miles.

There are three navigable approaches to the inner part of the bay which gives access at its north-western end to the St. Croix River, down which the boundary runs, viz (i) between the coast north-westward of West Quoddy Head and the south end of Campobello Island, thence between the latter island and Moose Island, thence between the latter island and the south-western end of Deer Island; (ii) north of Campobello Island, thence between that island and the east coast of Deer Island and then between the south-west coast of the latter and Moose Island; (iii) between Macmaster Island, with the islets and dangers south-eastward, all lying northeast of the northern end of Deer Island, and the mainland coast further north-eastward. Least depths in the fairways of these channels are: (i) dredged to 12 feet over a width of 500 feet; (ii) 17 fathoms; and (iii) $4\frac{3}{4}$ fathoms. Local knowledge is essential for the navigation of (i) and (iii) for, besides being narrow, these fairways are tortuous and the tidal streams are strong. The rise and fall of the tide is about 20 feet. In general, depths in the middle of the main part of Passamaquoddy Bay are between about 10 and 24 fathoms.

At the south-western end of the bay, south of Moose Island, is the only entrance to Cobscook Bay and several other irregular-shaped bays cluttered with islands.

Small ports within the area are: On the United States side—Lubec, opposite the south-west end of Campobello Island and Eastport on the south-east of Moose Island. On the Canadian side—St. Andrews, on the south-east side of the entrance to St. Croix River; Chamcook Harbour, about 3 miles north of St. Andrews; Welshpool, on the western side of Campobello Island; and Lords Cove on the north-eastern side of Deer Island.

Very approximately, about a third to a half of the coastline of the bay is United States territory (excluding that of the islands).

The Wolves, a group of five islands and a number of rocks, front the entrance to the bay towards the northern end. The southernmost is situated approximately 12 miles north-east of West Quoddy Head and the northern about $6\frac{1}{2}$ miles east of Bliss Island and $4\frac{1}{2}$ miles offshore.

The sum of the lengths of possible closing lines between West Quoddy Head-Campobello Island-Bliss Island could be 8 miles. The bay conforms to the Law Commission's definition in article 7 of the 1956 report.

The sum of the lengths of possible closing lines between West Quoddy Head-Wolves-Bliss Island total about 19 miles, and so the bay in this case would fall outside that definition.

The boundary from the St. Croix River passes in a straight line to the passage between Deer Island and the American coast, thence about midway between that island and Moose Island; after which it continues in straight lines about midway between Moose Island and

the southern end of Campobello Island, to continue between the south-western end of the island and the mainland coast to the Bay of Fundy. About midway between the coast of Campobello Island and Grand Manan Island, it turns south-westward and then runs midway between the latter island and the United States coast.

The boundary lines towards the south-west end of Campobello Island were established after consideration of the fishing and other interests of the two States and do not form a median line or "thalweg". The navigable part of the channel at one place is on the United States side of the boundary.

2. Gulf of Honduras (Annex, map No 11)

References: Charts, Nos. 1573, 1219

West Indies Pilot, Volume I, Tenth Edition, 1941

The Gulf of Honduras at the western end of the Caribbean Sea is about 50 miles across at its entrance and penetrates about 46 miles. At the south-western end is Honduras Bay, roughly rectangular in shape, with an entrance $12\frac{1}{2}$ miles across between Cape Three Points and Orange Point and a penetration of $12\frac{1}{4}$ miles in a south-westerly direction and about 20 miles in a southerly direction. The boundary between British Honduras and Guatemala is the River Sarstoon, which enters the bay on its western side about 12 miles south-westward of Orange Point. From Cape Three Points the coast trends in a straight line south-eastward for about 33 miles, then turns abruptly north-eastward for 27 miles. About 21 miles south-east of Cape Three Points, the Rio Moncagua enters the sea; this is the boundary between Guatemala and Honduras.

Fronting the coast of British Honduras up to a distance of about 5 miles off shore for a distance of 18 miles north-eastward of Orange Point are a number of sand cays and shoals. Depths in the bay shoal from about 12 fathoms in the middle gradually to the shore. A dangerous spit extends about $7\frac{1}{2}$ miles off shore from a position 7 miles south-south-eastward of Cape Three Points. There are several detached shoals charted.

From a position about 17 miles north of the mouth of the Rio Moncagua, a string of sand cays, reefs and dangers extends north-north-eastwards and northwards to front the coast of British Honduras up to 20 miles off-shore. The main shipping tracks to Honduras Bay and northwards to Belize and other ports of British Honduras pass between the cays and dangers on the northern side and the mainland southward.

The coast trends south-eastwards from the mouth of the Rio Moncagua for about 6 miles and then turns north-eastward to Omoa Harbour. The distance from the mouth of the river to the harbour is 15 miles, but the bight does not conform to the definition of a "bay" in the Law Commission's 1956 report.

There are no islands or drying features in Honduras Bay nor in the vicinity of the coast near the mouth of the Rio Moncagua.

Guatemalan ports within Honduras Bay are Port Livingstone at the entrance to the River Dulce, leading to an extensive lake—vessels drawing more than 6 feet

anchor off; Santo Tomas, in a small bight in the south-east corner of the bay, has a channel dredged to 30 feet leading to a wharf; Puerto Barrios, in the same bight, has a pier with a berth of 25 feet alongside.

The coastline of Honduras Bay measures very approximately about 70 miles, out of which about 14 miles are in the territory of British Honduras.

3. Gulf of Fonseca (Annex, map No 12)

References: Charts, Nos. 1960, 1049

West Coasts of Central America and United States Pilot, Sixth Edition, 1950

The entrance to this gulf lies between Punta Cosequina on the south and Punta Amapala, 9 miles north-westward. The gulf is shaped somewhat like that of a hand with "fingers" formed by a bay in which is Puerto La Union, Bahia Cismuyo, Bahia San Lorenzo and the "thumb" by the indentation in which is Money Penny Anchorage and into which the Negro River, Estero Blanco and Estero Real flow. The penetration inland from the line joining the entrance points to the various "fingers" are: 30, 27, and 32; it is 32 miles to the end of the "thumb".

A large proportion of the coastline of the gulf is mangrove swamp, while other parts form the steep coastline round nearby volcanos. There are a number of islands in the gulf, the principal ones are: Farallones, about 9 miles within the entrance and 5 miles from the eastern shore; Meanguera and Meanguerita, near the middle of the "palm" 10 miles within the entrance and 6 miles from the north-west shore; Conchaguita, midway between Meanguera and the shore and the shore north-westward; Tigre, about 3½ miles north-east of Meanguera; Martin Perez, 2 miles north of Conchaguita, with Isla Punta Sacate three-quarters of a mile north-westwards and the same distance off shore; Exposicion, about 1½ miles north-west of Tigre with Inglesera, Violin, Coyote and Garova within 2½ miles westward of it, and all lying in the approach to Bahia Cismuyo; Sacate Grande, about a mile north of Tigre, between Bahia Cismuyo and Bahia San Lorenzo and separated from the mainland by a narrow creek.

The boundary between El Salvador and Honduras meets the gulf in the entrance to Rio Goascoran, on the north side of the "finger" in which is Puerto La Union; the boundary between Honduras and Nicaragua meets the sea in the "thumb" in the vicinity of the mouths of the Negro River and Estero Blanco. Of the islands, Meanguera, Conchaguita, Martin Perez and Isla Punta Sacate are territory of El Salvador and Sacate Grande, Tigre, Exposicion, Inglesera, Violin, Coyote and Garova are territory of Honduras.

Depths in the entrance to the gulf are about 20 fathoms, these in general graduate to the shores; north-eastwards, northwards and north-westwards of Meanguera depths are everywhere less than 6 fathoms. In the "fingers" drying banks extend off shore as far as 1½ miles in places, with shallow depths a considerable way seaward of the low-water lines. Nearly the whole of the western side of Bahia San Lorenzo is filled by an extensive detached drying bank. Another

small drying bank lies south of this bay and 3½ miles east of Tigre. Except for a few channels, the whole of the northern end of the gulf is shallow.

Ports within the gulf are: Amapala, a port of entry and the only accessible one on the Pacific coast of Honduras, at the north-west corner of Tigre. It has an open anchorage in depths of 7 fathoms, but limiting depths in the approach are 3½ fathoms. The fairways lie on either side of Meanguera.

Puerto La Union, or Cutuco, in the north-west "finger" of the gulf, is a land-locked harbour and the principal port of entry for El Salvador; there is a wharf with 30 feet of water alongside, but the limiting depth is 24 feet on the bar in the approach; the fairway runs between Conchaguita and the mainland westward.

Estero Real in Nicaragua is navigable for about 20 miles by vessels which can cross the bar, which has 18 feet over it. There are a few trading stations in this river. Well-sheltered anchorage may be obtained in Money Penny Anchorage in the approach to this river.

As a very approximate estimation, about half the coastline of the gulf is territory of Honduras and the other two States have about a quarter each.

In 1916-1917 the question of the status of the Gulf was brought before the International Court of Central American Republics. Briefly, the Court in its Judgment stated that the gulf was an "historic possessed of a character of a closed sea", and that, outside the three-mile limits of territorial waters enclosing the exclusive property of each of the three States, co-partnership should exist in the ownership of the remaining waters.

4. Salinas Bay (Annex, map No 13)

References: Charts, Nos. 587 (Plan), 1049, 2145

West Coasts of Central America and United States Pilot, Sixth Edition, 1950

The boundary between Costa Rica and Nicaragua meets the sea on the northern side of Salinas Bay on the Pacific side of Central America.

The bay, running in a general east-south-easterly direction, is entered between Punta Sacate and Punta Arranca Barba about 2½ miles north-north-westward. It has a length of 4½ miles, and minimum and maximum widths of 2 and 3 miles. About 1¼ miles east of Punta Sacate, and three-quarters of a mile off shore, lies the island of Salinas; south-eastward of this, and extending up to half a mile off shore, lies a group of detached drying rocks. A group of smaller rocks, some above-water and others drying, lies 400 yards off shore, half a mile east of Punta Arranca Barba. The head of the bay dries out in places for nearly half a mile.

Depths in the entrance are from 11 to 15 fathoms, further in towards the middle of the bay, they are 6 to 9 fathoms; the coastal banks, with less than 3 fathoms over them, extend up to half a mile off shore and rather more than a quarter of a mile east and south of the island of Salinas. On the latter, and 200 yards north-west of the island, is a small above-water rock and a drying rock about 400 yards east of the island. Good sheltered anchorage from a westerly blow may be obtained south-

south-westward of the island of Salinas. There are no ports in the bay.

The international boundary meets the coast about two-thirds of the way along the northern shore, thus about one-third of the coastline is Nicaraguan territory.

The bay conforms to the definition in article 7 of the Law Commission's 1956 report.

A promontory, of which Punta Sacate forms the northern point, separates Salinas Bay from Elena Bay, the south-western entrance point of which is Punta Blanca, about 11 miles south-westward of Punta Sacate. A line 15 miles long running northwards to the Nicaraguan coast, would enclose an area of sea which conforms to the Law Commission's definition of a "bay" in its 1956 report. Considering these two bays as one indentation, about one-quarter of the coastline would form Nicaraguan territory.

5. Chetumal Bay (Annex, map No 14)

References : Chart No. 1204

West Indies Pilot, Volume I, Tenth Edition, 1941

Chetumal Bay, the entrance to which lies about 25 miles north of Belize, runs in a general northerly direction. Its western side is formed by the coasts of British Honduras and Mexico, its eastern side by the Mexican coast and by the west coast of Ambergris Cay, which is territory of British Honduras. The entrance to the bay lies between the south end of Ambergris Cay and the coast of British Honduras 12 miles westward. The penetration of the bay is 57 miles. The general width is about 13 miles and the extreme width about 20 miles.

Ambergris Cay is about 19 miles long in a north-north-easterly direction, and has an average width of about $3\frac{1}{2}$ miles; between this and the mainland are a number of cays, the principal of which are Mosquito, Guana, Blackadore Swab and Deer Cays. Other islets are Shipstern Cay, close to the mainland coast of British Honduras and 24 miles within the entrance; Tamalca Island on the west side, close off the Mexican coast and 43 miles within the entrance; also an unnamed cay, about a mile north-west of Ambergris Cay.

Rivers flowing into the bay, each forming a highway for inland communication, are, on the west side, New River, Hondo River and Rio S. Jose; on the north side, Rio Kirk. New River is in British Honduras; the Hondo River forms the land boundary and the others are in Mexico.

The whole of the bay is shallow. A bar of mud, with depths of 5 feet over it, extends right across the entrance to the bay; channels within the bay leading to the mouths of the rivers are marked by beacons and have depths of from 8 to 12 feet.

There are settlements at Corosal near the mouth of the New River and at Consejo, about 6 miles north-eastward, in British Honduras; and at Payo Obispo or Chetumal, close north of the Hondo River, at Calderitas and Ubero, about 4 and 10 miles, respectively, northward of that river, in Mexico.

The boundary through the bay has been laid down

in straight lines as indicated on the chartlet; it meets the sea after passing through the narrow channel, named Boca Bacalar, between the north end of Ambergris Cay and the southern tip of the Mexican coast. A narrow canal is charted cutting through this southern tip of the Mexican coast and thus giving access to the Mexican part of the bay entirely through Mexican territory.

Very approximately, half the coastline is in the territory of each state.

6. San Juan River (Annex, map No 15)

References : Chart No. 1139

West Indies Pilot, Volume I, Tenth Edition, 1941

The San Juan River forms the boundary between Costa Rica and Nicaragua on the Caribbean side of Central America. The river reaches the sea through a delta and the boundary follows the principal branch, close to the mouth of which is the small port of San Juan del Norte or Greytown Harbour. Owing to silting, this port is almost disused now. Southward of the delta, the coast runs in a south-south-easterly direction for many miles and is comparatively straight. The coast, at the delta itself, trends at right angles to this stretch for about 5 miles whence the main coasts run northwards and north-north-eastward to form a narrow indentation with a length across its entrance of nearly 40 miles and a maximum penetration of about 12 miles. This in no way conforms to the definition of a "bay" in article 7 of the Law Commission's 1956 report.

The delta is formed primarily of swamp, low sand and mud bars, and is fronted by spits, on which the sea continually breaks heavily, enclosing shallow lagoons; all are liable to frequent changes. In 1937, the main channel entrance had but 5 feet over the bar.

The best anchorage is about $2\frac{1}{2}$ to 3 miles northward of a disused light tower towards the western end of the delta, in depths of about 10 fathoms, and always at least a mile outside the breakers, which extend up to half a mile off shore. Eastward and southward of the delta, depths of 100 fathoms lie 7 or 8 miles off shore, but 5 miles northward they are 15 miles off. There are no dangers in the approach other than the coastal banks.

7. Mazanillo Bay (Annex, map No 16)

References : Charts, Nos. 463, 486; U.S.H.O. No. 2646

West Indies Pilot, Volume III, Fourth Edition, 1946

Mazanillo Bay may be considered to lie between Icacos Point and the eastern extreme of the entrance to Fort Liberté Bay about 6 miles south-westward, and to lie in the angle of the coast where the north coast of the Dominican Republic turns from a general south-westerly direction to the westerly direction of the coast of Haiti. The penetration inland is 5 miles. Icacos Point is situated on the north-west side of a peninsula of which Monzillo Point is the southern extreme. For this extreme, the coast turns north-north-eastwards for $2\frac{1}{2}$ miles and thence trends southward for about $5\frac{1}{4}$ miles to the entrance to Estero Balza, a shallow lagoon, the entrance of which is now closed by mangroves, thence the coast

turns abruptly westward. The mouth of the Massacre River, which forms the boundary between the Dominican Republic and Haiti, is $1\frac{1}{2}$ miles west of the entrance to Estero Balza.

Mangrove swamps form the northern and eastern sides of the bay; in the latter side are two shallow indentations or lagoons, most of which lie behind the coast, the southern of these is fronted by a mangrove islet named Barriga de Vaca.

The bay is deep except on its northern and eastern sides. There are depths of 320 fathoms in the entrance, and depths of 100 fathoms are found less than half a mile from the southern shore, within a mile of Monzillo Point and about $1\frac{1}{4}$ miles from the south-east corner of the bay. East and south-east of the promontory on which is Monzillo Point is a shallow coastal bank with depths of less than 3 fathoms; depths to 10 fathoms extend up to half a mile from this bank. About a mile east of the mouth of the Massacre River is Puerto Libertador, a small settlement with a pier, 745 feet long, having a depth of 46 feet at its outer end, decreasing to 10 feet at its inner end.

Approximately one-third of the coastline of the bay as described above lies in the territory of Haiti.

North and north-west of the promontory at the northern end of the bay are the Seven Brothers, small islets lying at the western end of the extensive shallow Monte Cristi Bank. Arenas, the outermost, lies 7 miles offshore and Torotu, the innermost, is $2\frac{1}{2}$ miles offshore.

Close beyond the bay westwards is the narrow entrance, about $1\frac{1}{2}$ miles long, leading to Fort Liberté Bay, which is land-locked with a length of about 5 miles and a general width of about a mile. There is a good anchorage in depths of 9 fathoms off the settlement of Fort Liberté.

8. Gulf of Paria (Annex, map No 17)

References : Charts, Nos. 1480, 1801, 483A
West Indies Pilot, Volume II, Tenth Edition, 1955

The Gulf of Paria is an extensive gulf roughly rectangular in shape, with an east-west length of about 70 miles and a north-south breadth of about 30 miles. It is entered near its north-east corner through the Dragon's Mouth, and near the middle of the southern side through the Serpent's Mouth. Both these entrances are described in the study on "Straits which constitute Routes for International Traffic" (A/CONF.13/6)².

The north-eastern, eastern and approximately half the southern shore are formed by the coasts of Trinidad and the remainder by the coast of Venezuela.

Depths in the middle of the Gulf are from 16 to 10 fathoms. The western and south-western shores are fronted by extensive, shallow coastal banks, depths of less than 3 fathoms being found in places up to 10 miles offshore. The western and south-western sides form part of the delta of the Orinoco River.

Guiria, on the Venezuelan coast on the north side of the Gulf, is a port of entry for the San Juan River which empties into the western end of the gulf. There is a pier 200 feet long with a depth of 15 feet alongside. The important oil shipping of Caripito is 53 miles up the San Juan River; vessels with a draught of 32 feet in fresh water can berth there.

Pedernales and Capure on the south side of the Gulf have important oil installations near them.

Ports in Trinidad are Point Fortin and Brighton on the south shore, Point à Pierre on the east shore and Port of Spain on the north-east shore. All are oil-loading ports and can accommodate deep draught vessels.

In 1942, a treaty was signed between the Governments of the United Kingdom and Venezuela dividing the submarine areas of the Gulf. This dividing line runs approximately in a straight line from the south-western end of the Dragon's Mouth to the Serpent's Mouth. This has no relation to the status of the waters above the continental shelf.

The following regulations are enforced by Venezuela: in Venezuelan territorial waters the Venezuelan flag must be displayed continuously at the fore; at night, on demand, the name of the vessel must be signalled by morse lamp.

9. Bay of Ancón de Sardinias (Annex, map No 18)

References : Chart No. 2257
South America Pilot, Volume III, Fourth Edition, 1954

Bahia de Ancón de Sardinias is a shallow bight in the coast between the mouth of Rio Vainillita and Punta Mangles, 33 miles north-north-eastward. Its penetration is about 12 miles. In the bight are four large openings which resemble river mouths and are the entrances to a complex system of creeks resembling a delta.

From south to north these are: R. Santiago, the entrance to which is reputed to be shallow; La posa del Puerto, about 4 miles long in a south-easterly direction and three-quarters of a mile wide, with depths of from $2\frac{1}{2}$ to 4 fathoms, but depths in the approach are 2 fathoms; Bahia San Lorenzo, also with depths of 2 fathoms in the approach, is about 4 miles long with widths varying between $1\frac{1}{2}$ miles and half a mile and it has depths of from 6 to 10 fathoms; Panguapi Bay, about 2 miles wide, is the estuary of the River Mataje which forms the boundary between Ecuador and Colombia; no details are available, but the estuary appears to be shallow. North of Panguapi Bay is the southernmost mouth of the delta of the River Ancón.

The whole of the eastern side of the bay is filled with shallow and drying banks and local knowledge for navigation to the entrances named above is essential; the whole coast is low and featureless. Vessels should not normally approach the coast within depths of 10 fathoms, which lie between 4 and 8 miles offshore.

Población de la Tola, a small port, lies about a mile within the River Santiago. Puerto de San Lorenzo lies at the head of Bahia San Lorenzo and about 12 miles east-north-east of La Tola; it has rail communication with Quito, the capital of Ecuador.

² *Supra*, p. 114.

Including only the most seaward coastlines of the outer islands, about one-third of the coastline of the bay lies in Colombia.

Available charts are inadequate for a fuller description.

10. Bay of Oyapok (Annex, map No 19)

References : Chart No. 1802

West Indies Pilot, Volume II, Tenth Edition, 1955

The Bay of Oyapok is the estuary of the River Oyapok which forms the boundary between French Guiana on the west and Brazil on the east. The coast of the estuary on its eastern side trends north-north-eastwards to Cape Orange, the natural entrance point, where it turns south-eastwards; that on the western side trends northward to a prominent point abreast Mont d'Argent, and then trends north-westwards, past a point fronting a hill called Fausse Mont d'Argent, about 5 miles from Mont d'Argent. With the exception of these hills, the whole coast is low and fronted with mangroves. Cape Orange is a rounded cape; the low-water line is charted as lying up to 3 miles northward of it.

The entrance to the estuary may be considered as lying between the low-water line off Cape Orange and the point close to Mont d'Argent, a distance of 10 miles, or between that cape and the coast off Fausse Mont d'Argent, a distance of about 12½ miles. The penetration to where the River Oyapok narrows to about 2 miles is in the first case about 12 miles, and in the second about 15 miles.

The River Uassa enters the estuary on the eastern side about 6 miles south-south-west of Cape Orange; it has depths in its entrance of 8 feet.

The River Uanares flows into the western side of the estuary about 8 miles south of Mont d'Argent; it also is shallow.

The estuary is encumbered with shoals on which the sea breaks heavily during the winter; it has not been completely surveyed and navigation in it is difficult and dangerous. The 3-fathom depth contour is charted 7 miles offshore in the approaches. Two drying banks are charted off the mouth of the River Uanares, but the survey is old and there is little doubt that depths and drying features in the estuary are liable to frequent changes.

Vessels of less than 10-foot draught can anchor about a mile off the coast near Point d'Argent, where there is a small jetty. Vessels of light draught can ascend the River Oyapok for about 30 miles to St. George.

About half the coastline is Brazilian territory.

11. Estuary of the Maroni River (Annex, map No 20)

References : Charts, Nos. 534, 1802

West Indies Pilot, Volume II, Tenth Edition, 1955

The River Maroni forms the boundary, near its mouth, between French Guiana and Surinam; it enters the sea through a comparatively straight stretch of coast-

line which runs in a general west-north-westerly direction for many miles. The entrance to the river proper lies between Pointe Française on the east and Galibi Point about 2 miles westward. From the latter point the coast runs north-north-westward for 5¾ miles to Kaaimanshoofd, the western natural entrance point of the estuary, and thence turns westward. From Pointe Française, the coast turns abruptly east to form the mouth of Rivière La Mana which, flowing west-north-westwards, is separated from the sea by a narrow neck of land terminating at Pointe Isère, the eastern natural entrance point, about 3 miles east-north-east of Pointe Française. The low-water lines of the coast extend about 1½ miles and half a mile north of Pointe Isère and Kaaimanshoofd respectively. The estuary thus has an entrance about 8½ miles wide, with a penetration of about 4½ miles.

The estuary is shallow, but the tide rises about 8 feet at spring tides. It is approached between Tijger Bank on the west and Banc Français on the east. The former, with depths of less than 6 feet, extends about 8 miles north of Galibi Point—there is a drying patch about 3½ miles north of that point; the latter, with similar depths, extends about 6 miles north of Pointe Française. In 1955, least depths on the recommended track through the estuary were 7 feet, and ships of about 15-foot draught could reach Albina in Surinam and St. Laurent in French Guiana, both about 15 miles above Galibi Point, Rivière La Mana can be navigated by vessels of about 12-foot draught to Mana, a French settlement, about 10 miles within Pointe Isère.

The recommended track into the Maroni River passes close to the French shore at and within Pointe Française. The track from seaward is marked by buoys, which are moved to conform with the alterations in depths between and over the banks. Local knowledge is essential.

About one-third of the coastline of the estuary is French.

12. Estuary of the Corentyn River (Annex, map No 21)

References : Charts, Nos. 99, 1801

West Indies Pilot, Volume II, Tenth Edition, 1955

The boundary between British Guiana and Surinam follows the Corentyn River near its mouth. The estuary of the river may be considered to extend seaward from a line joining Bluff Point on the east bank to a position on the British Guiana coast 4½ miles westward. The coast from Bluff Point trends north-eastward for 7 miles, and then turns eastward; Turtle Bank, which dries, extends up to 2½ miles offshore from this latter bend in the coast. The Nickerie River enters the estuary on its south-eastern side about 3 miles north-east of Bluff Point. The coast from opposite Bluff Point trends northward for about 5 miles, and then gradually trends in a curve north-north-westward and north-westward. The outer end of the estuary may be considered as a line joining the north-west corner of Turtle Bank to a position on the coast of British Guiana 15 miles west-north-westward.

The estuary is shallow; the 3-fathom contour lies about 2 miles north of Turtle Bank and continues in a north-westerly direction across the approach to the estuary; at the north-western end it is about 8½ miles off shore. Near the middle of the estuary are two banks, close together and shallower than the rest of the estuary; navigation channels lie both east and west of them. Depths in the channels across the bar are about 8 feet and the rise of the tide is about 8½ feet. Tidal streams are strong near the river mouths.

Five drying banks are charted in the estuary; these lie 1¾ miles north-west of Bluff Point; 4 miles west-north-west of that point and three-quarters of a mile off shore; 5¼ miles north-west of the point and three-quarters of a mile off shore; 5½ miles north-west of the point and nearly 1½ miles off shore; and 4¾ miles north-west of the point and 2¾ miles off shore.

In the winter, heavy seas occur in the estuary and ships of 9 feet draught only can enter the river—in the summer a draught of 16 feet is possible. The river gives access to the settlement of Tropic in Surinam about 60 miles up the river.

The small ports of Niew Nickerie and Wageningen lie about 2½ and 24 miles within the Nickerie River. They can be reached by vessels with a 13½-foot draught.

About half the coastline of the estuary is Surinam territory.

13. Boca de Capones (Annex, map No 22)

References: Charts, Nos. 586, 1813

South America Pilot, Volume III, Fourth Edition, 1954

The boundary between Peru and Ecuador runs northwards to meet the coast in Boca de Capones, a narrow inlet running approximately east and west between the mainland on the south side of Golfo de Guayaquil and several islands close off shore. The eastern end of Boca de Capones connects with Estero Grande, a similar, but wider inlet, and its western end with the Pacific Ocean.

Abreast the termination of the land boundary, the waterway is about a mile wide between the mainland and the south side of Isla Templeque, but is obstructed near its middle by an islet about a mile long and half a mile wide. About a mile west of the boundary, the waterway is constricted to about half a mile in width. It then continues westward between the north side of Isla Mato Palo and the south coast of an unnamed island of which Punta Payana is the north point; Boca Payana separates this island and Isla Templeque. The waterway thence widens to a general breadth of nearly 1¼ miles and continues westward for about 3½ miles; it is, however, obstructed by Isla Correa, about 3 miles long and half a mile wide, and by three islets in the channel south of the island and two islets and two drying mud flats north of the island. The waterway thence continues north-westward for about 2 miles to its entrance into the Pacific, having a general breadth of rather more than half a mile. Within three-quarters of a mile seaward of the entrance are two drying mud banks. South of Isla Correa, a creek named Estero del Salto leads west-south-westward to Bahía de Tumbes.

Depths in both Boca de Capones and Estero Grande are shallow and in general vary between one and 7 feet. The rise of the tide is about 6 feet.

It is most probable that the coastline and depths in the area are subject to continual change.

There are no ports within the area.

Accepting that the islands north of Boca de Capones are territory of Ecuador, the coastlines are about equally divided between that state and Peru.

14. Rio de la Plata (Annex, map No 23)

References: Charts, Nos. 2522, 3064, 3561, 1749, 2039

South America Pilot, Part I, Ninth Edition, 1945

Rio de la Plata is an extensive, funnel-shaped estuary formed by the confluence of Rio Parana and Rio Uruguay; the latter river forms the boundary between Uruguay and Argentina. The northern shore of the estuary is Uruguayan territory and the south-western Argentinian. As generally accepted, the entrance lies between Punta del Este and Cabo San Antonio, 120 miles south-westward; the penetration inland is about 160 miles. The estuary is remarkably shallow. The outer part seaward of Montevideo and Punta Piedras, about 57 miles south-westward, is divided into two channels by the extensive shoals Rouen Bank, 50 miles north-east of Cabo San Antonio, and Banco Ingles, together with Archimedes Bank, about 35 miles further northward. Several islets lie off the Uruguayan coast between Punta del Este and Montevideo, the most seaward of these are I. de Lobos, 4½ miles south-south-east of Punta del Este, and I. de Flores, about 6 miles off shore and about 12 miles east of Montevideo.

The inner part is encumbered with extensive shallow banks with less than 3 fathoms over them, which almost fill the estuary. The principal of these are Banco Ortiz, extending from the northern shore; Banco Chico, midway between that bank and the coastal bank extending from the Argentinian shore; and Playa Honda, filling the north-western end of the estuary. Channels, marked by buoys and beacons, have been dredged through these banks to give access to the various ports.

Isla Farallon, the most seaward of a group of islands, lies 3½ miles west of Colonia, about 88 miles above Montevideo; the estuary here is about 20 miles wide. About 24 miles north-west of this island is Isla Martin Garcia; this lies in the mouth of the Rio Uruguay and abreast the delta of the Rio Parana. The estuary is here about 12¾ miles wide. About 10 miles further north, the mouth of the Rio Uruguay narrows to a width of about 4 miles.

The principal ports in the estuary are:

On the coast of Uruguay: Montevideo, about 60 miles west of Punta del Este, channel dredged to 33 feet; Colonia Roads, about 88 miles above Montevideo, which vessels with draughts of less than 15 feet can reach.

On the coast of Argentina: La Plata, about 21 miles south of Colonia, channel dredged to 25½ feet; Buenos Aires, 27 miles north-westward of La Plata, dredged to 27½ feet.

Depths are maintained in the entrance to the Rio Uruguay to allow vessels drawing up to 23 feet to enter and navigate for about 100 miles.

Pilotage is compulsory in the estuary, except for coasting vessels, beyond a line joining Montevideo to Punta Piedras. A vessel bound for an Uruguayan port on Rio Uruguay should either pick up an Uruguayan pilot at Montevideo or take an Argentine pilot, who will conduct her as far as the roadstead of the Uruguayan port.

About half the coastline of the estuary is Uruguayan.

15. Estuary of the Coco (Wanks) River (Annex, map No 24)

References : Charts, Nos. 2425, 1218
West Indies Pilot, Volume I, Tenth Edition, 1941

Information regarding the estuary is scanty and old ; it is known that the coastline and depths are liable to frequent changes due to the alluvial deposits from this large river.

The river near its mouth forms the boundary between Honduras on the north and Nicaragua on the south. The land everywhere near the entrance is low and swampy and covered with trees.

Almost filling the entrance in the delta is Isla Martinez, an island about $1\frac{3}{4}$ miles long and nearly a mile wide. The main entrance to the river, less than a quarter of a mile wide, lies southward of this island, between it and Isla San Pio, a long narrow islet. Southward of the latter is a shallow lagoon about $1\frac{1}{2}$ miles long and half a mile wide, almost enclosed by other islets. There is a secondary narrow and shallow entrance channel west of Isla Martinez.

Within a mile eastward and south-south-eastward of Isla Martinez lie other islets. Depths of less than 3 fathoms are charted within $1\frac{3}{4}$ miles north, east and south-east of Isla Martinez and these shallow depths are reported to be extending. A shifting bar fronts the river entrances, having depths from 3 to 6 feet, and the sea constantly breaks on it. At high water, vessels drawing 4 feet can at times cross the bar to reach Puerto Cabo Gracias a Dios on the south side of Isla Martinez.

16. Rio Grande (Annex, map No 25)

References : Charts, Nos. 3980 ; U.S.C. and G. 1117
West Indies Pilot, Volume I, Tenth Edition, 1941

The Rio Grande separates Mexico on the south from the United States of America on the north. The river enters the sea in a north-easterly direction through a comparatively straight stretch of coastline running in a general north-south direction for many miles. The river mouth is narrow, and is fronted by a bar over which it is reported that a depth of about 4 feet can be carried. No recent survey has been made and the channel is changeable.

By international agreement the river is not used for navigation, and special permission is necessary for any boat to enter it. The port of Brownsville lies on the

northern bank about 55 miles from the mouth by river, but about 20 miles in a direct line. This port is reached by a canal leading from Brazos Santiago, about 6 miles north of the river entrance. Brazos Santiago is a narrow pass leading into Laguna Madre, an extensive, shallow lagoon, separated from the sea by Brazos and Padre Islands, two long and very narrow strips of land. The former, in 1940, was no longer an island, but joined the mainland immediately north of the mouth of the Rio Grande.

III. ASIA

1. Gulf of Aqaba (Annex, map No 26)

References : Charts, Nos. 756, 3595
Red Sea and Gulf of Aden Pilot, Tenth Edition, 1955

The Gulf of Aqaba is a long narrow gulf on the eastern side of the Sinai Peninsula. The western shore is Egyptian, the eastern shore is Saudi-Arabian and the head of the gulf is Israeli and Jordanian territory. The islands of Tiran and Sinafar front the entrance. The length of the gulf is about 96 miles. The breadth at the entrance between Nabq and Ras Fartak is $5\frac{3}{4}$ miles. About 17 miles above Ras Fartak the breadth is $14\frac{1}{2}$ miles, which is the widest part of the gulf ; thence abreast El Kura it is $12\frac{1}{2}$ miles wide, abreast El Mamlah, the width is 9 miles, thence this general width is maintained, varying from between $8\frac{1}{2}$ and 11 miles, to within 15 miles of the head. The head then narrows to a width of 4 miles abreast Ras el Masri, whence a general width of about 3 miles is maintained for 4 miles to the head.

The whole of the gulf is deep ; depths of over 800 fathoms occur near its middle.

The only islets inside the gulf are Humaidha and Fara Un, both close inshore, the former off the eastern side $20\frac{1}{2}$ miles from the head, and the latter off the western side $7\frac{1}{2}$ miles from the head.

Tiran Island, in the approach, is separated from the Egyptian coast by the Strait of Tiran, about 3 miles wide ; it lies about $4\frac{1}{2}$ miles south of Ras Fartak ; Sinafar Island lies about $1\frac{1}{2}$ miles east of Tiran, with a reef in between. The north-west, north and east coasts of these islands are fronted by drying coral reefs. About midway between the west side of Tiran Island and the Sinai coast, westward, a line of drying coral reefs lies diagonally across the strait, forming on the west, the Enterprise Passage and, on the east, the Grafton Passage. The former has a minimum breadth of 1,300 yards, and the latter a minimum breadth of 950 yards between the central reefs and those extending from the coasts. Both these passages are deep. East and north of Sinafar and Tiran islands there would appear to be a tortuous channel between the coral reefs into the gulf, with a least depth of 9 fathoms and a width of less than half a mile ; this area has not been surveyed in detail, and the available information is very old.

The Jordanian port of Aqaba lies on the eastern side at the head of the gulf, and the Israeli port of Eilath is on the western side of the head.

Of the coastline, over 100 miles are in the territory of both Egypt and Saudi Arabia, while about 3½ miles are territory of Jordan and about 6 miles are territory of Israel.

2. Shatt al-Arab (Annex, map No 27)

References : Charts, Nos. 2884, 3842
Persian Gulf Pilot, Tenth Edition, 1955

The Shatt al-Arab is a large river combining the waters of the Rivers Tigris and Euphrates, which enter the head of the Persian Gulf. Near its mouth, its eastern bank forms the boundary between Iraq to the west and Iran to the east.

The river mouth is funnel-shaped; at Fao, the river is about half a mile wide, it thence widens gradually over a distance of 5½ miles to its mouth, where it is about 4¾ miles wide, between Ras al Bishr and Ras al Abadan north-eastward. Both banks are very low and swampy and are fringed with drying mud banks.

Extensive drying mud banks extend south-eastward from Ras al Bishr and Ras al Abadan; the former, Maraqqat Abdullah, up to 8¾ miles offshore, and the latter, Maraqqat Abadan, up to 6½ miles; it is probable that both extend to seaward. Depths under 3 fathoms extend for about 4½ miles further seaward of these banks and form a bar. For a considerable distance seaward of the bar, depths are irregular. An artificial channel, marked by buoys, beacons and lights, has been dredged across the bar, giving access to vessels of about 32-foot draught at high water spring tides. The rise of the tide is about 9½ feet.

The principal ports in the river which can be reached by vessels of the above-mentioned draught are Fao and Basrah on the Iraqi side and Abadan and Khorramshahr on the Iranian side. Abreast the two latter ports, the international boundary leaves the bank and runs in the *thalweg* of the river.

Pilotage is compulsory within the river and its direct approach. The limits of the port of Basrah extend from the sea for 88 miles up the river. There are various regulations in force regarding speed, overtaking, entering the dredged channels on a falling tide, etc.

The amount of coastline at the river mouth appertaining to Iraq and Iran is about equally divided, but it should be remarked that the international boundary is the Iranian bank of the river.

3. Khor Abdullah (Annex, map No 28)

References : Chart No. 2884
Persian Gulf Pilot, Tenth Edition, 1955

Khor Abdullah separates the eastern side of the large island of Jazirat Bubiyan from the mainland of Iraq; Khor Sabya, a narrow creek only available for boats at half-tide, runs between the island and the mainland of Kuwait.

The entrance to Khor Abdullah may be considered as a line joining the southern corner of Maraqqat Abdullah, the extensive mudbank fronting the coast of

Iraq westward of Ras al Bishr, and the edge of the drying mudbank off Jazirat Bubiyan, about 6½ miles south of Ras al Qaid. The breadth of the entrance is thus about 14 miles. The inner end of the Khor may be considered as where the waterway divides to pass on each side of Jazirat Warba; the penetration is thus 23 miles. Both banks are low, alluvial land covered in places with reeds and grass; drying mudbanks extend into the Khor for about 1¾ miles from the line of the coast, except off the south-east end where the bank itself continues in a south-easterly direction for about 8 miles between the Khor and the approach to the Shatt al-Arab.

Depths across the entrance are varied; there are a number of shoals with depths of less than 3 fathoms lying in line with the main direction of the Khor. Fasht al Aik, a small bank lying about 6¾ miles east-south-eastward of Ras al Qaid, dries 3 feet; a similar bank lies 3¼ miles eastward of the same point, and one drying 4 feet lies between the latter and that point. The least depth charted in the main channel and its approach is 22 feet. Buoys mark the line of the channel. In 1955, this marked channel entered the Khor near its middle, but about 3½ miles above Ras al Qaid it lay nearer to Jazirat Bubiyan than the Iraqi shore.

Anchorage may be obtained by vessels with local knowledge anywhere in the Khor, according to draught, but anchorage should not be taken up at the east-south-eastern end on account of submarine cables. Vessels may also find anchorage off Umm Qasr, where there is a jetty, about 12 miles above the eastern end of Jazirat Warba.

The boundary between Kuwait and Iraq runs through the Khor Abdullah, so about half the low-water coastline is in the territory of each state.

The Iraqi waters of the inlet are included in the port of Basrah.

4. The Sunderbans (Hariabhanga and Raimangal Rivers) (Annex, map No 29)

References : Chart No. 859
Bay of Bengal Pilot, Eighth Edition, 1953

The boundary between India and East Pakistan reaches the sea in the vicinity of the mouths of the Hariabhanga and Raimangal Rivers, two of the rivers forming part of the delta of the River Ganges.

These two rivers meet in a common estuary, with an entrance about 4½ miles wide, and are separated near their mouths by an island 12½ miles long in a north-south direction with a general width of about 2½ miles. The southern end of this island lies back about 5 miles from the general line of the coast formed by the other islands of the delta. Thus, the estuary of the two rivers has a penetration of about 5 miles, a width at the entrance of about 4½ miles and a maximum width of 7¾ miles. The breadth of the Hariabhanga River when it enters the estuary at the north-west corner is about 2 miles wide and the breadth of the Raimangal River in the north-east corner is 2½ miles.

The deep channels from the river mouths, with depths of from 4 to 10 fathoms, lie towards the sides of the estuary, leaving a shallow bank between and south

of the island separating the rivers. A small area, dry at low water, is charted on this bank and about a mile south of the island; depths of between a half and 3 fathoms extend from the island as far southward as the entrance to the estuary. Seaward of the entrance, the channels unite to form a single approach over a distance of about 15 miles between the coastal banks, with depths of less than 3 fathoms. The general breadth of the approach channel is $1\frac{1}{2}$ miles; depths therein are from $3\frac{1}{2}$ to 8 fathoms. On the western coastal bank are three patches, marked by breakers and which probably dry at low water; these lie $1\frac{1}{2}$, 5 and 10 miles south of the entrance to the estuary.

Tidal streams are almost certainly strong and local knowledge is essential for navigating in the vicinity, as the banks are subject to change; the land is low and there are no navigational marks.

About half the coastline of the estuary is Indian and the remainder Pakistan.

5. Sir Creek (Annex, map No 30)

References : Chart No. 118

West Coast of India Pilot, Ninth Edition, 1950

The north-west bank of the Sir River forms the boundary between Pakistan and India. This river forms one of the mouths of the delta of the River Indus.

The coast is low and flat throughout and partially flooded at high water to a considerable distance inland. It was reported in 1952 that the whole of the Indus delta coastline, coastal flats and depth contours had extended seaward as much as 5 miles in places; that the sea-face was generally formed by a narrow belt of low sand hills, fronted by drying sandbanks and backed by mangrove swamps interspersed by mud-banked tidal creeks. In consequence, therefore, the following description from the existing chart, based on an old survey, must be treated with reserve. It is not normal for any vessels except of light draught and up-to-date local knowledge to approach the coast within depths of 10 fathoms.

The following description is from the chart :

The entrance was funnel-shaped and ran in a north-easterly direction from the general north-westerly trend of the coast of the Indus delta. Its southern entrance point, which was low, flat land about 2 feet high, was fronted up to a distance of about 2 miles by a sandbank which dried in places. The north-western entrance point was formed by an islet from 2 to 4 feet high, about 8 miles north-west of the southern entrance point. The penetration of the inlet was about 6 miles to the restriction of the creek to a breadth of about $1\frac{3}{4}$ miles. The northern shore consisted of sand and mud which dried from 2 to 5 feet, the south-eastern side was of sand and mud with scattered mangroves intersected by creeks. Extending from the northern side was an extensive flat with depths of only a few feet and on which were these drying banks. The entrance channel, with depths of up to 7 fathoms, lay close to the southern shore and was about a mile wide, but approach thereto was restricted by an extensive bar lying seaward of the estuary, over which there was a limiting depth of 2 fathoms. There are no ports within the estuary. It was possible for light draught craft which could cross the bar to navigate the Sir River for a considerable distance.

During the south-west monsoon, the whole of the coast is fronted by breakers when the sea breaks in depths greater than 3 fathoms, which are found many miles off shore.

Rather more than half the coastline of the estuary lies on the Pakistan side.

6. Naaf River (Annex, map No 31)

References : Chart No. 3493

Bay of Bengal Pilot, Eighth Edition, 1953

The Naaf River near its mouth forms the boundary between Pakistan and Burma. The river discharges into the sea between Shahpuri Point and Cypress Point, about a mile east-south-eastward. An extensive drying sand and mud flat extends about $1\frac{1}{2}$ miles southwards and nearly 2 miles south-eastwards of the latter point: on this flat and about half a mile south of the point is a small, low islet. Off the northern side of the entrance there are no drying features. Inside the entrance, the river has a comparatively uniform width of about a mile for a distance of 10 miles, and runs approximately parallel to the coast; depths in the middle vary between 12 and $5\frac{1}{4}$ fathoms; thence the river widens and becomes shallower.

A closing line tangential to the low water lines of the coast on either side of the river entrance has a length of about $3\frac{1}{2}$ miles, and the penetration from this to the line joining the natural entrance points of the river is three-quarters of a mile.

The entrance is fronted by shallow flats which form a bar; that south-west of Shahpuri Point is named Shahpuri Flat and that south of Cypress Point, Cypress Sands. These have depths of less than 3 fathoms over them and extend for $4\frac{1}{2}$ miles southward and westward of the former point, their least depths in places are about a foot. St. Martin's Island, consisting of an island about 3 miles long and two islets southward of it, all joined by a reef, is connected to the south-western end of Cypress Sands and lies about $5\frac{1}{2}$ miles south-south-west of Shahpuri Point. St. Martin's Reef, a ridge of sunken rocks, lies about $5\frac{3}{4}$ miles west of the northern end of the island. Sitaparokia Patches, with about $1\frac{1}{2}$ fathoms over them, lie from $4\frac{1}{2}$ to 8 miles south-east of the island.

In 1944, there were two channels across the bar, one north-west of St. Martin's Island, had a least depth of 8 feet, the other, named Patrick's Gut, had a depth of 11 feet and lay north-east of the island; the latter is marked by a buoy. The tidal streams set across the approaches to the bar at about one knot.

The principal anchorage is off Maungdaw, a town on a creek in the eastern bank of the river about 7 miles above the entrance. Depth of water there is about $4\frac{1}{2}$ fathoms.

7. Estuary of the Pakchan River (Annex, map No 32)

References : Charts, Nos. 3051, 3052

Bay of Bengal Pilot, Eighth Edition, 1953

The Pakchan River, near its mouth, forms the boundary between Burma and Thailand. The river entrance lies between Victoria Point, the southern extreme of

Burma, and the low-water line of the mainland about $3\frac{1}{4}$ miles southward. Pulau Ru lies between one and $3\frac{1}{2}$ miles south-south-westward of Victoria Point and fronts the river entrance, Pulau Ganga lies about 2 miles west of the island. South-south-westward of this island, a chain of islands and islets fronts the Thailand coast up to a distance of 10 miles off shore; the longest of these are: Pulau Pingngwe, Goh Chang and Goh Piam. West and north-west of Victoria Point lies another group of islands extending up to $5\frac{1}{2}$ miles off shore; the principal of these are Pulau Besin, Pulau Perlin, Pulau Jungis and Pulau Tonton, the last connected to the coast by a drying bank. Fifteen miles west of Victoria Point is St. Mathew's Island, a large island forming one of an extensive chain fronting the coasts of both Burma and Thailand.

The river, for about 9 miles within, has a general breadth of about $2\frac{1}{4}$ miles, with depths of from $4\frac{1}{2}$ to 11 fathoms. The approaches to the river mouth are encumbered by numerous islands, reefs and shoals; depths of less than 3 fathoms extend up to 9 miles north-west, $5\frac{1}{2}$ miles west and $8\frac{1}{2}$ miles south-west of Pulau Ru, but there are three main channels of approach. The northern passes between Pulau Jungis and Pulau Tonton, thence north of Pulau Ru; this channel has a least depth of 11 feet; the western lies between Pulau Perlin and a reef less than a mile southward of that island, thence north of Pulau Ru, and this channel has a least depth of 20 feet in it; the southern passes between Goh Chang and the shallower water south of Pulau Pingngwe, then east of that island, of Pulau Saung Kharan and the islets southward and eastward of it, and thence south-eastward of Pulau Ru, the least depth in this channel is 30 feet. As none of these channels are buoyed, great caution is necessary in their navigation.

Vessels usually anchor about half a mile south of Victoria Point in depths of from 5 to 10 fathoms. Small craft can also anchor in Victoria Point Harbour, a small area with depths of about 15 feet close north-east of the point or in similar depths off the entrance to Ra-Nohng Creek. The Burmese settlement of Kawsong is on Victoria Point and the Thai town of Ra-Nohng is about 2 miles up the creek of that name.

The international boundary runs eastward and south-eastward of Victoria Point, thence east of Pulau Ru, thence between that island and Pulau Saung Kharong. Goh Chang and Goh Piam are Thai territory. St. Mathew's Island, with the islands lying within 17 miles south-south-westward of it, are Burmese territory.

8. Sibuko Bay (Annex, map No 33).

References: Charts, Nos. 2576, 2099, 1861
Eastern Archipelago Pilot, Volume I, Sixth Edition, 1950

Sibuko Bay is a large indentation in the coast of Borneo between Bum-Bum Island and Mandul Island, 71 miles south-westwards. The northern part of the bay is territory of North Borneo and the southern part is Indonesian. Bum-Bum Island, also forming the southern entrance point to Darvel Bay, is separated from the mainland by a channel about half a mile wide, and is

fronted on its south side by extensive reefs lying up to $7\frac{1}{2}$ miles from it. Mandul Island is a large island in the delta of the Sungei Sesayap. The coast of the western part of the bay is cut into by the mouths of numerous rivers, the largest of which are the Simengaris and Sibuko on the south-western side and the Kalabakang. The penetration of the bay is about 43 miles. The inner portion is almost completely filled by the large islands of East Nunukan and Sibetik. The former is separated from the islands south-east of the delta of Sungei Sibuko by a channel about $2\frac{1}{2}$ miles wide, from Sibetik Island by a channel 4 miles wide which is nearly filled by an island. Sibetik Island is about 19 miles long, and is separated from the mainland northward by distances varying between 4 and $5\frac{1}{2}$ miles. The water extending off the north-eastern and northern coasts of the island and north-westwards as far as the mouths of the Kalabakang River is known as Cowie Bay. The north-western and western coasts of Sibetik Island are separated from the mainland by Coalmine Reach, a narrow channel with a least width of about half a mile.

The northern coast of Sibuko Bay is fronted by coral reefs; the principal of these are Ligitan Reefs, lying from about 5 miles south-westward to 12 miles west-south-westward of the southern end of the reef extending from Bum-Bum Island, and about $4\frac{1}{2}$ miles from the mainland coast; several other reefs lie within 7 miles west-south-westward of these. There are numerous dangers lying up to $11\frac{1}{2}$ miles off shore. A rock, which dries one foot, lies about $9\frac{1}{2}$ miles south-east of the eastern end of Sibetik Island, and Makasser Banks, which are awash at low water, lie 5 miles east-south-eastward of the south end of the island. Drying spits extend about 3 miles south-east of East Nunukan and about $4\frac{1}{2}$ miles from Ahus, an island about 4 miles north of Mandul.

Depths at the northern end of the outer part of the bay are over 100 fathoms; the whole of the southern half is shallower and depths vary between about 30 and 4 fathoms. The channels south and north of East Nunukan Island are from 4 to 7 fathoms; in the approach to and in Cowie Bay the depths are from 4 to 10 fathoms, but there are depths, however, up to 17 fathoms in that part off Tawau; in the north-west end of Cowie Bay, which part has not been surveyed in detail, depths would appear to be shallower. In Coalmine Reach depths are between 6 and 12 fathoms; the channels leading south-eastward from it to that between Sibetik and East Nunukan Islands are shallower and have depths of about 2 fathoms.

Tawau, on the North Borneo coast opposite the middle of Sibetik Island, is the only port of consequence in the area. It has a pier with 17 feet of water alongside. Vessels also load logs at an anchorage at the north-east end of Coalmine Reach. Semporna, in the channel between Bum-Bum Island and the mainland, is a small fishing port.

Tidal streams in Cowie Bay and its approach run up to $2\frac{3}{4}$ knots. There are several beacons marking some of the reefs and there are navigational lights at Tawau and on the coast about 6 miles eastwards to assist approach at night.

Cowie Bay and its approach have a breadth at the entrance, from the east end of Sibetik Island to the main-

land north-north-eastward, of about 11½ miles and a penetration of 29 miles.

The international boundary runs through the Sino Solan River, thence midway between its eastern entrance point and the north end of East Nunukan Island to the parallel of 4° 10' North, thence it crosses Sibetik Island on this parallel.

Thus, in Cowie Bay and its approaches about one-eighth of the coastline is Indonesian and the remainder territory of North Borneo. In Sibuko Bay as a whole, when including the coastline of Sibetik and Nunukan Islands, as a rough approximation about half the coastline belongs to each State.

IV. CHINA

1. The Hong Kong area

References : Charts, Nos. 3026, 2562, 3605

China Sea Pilot, Volume I, Second Edition, 1951

The Hong Kong area involves the territories of three states, that of China, the Portuguese territory of Macao and the British territory of Hong Kong and its leased territory; these will be dealt with in three parts: (a) the China and Hong Kong territory on the west; (b) the China and Hong Kong territory on the east; and (c) Macao.

(a) Deep Bay (Annex, map No 34)

On the west, the Treaty boundary between China and Hong Kong crosses the neck of the promontory at the southern end of which is the island of Hong Kong, and reaches the coast close westward of the mouth of the river which enters the sea at the head of Deep Bay or Hau Hoi Wan. The boundary thence follows the high water line of the northern and western shores of the bay to South-West Point, its northern natural entrance point.

Deep Bay is entered between South-West Point and Black Point, 4 miles southwards, and has a penetration of about 8½ miles. The narrowest part of the bay lies about 4 miles within the entrance and is 2 miles wide. Mud flats, which dry, extend up to about three-quarters of a mile from the coast on all sides of the inner part of the bay. About 3¾ miles within South-West Point, and about a mile from the north-west shore, is a small drying rock; a similar rock lies nearly half a mile off the south-east shore and about 6¾ miles within Black Point.

North-west of the bay lies the entrance to the Chu Chiang or Canton River. Near the middle of this entrance, and fronting Deep Bay, is the Chinese island of Nei-Ling-Ting; this island is 5 miles south-west of the northern entrance point of Deep Bay and 4¾ miles west of its southern entrance point. About 2 miles south-west of Black Point is Tung Kwu, an islet, the northern of a group extending about 2½ miles southward, all of which are Hong Kong territory.

Depths in the bay are between one and 3 fathoms at the south-western end and less than one fathom at the head of the bay. A deep channel leading past the north end of Lantao, from the waters of Hong Kong

harbour, leads across the entrance to the bay and eastwards of an extensive bank with less than 3 fathoms over it, on which lies Nei-Ling-Ting, into the Chu Chiang.

There are no ports within the bay.

Approximately half the high water coastline of the bay is in Chinese territory and the remainder is territory of Hong Kong.

(b) Mirs Bay (Annex, map No 35)

On the east, the Treaty boundary between Chinese and Hong Kong territory meets the coast close eastward of Sha Tau Kok, a village near the head of Starling Inlet, an indentation at the north-west end of Mirs Bay. The boundary thence runs north-eastwards along the high water line of Mirs Bay to Chun Pei Ngaam, the eastern natural entrance point of Mirs Bay.

Mirs Bay is entered between Chun Pei Ngaam and Tam Long Sui, a headland about 5¾ miles west-south-westward. The penetration of the bay to its north-western end is about 14 miles. Its eastern and northern shores are comparatively regular, but the western side has many deep indentations. The principal of these are Tolo Channel and Starling Inlet.

Tolo Channel, about the middle of the west coast of the bay, is about 6 miles long and about three-quarters of a mile wide; its south-western end widens into an area about 5½ miles long, with a maximum width of about 3 miles, somewhat encumbered with islands, forming Tolo Harbour, Plover Cove and Tide Cove.

Starling Inlet at the north-west end of the bay runs in a south-westerly direction for about 3½ miles, with a general breadth of about three-quarters of a mile.

There are a number of islands and islets in Mirs Bay; the most important of these are as follows:

Gau Tau, an islet, near the middle of the bay and 2¾ miles within the entrance; a drying rock lies about half a mile south-west of it.

South Gau, about 2¼ miles within the entrance and more than a mile off the western shore.

Peng Chan, about 6¼ miles within the entrance and about 1¼ miles from the north-east shore.

Peak Rock, near the middle of the northern side of the bay and a third of a mile off shore.

In the southern approach to Tolo Channel are Tap Mun Chau and Chik Chau, with several islets near them.

Between Tolo Channel and Starling Inlet are Ngo Mei Chau, Pak Sha Chou and Crooked Island with other islets and rocks between them and the mainland.

Depths in Mirs Bay are in general between 7 and 12 fathoms, but are less in Tolo Harbour, Starling Inlet and the various coves around the bay. In general, the coasts are steep-to, but the ends of Tolo Harbour, Tide Cove and Starling Inlet all dry out.

Navigation within the bay is not difficult, but care must be taken to avoid numerous fishing stakes, some of which are situated in depths up to 9 fathoms. There are no ports in the bay, but there are several snug anchorages for vessels with local knowledge. Good anchorage may be obtained in the bay during typhoons.

Excluding the coastlines of the many islands and that of the inlet of Tolo Channel, about half the high water coastline of the bay is Chinese and the other half the territory of Hong Kong.

(c) *The Macao area* (Annex, map No 36)

The Portuguese settlement of Macao consists of the small peninsula at the south-eastern end of Aomen Tao, a large Chinese island towards the south end of the delta of the Chu Kiang, Ilha de Taipa and Ilha de Coloane. The northern boundary is on the narrow isthmus joining the peninsula to Aomen Tao. The peninsula is about 2½ miles long and about 1½ miles wide. I. de Taipa lies about 1½ miles southwards of the southern extremity of the peninsula and I. de Coloane about a mile southward of the I. de Taipa.

A breakwater extends nearly 2 miles south-eastward from the south-eastern end of the peninsula, and off its end there is a short detached breakwater parallel to it. A drying bank surrounds I. de Taipa, and a similar bank connects I. de Coloane to the Chinese islands north-westward and westward of it. Between the peninsula and I. de Taipa, a narrow drying spit extends eastward from the southern side of the island close westward of the peninsula. Close off the eastern end of I. de Taipa is a small rock 36 feet high and, nearly a mile northward of it, is a drying rock.

The whole of the area lies within the one-fathom depth contour, and the port is liable to silting. At high water, vessels of less than 14-foot draught can enter; the rise of the tide is about 9 feet at springs.

About 3½ miles north-east of the peninsula, and up to 2 miles off shore, lie the Chinese islets of Ta-Chou-Chou. About 2¼ miles south of the southern side of I. de Coloane is the south-east extremity of the Chinese island of Ta-Heng-Chin. About 8 miles eastward of the extremity of the breakwater lies the Chinese islet of Ching Chou; this is the northern of a chain of islets which extends about 10 miles south-south-westward.

Pilotage is compulsory in the port of Macao.

2. Yalu River (Annex, map No 37)

References : Charts, Nos. 1256, 1257, 3652

China Sea Pilot, Volume III, Second Edition, 1954

The Yalu River forms the boundary between China and North Korea and flows into the northern side of the Hwang Hai or Yellow Sea. Its estuary may be considered as lying north of a line joining Tefa To, an island 8 miles south of the southern extremity of Chorusan Peninsula on the east side of the estuary, to Kulungshan on the western shore about 34 miles north-westward. The estuary is funnel-shaped and has a penetration northwards of about 17 miles to where the river narrows to a width of 3 miles.

A number of islands and islets lie within the estuary, the principal of these are :

Ka To and several islets lying between the Chorusan Peninsula and Tefa To.

Banjo Islands, 6 in number, about 10 miles west of the western coast of the Chorusan Peninsula.

Oyan To, about midway between Ka To and the Banjo Islands.

Un To, about 2½ miles north of the western islands in the Banjo group.

Katchiri To, about 3½ miles north-east of Un To.

Tashi To, about 4 miles north of Un To.

Shinto Islands, comprising a large island and several islets, about 11 miles north-west of the Banjo Islands and about 6 miles from the western shore of the estuary. Northward of these islands towards the part where the estuary rapidly narrows are several low, flat, swampy islands.

The Banjo Islands lie on a large drying bank which extends 4 miles southward of them. Westward and northward of this bank, almost the whole of the estuary is filled with numerous banks of sand and mud, most of which dry; these banks are intersected by many channels which are constantly shifting. Drying mud flats also extend up to 3 miles from the western side of Chorusan Peninsula; between these and the banks off the Banjo Islands are two deep-water channels which are obstructed by flats at the northern ends.

There are only two practical channels into the river, one west of the Banjo Islands and the other west of the Shin To Islands; the former is that more generally used, as the northern end of the latter is liable to shift. The fairways and depths in the river vary from month to month, and the limiting draught of vessels using them are determined from time to time by the pilots. Vessels with a draught of 13 feet can usually reach Ryuganpo on the east bank, about 10 miles above the Shin To Islands, and those with a 10-foot draught might reach Shingishu on the east bank and Antung on the west bank about 13 miles further up river. There is anchorage near Tashi To, to which goods are transported by lighter. Close north-eastward of this, on reclaimed land extending from the mainland, is an artificial port with depths up to 30 feet alongside, whence iron and aluminium are shipped. This was still being completed in 1949 when the depth in the approach channel was 20 feet. In the estuary, the rise of the tide at springs is about 21 feet and at Antung it is about 10 feet. The channels are marked by buoys and beacons which are frequently moved as the channels alter. Tidal streams in the estuary are strong and may run at a rate of 3¾ knots, while in the river at time of floods, a rate of 5 knots with the ebb may occur. From the end of October to the beginning of May, the river may be closed by ice. It is dangerous to take the ground in the estuary or river as the sand banks are very steep and with a falling tide a vessel is liable to capsize; this is a particular danger owing to scour should a vessel be grounded athwart the channel. All vessels should employ a pilot.

The international boundary lies towards the western side of the estuary. Approximately one-third of the coastline of the mainland of the estuary lies in Chinese territory.

3. Mouth of the Tyumen River (Annex, map No 38)

References : Chart No. 2432

South and East Coasts of Korea, East Coast of Siberia and Sea of Okhotsk Pilot, Fourth Edition, 1952

The Tyumen River near its mouth forms the boundary between North Korea on the south and the Union of Soviet Socialist Republics on the north. The western bank is high, but the eastern bank is a marshy plain. At the time of the survey for the chart, the river had an entrance about $1\frac{1}{4}$ miles wide which was nearly closed by a narrow islet about three quarters of a mile long, the seaward coast of which followed the general direction of the shore. There were only narrow channels on each side of the islet leading into the river and that on its north-eastern side was the wider. Within this islet, and towards the Korean side, were several other islets extending about $1\frac{3}{4}$ miles up the river.

Depths close off the islet in the entrance are charted as 3 and $1\frac{3}{4}$ fathoms, but in 1923, the date of the last available information, the average depth in the entrance was about 6 feet. Small craft with local knowledge could then enter the river in calm weather. The river is much swollen in spring when the snow melts and after heavy rains; it is frozen over for several of the winter months. A high-power coastal navigational light is situated on the eastern side of the mouth of the river; there is another about 3 miles south-west of it.

It is believed that the international boundary passes through the channel on the north-eastern side of the islet in the entrance.

V. EUROPE

1. Gulf of Trieste (Annex, map No 39)

References : Charts, Nos. 201, 1434

Mediterranean Pilot, Volume III, Seventh Edition, 1946

The Gulf of Trieste lies at the north-east corner of the Adriatic Sea. The international boundary between Italy and Yugoslavia meets the sea in a small bay formed between Grossa Point and Sottile Point on its south-eastern side.³

The Gulf may be considered to extend from Salvore Point, the north-westernmost point of the Istria Peninsula and Porto Grado about 12 miles north-north-westward. The gulf is roughly in the shape of a rectangle, and has a penetration of about $13\frac{1}{2}$ miles. The narrowest part is about $9\frac{1}{2}$ miles wide. Its south-eastern shore is steep-to and is indented by several small bays, the principal being Perano Bay, Capo D'Istria Bay, San Bartolomeo Bay and Muggia Bay. The north-eastern shore is also steep-to and is comparatively straight; the north-western shore is low, swampy, intersected by a

³ See now the Memorandum of Understanding between Italy, the United Kingdom, the United States of America and Yugoslavia regarding the Free Territory of Trieste, London, 5 October 1954. Annex I to this Memorandum gives the new agreed boundary. U.K. Cmd. 9288, Miscellaneous No. 30 (1954) Trieste.

number of creeks and is fronted by a drying mud bank. Panzano Bay, about 3 miles across, cuts into the north corner of the gulf.

Depths in the gulf are in general between 12 and 8 fathoms. In the small bays on the south-eastern shore, they are slightly less, and depths less than 6 fathoms extend up to 3 miles from the north-western side. About 3 miles east of the entrance to Porto Grado the drying mud bank extends up to a mile offshore, and off the mouths of the Isonzo River, about 6 miles north-eastward, the drying banks extend up to a similar distance.

The modern port of Trieste lies on the coast close northward of Muggia Bay which also forms part of it. This bay is partially enclosed by a detached breakwater. The largest ships can be accommodated. Trieste is a free port. Monfalcone lies inside the head of Panzano Bay and is the centre of a ship-building industry.

The international boundary meets the coast near the head of San Bartolomeo Bay, which lies 10 miles north-eastward of Salvore Point. It is a small indentation between Grossa Point and Sottile Point about a mile north-eastward, the penetration is a little more than half a mile, but does not conform to the definition of a bay in article 7 of the International Law Commission's 1956 report. The Italian quarantine station for Trieste is situated at the northern end of the bay.

Other than the banks and shallows on the north-western side and a few submerged wrecks, there are no navigational dangers in the Gulf and navigation is simple. For night navigation there are ample high-powered lights. There is a rise of only one to 2 feet in tide, but the general water level, with prolonged winds, may alter by several feet. The Gulf is subject to Boras, which are gale force winds and violent squalls from between north and east which frequently set in with little or no warning and may blow for several days.

Very approximately, a quarter of the coastline of the Gulf is in Yugoslav territory.

2. Ems and Dollart (Annex, map No 40)

References : Charts, Nos. 2181, 3761, 3509

North Sea Pilot, Part IV, Tenth Edition, 1950

The estuary of the River Ems, between the high water lines, is shaped roughly like a bent funnel, and for the main part lies between the East Friesian coast of Germany and the Groningen coast of the Netherlands. Its seaward limit may be considered as extending from Norddeich on its northern side to the Netherlands coast about 18 miles south-westward. The penetration inland is about 20 miles. The coasts on both sides are low and flat and for considerable distances are formed by dykes. That from Norddeich trends south-south-westwards and southwards for about 18 miles to Knock, and then turns abruptly eastward for about 7 miles to the mouth of the River Ems, which is about three-quarters of a mile wide. At the river mouth, the coast turns to a southerly direction for about $5\frac{1}{2}$ miles, thence westward for about 5 miles, and thence in a curve northward and north-westward for a similar distance to form The

Dollart. From the western entrance point of The Dollart, the coast turns to a west-north-westerly direction for about 6 miles to Delfzijl, and thence in a northerly direction for the same distance, whence it turns west-north-westward for about 6 miles to the south-western end of the estuary. The coast then continues westward and west-south-westwards. Thus The Dollart is a bay at the inner end of the estuary, roughly square in shape with an entrance about 5 miles wide, a penetration of a similar distance and a maximum width of just over 6 miles.

A number of islands front the estuary. The most important is Borkum, lying about 12 miles west of Norddeich and about 6 miles from the Netherlands coast. This island lies on a drying bank which extends about 6 miles south-eastwards from it and into the estuary. About 2½ miles north-east of Borkum lies the island named Memmert Sand, with the western end of Juist about half a mile northward of it. Both these islands lie on an extensive drying bank which stretches up to 10 miles from the coast south-south-westwards from Norddeich. Rottumer Oog, with Rottumer Plaat 1¼ miles westward, lies about 3 miles south-west of Borkum on the extensive drying bank which stretches nearly 7½ miles northward of the Netherlands coast at the western end of the estuary as described above.

Detached drying sand banks lie up to 2½ miles north-west of Borkum. Inside the estuary at its northern end, the low water line is situated about a mile from the coasts on either side, but further in, from Knock eastwards and off Delfzijl, it is close to the coast. Parallel to the coast, off the latter port, however, there are three extensive detached drying banks which nearly fill the estuary. The narrow channel leading to Emden and the River Ems is confined on its southern side by a large drying bank extending from the east shore of The Dollart, which bay or indentation is almost completely filled by a drying bank.

Except for the main navigational channels, depths in the estuary are shallow. Shoal water also extends 10 miles west and 6 miles north-west of Borkum. There are channels on both sides of Borkum, that on the north is named Oster Ems and that on the south Wester Ems; the former is not of importance to sea-going traffic, the latter is divided into two by a shallow bank. Depths in all the channels in the estuary are liable to frequent change. Between Knock and Emden the channel is dredged over a narrow width and a depth of 23 feet is maintained. Vessels drawing up to 29 feet can, at high water, reach Emden on the north side of the estuary and Delfzijl on the western side; both these ports have berthing accommodation and all modern facilities. They both give access to extensive inland canal systems. Delfzijl can be reached by the deeper draught vessels by passing east, south and then west of the extensive detached drying banks lying off this port, or by light draught vessels by a direct channel between them and the Netherlands coast. The main channels are all well buoyed and marked by beacons and lights. The rise of the tide is about 10 feet at spring tides. In winter the channels are seldom completely frozen over. Pilotage is strongly recommended for ships without local knowledge. Other small ports in the estuary are Norddeich, which has a depth of about 7 feet in the approach;

Termunterzijl, about 4 miles east-south-east of Delfzijl, which has about 4 feet in the approach channel, and Nieuwe Statenzijl in The Dollart; both the latter ports give access to the Netherlands inland waterway system. The River Ems is navigable for sea-going vessels for about 22 miles.

The international boundary between Germany and the Netherlands meets the coast near the south-east corner of The Dollart, thence runs northward to a line joining the entrance points of that inlet, whence it turns westward along this line and continues westwards and northwards near the Netherlands coast to a position about 5 miles north of Delfzijl; it there leaves the immediate vicinity of the coast and continues seaward in a curve to a position between the islands of Borkum and Rottumer Oog.

3. Lough Carlingford (Annex, map No 41)

References : Charts, Nos. 44, 2800, 2810

Irish Coast Pilot, Tenth Edition, 1954

Lough Carlingford lies between Eire and Northern Ireland; the international boundary meets the west bank of the Newry River about 1¼ miles above Warrenpoint at the head of the lough. The entrance to the lough is between Cranfield Point in Northern Ireland and Ballagan Point in Eire, 2 miles south-westward. The lough is restricted 2 miles within the entrance to a width of one mile and thence abruptly widens to 3 miles. A general width between one and 2 miles is thence maintained to the head into which the Newry River flows abreast Warrenpoint. The penetration of the lough is about 8 miles.

The low-water line extends for about 300 yards off Cranfield Point and a drying rock lies about 400 yards further seaward. Off Ballagan Point, the low-water line extends as a spit about half a mile south-eastwards; there are a few detached drying rocks within 300 yards of the end of this spit. Close within the entrance, the lough is almost completely obstructed by shoals and drying rocks lying near the middle, whose positions can best be seen on the chart; on the largest of these is a small island named Block House Island. About 1¼ miles within, towards the north-eastern side, is Green Island, with drying rocks between it and the coast eastwards. Northward of this island, where the lough widens abruptly, the low water lines extend from the eastern shore for about 1¼ miles and from the western for about three-quarters of a mile over a distance of about 1½ miles; there are several drying patches near the middle of the lough here. Elsewhere within the lough, the low water line is, in general, less than a quarter of a mile off shore.

The following small ports lie within the lough :

(i) *On the Eire side* : Greenore, with about 14 feet of water at its pier, lying about 2 miles within the entrance; Carlingford, about 1¼ miles further in where there is a small tidal harbour which dries out.

(ii) *In Northern Ireland* : Warrenpoint, at the head of the lough on the eastern side of the Newry River, where there are small quays which dry out and a patent slip; Victoria Lock, 2½ miles within the Newry River and at the entrance to a ship canal, where there are

quays with 16 feet of water alongside; and Port Newry, $5\frac{1}{2}$ miles north-west of Warrenpoint and reached by the ship canal, where there is a wet dock with a depth of 13 feet.

There are two approach channels to the lough between shoals lying in the entrance; the eastern is that most generally used and it runs about a quarter of a mile west of the low water line off Cranfield Point; a depth of 17 feet is maintained therein by dredging. The channel thence passes eastward of Block House Island and the drying rocks in the entrance. Sheltered anchorage may be obtained in depths of from 7 to 10 fathoms between these rocks and those off Green Island. Above Greenore, there is a bar across the lough with a least depth of 11 feet on the leading line. Above this, the depths near the middle of the lough increase to between 30 and 42 feet in the fairway. For $2\frac{1}{2}$ miles from the head of the lough, the water shoals gradually to a depth of about 4 feet off the entrance to the Newry River. The intricate channels into the lough are well marked by buoys and navigational lights. The rise of the tide is 15 feet at springs. Tidal streams are strong; in the entrance they may run up to a rate of $3\frac{1}{2}$ knots, and off Greenore up to 5 knots. It is recommended that vessels take a pilot.

Approximately half the coastline of the lough is territory of Eire.

4. Lough Foyle (Annex, map No 42)

References: Charts, Nos. 46, 2499, 2486

Irish Coast Pilot, Tenth Edition, 1954

On the north coast of Ireland, the boundary between Eire and Northern Ireland meets the coast in the south-west corner of Lough Foyle. This lough is the extensive estuary of the River Foyle which flows into its head. It is entered between Magilligan Point in Northern Ireland and the Eire coast little more than half a mile north-westward; the penetration is about $12\frac{1}{2}$ miles. From Magilligan Point, the lough gradually broadens to reach a maximum breadth of $6\frac{3}{4}$ miles about 7 miles within the entrance; it then gradually narrows again to the head where the River Foyle, at its entrance, is about half a mile wide. The greater part of the lough is occupied by shoals. The low-water line on the eastern side of the lough extends up to $1\frac{1}{2}$ miles off shore in places, while off the north-western shore it is comparatively close in. There are a number of drying patches within the lough, the principal of these are on the following banks, the positions of which can best be seen on the chart; the sizes, shapes and exact positions of the drying patches are liable to frequent changes: McKinneys Bank, North Middle Bank, Great Bank, South Middle Bank and Roof Banks.

The channel through the entrance is deep and continues for a distance of about 4 miles, having an average width of about half a mile, with depths greater than 6 fathoms; this area affords secure anchorage for large vessels and there are a number of mooring buoys. The navigational channel thence continues between the coastal bank on the north-west side of the lough and the North Middle and Great Banks to the entrance to the River Foyle. The axis of this channel lies at a maximum

distance of just over half a mile from the low water line off the Eire shore. A constant depth of 20 feet at low water is maintained in the channel by dredging operations carried out by the Londonderry Port and Harbour Commissioners. The rise of the tide at springs is about 8 feet. Tidal streams run at maximum rates of between 2 and $3\frac{1}{2}$ knots, the latter rate in the entrance. This channel is amply marked by beacons carrying navigational lights.

The area south-east of this main channel consists primarily of sand and mud banks with little or no water on them at low tide, interspersed with channels running in the general direction of the lough; none of these, however, give access to the River Foyle.

Londonderry is the only port within the lough; it lies in Northern Ireland about 5 miles up the River Foyle. There are berths there with modern facilities which can accommodate vessels up to $23\frac{1}{2}$ -foot draught. Moville is a town on the Eire coast about $2\frac{1}{4}$ miles within the entrance, it has a small boat harbour and landing can be effected.

Pilotage is compulsory within the lough. The pilot station is close southward of Inishowen Head (see below).

The land boundary between Eire and Northern Ireland meets the coast in the vicinity of Muff, on the western side of the lough near its head.

Rather more than half the coastline of the lough is territory of Northern Ireland.

Outside the entrance to the lough, the Eire coast continues in a north-easterly direction for about $2\frac{1}{2}$ miles to Inishowen Head and thence turns north-westwards; the coast of Northern Ireland at Magilligan Point turns south-eastwards and eastwards in a curve for about $8\frac{1}{2}$ miles; it then trends northward and north-eastwards to Ramore Head, whence it takes a general east-north-easterly direction. The approach to Lough Foyle may be considered as lying between Inishowen Head and Ramore Head, 9 miles eastward. Northwards of Magilligan Point, a shallow bank named The Tuns extends for 3 miles with its western edge parallel to and about three-quarters of a mile from the Eire coast. This bank is separated from the coast of Northern Ireland by a narrow channel with a least depth of 12 feet. The channel between the bank and the Eire bank is deep and is that normally used. Eastward of The Tuns is a trawling ground.

5. Flensburg Fjord or Flensburger Förde (Annex, map No 43)

References: Charts No. 3562, 2117

Baltic Sea Pilot, Volume I, Seventh Edition, 1944

The Flensburg Fjord or Flensborger Förde, as known to the Germans, is a narrow, winding fjord projecting westwards into the land from the extensive water area south of the Little Belt in the western end of the Baltic. Its entrance points may be considered as Pøls Huk, the south-eastern extreme of the Danish island of Als, and

Falshöft, the north-western entrance point of Kiel Bay about 7 miles south-westward. The entrance is rapidly narrowed to a width of about $3\frac{1}{2}$ miles between Kegnes, a peninsula on the south side of Als, and Birknack, a prominent point on the German mainland which forms the north-eastern entrance point of Geltinger Bucht. The fjord is then widened to its maximum breadth of $9\frac{3}{4}$ miles by Geltinger Bucht on the south side and Sønderborg Bucht on the north. The former bay has an entrance 4 miles wide and a penetration of $2\frac{3}{4}$ miles; the latter has a breadth at its entrance of 5 miles and a penetration of about $3\frac{1}{2}$ miles; Als Sund, the narrow strait separating the island of Als from the mainland of Denmark, leads from the head of the bay. West of these bays and $9\frac{1}{2}$ miles within the entrance, the fjord narrows to a breadth of about $1\frac{3}{4}$ miles; thence general widths of one to $1\frac{3}{4}$ miles are retained to its head. About 14 miles within its entrance, the fjord changes its general westerly direction to a northerly one for about $2\frac{1}{4}$ miles; thence, doubling round the northern end of the peninsula of Holnis, it takes a general south-westerly direction for about $7\frac{1}{2}$ miles to its head. North of Holnis, the northern shore is indented by Nybøl Nor, a sheet of water about 2 miles long and nearly a mile wide which is entered by the very narrow Egersund. West of Holnis is the narrowest part of the fjord, where it is about three-quarters of a mile wide. There are two islands within the fjord; these lie close together with their extremes about half a mile from the Danish shore, about midway along the innermost reach of the fjord.

Depths in the fairway through the outer part of the fjord as far as the western extreme of Sønderborg Bucht are no less than 10 fathoms, thence they decrease to general depths of more than 5 fathoms, except in the narrows off Holnis where there are some shoals, the least depth on the leading line there is about 22 feet. Under ordinary conditions, vessels with a draught of $19\frac{1}{2}$ feet can berth at Flensburg. Shoal water, in general, extends seaward off most of the prominent points. An extensive bank, with less than 6 fathoms over it and a least depth of one fathom, lies in the middle of the entrance to the fjord, the main approach channel for larger ships leads south of this. The main fairway through the fjord is well marked by buoys and leading beacons. There are ample lights for night navigation.

There is no appreciable tidal movement, but the water level may alter dependent on the direction, strength and duration of the wind. The ordinary variation is only about a foot, but prolonged gales between west and north-west lower it, at times, from 5 to 7 feet below the mean level. The fjord freezes completely over only in severe winters, when it may be closed from one to two months.

The main ports within the area are Flensburg, on the German side, and Sønderborg and Egersund on the Danish side. Besides these, there are a number of small fishing harbours and piers for the shipping of tiles and other local manufactures. Flensburg has considerable quays and can berth vessels drawing $19\frac{1}{2}$ feet; there are modern facilities and repairs can be executed. Sønderborg, lying close within Als Sund, has piers and wharves with depths of from 8 to 24 feet alongside and

other facilities. Egersund has a number of small piers with depths alongside of from 12 to 15 feet.

The international boundary meets the coast at the north-western corner of the head of the fjord, and thence continues eastwards to approximately the axis of the fairway through the fjord, which it follows to the entrance. The boundary is marked for the most part by leading beacons and lights.

Both German and Danish pilots may serve in the waters of either country but a vessel may be piloted into a harbour only by a pilot of the country which owns the harbour.

Vessels navigating in the fjord are forbidden to close either the German or Danish coasts within a distance of 200 metres without special permission, except in the case of ordinary navigation through the narrow channel west of Holnis. Navigation is also forbidden in the waters between the northern side of the Kegnes Peninsula and the coast northwards. Landing from Danish territorial waters may only be effected at Sønderborg, Egersund and Graasten, and police permission is required to do so. The above regulations apply west of a line joining the south-east extremity of Kegnes and Birknack.

Intensive fishing is carried out throughout the year in the whole fjord.

Approximately half the coastline is Danish and the other half is German.

6. Estuary of the Bidasoa River (Annex, map No 44)

References: Chart No. 2665 and plan

Bay of Biscay Pilot, Fourth Edition, 1956

The Bidasoa River for the last few miles of its course forms the international boundary between France and Spain. At the international bridge at Hendaye, the river flows into an estuary almost completely filled with banks which dry several feet at low water. This estuary is about $1\frac{3}{4}$ miles long and has a maximum width of about three-quarters of a mile; its seaward end is constricted to a width of about a quarter of a mile by a low sand spit terminating in Pointe Française. There are breakwaters from this point and the opposite shore. The estuary then opens out into a bay named Higuier Road. The entrance to this bay lies between Cabo Higuier, the northern point of an islet on a drying ledge extending from the northern end of Punta Erdico on the Spanish coast, and Pointe Ste. Anne on the French coast nearly two miles east-south-eastward. The penetration of the bay to Pointe Française is about $1\frac{1}{4}$ miles. Les Briquets are detached rocks, which dry 6 feet with their outer edge three-quarters of a mile north of Pointe Ste. Anne; Roches Noire are some small detached above-water rocks lying on a drying ledge which extends about a quarter of a mile northward of that point.

Depths in the entrance to the bay are about 11 fathoms. These depths decrease to the head where the drying banks intersected by the winding channel from the river extend nearly half a mile northward of Pointe Française and for a similar distance from the south-western shore. The narrow channel into the river has about a foot of water in it at low tide.

Anchorage may be obtained in the bay, sheltered from winds from the east through south to west. With winds from seaward this anchorage is unsafe. There is a small harbour of refuge formed by two short moles about a quarter of a mile southward of Punta Erdico; its entrance is 100 feet wide and depths within from 9 to 20 feet. The rise of the tide at springs is about 14 feet.

Fuenterrabia is a small fishing centre on the Spanish side of the estuary nearly opposite Hendaye.

Within the bay is a "neutral area" for the use of both French and Spanish vessels; this is marked by the alignment of beacons on the shore. This area to the low-water line at the head of the bay is less than three-quarters of a mile long and nearly a mile wide and encloses the best anchorage. From the northern end of this area, the international boundary through the territorial sea passes northward about equidistant from Cabo Higuer and Les Briquets.

About half the coastline is French and the other half is Spanish.

7. The mouth of the River Mino (Annex, map No 45)

References : Chart 1752

West Coasts of Spain and Portugal Pilot, Third Edition, 1946

Owing to the small scale of the available charts, this description is perforce brief.

The lower reaches of the River Mino form the boundary between Spain on the north and Portugal on the south. The entrance lies between Punta de los Picos and Ponta Ruiva about three-quarters of a mile southward. About a quarter of a mile westward of the latter point is a low islet with a fort on it, named Ilha Insua. The river mouth is fronted by a rocky bar; there are, however, channels leading on both sides of Ilha Insua; that on the north is widest and is encumbered with rocks but has a depth of about 10 feet in the fairway at high water springs; that on the south side also has many shoals and a depth of 13 feet at high-water springs. The sea breaks across both channels if there is any swell; the depths are variable.

Within the river are many shifting shoals and banks; entry and passage can, however, be made by light draught craft with the aid of an experienced pilot. About 1½ and 2 miles within the entrance are two fishing villages one on each bank of the river; anchorage may be obtained off them in depths of about 10 feet.

Both Spanish and Portuguese pilots can be obtained.

8. Idefjord and its approaches (Annex, map No 46)

References : Charts Nos. 3160, 2330, 121

Norway Pilot, Part I, Seventh Edition, 1948

The boundary between Sweden and Norway meets the sea near the western side of the head of Idefjord, thence passes through this fjord, through Ringdalsfjord, Svinesund, Saekken and thence seaward through the islands and rocks off-lying the coast. This description will follow the above order.

Idefjord is a long, straight fjord, running in a north-north-westerly direction, about 9 miles long with a general width of less than half a mile. Its maximum and minimum breadths are three-quarters of a mile and about 300 yards. Its general depths are from 18 to 5½ fathoms, except for about 1¾ miles from the head which shoals from depths of 2 fathoms. The small islet of Halleholm lies about 6 miles from the head towards the eastern side and is territory of Sweden.

The north-eastern end of the fjord widens somewhat but is partially filled by the islands of Brattøen and Sauøen, both of which lie on the Norwegian side of the boundary. At the north-eastern corner of the fjord lies the small port of Halden, where there are berths alongside in 16 to 25 feet.

At the north-western end of Idefjord, the waterway turns abruptly south-westwards to become Ringdals Fjord and then Svinesund. Ringdals Fjord is about 1¾ miles long with a general width of about a quarter of a mile. The channel is restricted at the north-western end to a breadth of little more than 100 yards by the Norwegian islet of Knivsvø.

Svinesund joins Ringdals Fjord to Saekken; it is about 2½ miles long and is extremely narrow. About half way along it is crossed by a bridge with a height of 190 feet. Westward of this is a dredged part of the channel having a breadth of 128 feet with a depth of 23 feet.

Saekken is the continuation of the channel seaward. This cuts across the southern end of the sheet of water lying between the mainland and the islands of Kirkø and Singlø, known as Single Fjord, thence continues in a south-south-westerly direction between the Norwegian islands of North and South Sandø and the Swedish mainland, and thence between the Norwegian island of Herføl and the Swedish islets of Tjurholm and North Hallsø to the northern end of Koster Fjord.

This stretch of the channel is about 8 miles long and has a maximum width of rather less than half a mile; it is deep with depths of from 25 to 60 fathoms. Herføl, South and North Sandø, with a few rocks lying off them, are the south-easternmost of a chain of islands and islets of which Kirkø and Vesterø are the largest, extending 11 miles north-westward from the Swedish mainland and about 7 miles southward of the Norwegian mainland.

Tjurholm and N. Hallsø are the northernmost of a chain of islands extending southwards for many miles, separated from the Swedish mainland and each other by very narrow channels. In general, their western extremities lie from about 1½ to 3 miles from the mainland.

Seaward of Herføl and N. Hallsø, the channel and boundary take a west-south-westerly direction for about 8 miles to the main waters of the Skaggearrak, close northward of Grisbadarna, a group of shoals with a least depth of one fathom.

South-westward of the chain of islands of which Herføl forms the southernmost, and on the Norwegian side of the boundary, are a number of shoals and detached above-water rocks and islets; these lie in two groups. The inner group extends about 2 miles north-

westward and lies from about 2 to 3½ miles westwards of Herfjøl; the largest islet is Tisler, and the most southern above-water rock is Svarteskjoer, which lies about 2 miles from Herfjøl and a mile north of the boundary. The outer group, enclosed within an area about three-quarters of a mile wide, extends about 4 miles north-westwards from Knubben, a small above-water rock close south of Heia, the largest in the group, lying about 5¼ miles west-south-westward of Herfjøl. Heiftuene is a group of sunken rocks, some of which are awash at low water, lying up to half a mile south-east of Knubben.

On the Swedish side of the border, a chain of islands, islets and rocks lies approximately parallel to the outer edge of the islands mentioned above, lying south of Tjurholm and close to the mainland coast; Koster Fjord about 1½ miles wide separates these two chains. This outer group extends southward for about 11 miles from Kostersten, a small above-water rock, lying 2 miles south-west of N. Hallsø. The largest islands in the group are N. Koster and S. Koster; the most north-western above-water rock is St. Drammen; this lies about 2¼ miles south-west of Kostersten and just over a mile from the international boundary. About 3 miles west of this rock are the Grisbadarna shoals.

On the Swedish mainland coast about 5 miles east of Kostersten is the small port Strømstad. On the Norwegian mainland about 10 miles north-west of the entrance to Svinesund is the port of Frederikstad.

The international boundary for about 4 miles from Grisbadarna is marked by buoys, and thence by leading beacons.

South-eastward of the boundary, between Grisbadarna and North Koster, is a fishing ground in which it is prohibited to anchor.

9. Head of Bottenviken (Annex, map No 47)

References : Chart 2302

Baltic Pilot, Volume III, Fourth Edition, 1951

The boundary between Sweden and Finland meets the coast at the mouth of the Torne River, which discharges into the head of Bottenviken; it thence continues southward between the numerous islets lying off that part of the coast. The river mouth, about a quarter of a mile wide, enters the sea between the Swedish mainland and the Finnish island of Pirkkiö and about 1½ miles south of the Finnish town of Turniö. Sellei is an island close south of Pirkkiö; its southern end is about 5 miles south of Turniö.

From the river mouth, the mainland coast of Finland runs in a general south-easterly direction for about 17 miles to a promontory named Maksniemi; the mainland coast of Sweden runs in a general west-south-westerly direction from the river mouth for about 25 miles. A large number of islands and above-water rocks front the coast up to a distance of nearly 14½ miles, their positions can best be seen on the chart; only the principal ones will be mentioned here.

The largest islands, 3½ miles long and 3 miles wide is Seskar lying 10 miles south-west of the river mouth.

Puukko is a small islet about 1½ miles southward. About 11 miles southward of Seskar is Malören, the southernmost in this area. Sandskar lies about 5 miles north-east of Malören, with Seskarfurö between it and Seskar. About 10 miles east-north-east of Sandskar, with several islets in between, lies the islet of Sarvi, with another close north-eastward. These latter two are close westward of the Swedish-Finnish boundary which runs about midway between them and a group of four islets about half a mile eastward, the north-eastern of these is Maasarvi. Möyly, a small above-water rock, lies 4 miles south-eastward of this group and is the southernmost Finnish above-water feature in the area now described; it lies about 10 miles west-south-westward of Maksniemi.

Other islets and rocks lying near the boundary are: Knifskär, two islets and a rock, 3 miles north of Sarvi on the Swedish side; a group of five islets and rocks of which Pensaskari is the largest, about 1½ miles east of Knifskär; Kataja, an islet 2 miles north of Knifskär with the two islets of Hamnskär westward and a group of four islets and rocks close south-south-westward, the largest of which is Inakari. The boundary passes west of the islet close southward of Inakari, thence between them and thence east of Kataja. Northward of Kataja, a chain of above-water rocks extends for 2 miles, the northernmost of these is named Launikari. About 1½ miles eastward of Launikari and within a mile southward of Sellei, on the Finnish side of the boundary, lies a chain of rocks extending from the latter island. The boundary runs between Sellei and two islets lying about half a mile west of its western extreme. Kraseli and another Swedish islet close northward lie off the mouth of the Torne River.

Two buoys mark the outer line of the boundary between Maasarvi and Knifskär, thence to the Torne River the boundary is indicated by the alignments of pairs of beacons set up on the islets and rocks.

The whole area is encumbered with innumerable shoals and dangers; the fairways in use between them are marked by beacons, buoys and lights. The area is likely to be closed by ice from the middle of November to the middle of May. With strong and prolonged winds from the northern quarters the water level is liable to drop by several feet; conversely, with winds from the southern quarters, it is likely to rise. There is no tide as such.

The principal ports within the area are:

On the Finnish side, Kemi, about 11½ miles south-east of the entrance to the Torne River, where there are depths at the quays of from 10 to 21 feet and in the roads up to 24 feet; Röyttä, the port for the town of Tornio lying a short way up the river, which is on the west side of Sellei and where there are depths of 20 feet at the quays.

On the Swedish side, Haparanda, on the mainland opposite Tornio, where there is a quay with a depth of 19 feet alongside, and Neder Kalix, about 24 miles west of Tornio, where there is a depth in the roads of 27 feet. There are several landing places between Kemi and Röyttä and also on the Swedish coast west of the river entrance.

Pilotage is compulsory for navigation in both Finnish and Swedish waters. Finnish customs regulations prescribe that vessels bound for Kemi must adhere to the route past Kemi lightvessel, or past Ulkokrunni and, if bound for Tornio, to the route past Malören lighthouse and Puukko in Swedish waters or past Kemi lightvessel to Röyttä.

10. The area of Viro Lachti (Annex, map No 48)

References : Chart No. 2247

Baltic Pilot, Volume III, Fourth Edition, 1951

The boundary between Finland and the USSR cuts the coast in the south-east corner of Viro Lachti, an indentation lying between Gevonemi and a point on the mainland 3 miles north-north-eastward. Extending 5 miles seaward of the latter point are the islands Laid-salm, Padio and Pukion Sari, all territory of the USSR, these are separated by very narrow channels. The penetration of Viro Lachti, from a line joining Gevonemi to the west extreme of Padio, is $5\frac{3}{4}$ miles. Within these limits about one-third of the coastline is USSR territory and two-thirds is Finnish.

Numerous islets lie within 3 miles of the coast westward of Gevonemi and east and south-east of Padio and Pukion Sari, which can best be seen on the chart. Less than half a mile south-east of Gevonemi is the Finnish islet of Vango with the USSR islet of Martin close south-east of it. Three-quarters of a mile west of the latter lies Santio, a Finnish islet, with Parrio another close westward. About $1\frac{1}{4}$ miles south of Parrio lies the islet of Kinnar, the largest of a group of islets and rocks, and the boundary runs through the group. About a mile south of this group is another cluster of above-water and submerged rocks, the largest of which is Gouör; the boundary passes northward, eastward and southward of it. Five and one-quarter miles southward of this cluster is Hallikarti, a smaller group, with Kivikari and Matakarti, two similar groups, lying $1\frac{1}{2}$ and $2\frac{1}{4}$ miles north-westward and westward respectively of the latter, with the boundary passing between. The southern end of the demarcated boundary lies 4 miles south-south-westward of Matakari and about midway between the island of Sommars and Itakari, the easternmost of a large group of Finnish islands and rocks $9\frac{1}{2}$ miles north-westward. The boundary throughout is marked by buoys and beacons.

Depths throughout the whole area are irregular and there are many shoals and submerged rocks; Viro Lachti itself is encumbered by islets, above-water rocks and shoals.

There are no ports of any consequence; a loading place is situated about $1\frac{1}{4}$ miles within Gevonemi which vessels drawing 24 feet can reach; an authorized track for vessels drawing up to 10 feet leads to the head of the bay. Shtandar or Kavö Road, situated between Martin and Padio, is sheltered except for the south-eastern quarter and there are depths of from 8 to 10 fathoms.

Anchorage may be obtained in Finnish waters north of Santio in depths of about 7 fathoms. The dangers in the approaches to both these anchorages are buoyed.

The area is likely to be closed by ice from January to April.

There is no tide, but prolonged winds from east or west are liable to effect a change in water-level.

Pilotage is compulsory in both Finnish and USSR waters.

11. Estuary of River Guadiana (Annex, map No 49)

References : Charts, Nos. 2680, 92

West Coasts of Spain and Portugal Pilot, Third Edition, 1946

The River Guadiana for the last few miles of its course forms the boundary between Portugal and Spain. It discharges through a comparatively straight stretch of coast running in an east-north-easterly direction for about 20 miles. About $1\frac{1}{2}$ and $2\frac{1}{4}$ miles within the entrance, two narrow creeks lead eastward off the main river to discharge into the sea through the River Higuierita, about $2\frac{1}{2}$ miles eastward of the main mouth, thus forming the islands of Canela and Salon; both these channels almost dry at low water.

On the western side of the entrance to River Guadiana, a drying sandspit extends nearly $2\frac{1}{4}$ miles south-eastward, and drying banks extend about a quarter of a mile south of Isla Canela. The distance between the end of this spit and the drying banks is about three-quarters of a mile. This entrance is fronted by a bar composed of sand banks which completely change at times of heavy floods in winter and of onshore gales. At times, some of these banks may be above water. The entrance channel is marked by buoys which are moved after alterations in the channel.

The small port of Villa Real de Santo Antonio lies on the Portuguese side about a mile within the entrance. Vessels drawing up to about 18 feet can reach this port and those drawing 17 feet can reach the piers at Pomarao about 22 miles up river. Tunny fishing nets may be found at times up to $5\frac{1}{2}$ miles off shore and a large sardine fishery takes places near the river entrance.

The rise of the tide is about 11 feet at springs.

Pilotage is compulsory.

12. The mouths of the River Evros (Annex, map No 37)

References : Chart No. 1086

Mediterranean Pilot, Volume IV, Eighth Edition, 1955

The principal mouth of the River Evros, known to the Turks as Meric and once known as Maritsa, forms the boundary between Greece and Turkey. The river discharges through a delta on the eastern side of a bight lying between the coast about 3 miles north-west of Grenea Burnu and Ak Makri about 20 miles north-westward. The penetration of this bight is $6\frac{1}{2}$ miles. The island of Samothraki, about 21 miles off shore, fronts the bight.

The coast of the delta extends for about $6\frac{1}{2}$ miles in the northerly direction. The principal of the river

mouths lies at the southern end. The mouths through the delta and its coast are liable to alteration. At the time of the survey for the chart, several low, narrow islets fronted the delta, lying up to half a mile off shore.

On the eastern side of the bight, depths of less than 3 fathoms are found up to 1½ miles off shore, the northern side is comparatively steep-to.

Depths on the bar of the principal mouth are usually

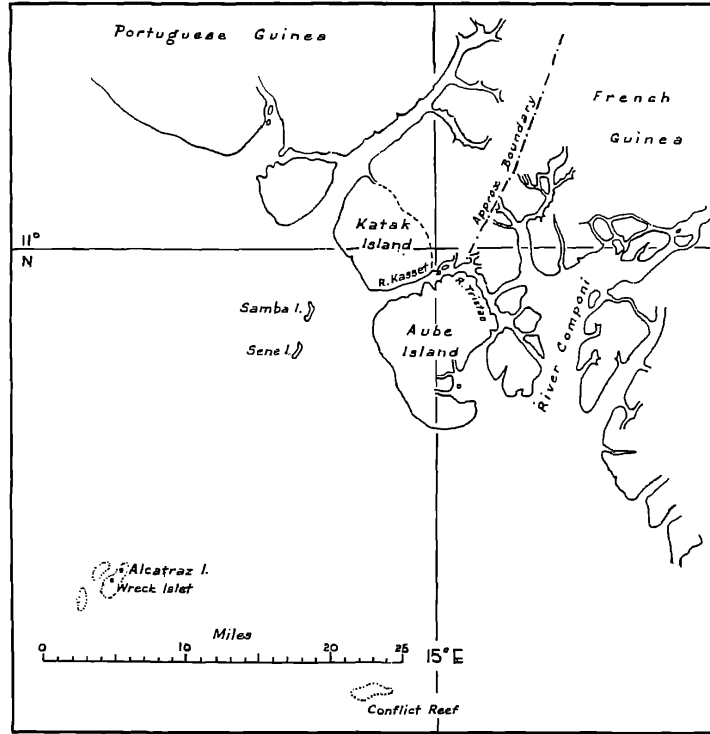
about 3½ feet. There is trade by small craft with the Turkish town of Enez, 2 miles within the principal mouth; Edirne, 70 miles up river, can be reached by barges. The port of Alexandroupolis, which has a small harbour with depths of about 18 feet, lies about 7 miles east of Ak Makri.

About a quarter of the coastline of the bight described above is in Turkish territory.

ANNEX

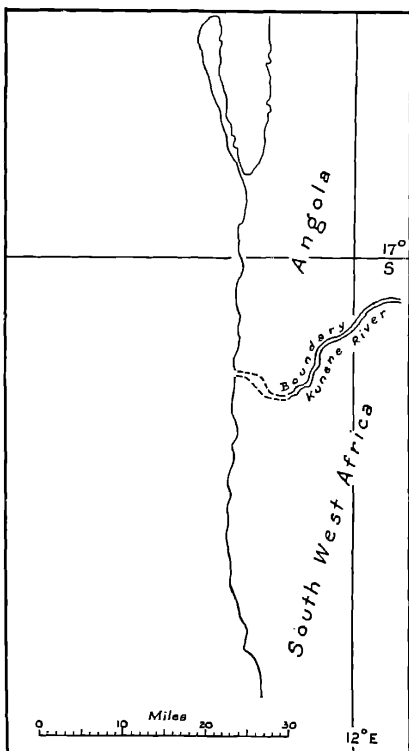
MAP NO. 1

Waterway at 11°N, 15°W (approx.) between French and Portuguese Guinea



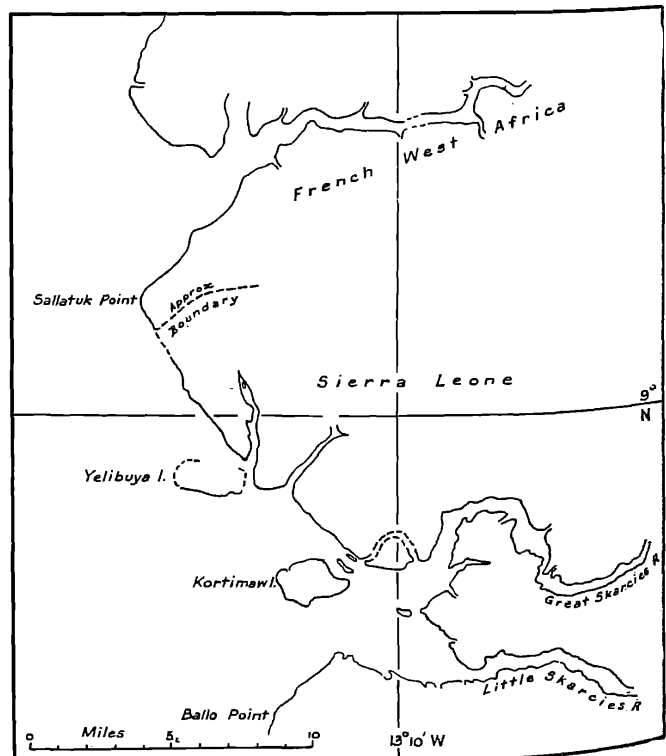
MAP NO. 2

Estuary of Kunene River

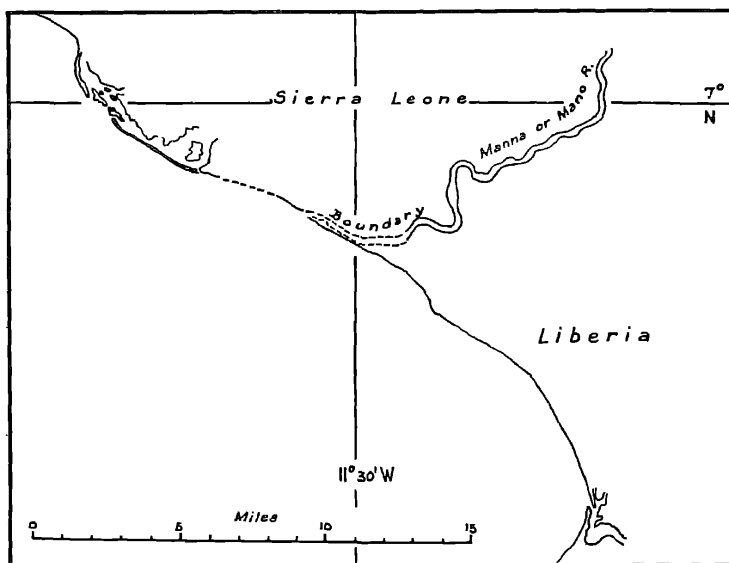


MAP NO. 3

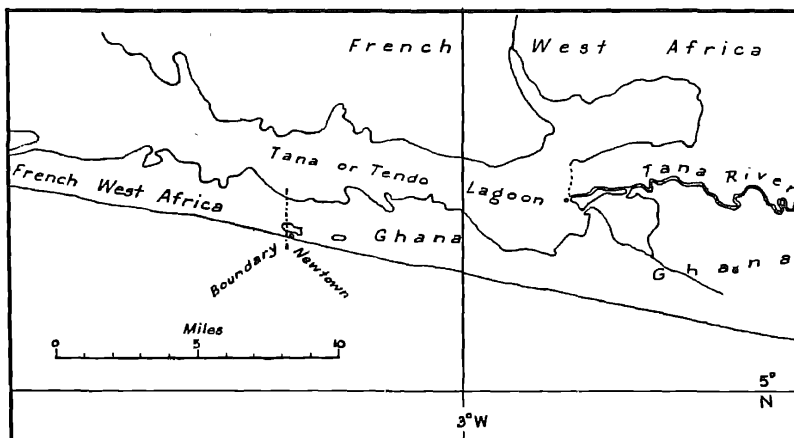
Estuary of Kolente or Great Skarcies River



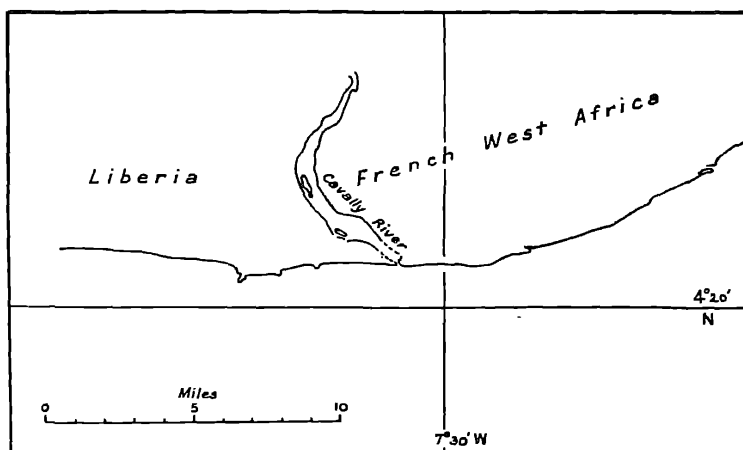
MAP NO. 4
Mouth of Manna or Mano River



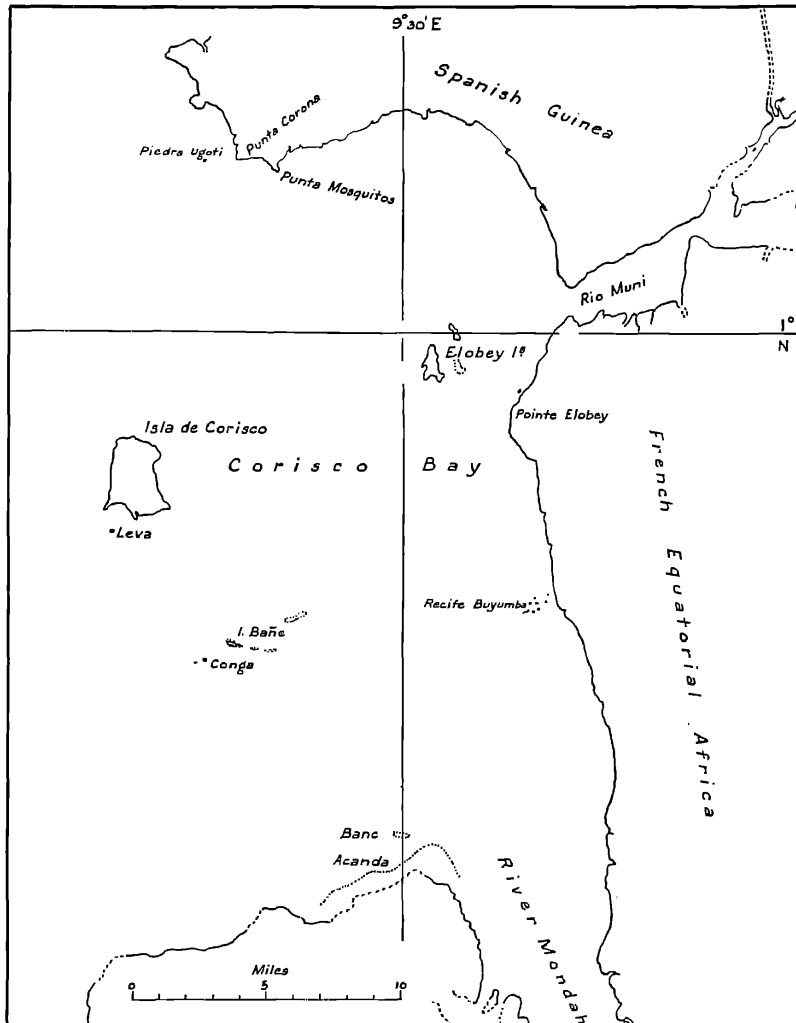
MAP NO. 5
Tana River



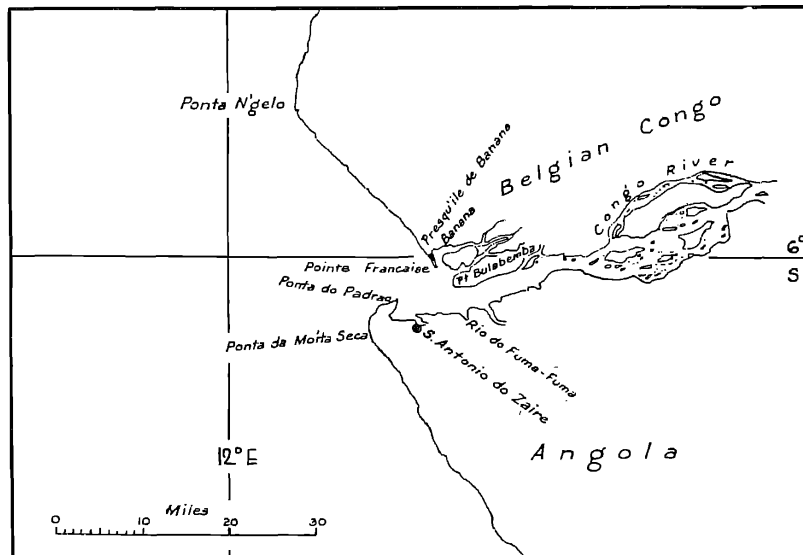
MAP NO. 6
Cavally River



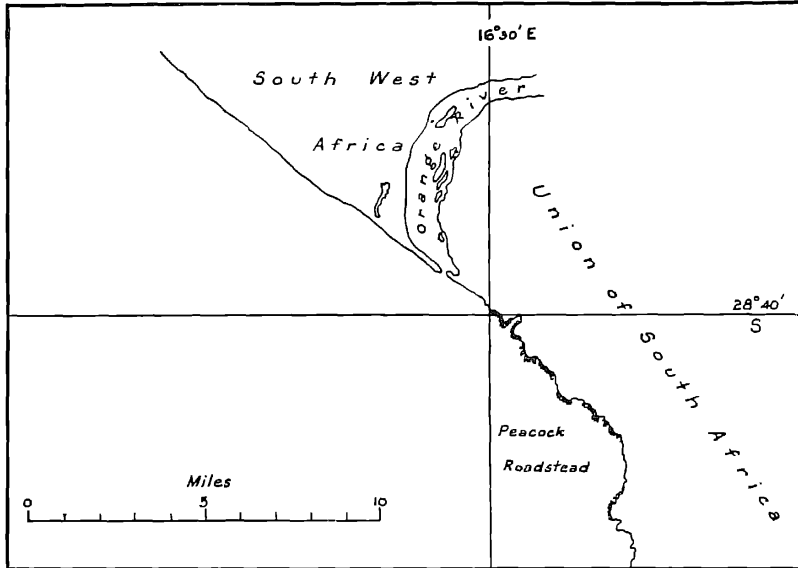
MAP NO. 7
Estuary of Rio Muni



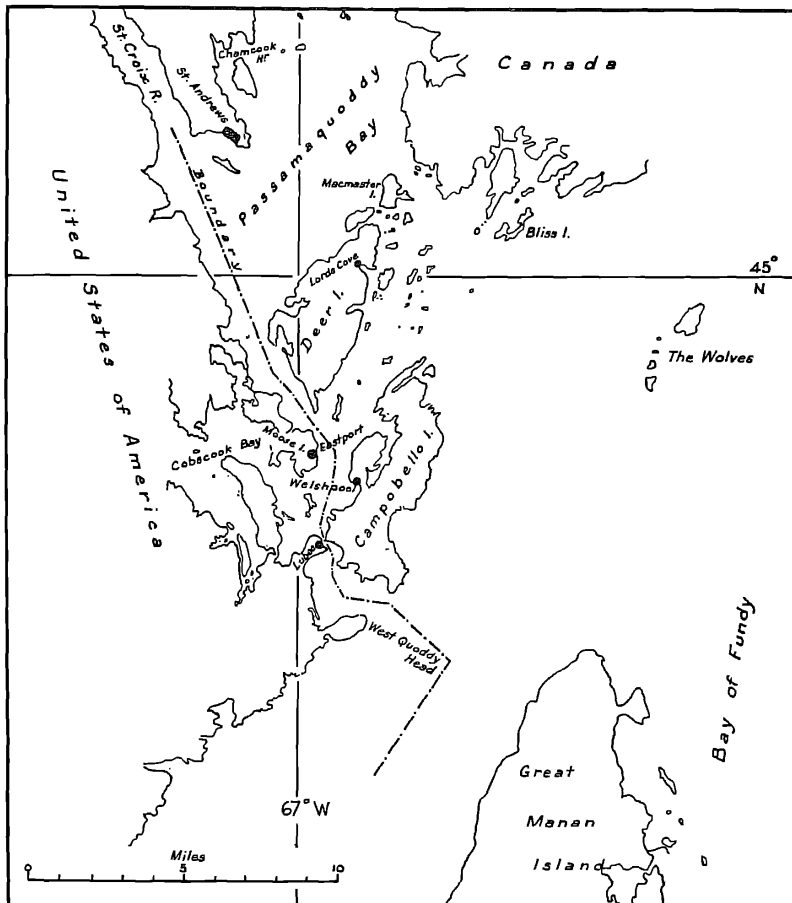
MAP NO. 8
Estuary of Congo River



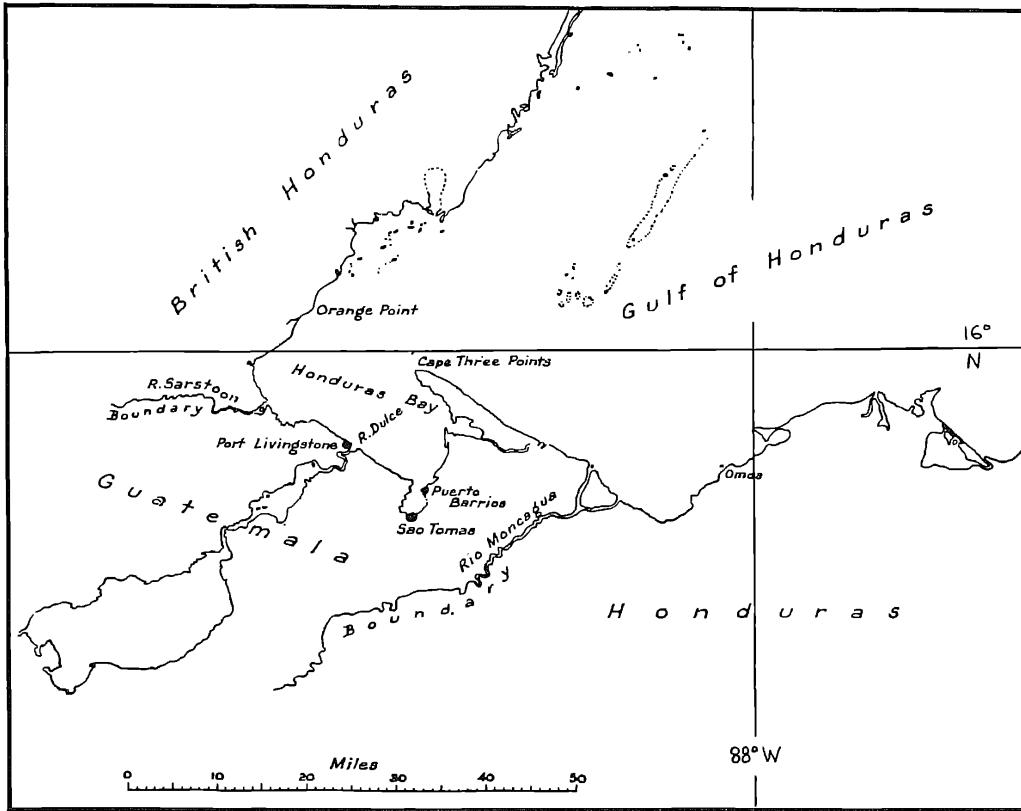
MAP NO. 9
Mouth of the Orange River



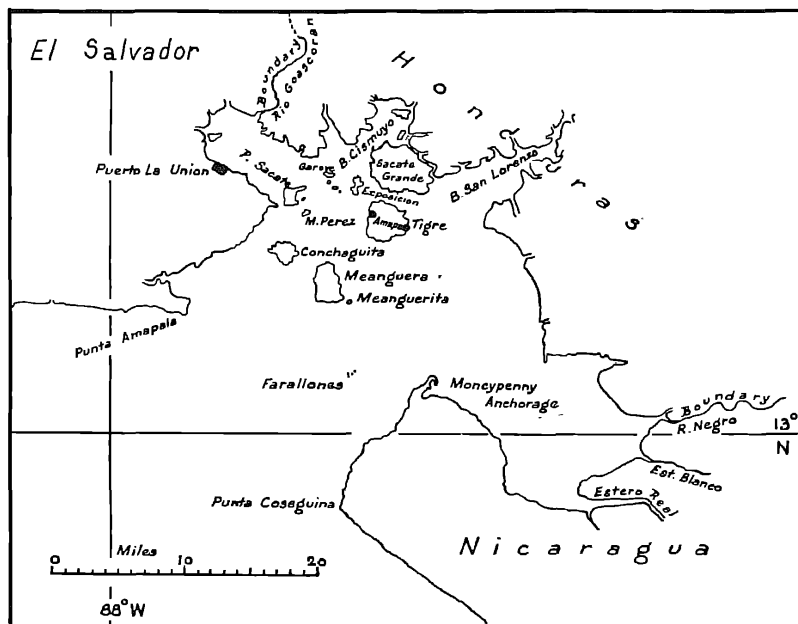
MAP NO. 10
Passamaquoddy Bay



MAP NO. 11
Gulf of Honduras

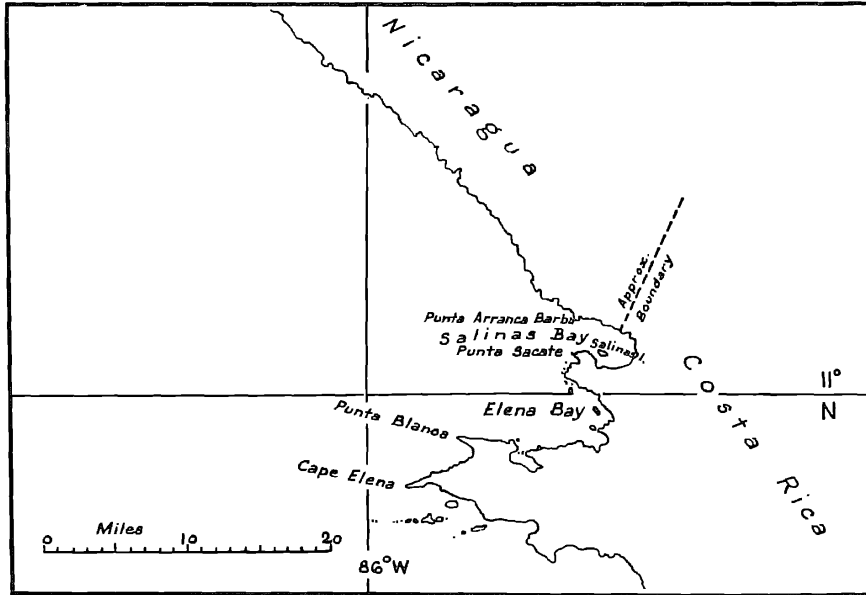


MAP NO. 12
Gulf of Fonseca



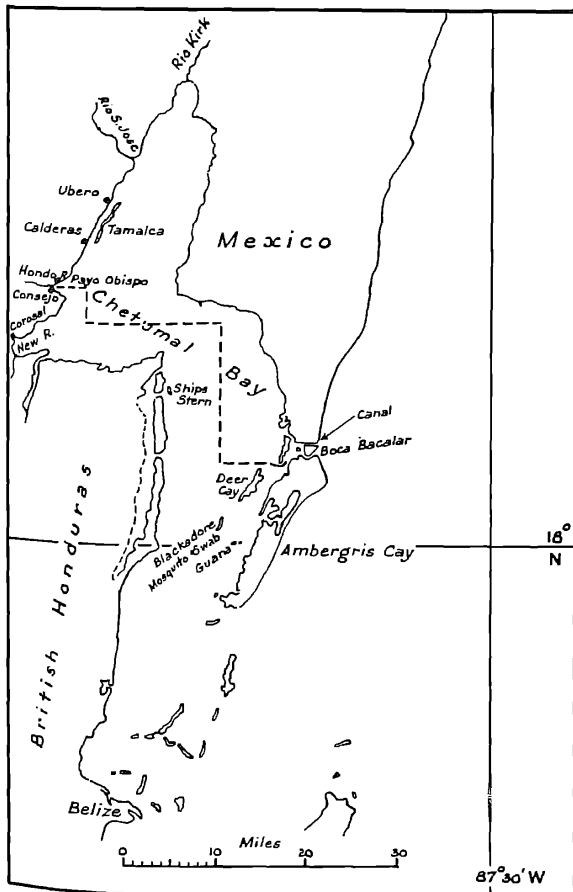
MAP NO. 13

Salinas Bay



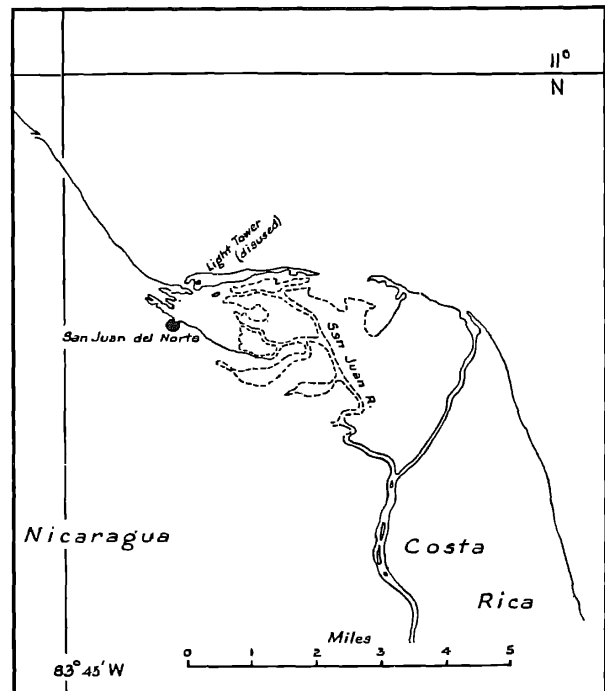
MAP NO. 14

Chetumal Bay



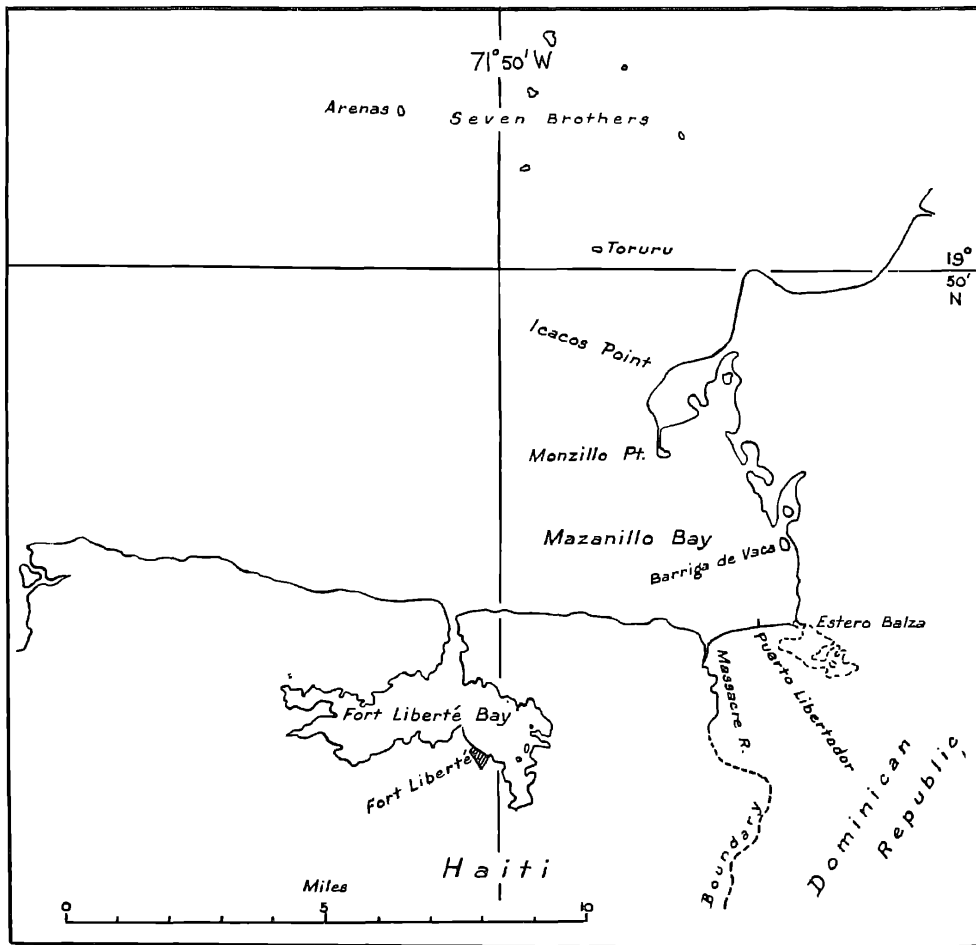
MAP NO. 15

San Juan River



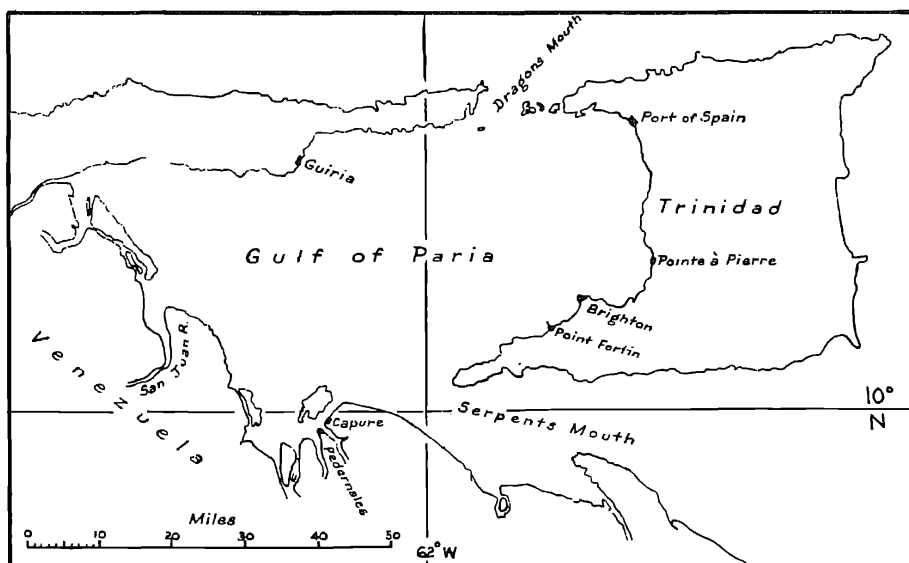
MAP NO. 16

Mazanillo Bay

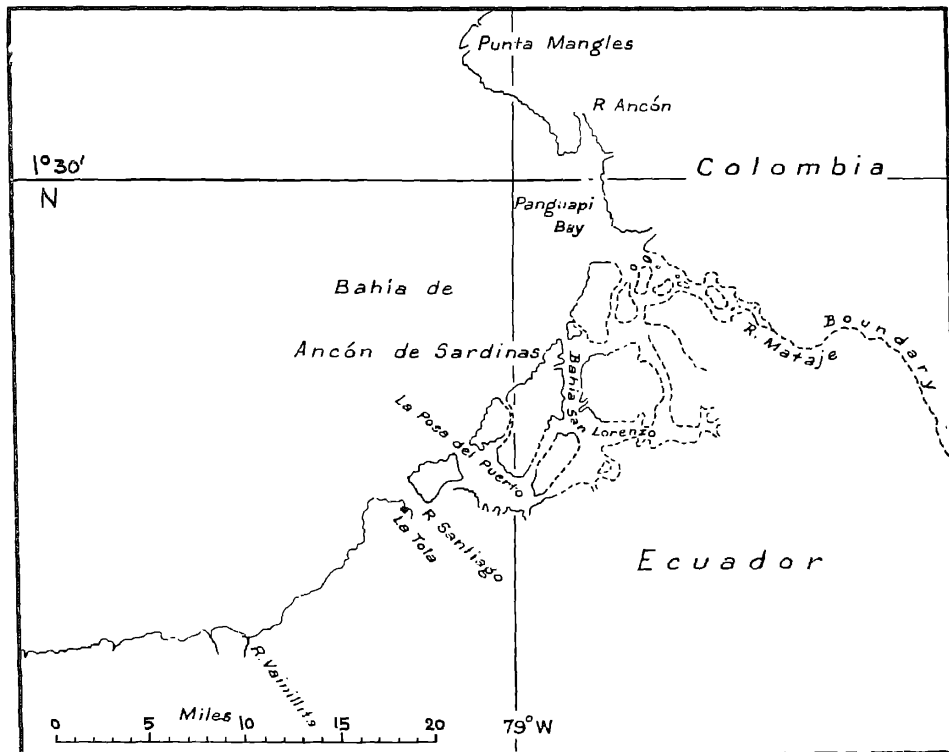


MAP NO. 17

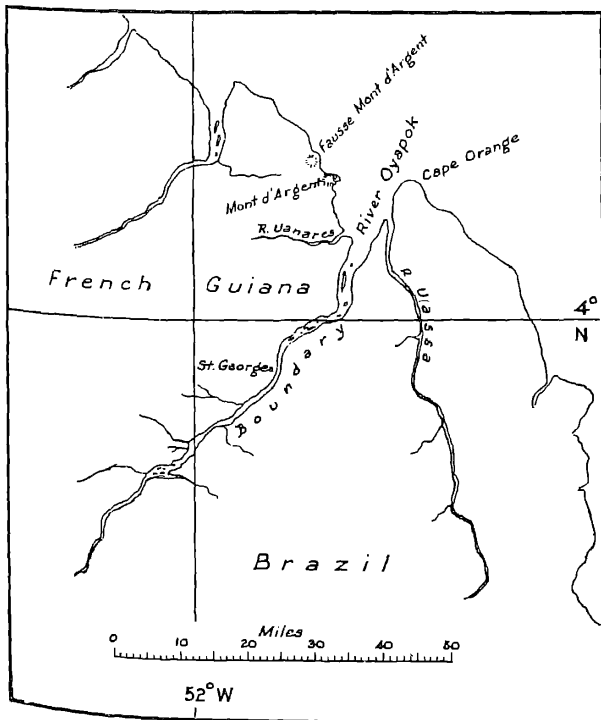
Gulf of Paria



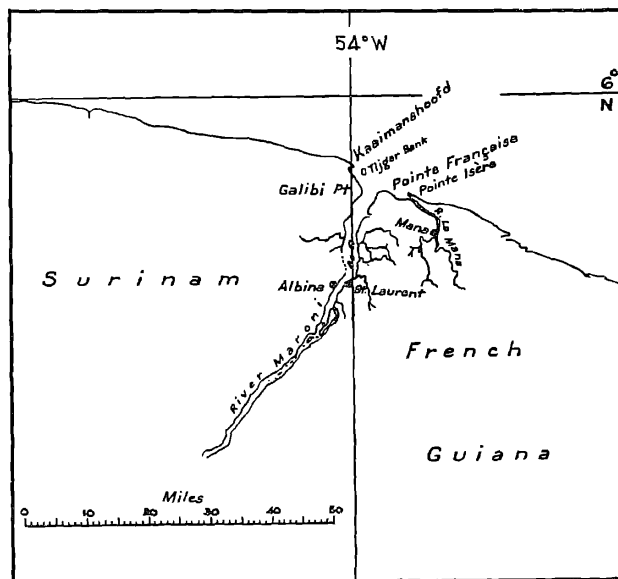
MAP NO. 18
Bay of Ancón de Sardinias



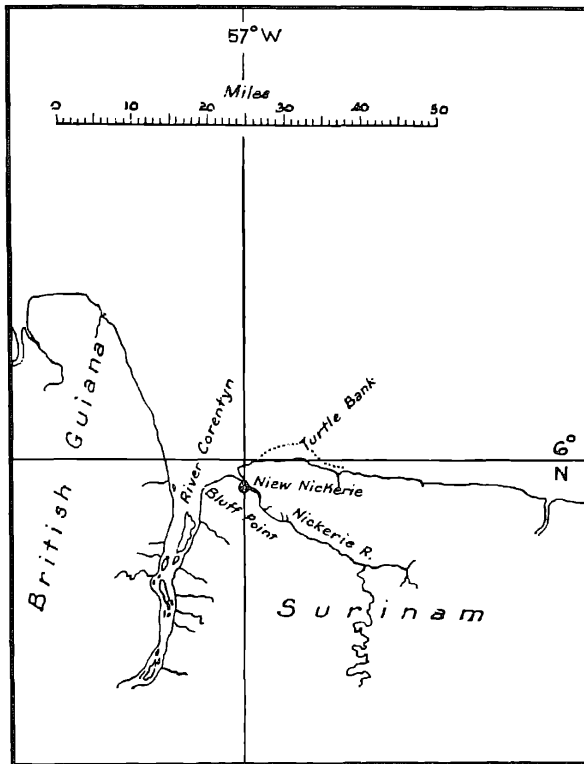
MAP NO. 19
Bay of Oyapok



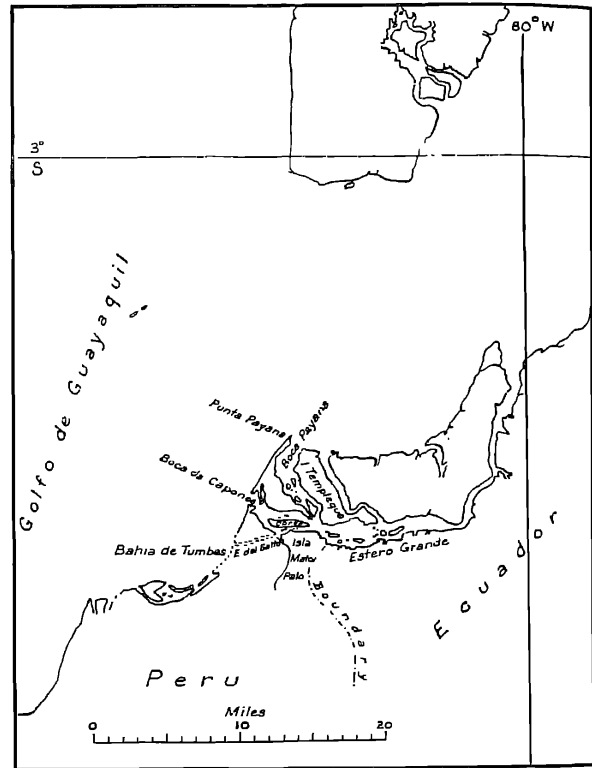
MAP NO. 20
Estuary of Maroni



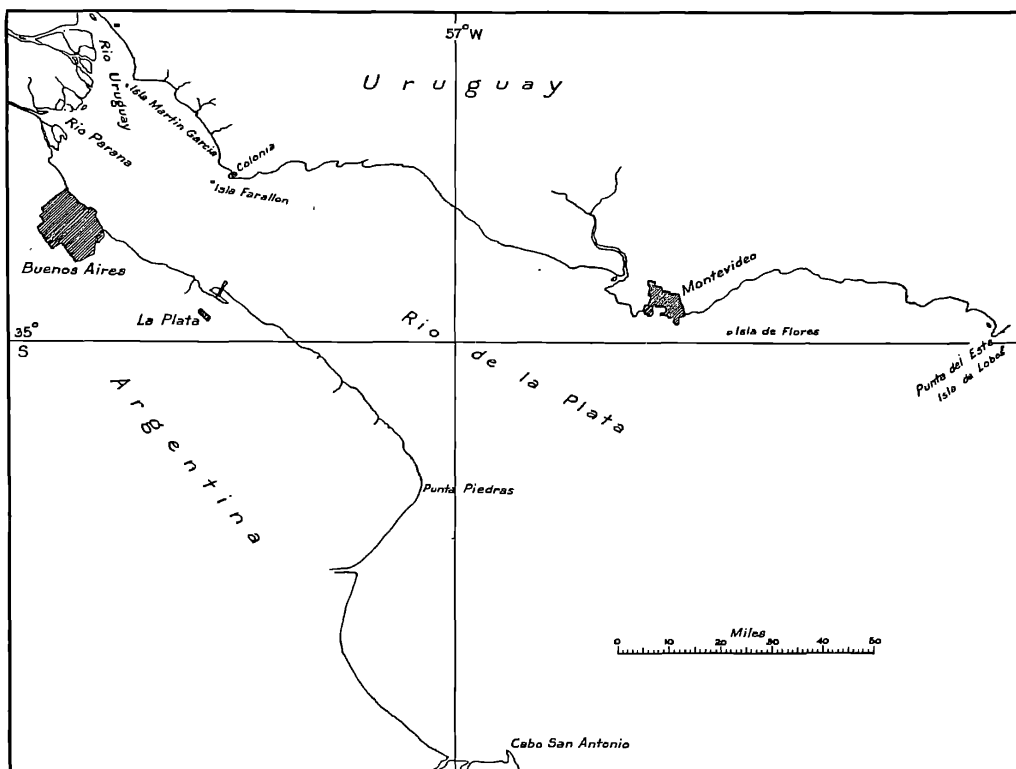
MAP NO. 21
Corentyn River



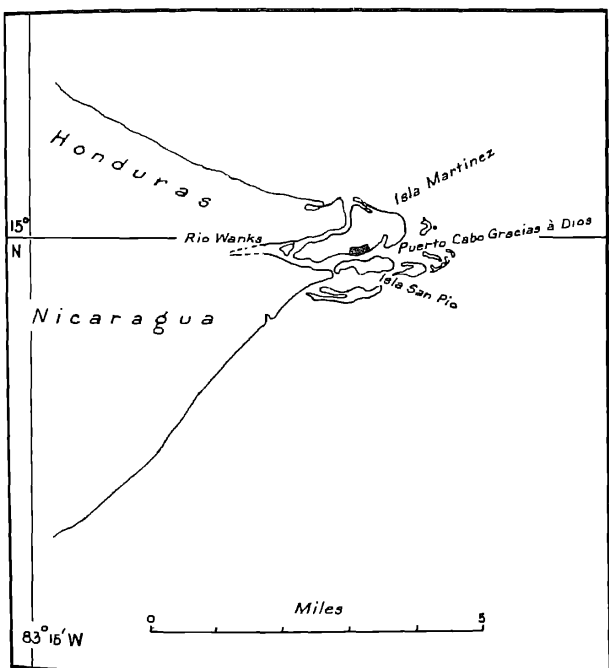
MAP NO. 22
Boca de Capones



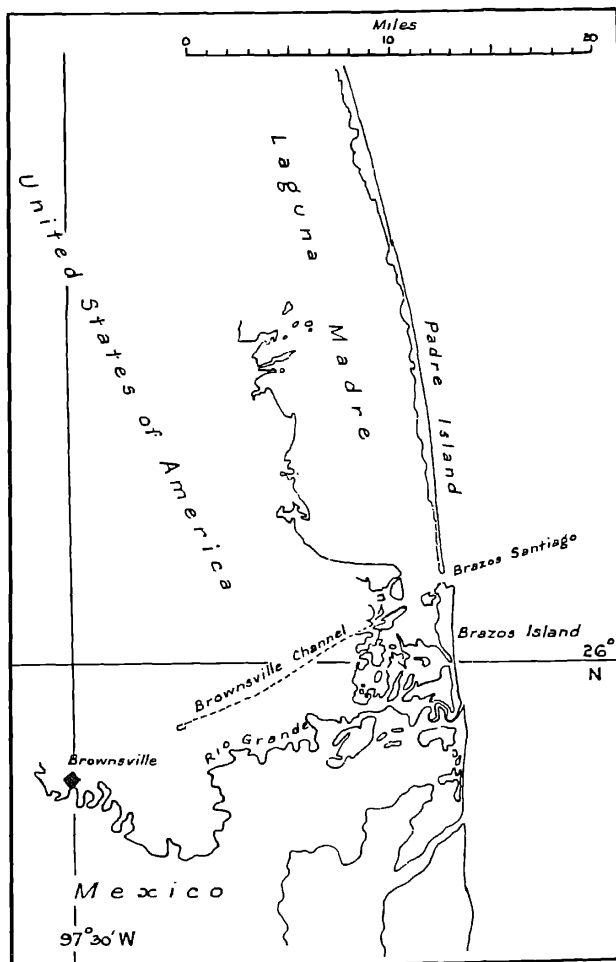
MAP NO. 23
Rio de la Plata



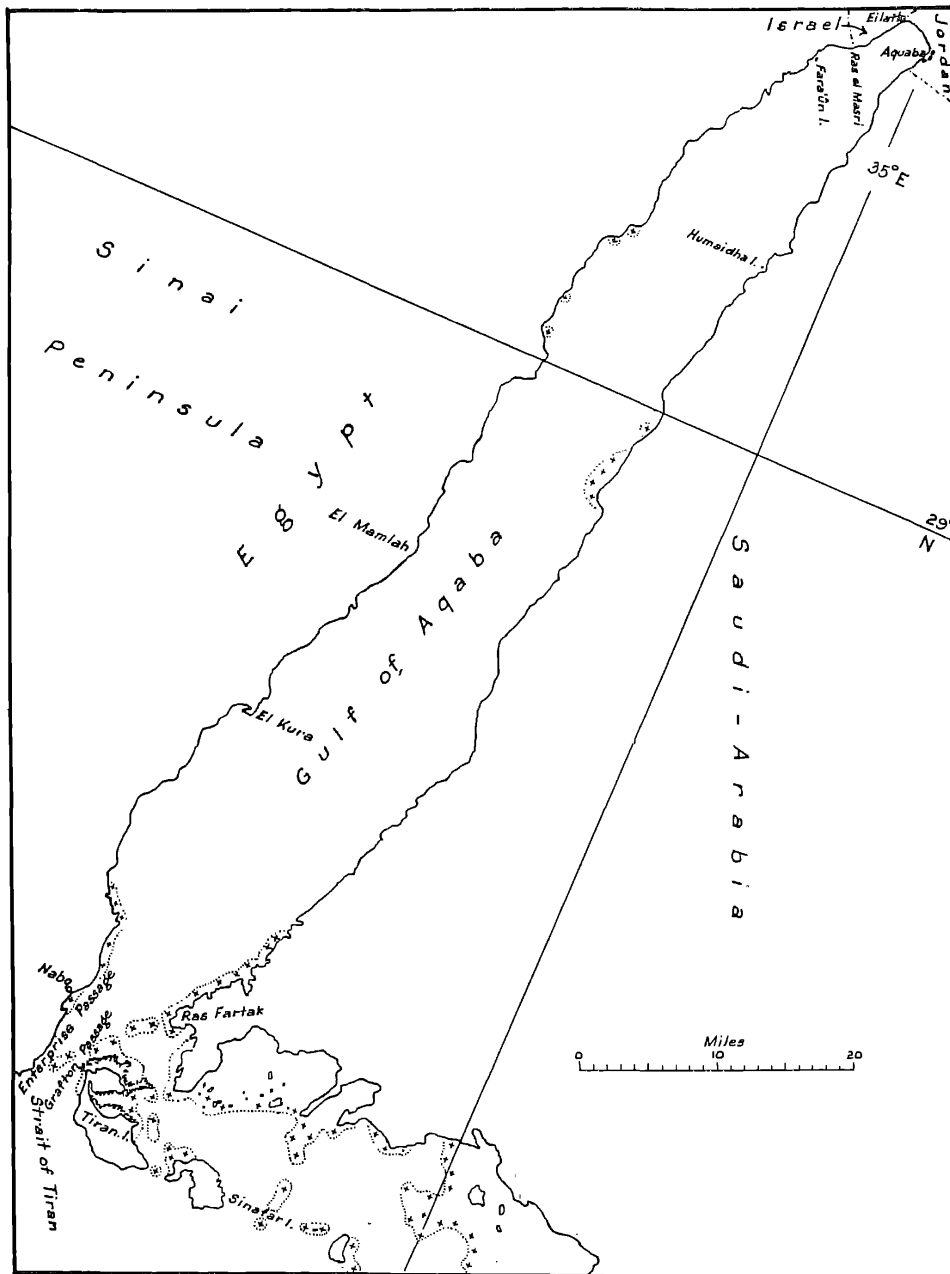
MAP NO. 24
Estuary of Coco (Wanks) River



MAP No. 25
Rio Grande

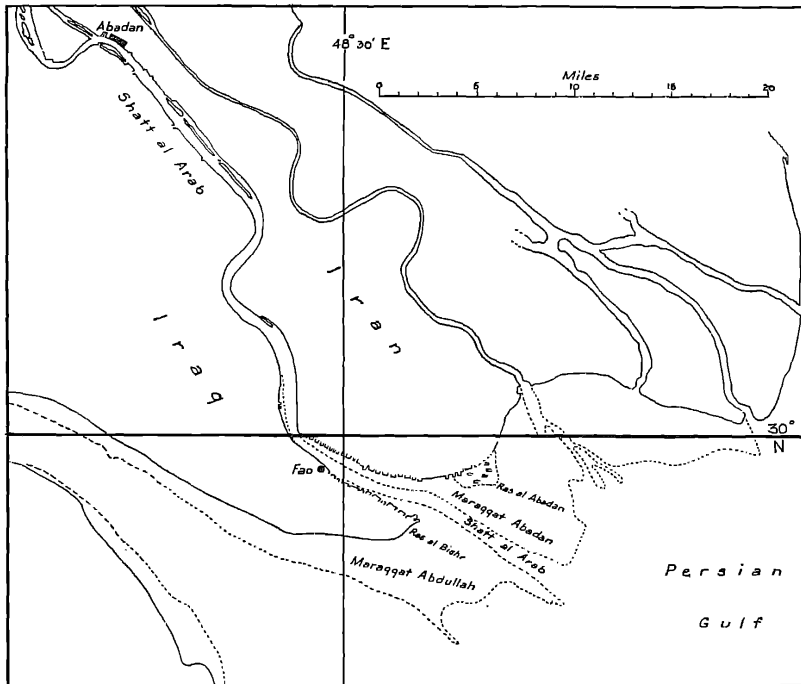


MAP NO. 26
Gulf of Aqaba



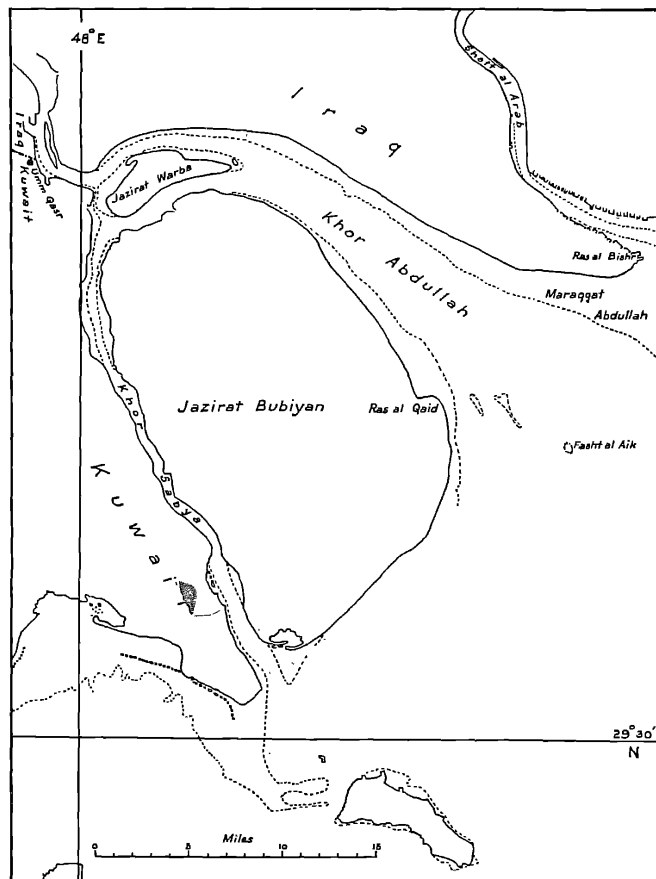
MAP No. 27

Shatt al-Arab



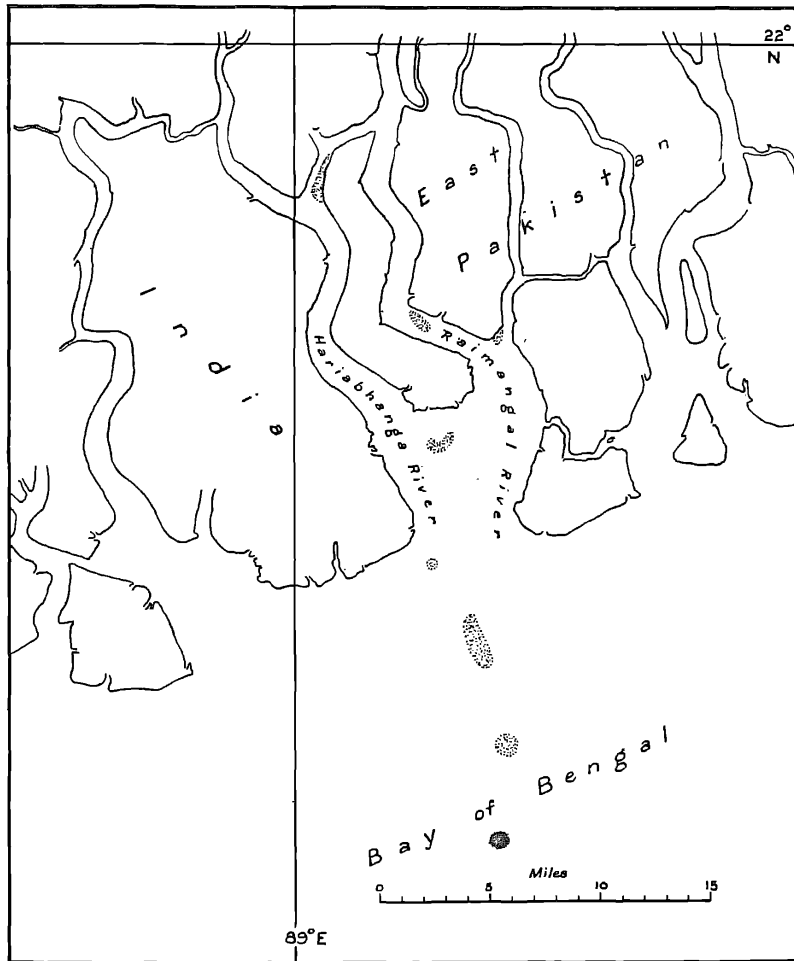
MAP No. 28

Khor Abdullah



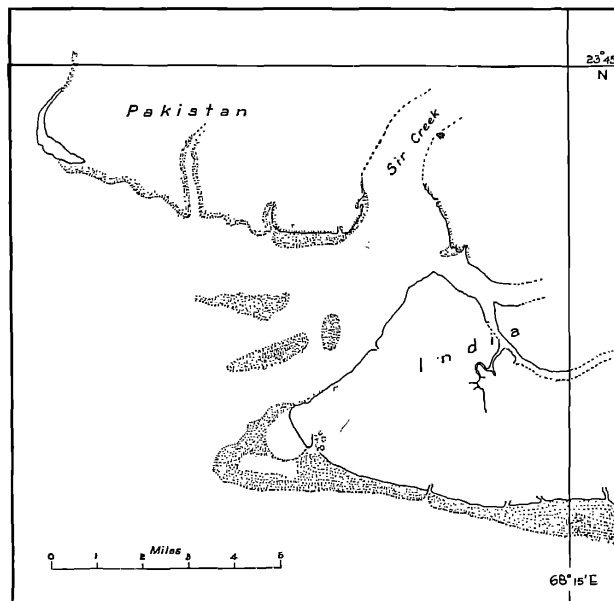
MAP NO. 29

The Sundarbans (Hariabhanga and Raimangal Rivers)



MAP NO. 30

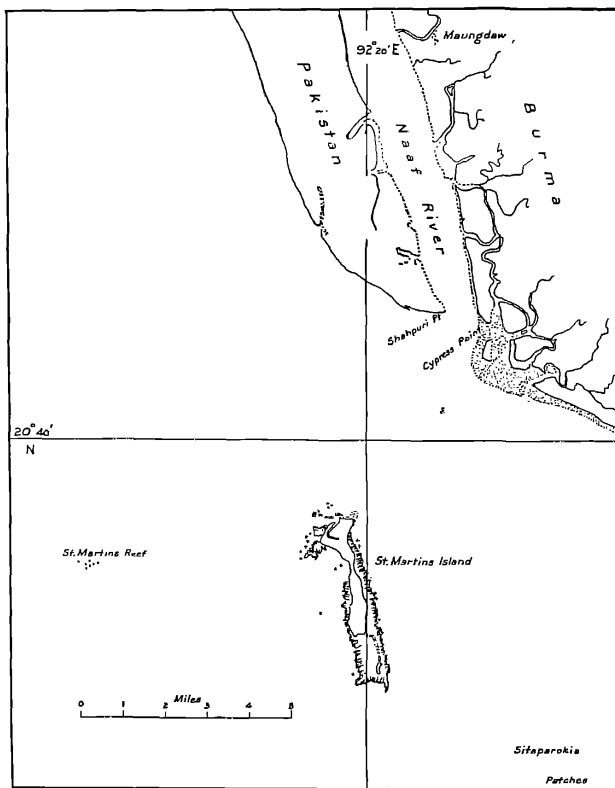
Sir Creek



Silt and sand banks covered at high tide

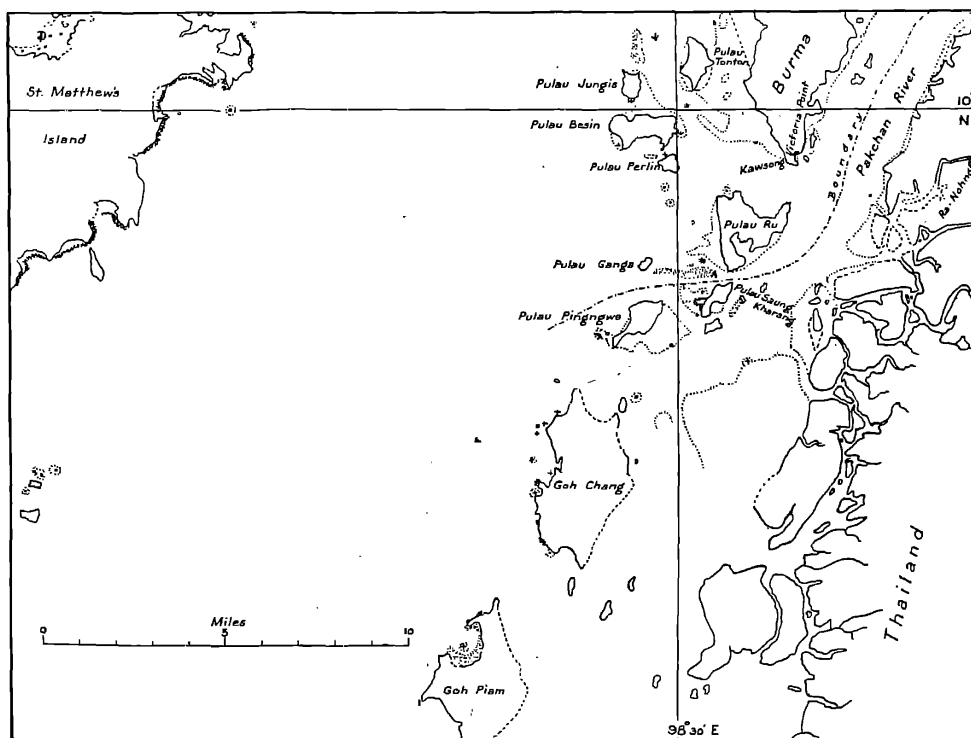
MAP NO. 31

Naaf River



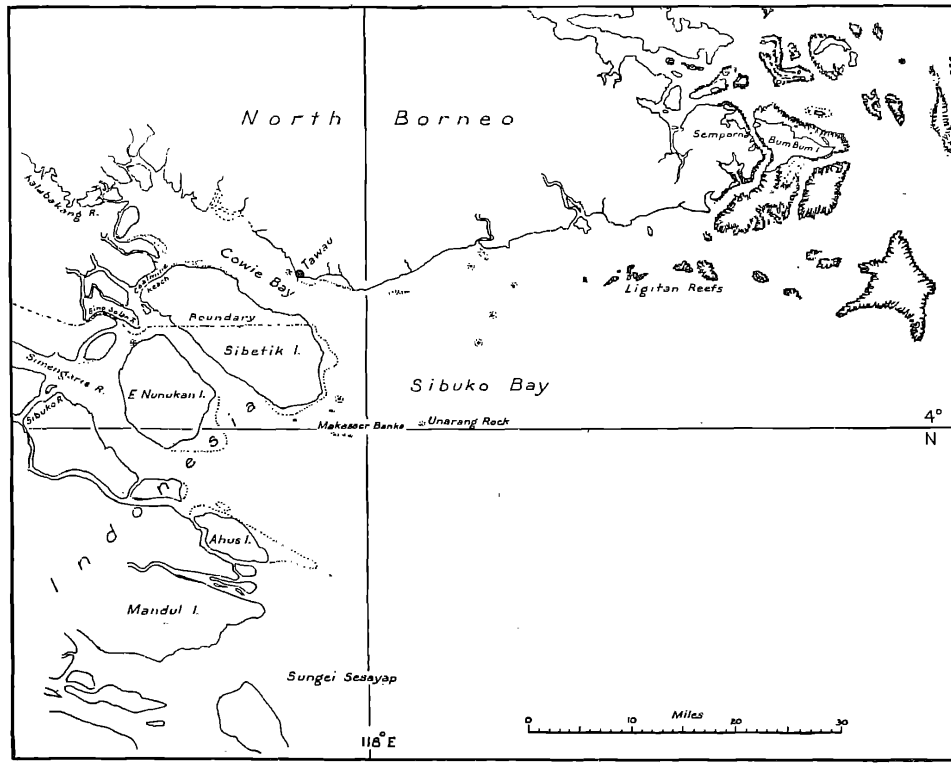
MAP NO. 32

Estuary of Pakchan River



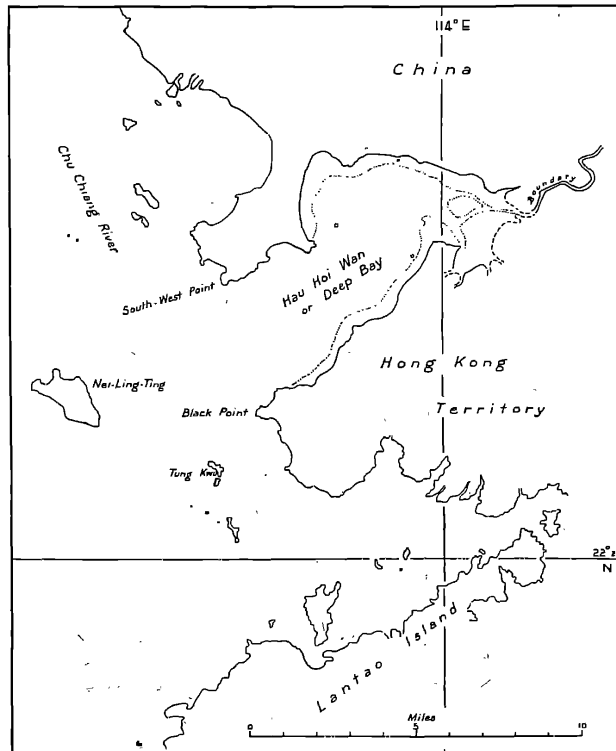
MAP NO. 33

Sibuko Bay

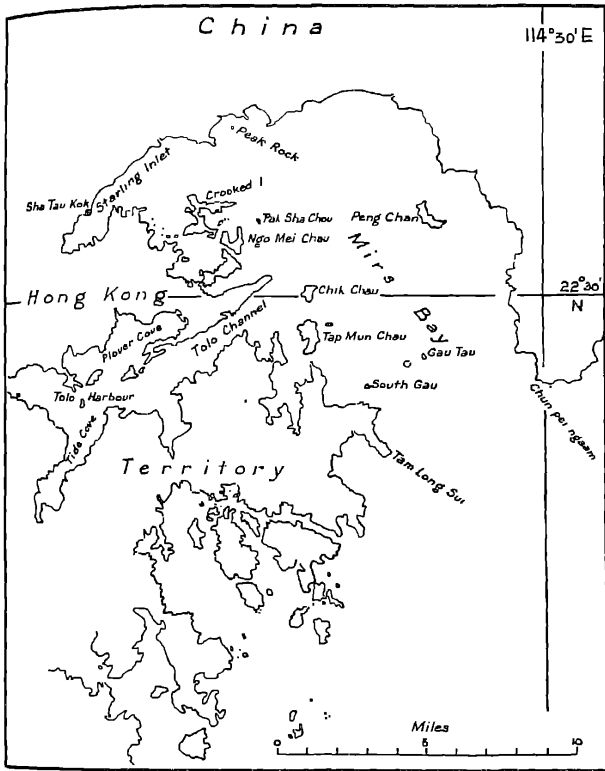


MAP NO. 34

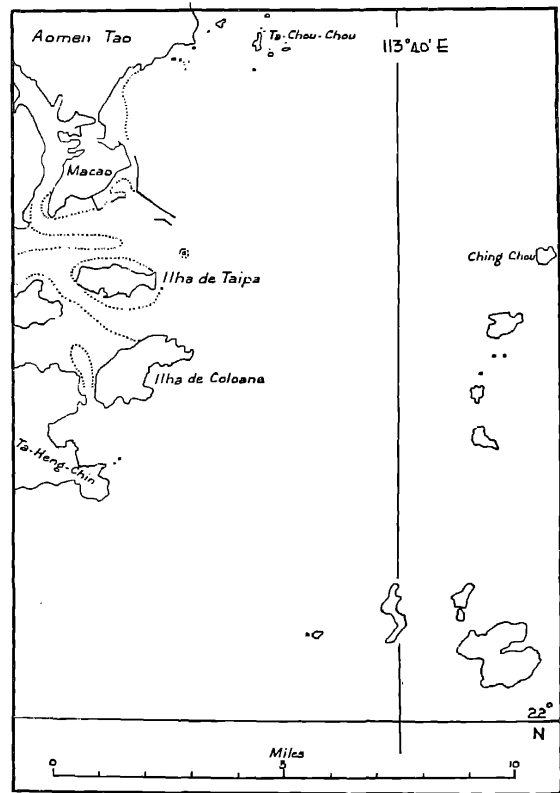
Hong Kong - Deep Bay



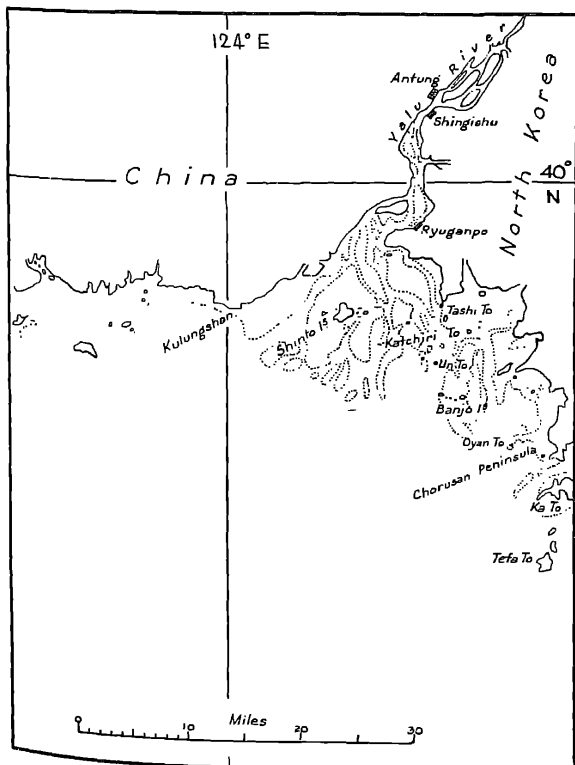
MAP NO. 35
Hong Kong - Mirs Bay



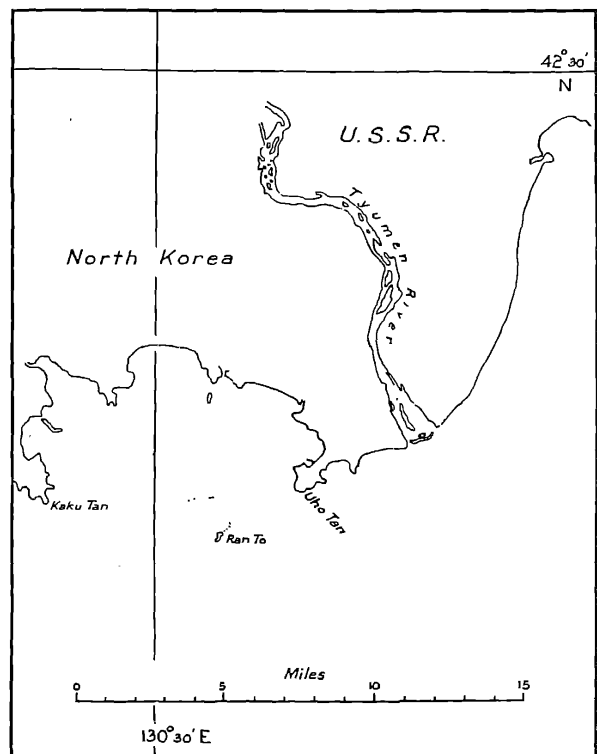
MAP NO. 36
Macao Area



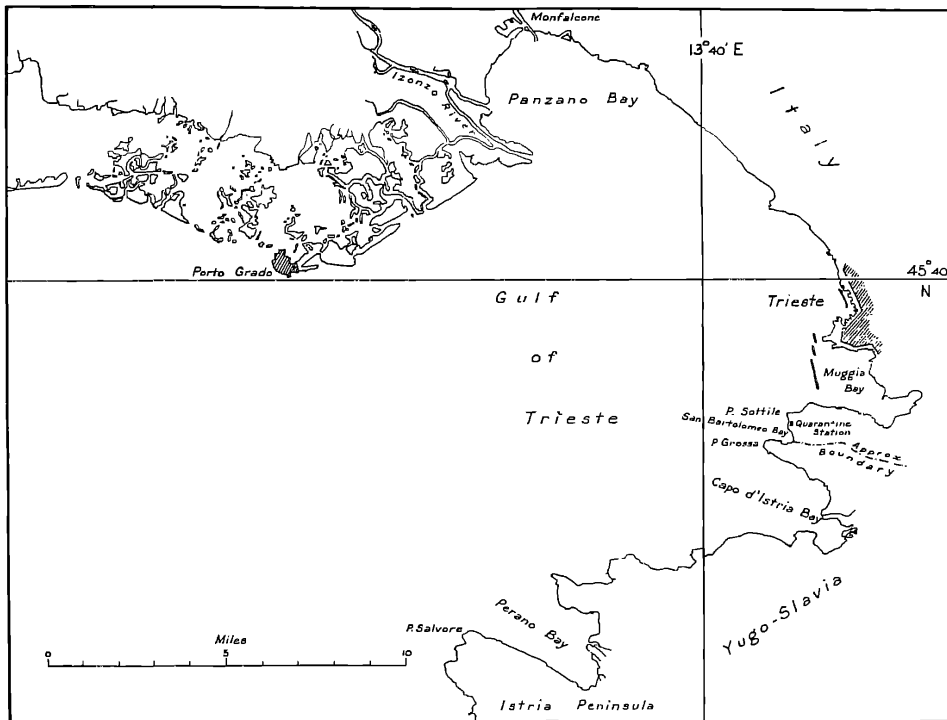
MAP NO. 37
Yalu River



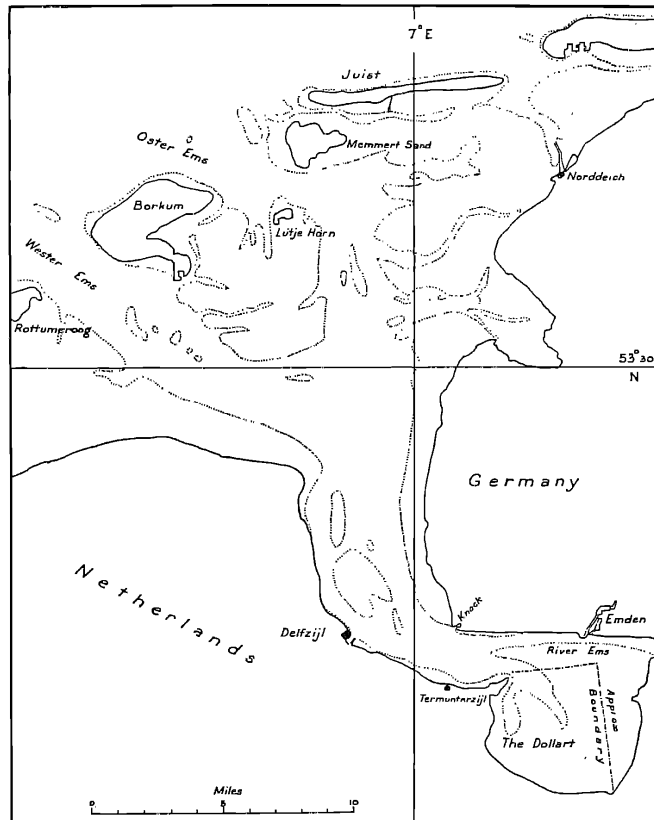
MAP NO. 38
Tyumen River



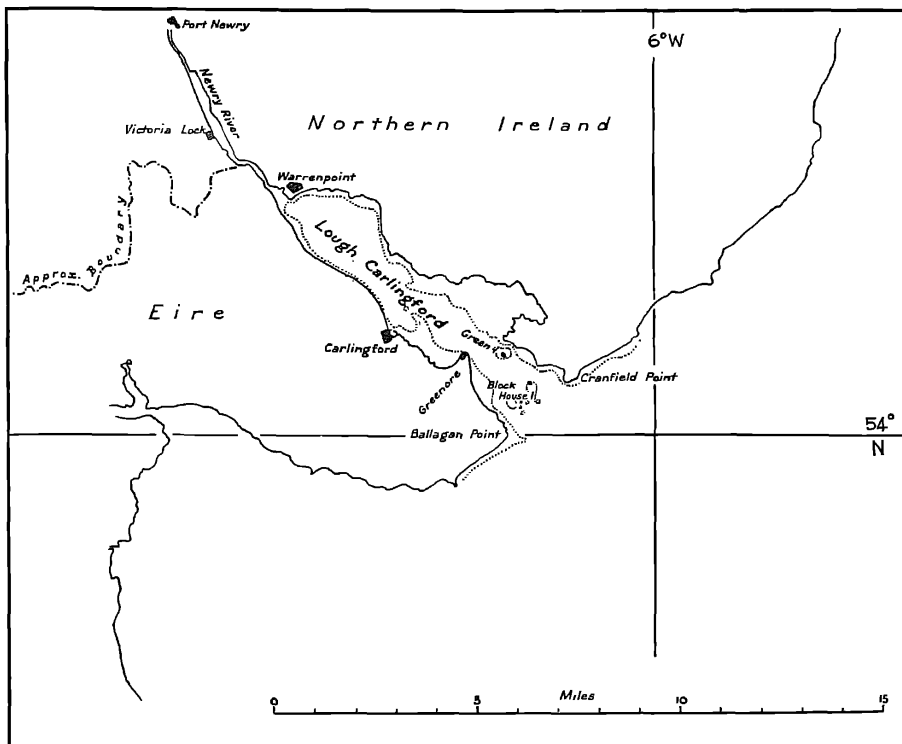
MAP No. 39
Gulf of Trieste



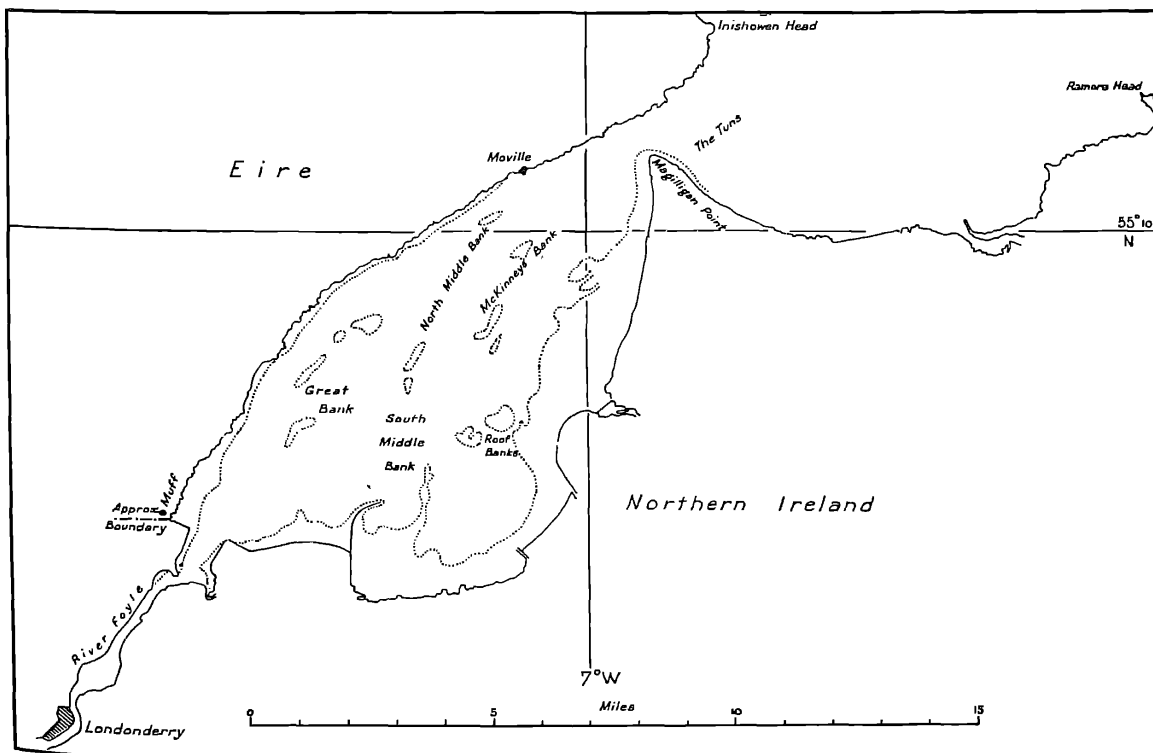
MAP No. 40
Ems and Dollart



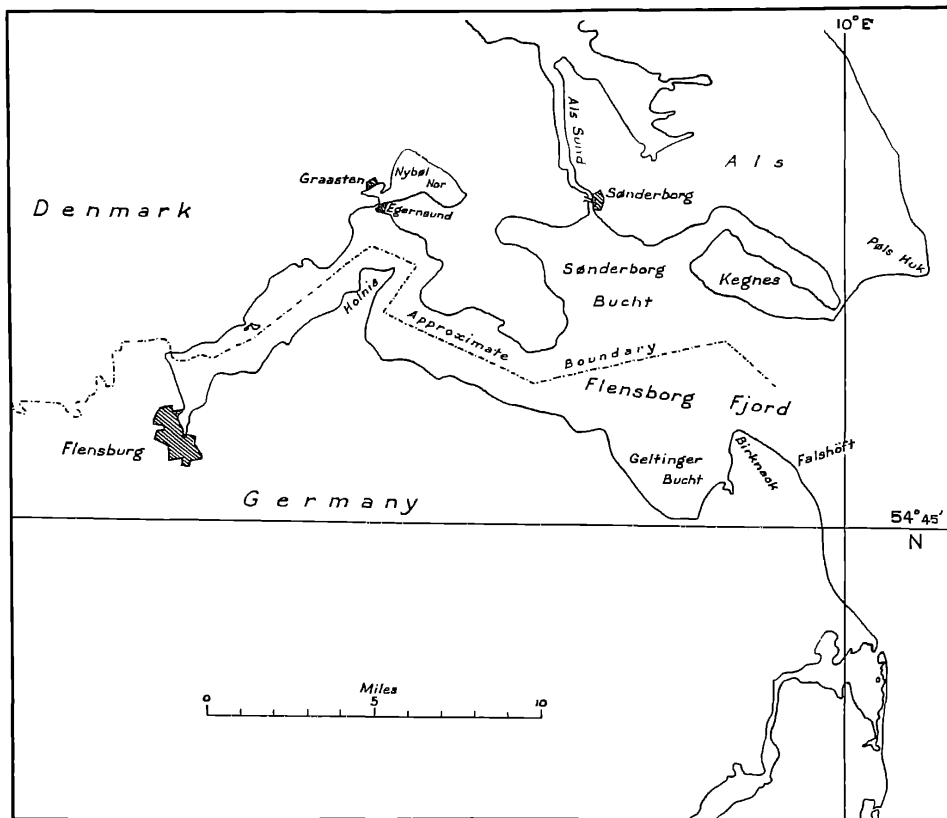
MAP NO. 41
Lough Carlingford



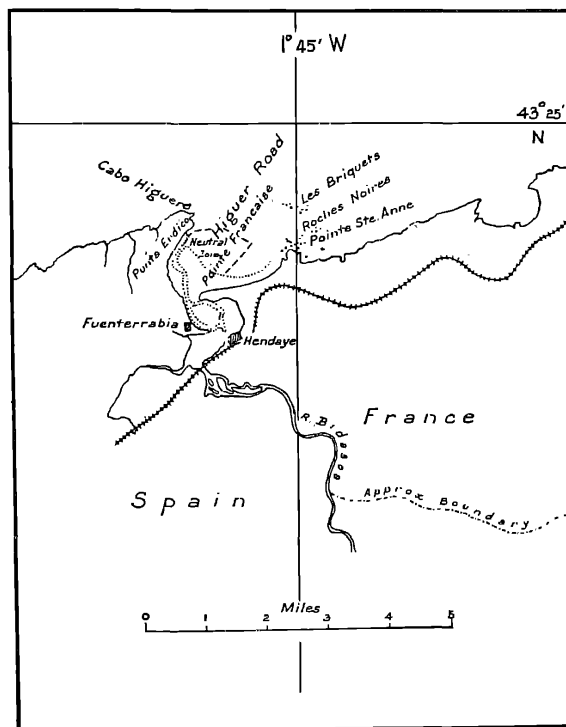
MAP NO. 42
Lough Foyle



MAP NO. 43
Flensburg Fjord

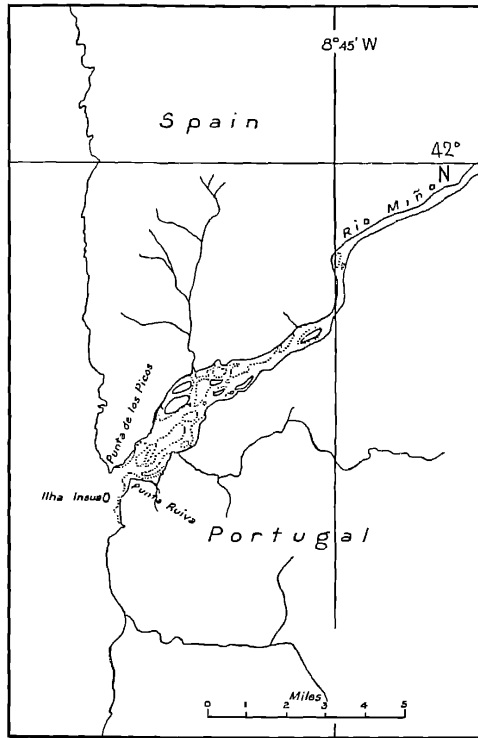


MAP NO. 44
Bidasoa River



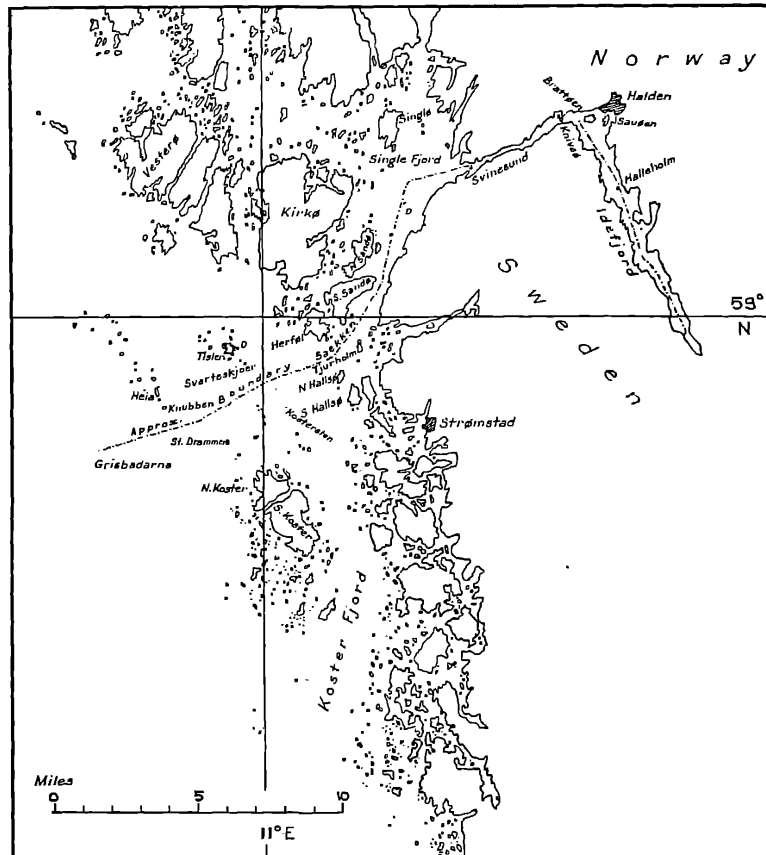
MAP No. 45

River Miño

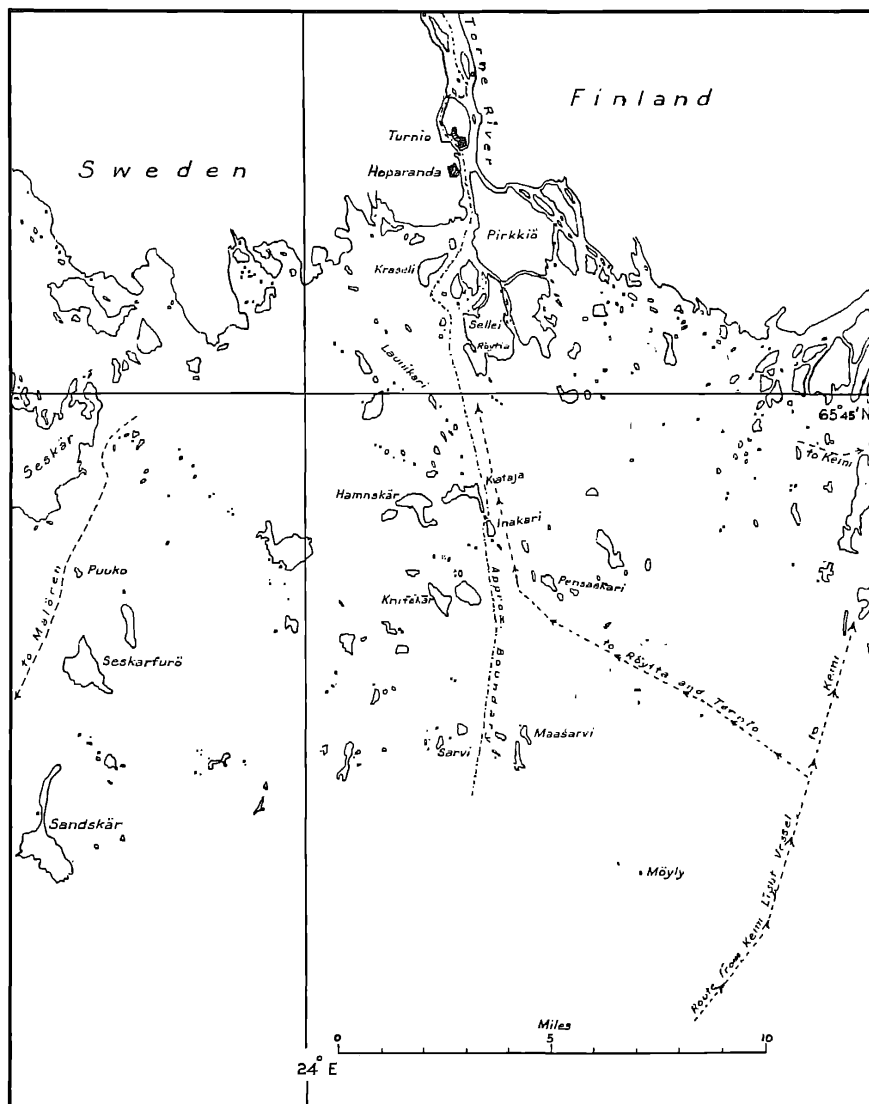


MAP No. 46

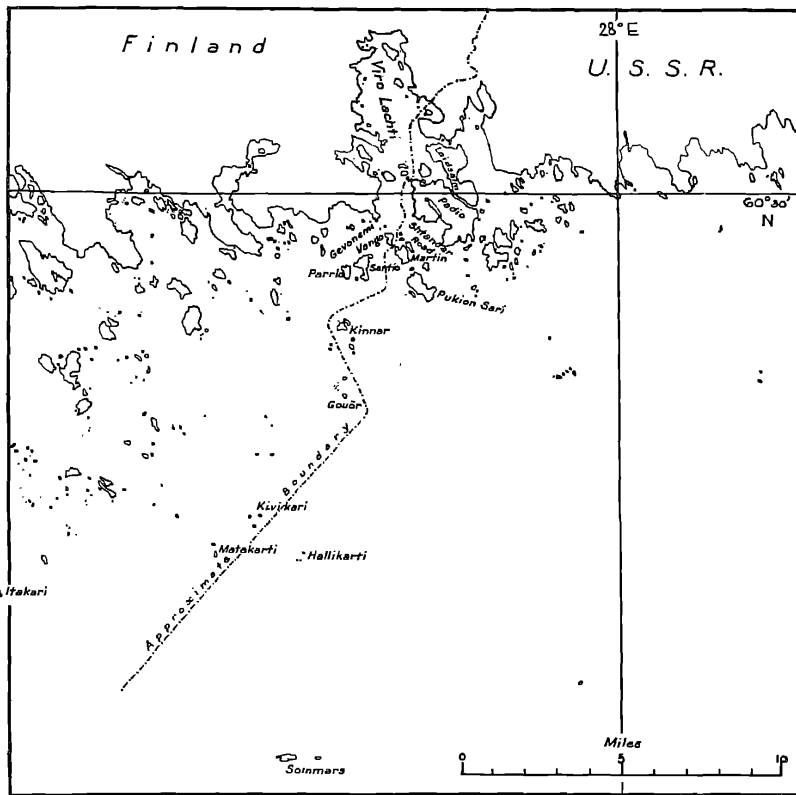
Idefjord



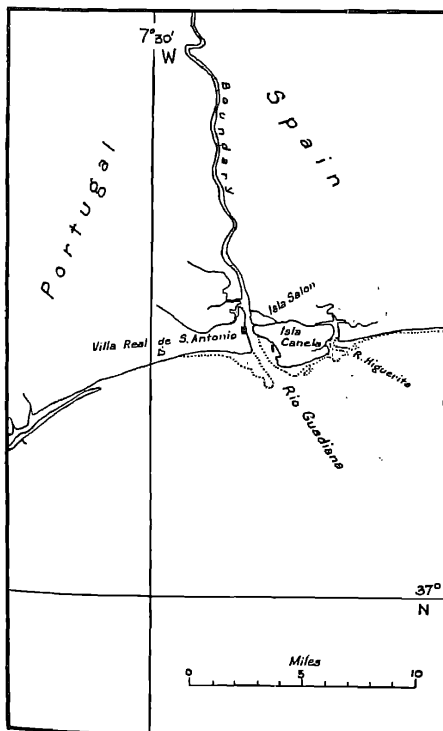
MAP NO. 47
Head of Bottenviken



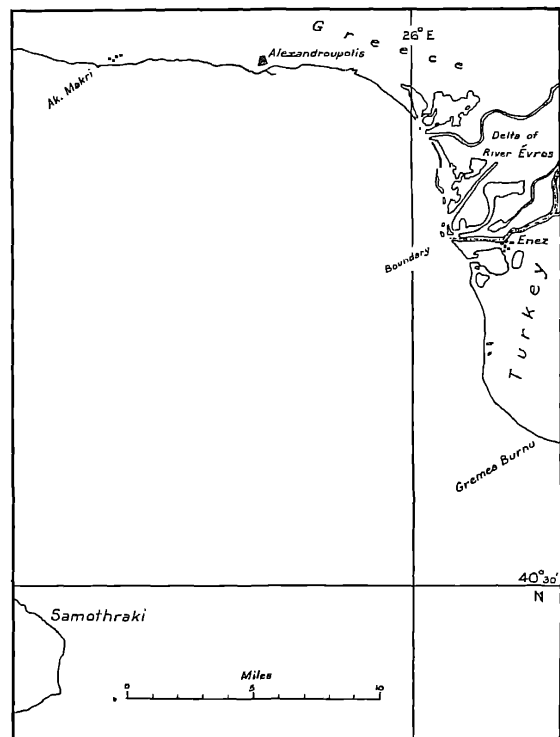
MAP No. 48
Viro Lachti Area



MAP No. 49
River Guadiana



MAP No. 50
River Evros



Annex RJ-4

F. Blasco, E. Janodet and M.F. Bellan, "Natural Hazards and Mangroves in the Bay of Bengal", *Journal of Coastal Research Special Issue No. 12: Coastal Hazards*, 1994, pp. 277-288.

Natural Hazards and Mangroves in the Bay of Bengal

F. Blasco, E. Janodet and M.F. Bellan

Institute for the International Map of the Vegetation, Université Paul Sabatier - CNRS,
39, Allées Jules Guesde, 31062 Toulouse Cedex, France

ABSTRACT: Mangroves are commonly found in the intertidal zone of tropical and subtropical sheltered coastlines. They are not affected by forest fires, but about 50% (50,000 km²) of their total areal extent, particularly in Asia, Australia, Madagascar and the Caribbean, are potentially exposed to tropical cyclones, typhoons and hurricanes.

In the mangroves of India and Bangladesh, especially at the mouth of the Ganges, the threat from strong winds, surges driven by storm waves and floods, is one of the most deadly in the world. Paradoxically this mangrove area, known as "The Sunderbans," bears the largest natural mangroves of the world in a single block (about 6,050 km², *i.e.*, 2,000 km² in India and 4,050 km² in Bangladesh).

Emphasis in this paper is on the impacts of windstorms in the mangroves of the Bay of Bengal, deduced from field observations and satellite image analysis, including forest destructions and forest alterations like defoliation. The final result of our analysis is that mangrove species are able, in this part of the world, to heal cyclonic wounds and maintain their total areal extent constant in the absence of human interference.

INTRODUCTION

The total areal extent of mangroves around the world is not accurately known. It probably oscillates between 80,000 and 100,000 km² (SAENGER *et al.*, 1983). Nearly 50% of these forest communities are periodically affected by spectacular windstorms accompanied by heavy rains such as cyclonic storms (Bay of Bengal, Southern Pacific), hurricanes (Caribbean, Gulf of Mexico), and typhoons (Far East). They are also influenced by entirely different natural hazards such as tectonic movements (Ganges), over-sedimentation and rapid coastal erosion (The Guayanas, Southern Madagascar), fluctuating water and soil salinity (West African coastal lagunes) and long periods of constant flooding.

These ecosystems have formed since the beginning of the Tertiary (lower Miocene). They are able to withstand most adverse environmental conditions such as muddy soils with high salt and water content, destructive tidal effects and redoubtable windstorms crossing flat areas on which the mangroves (shallow-rooted species, thriving on unstable substrate) grow.

Since the beginning of this century, mangrove regression is mainly due to their conversion to agriculture and to the diversion of fresh water. Since the 1950's, the development of aquaculture has led to massive mangrove destruction, particularly in the Indo-Pacific region where at least 1.5 million hectares of coastal forests have been converted to aquaculture.

Using field observations and satellite images analysis, we have observed how woody mangrove species survive catastrophic events such as cyclones in the Bay of Bengal. We have also observed how certain species appear to take advantage of these natural disturbances to activate their normal dynamic processes of cicatrization and territorial

expansion in coastal areas. *An analysis of digital SPOT data at four dates (1987, 1988 and 1989) after moderate and severe cyclones confirms that forest damage is usually concentrated in a limited fraction of the total mangrove forest.*

METHODS AND BASIC FIELD DATA

This study is centered on the Sunderbans at the top of the Bay of Bengal. Other mangrove types located elsewhere around the Bay of Bengal are less affected by cyclones and have almost the same floristic components. The mangroves on the latter sites provide basic data for comparison.

The method adopted for the Sunderbans analyses was field observations and satellite digital image before and after cyclones of different intensities (from moderate to highly destructive events). The method employed for the processing of the images is described in the section "Remote sensing applied to mangroves." Field observations, for security reasons, are almost impossible in the Sunderbans during the rainy season, April to November. Our comments concerning these mangroves are based on data collected during the dry season (February) and from satellite data recorded on 7th November 1987 and 26th October 1988, after moderate and severe cyclones. Elsewhere, coastal field studies are much easier throughout the year. Detailed descriptions and ecological analysis of the mangroves of India and Bangladesh have been given by CURTIS (1933), BLASCO (1977), UNTAWALE (1984), CHAUDHURY (1989) and DAGAR *et al.* (1991). *Data concerning the impacts of cyclones and floods on mangrove ecosystems are almost non-existent.*

As shown in Figures 1 and 2 and Tables 1 and 2, the mangroves of the area have a total extent of about 11,065 km², of which about 77% is located in the Bay of Bengal

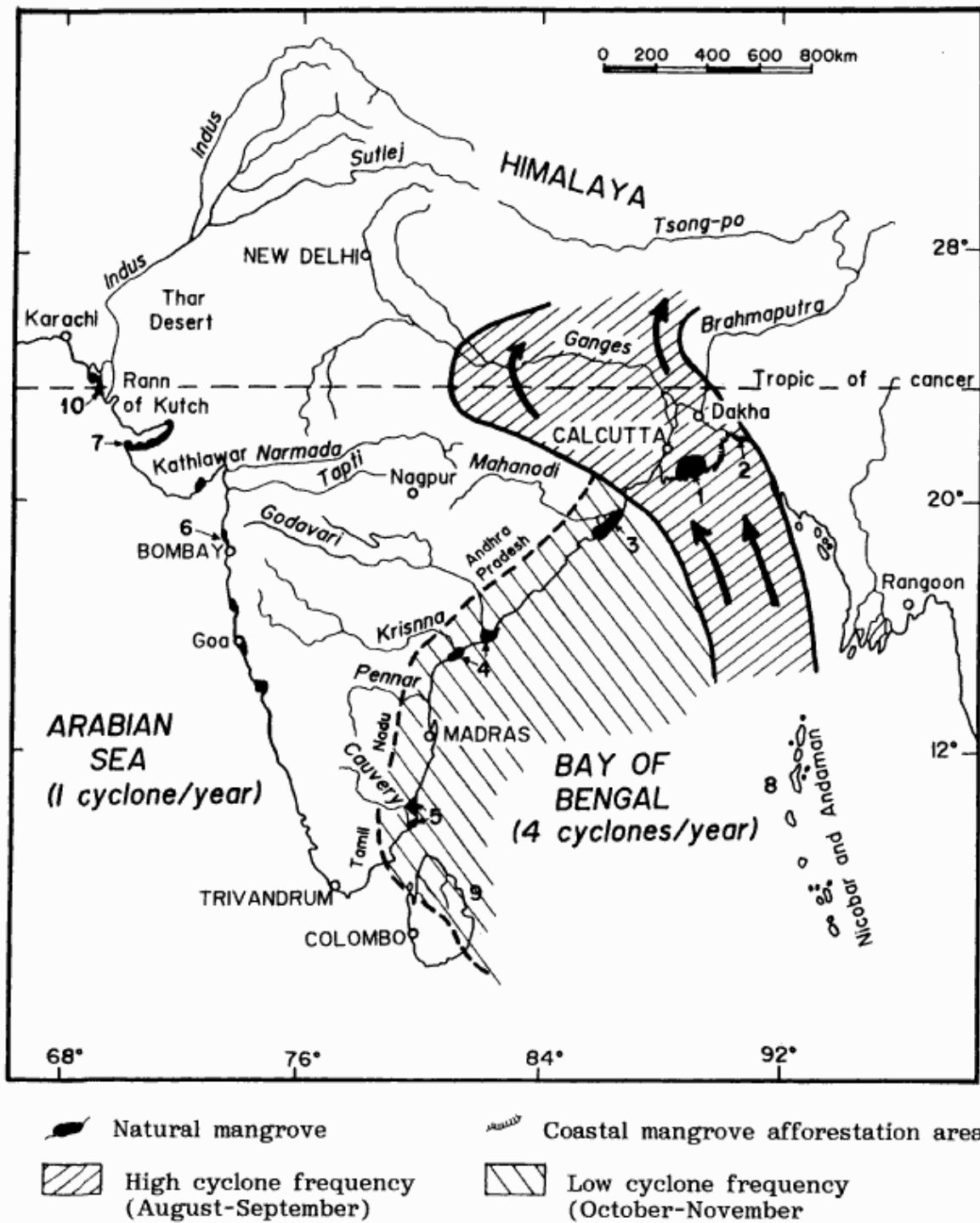


Figure 1. Cyclonic tracks in the Bay of Bengal and location of mangroves (figures refer to Table 1).

where cyclonic storms are frequent and often disastrous. From 1891 to 1970, 363 cyclones, among which 133 were of a severe nature, were recorded in the Bay of Bengal in contrast to 98 in the Arabian Sea (Table 2). The mangroves of the Bay of Bengal belong to two main categories: those

that are located in the Sunderbans, at the top of the Bay of Bengal in India and Bangladesh (7,550 km²), which are directly and frequently hit by tropical cyclones; and those that are protected in deeply indented coastlines (Andaman and Nicobar, roughly 780 km² of mangroves) or in creeks

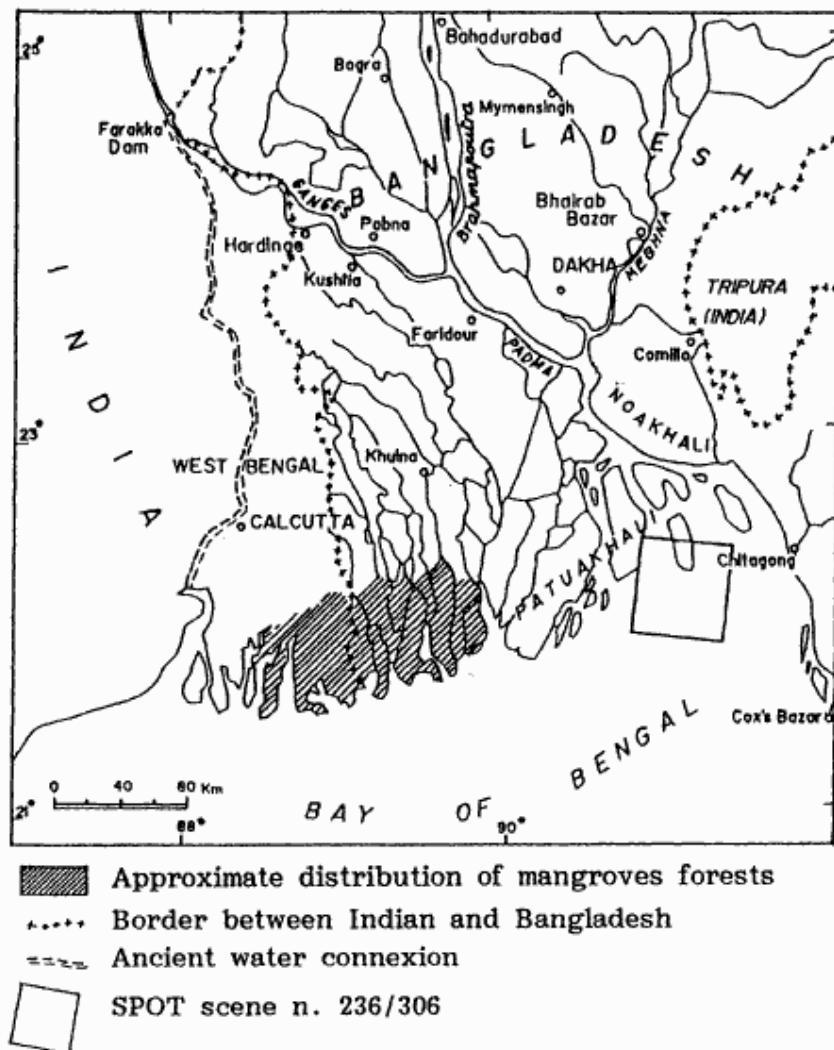


Figure 2. Location of the Sunderbans (India and Bangladesh).

and bays along the eastern Indian Coast and in Sri Lanka (about 200 km² of mangroves), which are less exposed to cyclones.

Universal features of mangroves are as follows: (1) limited number of species (about 60 woody species around the world), (2) reduced number of strata, (3) reduced size of many woody species, (4) the relatively small size of leaves, and (5) absence or rarity of vascular epiphytes. These characteristics are found in both cyclone-prone and cyclone-free forests. The simple floristics and architectures are primarily related to very selective soil conditions.

In the Sunderbans and other areas where cyclones are frequent and violent, the zonation may be considerably disturbed and many trees may have multidirectional inclinations. In addition, the trees on sea face are often smaller than inland. Cyclonic storms affecting these mangroves influence their structure and morphology. These relationships are also recognized for the mangroves of the Antilla,

often affected by cyclones, in contrast to those of the Guyanas (LESCURE and TOSTAIN, 1989). The spatial evolution of mangroves is also influenced by other physical parameters. In the Ganges, spatial relationships are strongly related to site factors. For example, soils and rivers are less saline in the eastern part (15 to 20‰) than in the western part (28 to 32‰). Consequently the size of the forest evolves from about 15–20 m in height in the east (*Heritiera fomes* Buch-Ham.) to 3–7 m in the west (*Excoecaria agallocha* L.).

In addition to these complex and little known effects of cyclones, conspicuous damage is observed after each catclysm. The damage can be classified into two causal categories, mangrove destructions and forest alterations. Forest destruction, including forest gaps and bank erosion, alters the long-term dynamics of the forest processes. However, mangrove alterations, like defoliation, lead only to temporary and superficial damage.

Table 1. Main mangrove areas in The Bay of Bengal and Arabian Sea (see Figure 1).

Bangladesh	1(a)	Sunderbans	4,050 km ²
	2	Mangrove afforestation	1,500 km ²
India	1(b)	Sunderbans	2,000 km ²
	3	Orissa	50 km ²
	4	Andhra Pradesh	100 km ²
	5	Tamil Nadu	15 km ²
	6	Maharashtra + Goa	20 km ²
	7	Gujarat	20 km ²
	8	Andaman and Nicobar	780 km ²
Sri Lanka	9		35 km ²
Pakistan	10		2,495 km ²
			11,065 km ²

RESULTS

Forest Gaps, Mass Mortality and Forest Alteration

Wind Damage

During the most severe cyclonic storms (16th and 17th October 1909, 24th September 1919, 10th May 1961, 20th August 1987, and 6th September 1988) when the speed of wind reached about 200 km/hr followed by downpours of more than 200 mm in 24 hours, the mangroves of the Sunderbans were very heavily damaged. This was particularly true in parts of the Khulna district in Bangladesh (CHOUDHURY, 1962). Large areas of up to 50,000 hectares were either toppled or structurally damaged with broken tree tops and branches. This extensive and spectacular damage also occurred in other parts of the world. CINTRON and SCHAEFFER-NOVELLI (1983) reported that, in the Caribbean, wind speeds reaching 95 km/hr caused defoliation and winds exceeding 130–160 km/hr brought down trees.

The relation between the forest structure and its sensitivity to wind damage is difficult to assess. In the Caribbean, small trees are usually more resistant than taller stands (PAGNEY and BENITO-ESPINAL, 1991). The *Avicennia*, with a very shallow root system, seem to be especially sensitive to windthrow. On the contrary, *Rhizophora* are more resistant to violent winds because of their dense stilt-root systems, but regeneration is usually slower (STODDART, 1971, 1974).

Table 2. Frequency of tropical cyclones monthwise over Bay of Bengal and Arabian Sea—period 1891–1970 (KOTESWARAM, 1984). (Figures in parentheses are severe cyclones.)

Months	Bay of Bengal	Arabian Sea
January	5 (1)	2
February	1 (1)	0
March	4 (2)	0
April	19 (8)	5 (4)
May	39 (26)	16 (13)
June	35 (4)	15 (10)
July	38 (7)	3
August	26 (1)	2
September	32 (10)	5 (1)
October	62 (26)	20 (7)
November	68 (33)	25 (19)
December	34 (14)	5 (1)
Total	363 (133)	98 (55)

One of the most striking floristic peculiarities of the Sunderbans, the largest mangroves in the world, is the rarity of *Rhizophora*, whereas *R. apiculata* Bl. and *R. mucronata* Lamk. are usually very conspicuous and almost omnipresent in the mangroves of Asia, from Bombay to Malaysia, Thailand, Mekong, etc. This rarity of *Rhizophora* representatives in the Sunderbans and the high frequency of severe cyclones in this area is an unexplained coincidence. Little damage was observed in recently thinned areas. It is noteworthy that afforested mangrove areas (*Sonneratia apetala* Buch. Ham.) in most exposed coastal zones (Figure 3) successfully resist the combined actions of storms and tidal waves (BLASCO *et al.*, 1992). This may be related to the small size of the stands observed in Gadeloupe after cyclone Hugo (PAGNEY and BENITO-ESPINAL, 1991).

Over-Sedimentation and Environmental Effects

Southward, in much dryer coastal lagunes of the Tamil Nadu State (see Figure 1) where the frequency of cyclones is less, dying mangrove stands have been observed after storms. There are several causes, the most common being the modification of the hydric regime. Just as damming and fresh water diversion destroy thousands of hectares of mangrove, primarily in dry areas (Andhra Pradesh and Tamil Nadu), several cases of spectacular mangrove mortality have been observed after cyclones.

The mortality involves small gaps to practically all species inside a coastal lagune (Figure 4). Explanations vary little. Strong waves and winds can create in only a few hours sandy bars and sea-grass accumulations that form dykes at the entrance of coastal lagunes. In addition, tremendous volumes of sediments are deposited by continental rains (e.g., up to 390 mm in 24 hr in Sri Lanka) that disturb or hamper free circulation of water. *The daily tidal effect essential for mangrove survival declines or ceases, leading to mass mortalities of trees.* This was reported in North Florida Bay after Hurricane Donna (TABB and JONES, 1962; CRAIGHEAD and GILBERT, 1962; CRAIGHEAD, 1964).

Clay deposition over pneumatophores impairs gaseous exchanges, leading to rapid defoliation and widespread mortality. Moribund trees in the Bay of Bengal, generally belonging to *Avicennia officinalis* L. and *A. marina* Vierh., may survive for a few months, but the aerenchyma of their pneumatophores is rapidly attacked by microorganisms. Trees decline progressively and their recovery becomes impossible. The forest is replaced by a shrubby stand of halophytes, among which *Suaeda maritima* (L.) Dum and *S. monoica* Forsk. or *Acanthus ilicifolius* L. become conspicuous. In areas where the evapotranspiration is exceptionally high, there is a gradual soil compaction, creating localized depressions (salt swamps, see Figure 4) which are almost asylvatic. If a subsequent cyclone removes these dykes, allowing renewed tidal penetration and the deposition of fresh sediments accompanied by soil aeration during low tides, a new forest stand can replace these almost barren depressions; the new stands are dense (*Excoecaria agallocha* L. on sandy soils), even-aged and practically monospecific. If the lagoon is filled up with sediments, the mangrove will be definitely replaced by glycophytes or by crops.

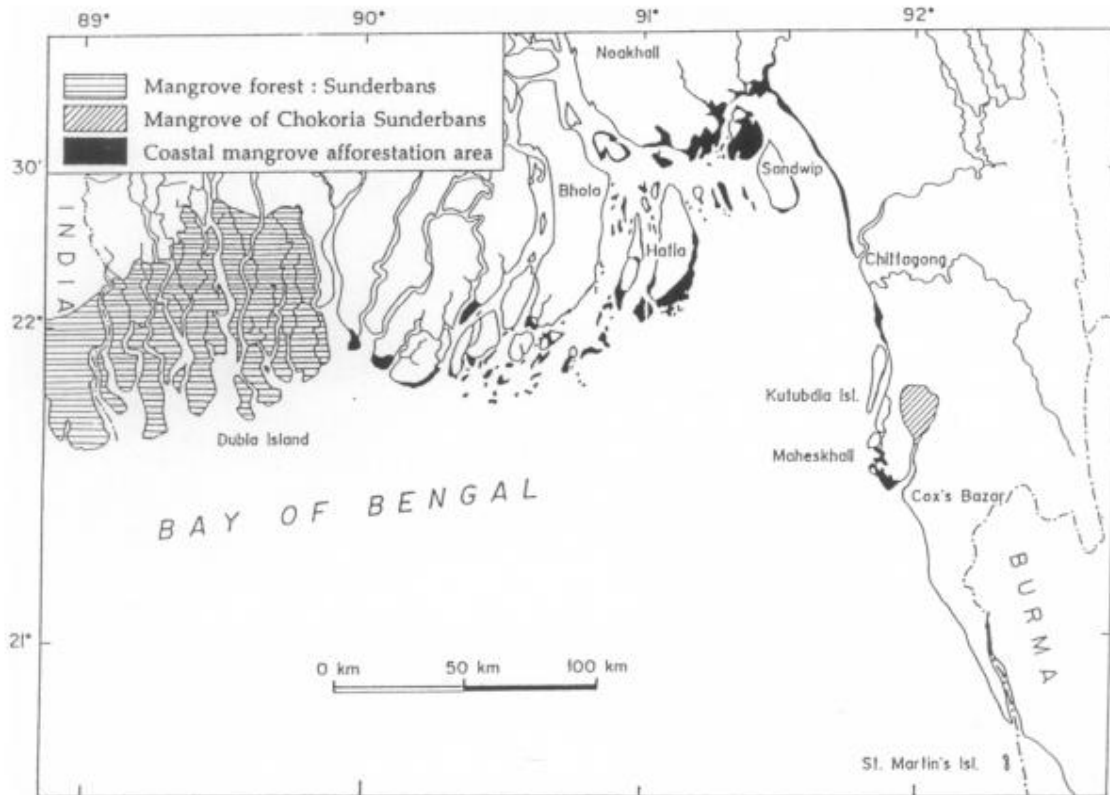


Figure 3. The extension of coastal areas, showing planted mangroves (from CHAUDHURY, 1989). They perfectly resist storms and tidal waves.

Erosive Factors

Erosion and accretion along the muddy river banks of the Sunderbans (where the width of main rivers varies from 2 to 6 km and the tidal amplitude averages about 3 to 5 meters) are part of continuous and normal processes that are suddenly accelerated during the cyclonic storms. The most conspicuous pioneering plant community of the river banks includes two palms, *Nypa fruticans* Wurmb. and *Phoenix paludosa* Roxb., with shrubby communities belonging to the *Avicennia* group mixed with *Ceriops tagal* (Perr.) Robins, *Excoecaria agallocha* L., etc. Uprooted and scattered scrubs and trees sink into river beds and disappear. The usual mechanisms along the sea face as well as on river banks cause a progressive deterioration of the substrate by the scouring of waves. The stability of sediments seems to be much greater in the mangrove forests of the Sunderbans than in the eastern part of the Delta along the deforested water course of the Ganges.

During a cyclonic storm, erosive processes are accentuated and accelerated. Fringing vegetation is washed away with the soft sediments, and there is no visible local forest damage. The river bank or the coastal line simply recedes for a few meters, usually less than 20 m. Our present mapping accuracy does not allow for fine-scaled monitoring of these coastal or river bank modifications because of the technical limitations, both geometric and temporal, of the existing satellite tools.

This accelerated bank erosion is compensated by newly accreted muddy or sandy deposits, elsewhere along river banks and coastal zones. The origins of these deposits are not properly documented. The greatest part of them seem to be of continental origin. According to CHAUDHURY (1989), the annual estimated total volume of sediments carried in suspension by the Ganges, the Brahmaputra and the Meghna Rivers is 2.5 billion metric tons. The greatest part is exported offshore. Over the period of 1972–1979, 1,157 km² of new land was created in southern Bangladesh. Soft loamy sediments are primarily and spontaneously consolidated by a wild salt tolerant rice, *Porteresia coarctata* (Roxb.) Takeoka, or by fast growing scrubs such as *Phoenix paludosa*, *Sonneratia apetala*, and *Excoecaria agallocha*. After three or four years, the resulting plant community is often a dense and narrow shrubland permanently threatened by currents and strong wave energy.

Defoliation by Cyclonic Storms

With the exception of *Excoecaria agallocha* L., which may be deciduous in some localities, all mangrove trees and shrubs are evergreen even along arid coastlines. In the case of the mangroves of Andaman and Nicobar (roughly 780 km²), located in the Bay of Bengal, the average litter production (7 to 11 tons·year⁻¹·hectare⁻¹) peaks during the windy seasons, August to October (DAGAR *et al.*, 1991). However, the average annual litter production in the man-

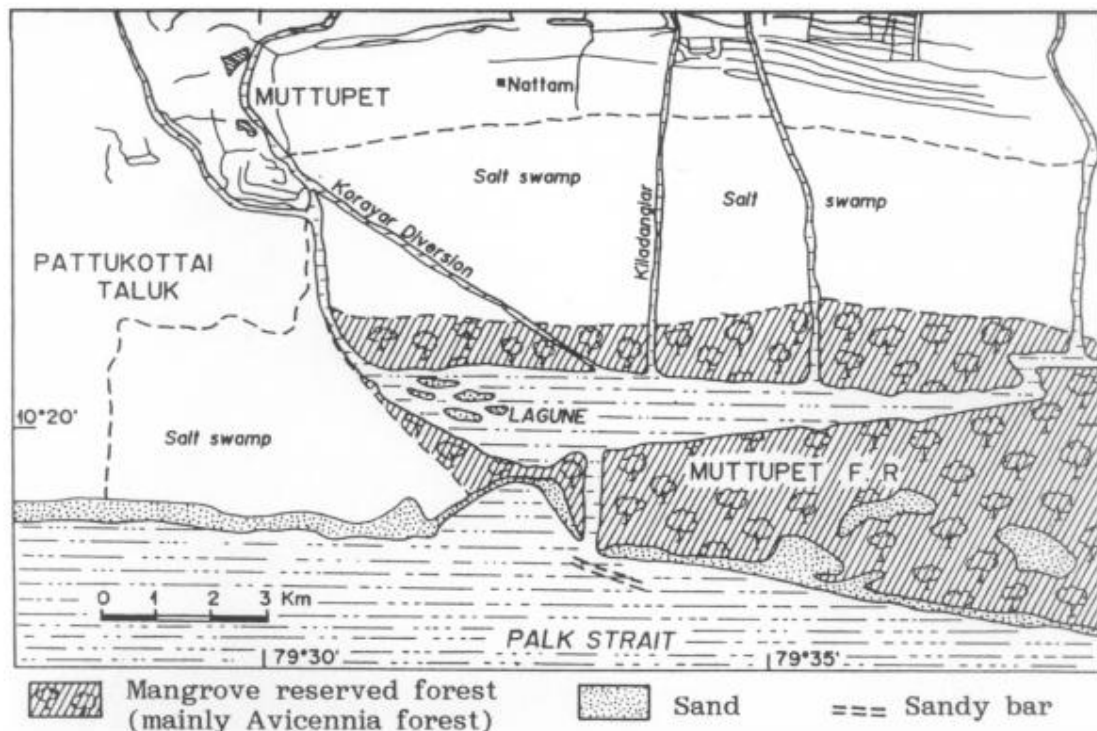


Figure 4. Regression of mangroves in coastal lagunes (see n. 5, Figure 1). This mangrove has been almost entirely destroyed by a cyclone in 1973 (Blasco, 1975). Salt swamps progressively replace forest stands.

groves of Andaman, where the flora has diversified to about 30 woody species, is similar to the annual values measured elsewhere. This is particularly true in the Caribbean where the flora is extremely simplified, 2 to 4 species (LUGO and SNEDAKER, 1974), and in the South Pacific (WOODROPPE and MOSS, 1984). Strong drying windstorms may defoliate large mangrove stretches in a few hours. In most cases, the majority of trees and shrubs are able to recover. This fact has also been observed in Florida after Hurricane Betsy (TAYLOR, 1967).

The activity of apical meristems of leafless branches seems to be stimulated, presumably because the heavy rains accompanying each cyclone dilute the sodium chloride in the topsoil. This lowering of the salinity induces a post cyclonic vitality. The stands usually recover their normal appearance in less than four months. The exact role of strong winds, and consecutive changes in salt concentrations, in influencing aspects of seed production of mangrove species is not well documented. Most mangrove seedlings float on brackish waters and there is a profound redistribution of germinating seeds throughout the forest during and after cyclonic storms. The numerous seedlings in the understory benefit from a greater amount of light intensity reaching the soil during the few weeks when the canopy is partly defoliated. Seedlings take this opportunity to accelerate their growth and develop strength until the older trees foliate.

These intermittent deciduous "phases" of mangrove trees, in areas with frequent and severe cyclones, and the con-

secutive phenological reactions, including the flowering of species, have not been studied. Presumably, cyclonic storms should be considered as one of the natural parameters, such as the aridity or soil salinity. These factors require additional research as they episodically play unknown roles in the biological rhythms of constitutive species.

Remote Sensing Applied to Mangrove Studies

Many studies are now available throughout the world concerning the use of Landsat TM or SPOT data for coastal studies. The mangroves of the Sunderbans have been recently studied with SPOT (CHAUDHURY, 1989), and an analysis of floods in Bangladesh through remote sensing data has been published (BLASCO *et al.*, 1992). The main input of the present contribution is to have a preliminary perception of mangroves with weather satellites (NOAA series) and to try to apply high resolution remote sensing technology to assess cyclonic damage.

NOAA AVHRR LAC Data for Mangrove Studies

The use of LAC (Local Area Coverage) from NOAA AVHRR (Advanced Very High Resolution Radiometer), acquired daily at 1.1 km of off-nadir resolution, has not yet been investigated for mangrove studies. The sizes of these landscape units are usually too small for the resolution of sensors. In large continental forest areas, such as the Amazon and Central Africa, channels 1 (visible, 0.58–0.68 μm) and 2 (near infrared, 0.725–1.1 μm) of this satellite

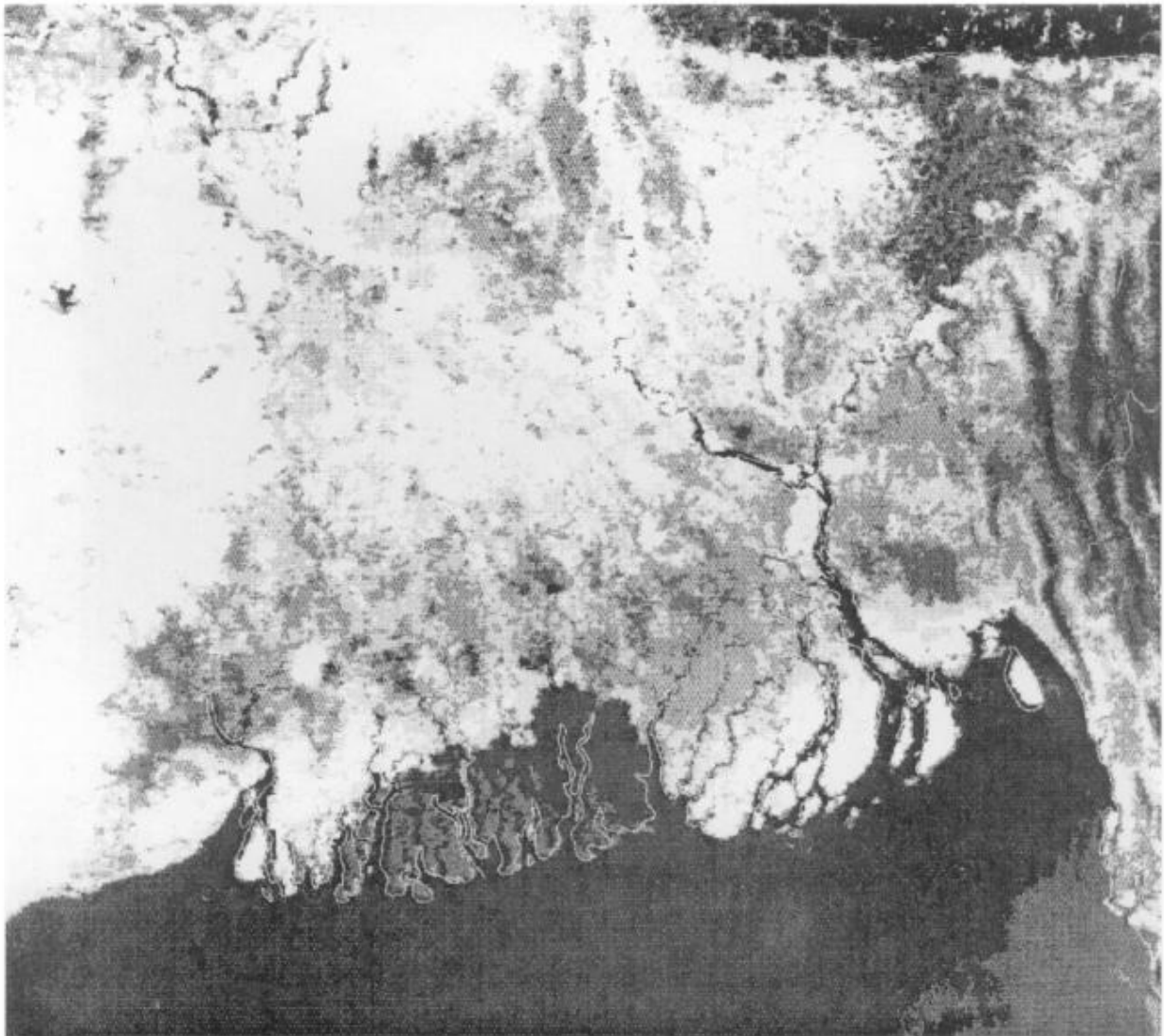


Photo 1. Black and white print of false color composite of NOAA AVHRR LAC channels 3, 2 and 1 over the Sunderbans (17th February 1991). NOAA AVHRR can be used for mangrove monitoring in the Sunderbans. This document is just an illustration of the potential capabilities of the instrument.

provide information about the biomass and the photosynthetic activity of the vegetation, generally studied using vegetation indices. Channel 3 ($3.55\text{--}3.95\ \mu\text{m}$) covers both reflection and emission domains of thermal infrared and is rather difficult to interpret. It seems, however, correlated with the hydrological conditions and functioning of the vegetation, like thermal infrared channels 4 ($10.5\text{--}11.3\ \mu\text{m}$) and 5 ($12.5\text{--}13.5\ \mu\text{m}$) which will not be examined here.

On the Sunderbans, the high frequency of the daily observations with NOAA could provide interesting results for discussion. Photo 1 shows a LAC-AVHRR image (channels 3, 1 and 2) over Bangladesh, acquired on 17th February 1991, on which the mangrove forests of the Sunderbans are clearly discriminated in green on the coastal area. The site quality gradient, particularly increasing salinity from east to west, is visible and two main mangrove types, with

high salinity in the west and low salinity in the east, can be discriminated. The potential applications of weather satellites are worthy of scientific investigations because they can provide information a few hours after each cyclonic impact. However, when this image is recorded during the dry season, no sign of alteration is visible.

Analysis of Mangrove Defoliation Using SPOT Data

High resolution sensors such as SPOT and Landsat TM provide accurate but scarce images. According to BLASCO *et al.* (1992), the mangroves of the Sunderbans seem to be unchanged after two successive cyclonic storms in 1987 and 1988. Nothing in these ecosystems has been profoundly altered by winds and surges according to spectral reflectivity captured from space. We observed the case of a more

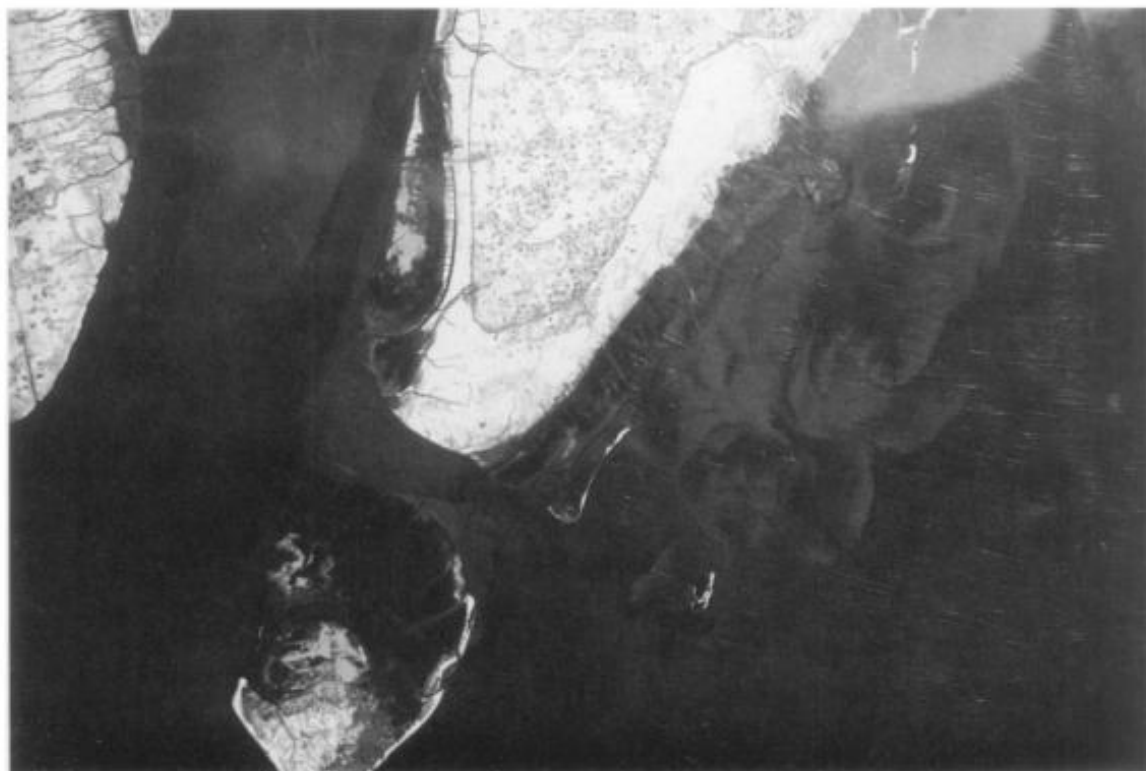


Photo 2. Black and white print of false color composite of SPOT channels XS3, XS2, XS1 over Hatia Island (scene 236/306). The image has been recorded during the dry season (25th February 1987).

exposed area, South Hatia Island, at the top of the Bay of Bengal (Figure 3). Along this coast, as well as along the whole coastline to the east of the Sunderbans, a dense afforestation program has been conducted by the Forest Department (Bangladesh) and the World Bank. This program started in 1964/65, with the aim of consolidating the sediment accretions. In South Hatia, plantations were realized in 1979/80, 1980/81 and probably in 1982/83. The most commonly planted species is *Sonneratia apetala*. The total re-afforested area exceeds 150,000 hectares.

For this region (SPOT scene K236/J306), satellite data

were available from 4 dates (Table 3). Beyond visual comparison of the various documents, digital processing was carried out on SPOT data with channels XS1 (0.5–0.59 μm), XS2 (0.615–0.68 μm) and XS3 (0.79–0.89 μm), and with the use of "Didactim" software. There was superimposition of 1987, 1988 and 1989 data in order to detect possible local accretion or erosion phenomena. In this very flat area, geometric corrections were not necessary. Consequently, there was the analysis of the mangrove spectral signatures and vegetation indices ($VI = (XS3 - XS2) / (XS3 + XS2)$) on the same training zones at different dates, to understand the radiometric behaviour of the forest.

The first question is to determine whether satellite imagery allows the detection of acceleration of coastal erosion accompanied by a simultaneous destruction of the mangroves from cyclonic storms. Erosion and accretion phenomena have been observed through comparison of SPOT data from the 25th February 1987 (Photo 2) to a map drawn from aerial photographs in 1981 (Figure 5). The conclusion of this investigation is that some changes can be observed after a medium or long period. These changes are obviously due to winds, waves and runoff effects, but they are not necessarily related to the cyclones. In any case, even violent cyclones in 1987 and 1988 seem to have been without geomorphological effects on South-Hatia Island.

The second investigation concerned the status of the mangroves viewed from satellites. A careful analysis of these mangroves after two severe or destructive cyclones, 20th August 1987 and 6th September 1988, clearly indi-

Table 3. List of data available for SPOT scene 236/306.

Date	Source	Technical Characteristics	Known Date of Cyclone	Peculiarity
1981	Afforestation map	1/200,000		basic data
25/02/87	SPOT	XS-1B-20 m v.a. 4°9 E		dry season
07/11/87	SPOT	XS-1B-20 m v.a. 1°6 W	20/08/87	after a moderate cyclone
26/10/88	SPOT	XS-1B-20 m v.a. 14°2 W	06/09/88	after a destructive cyclone
15/03/89	SPOT	XS-2-20 m v.a. 1°9 E		dry season

Meaning of abbreviations: XS: Spot Channel; 1B: preprocessing level including standard radiometric and geometric corrections; 2: preprocessing level including level 1B and bidirectional corrections on the basis of ground control points; v.a.: viewing angle

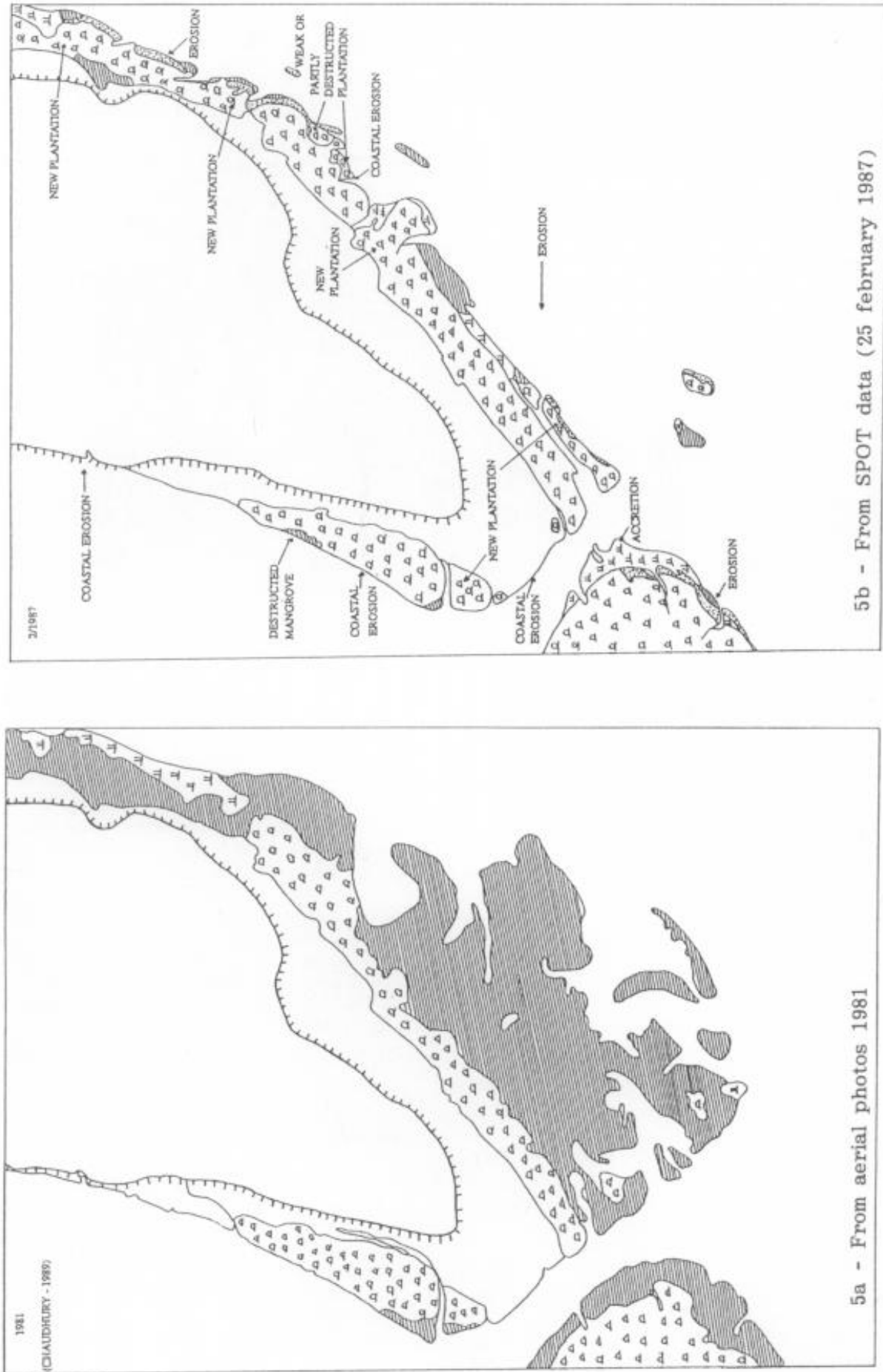


Figure 5. Evolution of South Hatia coastal area (scale 1/200,000). Although erosion is active in some places, the mangroves perfectly resist the annual cyclonic storms.

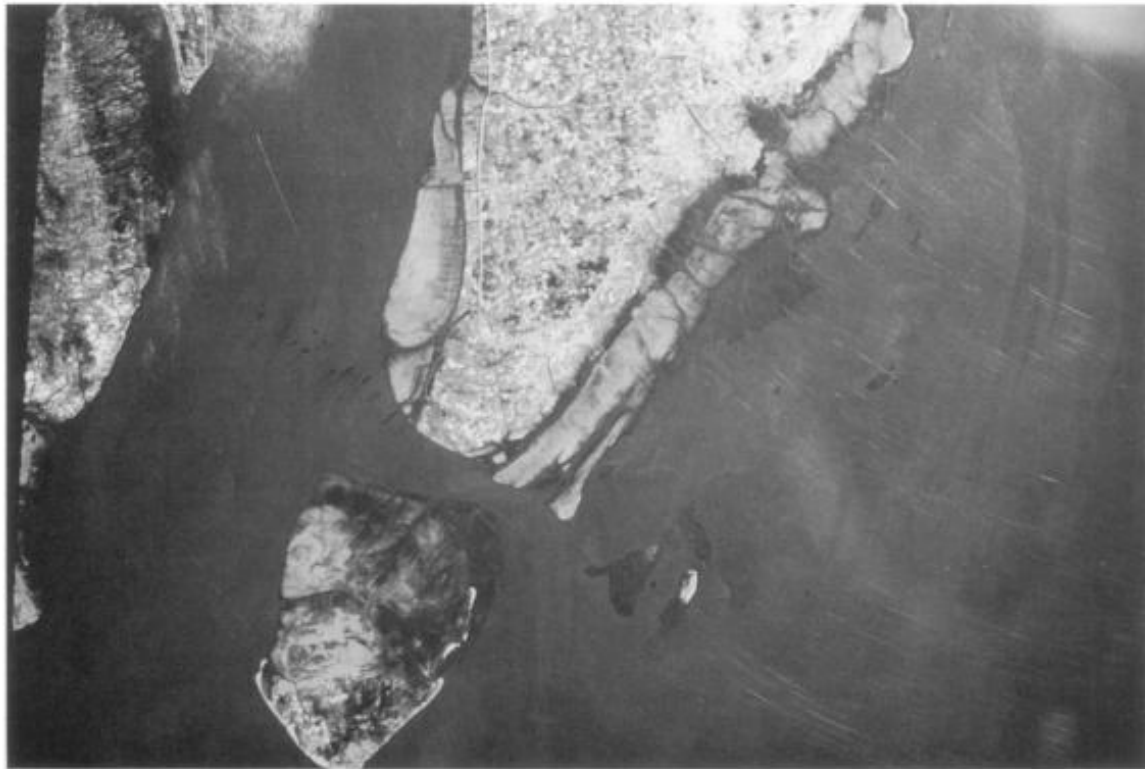


Photo 3. Black and white print of false color composite of SPOT channels XS3, XS2, XS1 over Hatia Island (scene 236/306). The image has been recorded after a cyclone (7th November 1987).

cates that the forests were subsequently healthy, dense and green on the 7th November 1987 (Photo 3) and 26th October 1988. The destructive effects recorded on populations, settlements and crops have not, so far, been detected on the coastal mangroves.

In the absence of storms during the dry season, SPOT data recorded on 25th February 1987 and 15th March 1989 indicate that coastal mangroves, dominated by *Sonneratia apetala*, are extensively defoliated although they are normally evergreen plant communities. Two main types of mangroves can then be discriminated according to their spectral signatures (Figure 6). Healthy forest types present important contrasts in their reflectances for red (XS2) and near infrared (XS3) channels because of their photosynthetic activity. This is illustrated by images recorded on 7th November 1987 and 26th October 1988 for the three classes of mangroves (Figure 6) and on those recorded on 25th February 1987 and 15th March 1989 for the class no. 1 (Figure 6). In contrast, the signature of the second type of mangrove is poorly differentiated and strongly influenced by the water background, and suggests that most trees have lost their leaves (Figure 6, class no. 1 on 25th February 1987 and classes no. 1 and 2 on 15th March 1989). Intermediary behaviour (Figure 6, class no. 2 on 25th February 1987) may correspond to a partially defoliated mangrove.

Of particular note is that younger plantations, planted in 1981 and 1982, remain dense and fully evergreen during the dry season, whereas the oldest ones, planted in 1979, are leafless. This is presumably because during the dry

season air humidity decreases and soil salinity increases because of a reduction of the fresh water input. Roughly 70% of the forest area was defoliated.

If information gathered from satellite data can be confirmed, it might indicate that evergreen mangrove trees such as *Sonneratia apetala* are able to develop a deciduous phase as an adaptative strategy to an environmental stress such as an increase of sodium chloride in water and soils. In this specific case, cyclones seem to have no effect on the greenness of the canopy, whereas fresh water shortages induce an immediate leaf-fall and hence a decrease in annual wood production. This could be one of the consequences of the Farakka Dam that was constructed across the Ganges. The dam is clearly visible on the NOAA AVHRR imagery (Photo 1 and Figure 2).

DISCUSSION AND CONCLUSION

Our field and laboratory investigations have shown that almost every delta located around the Bay of Bengal has its own mangrove forest type with distinct ecological conditions (soil and water salinities, tidal amplitude, etc.) and floristic compositions. About 77% of the total area of these coastal forests lie in the Gangetic delta where the frequency and severity of cyclonic storms is very high.

(1) The magnitude of cyclonic impacts ranges from simple provisional defoliation to windthrows. The latter forms of mangrove destruction are much less frequent and are usually restricted to small fractions of mangroves.

Almost all mangrove species seem to be resistant to winds of below 150 km/hr, but there is variability from one species

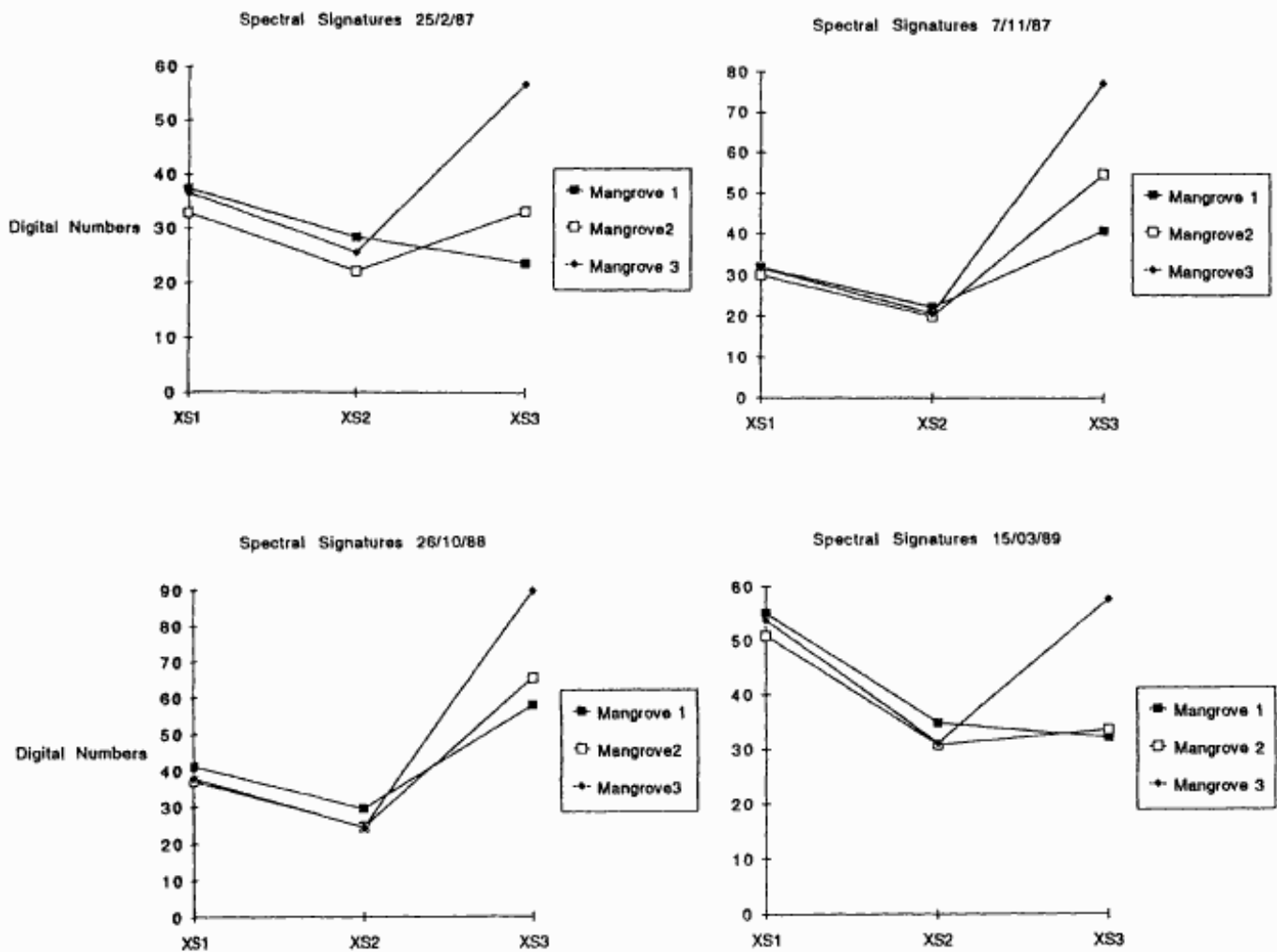


Figure 6. Spectral signatures of three mangrove classes (South Hatia Island).

to another in terms of wind tolerance. The re-afforested coastal zone dominated by *Sonneratia apetala* Buch. Ham. seems to be highly resistant to the most severe cyclones. Moreover, the temporal defoliation of mangrove trees has no apparent effect on primary production. Factors that stimulate growth and seed production have not been investigated.

Sandy banks are deposited at the mouths of rivers and on islands. Strong winds often create dunes able to spread to some distance into the mangrove. The redistribution of sediments due to strong wave actions and winds kills some mangrove stands, either by over-sedimentation or by a pronounced disturbance of the hydrologic regime.

(2) The natural disturbances in the mangroves induce new and dynamic successional phases. This can be interpreted as a common form of "rejuvenation," particularly in the outer fringes of the mangrove stands. It is noteworthy that the most common species around the Bay of Bengal are *Excoecaria agallocha* and *Avicennia* species and they have a wide ecological amplitude and remarkable regenerative capabilities. Although this aspect of the forest dynamism is still poorly documented, the assumption is that the mean age of trees in the mangroves of the Bay of

Bengal, i.e., in a cyclone-prone area, is directly related to the frequency of violent cyclones.

(3) During each cyclonic storm, erosive and accretion processes have suddenly intensified. Although our technical capability to monitor and to quantify these phenomena is still inadequate, the total area of these mangroves has remained almost constant in the absence of human interference: what has been lost here is spontaneously compensated elsewhere by newly created mangrove communities. From a practical point of view the frequency of cyclones has only local effects on the usual timber crop rotations. This is particularly true in the continental parts of the mangrove stands even if river bank mangrove belts were frequently reshaped.

(4) Concerning the use of satellite technology for the monitoring of cyclonic impacts on mangrove areas, the spatial and radiometric resolutions of SPOT and Landsat TM are sufficient for an evaluation of localized damage and forest destruction. On a practical basis, it takes 5 to 12 weeks after a cyclone to acquire images with adequate quality. This temporal resolution and timeliness of high resolution satellites creates substantial obstacles, and we cannot at present rely on the availability of exploitable

satellite data for evaluation of the cyclonic impacts on mangrove stands of the Sunderbans.

ACKNOWLEDGEMENTS

We would like to express our thanks to Dr. J. P. Malingreau and Dr. F. Achard (Institute for Remote Sensing Applications—Joint Research Center, Ispra, Italy) for providing the NOAA AVHRR satellite product. We thank Mrs C. Tertre for typing the manuscript.

LITERATURE CITED

- BLASCO, F., 1977. Outlines of ecology, botany and forestry of the mangals of Indian subcontinent. In: CHAPMAN, V.J., *Ecosystems of the World no. 1, Wet Coastal Ecosystems*. Amsterdam: Elsevier Scientific Publishing Company, Chapter 12, pp. 241-260.
- BLASCO, F.; BELLAN, M.F., and CHAUDHURY, M.U., 1992. Estimating the extent of floods in Bangladesh using SPOT data. *Remote Sensing of Environment*, 39(3), 167-178.
- CHAUDHURY, M.U., 1989. *Les mangroves du Bangladesh et leur analyse par télédétection spatiale*. Toulouse, France: Thèse Univ. Toulouse III, 150p.
- CHOUHURY, A.M., 1962. *Working Plan of Sunderbans Forest. Division for the Period 1960-61 to 1979-80*, vol. 1. Bangladesh: Dakha, 82p.
- CINTRON, G. and SCHAEFFER-NOVELLI, Y., 1983. Mangrove forests: Ecology response to natural and human induced stressors. In: UNESCO, Coral reefs, seagrass beds and mangroves: Their interaction in the coastal zones of the Caribbean. *Reports in Marine Science*, 23, 87-109.
- CRAIGHEAD, F.C., 1964. Land, mangroves and hurricanes. *Fairchild Tropical Garden Bulletin*, 19, 5-32.
- CRAIGHEAD, F.C., and GILBERT, V.C., 1962. The effects of Hurricane Donna on the vegetation of southern Florida. *Quarterly Journal of the Florida Academy of Sciences*, 25, 1-28.
- CURTIS, S.J., 1933. *Working Plan For the Sunderbans Division (1931-51)*. Bengal: Forest Department.
- DAGAR, J.T.; MONGIA, A.D., and BANDYOPADHYAY, A.K., 1991. *Mangroves of Andaman and Nicobar Islands*. New Delhi: Mohan Prinlani Pub., for Oxford & IBH Publishing Co. Pvt. Ltd., 166p.
- FOSBERG, F.R., 1971. Mangroves versus tidal waves. *Biological Conservation*, 4, 38-39.
- KOTESWARAM, P., 1984. Climate and mangrove forests. *Invited lecture at UNDP/UNESCO Second Training Course on Mangrove Environment*, (Goa) 1-25 November 1984.
- LESCURE, J.P. and TOSTAIN, O., 1989. Les mangroves guyanaises. *Bois et Forêts des Tropiques*, Guyane: CIRAD, Nogent sur Marne, France, Spécial 220, 35-42.
- LUGO, A.E. and SNEDAKER, S.C. (ed.), 1974. Properties of a mangrove forest in southern Florida. *Proceedings International Symposium on Mangroves* (Honolulu) 8/11 October 1974, 170-212.
- PAGNEY BENITO-ESPINAL, F. and BENITO-ESPINAL, E., 1991. *L'ouragan Hugo: Génèse, Incidences Géographiques et Écologiques Sur la Guadeloupe*, France: Univ. Dijon, 210p.
- SAENGER, P.; HEGGERL, E.J., and DAVIE, J.D.S. (ed.), 1983. Global status of mangrove ecosystems, *Working Group on Mangrove Ecosystems of the IUCN Commission on Ecology in Cooperation with the United Nation Environment Programme and the World Wildlife Fund*, Lausanne, Switzerland: Elsevier Sequoia S.A., 88p.
- STODDART, D.R., 1971. Coral reefs and islands and catastrophic storms. In: STEERS, J.A. (ed.), *Applied Coastal Geomorphology*, London: Macmillan, pp. 155-197.
- STODDART, D.R., 1974. Post-hurricane changes on the British Honduras reefs: Resurvey of 1972. *Proceedings 2nd International Coral Reef Symposium* (Brisbane) 2, 473-483.
- TABB, D.C. and JONES, A.C., 1962. Effects of Hurricane Donna on the aquatic fauna of North Florida Bay. *Transactions of the American Fisheries Society*, 91(4), 375-378.
- TAYLOR, R.A., 1967. Effect of Hurricane Betsy on the southeastern Everglades. *Quarterly Journal of the Florida Academy of Sciences*, 30, 10-24.
- UNTAWALE, A.G., 1985. Mangroves of Asia and the Pacific: Status and usage. Mangroves of India: Present status and multiple use practices. *Report for UNDP/UNESCO Regional Project, Research and Training Pilot Programme on Mangrove Ecosystems in Asia and the Pacific*, Goa, India: National Institute of Oceanography, 67p.
- WOODROFFE, C.D. and MOSS, 1984. Litterfall beneath *Rhizophora stylosa* Griff., Vaitupu, Tuvalu, South Pacific. *Aquatic Botany*, 18, 249-255.

Annex RJ-5

K. Furukawa, E. Wolanski, "Sedimentation in Mangrove Forests",
Mangroves and Salt Marshes, Vol. 1, 1996, pp. 3-10.

Sedimentation in mangrove forests

Keita Furukawa^{1,2} and Eric Wolanski²

¹Port and Harbour Research Institute, 1-1,3 Chome, Nagase, Yokosuka 239, Japan; ²Australian Institute of Marine Science, PMB No.3, Townsville MC, Queensland 4810, Australia

Keywords: Dense vegetation, flocculation, flow modelling, tidal pumping, turbulence

Abstract

The tidal currents in mangrove forests are impeded by the friction caused by the high vegetation density. The tidal currents are also complex comprising eddies, jets and stagnation zones. The sediment particles carried in suspension into the forest during tidal inundation are cohesive, mainly clay and fine silt, and form large flocs. These flocs remain in suspension as a result of the turbulence created by the flow around the vegetation. The intensity of sedimentation is largest for trees forming a complex matrix of roots such as *Rhizophora* sp. and smallest for single trees such as *Ceriops* sp. The flocs settle in the forest around slack high tide. At ebb tides the water currents are too small to re-entrain this sediment. Hence the inundation of coastal mangrove forests at tidal frequency works as a pump preferentially transporting fine, cohesive sediment from coastal waters to the mangroves. Mangroves are thus not just opportunistic trees colonising mud banks but actively contribute to the creation of mud banks.

Introduction

Mangrove forests are a buffer zone between the coast and the ocean. One of their presumed important functions is to provide a mechanism for trapping sediment. Suspended sediment is introduced to coastal areas by river discharge, dumping of dredged material and resuspension of bottom sediment by waves and ships (Holeman, 1968; Laronne and Mosley, 1982; Wolanski, 1994). Mangrove forests are believed to be an important sink for suspended sediment (Woodroffe, 1992; Wolanski *et al.*, 1992; Furukawa *et al.*, 1996; Wolanski, 1994; Wolanski, 1995).

Most coastal mangrove forests are connected to the sea via a tidal creek. Sediment transport mechanisms in these creeks have been investigated in detail. These mechanisms are dominated by hydrodynamic processes, as opposed to biological processes which prevail further offshore (Ayukai and Wolanski, 1996), and include the asymmetry of the tidal currents, the baroclinic circulation and shear-induced destruction of flocs (Gibbs, 1985; Woodroffe, 1985; Dyer, 1986; Wolanski *et al.*,

1988; Wolanski, 1995; Wolanski *et al.*, 1995; Wolanski and Gibbs, 1995; Mazda *et al.*, 1995). Sediment transport mechanisms in mangrove forests have received little attention though observations suggest a net inflow of fine sediment in mangroves (Furukawa *et al.*, 1996). The flows through mangrove forests are sluggish as a result of the high vegetation density increasing friction (Wolanski *et al.*, 1980; Mazda *et al.*, 1995 and 1996). In these latter studies, only overall friction coefficients have been estimated by averaging spatially over several tens of roots, tree trunks and pneumatophores. There have been no previous studies of the details of these flows around the vegetation and their role in the process of sedimentation in mangroves.

It has never been clear whether mangroves create their own environments (mud banks) or whether they are simply opportunistic colonisers of mud banks generated by other geomorphological processes. From a detailed study of flows through a mangrove forests and the resulting sedimentation processes, we show that mangroves actively create their own ecosystems by trapping

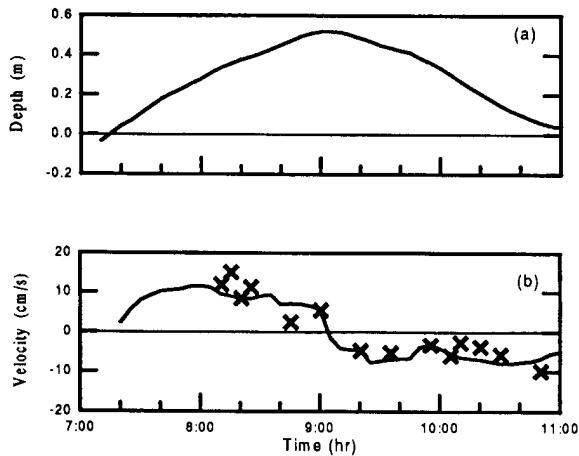


Fig. 1. Time series of (a) water depth and (b) observed (x) and numerically predicted (line) velocity at our study site in Cairns mangroves. Time is in hour on December 3, 1994.

sediment. The trapping mechanism is due to the high micro-turbulence created by the flow around the vegetation maintaining sediment in suspension at flood tidal currents. This sediment settles near the time of slack water high tide when turbulence vanishes. This sediment is not re-entrained by ebb tidal currents which are too sluggish because of the high vegetation density.

Tidal pumping

Our study site was the mangroves along the Cairns boardwalk, in wet, tropical Australia (see details in Furukawa *et al.*, 1996). The area is populated by a fringe of *Rhizophora* sp. trees along the banks of the tidal creek and by *Cerriops* and *Avicennia* trees further inland. The width of the mangrove forest is about 150 m. Macro-tides prevail, peaking at 3.5 m peak to trough, during which water depth never exceeds 1 m in the mangroves.

The water currents in the mangrove forest were controlled by the tides. Water spilled over from the tidal creek to inundate the forest at flood tide, this water drained back in the tidal creek at ebb tide (Fig. 1). The currents through the forest were sluggish, seldom exceeding 0.1 m s^{-1} . The driving force for this flow is the water surface slope I (i.e. the slope of the water surface from the tidal creek into the forest, Fig. 2) and the retarding force is the friction. The total friction is the sum of that at the

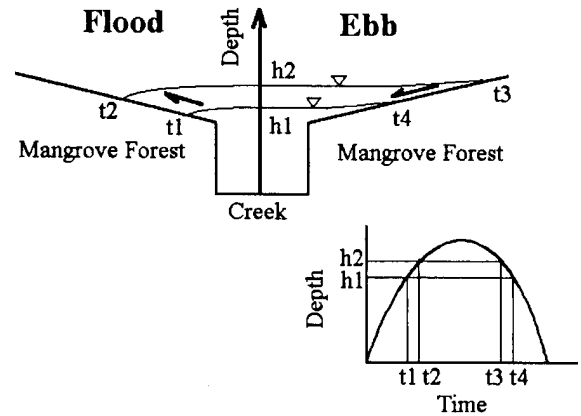


Fig. 2. Sketch of the water elevation in a tidal creek-mangrove swamp system at flood tide and ebb tide. The water surface slopes towards the creek at ebb tide but towards the mangroves at flood tide.

bottom and that caused by the flow around the tree trunks, roots and pneumatophores. These flows are complex, with eddies, jets and stagnation zones. Details of these micro-scale flows vanish if we average spatially over many roots, trunks and pneumatophores, so that only net currents remain. Inertia is negligible for these net currents because the flows are sluggish and the friction force balances the force created by the water surface slope. Thus

$$u = \frac{1}{n} h^{2/3} I^{1/2} \quad (1)$$

where u is the water velocity, n is the spatially-averaged Mannings friction coefficient, h is the water depth and I is the water surface slope.

The Mannings friction coefficient, n , is an important engineering parameter and has been the focus of much research by hydraulics engineers working with rivers and channels (e.g. Chow, 1959). Typical values of n for sandy channels are in the range 0.025-0.035. The value of n is believed to diminish for decreasing grain size of the sediment and indeed muddy estuaries can have an even smaller value of n ($n=0.015$; see King and Wolanski, 1995; Lixian & Wolanski, 1996). Hence, if only bottom friction was important, at first glance the value of n should be <0.025 in mangroves where the dominant sediment is mud. In fact that is not the case because flows around the vegetation increase friction. Wolanski *et al.* (1980)

and Wolanski *et al* (1992) found $n=0.2-0.4$ from field observations and $n=0.25$ from model studies in a heavily vegetated mangrove swamp at Hinchinbrook Island, Australia. Mangroves are as heavily vegetated as salt marshes and several authors have also reported a high value of the Mannings friction coefficient in such systems. Indeed, Burke and Stolzenbach (1983), Kjerfve *et al.* (1991) and Hosokawa and Furukawa (1994) modelled spatially-averaged flows through dense vegetation of *Spartina* salt marshes and deduced $n=0.1-0.2$.

Observed and predicted (assuming $n=0.1$) currents at our study site compare favourably (Fig. 1). Thus the vegetation increases Mannings friction coefficient by a factor of at least 5, hence the friction force by a factor of at least 25, from that expected for non-vegetated surfaces. This effect in turn inhibits water flows and the small velocities, seldom exceeding 0.1 m s^{-1} , that result are unable to resuspend the fine cohesive sediment for which a peak velocity of 0.3 m s^{-1} is needed (Wolanski *et al.*, 1995). What causes a sediment pump is, as shown below, the high turbulence as a result of complex flows around the vegetation which maintaining sediment in suspension until settling occurs at high tide.

Observed sedimentation rates

The net sedimentation rate at spring tides was measured at our study site on a transect from the bank of the tidal creek to the tidal limit in the mangrove forest. It decreases exponentially with distance, x , from the creek (Fig. 3).

This exponential decrease results from simple hydrodynamics. Sediment settles at a rate $w_o C$, where w_o is the settling velocity and C the suspended sediment concentration. The system is driven by the inflow of water from the creek, the water flowing into the mangroves at a velocity u over a depth h . At the creek bank the suspended sediment concentration is C_o and this is controlled by the dynamics of the tidal creek. The concentration of suspended sediment C in the waters in the mangroves decreases with distance from the creek because it progressively settles out, so that from continuity of sediment flux,

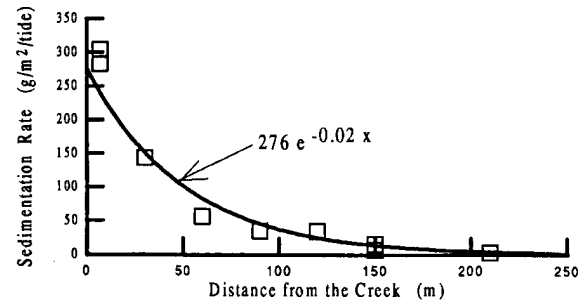


Fig. 3. Observed (\square) and numerically predicted (line) sedimentation rates across the Cairns mangrove with distance from the tidal creek, for the spring tide of December 3, 1994.

$$C = C_o \exp \left[-\frac{w_o x}{hu} \right] \quad (2)$$

where x = the distance into the mangrove forest from the tidal creek.

The sedimentation rate S is calculated from equation (2) as

$$S = -\frac{d(Chu)}{dx} = C_o w_o \exp \left[-\frac{w_o x}{hu} \right] \quad (3)$$

and the predicted sedimentation rate matches the observations well (Fig. 3). The predicted sedimentation rate was calculated assuming from the field observations that $h=0.4 \text{ m}$, $u = 0.1 \text{ m s}^{-1}$, and $w_o = 0.0005 \text{ m s}^{-1}$.

This simple model shows that nearly all the suspended sediment that entered the mangrove forest from the tidal creek, settled in the forest and was not re-entrained and exported at ebb tide.

It must be noted that we assume the sediment in the water column at point x is vertically well mixed by turbulence caused by mangrove roots and undulation of the bed. This assumption is justified by laboratory measurements for vertical velocity distribution in the *Spartina anglica* canopy which shows high complexity of the flow (Shi *et al.*, 1995). Woolnough *et al.* (1995) on the contrary, assume quiescent settlement, and get arc-tangential function for sedimentation rate for the salt marsh. The assumption of quiescent settlement has a risk of an over-estimate of settlement at the creek side and an under-estimate of settlement distant

from the creek for well mixed water. Thus, the selection of the settlement process is an important matter.

We show below that the high settling velocity of the suspended sediment is due to flocculation.

Flocculation

The particle size distribution of the suspended sediment at the study site shows the sediment to be muddy silt, composed mainly of fine silt and clay (Fig. 5) with a mean diameter of 5.6 μm , 40% by volume of the sediment being $< 4 \mu\text{m}$ and 20% less than 2 μm . If these sediment particles were not aggregated in flocs, their settling velocity as calculated by Stokes law would be around 0.00008 m s^{-1} .

This very low value of the settling velocity is however unrealistically low because in fact the sediment was flocculated. At our study sites, floc size was measured by two techniques, namely the special sampling slide - microscope technique of Gibbs and Konwar (1986) and in-situ micro-photographs. The latter technique samples less water and registers fewer flocs, can lead to loss of clarity particularly if flocs are packed too densely but has the advantage that it does not destroy flocs mechanically (Wells, 1989; Eisma *et al.*, 1990). Both techniques yielded similar results, which indicated that at least 99% of the suspended sediment was flocculated. The flocs in suspension at our study site (Fig. 4) had a loose structure, subdivided in zones of high and low density, and individual floc sizes varied between 30 and 300 μm . Mean floc size was 100 μm corresponding to a settling velocity of 0.005 m s^{-1} (Gibbs, 1985), this settling velocity is 100 times larger than that of the individual particles of clay and silt making up the floc.

Flocculation appears responsible for the rapid settling near high tide and the lower concentration in suspended sediment at ebb tide than at flood tide at our study site in the mangrove forest (Fig. 6). Most of the flocs settled within 30 min just prior to the high slack tide. The settlement removed preferentially (Fig. 6) the small particles ($< 4 \mu\text{m}$), the largest (rare) particles ($> 32 \mu\text{m}$) and all the large flocs ($> 250 \mu\text{m}$) and over 90% of the large

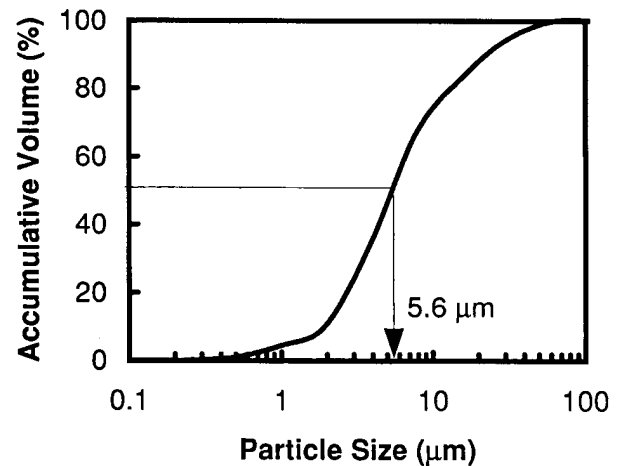


Fig. 4. Typical accumulative particle size distribution curve for suspended sediment in the water column at our study site.

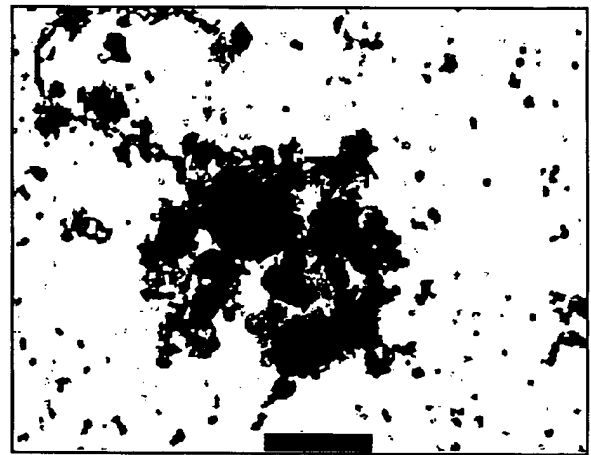


Fig. 5. Microphotograph of flocs in suspension in the water column at our study site in the mangroves. The bar represents 100 μm . The darker areas in the flocs represent zones of high packing density of particles, the lighter areas zone of low packing density.

flocs ($> 100 \mu\text{m}$). Thus preferential sedimentation of clay and fine silt occurred.

We show below that what maintained the flocs in suspension until near high tide was the high turbulence created by the water flow around tree trunks, roots and pneumatophores.

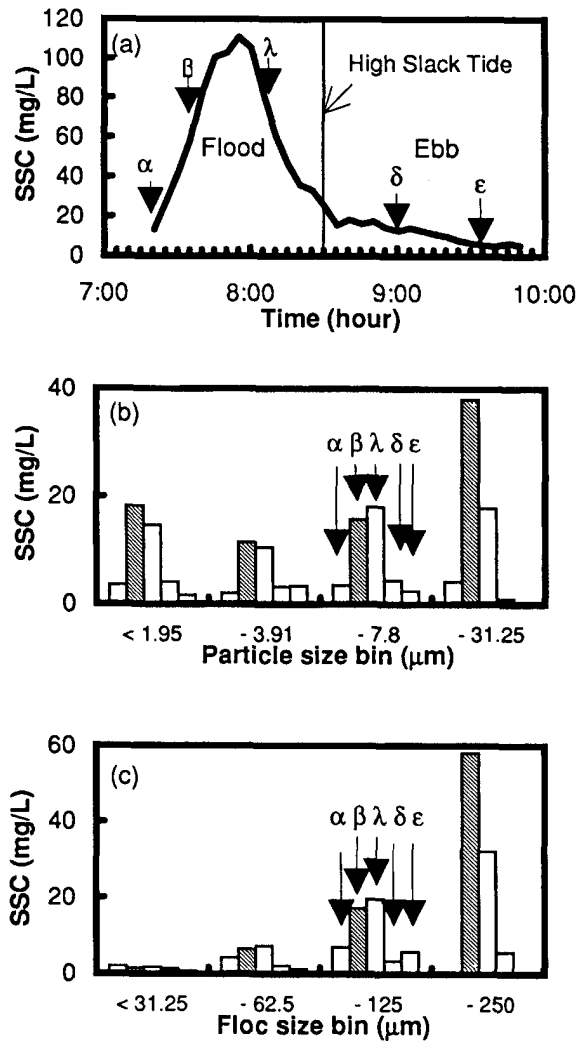


Fig. 6. (a) Time series plot of suspended sediment concentration (SSC) in the water column at our study site in the Cairns mangroves on December 2, 1994. (b) and (c) are respectively particle and floc size distributions for sampling times α - ϵ (shown in Fig. 6a). The bin sizes for particle and flocs are different. The particle bin sizes are <1.95 , $1.95-3.91$, $3.91-7.8$ and $7.8-31.25$ μm . The floc bin sizes are <31.25 , $31.25-62.5$, $62.5-125$ and $125-250$ μm .

Vegetation-induced turbulence

Observed flow patterns were visualised using downward-looking video cameras tracking small floats following the technique of Furukawa *et al.* (1996). The currents around the vegetation varied with the vegetation density. The simplest flows prevail around single tree trunks (e.g. *Ceriops* sp.)

and the most complex flows were found around the matrix of roots of *Rhizophora* sp.

Around *Ceriops* sp. (Fig. 7a) a wake was visible behind the tree. Such wakes are characterised by the Reynolds number

$$\text{Re} = \frac{UL}{\nu} \quad (4)$$

where U is the undisturbed velocity, L is the diameter of the tree trunk and ν is the kinematic viscosity. For $\text{Re} < 1$, no bubble exist. A steady wake exist for $\text{Re} < 100$, but the water in the eddy is then nearly stagnant, while long wakes exist for $\text{Re} = 100-400$. Unsteady turbulent flows prevail for larger values of Re . Our data suggest $\text{Re} = 100-400$ in the field. Such flows are very turbulent with peak three-dimensional turbulent velocities of the same order as U . Indeed we visually observed zones of high upwelling and downwelling and other zones with high turbulence especially in the shear zones near the vegetation. This turbulence is sufficient to maintain the flocs in suspension.

For *Rhizophora* sp. the higher vegetation density generated more complex flows comprising jets, eddies and stagnation zones (Fig. 7b). Individual wakes behind roots interacted one with the other. Turbulence was intense in the region which the flow becomes jet, and sedimentation occurred preferentially in the stagnation zones.

The important parameter for calculating sedimentation rates in mangroves is the turbulent velocity. This was calculated using the numerical model of Furukawa and Wolanski (1996) for two-dimensional flows. The model *Rhizophora* root matrix comprised 19 roots each with a diameter of 0.04 m. Two undisturbed velocities U were chosen, 0.05 and 0.2 m s^{-1} . The model is calibrated by its ability to reproduce mean flows obtained in the field (Fig. 7). The turbulent intensity is inferred from the model. For $U = 0.05$ m s^{-1} , the turbulence is practically negligible and the wake effect is restricted to very small regions around each root (Fig. 8a). However for $U=0.2$ m s^{-1} , jet flows are formed, the jets are deflected by the vegetation to interact with each other, in agreement with observations (Fig. 7). The model predicts that in such conditions the turbulent intensity is 2-3 times larger than the mean velocity. This turbulence is three-

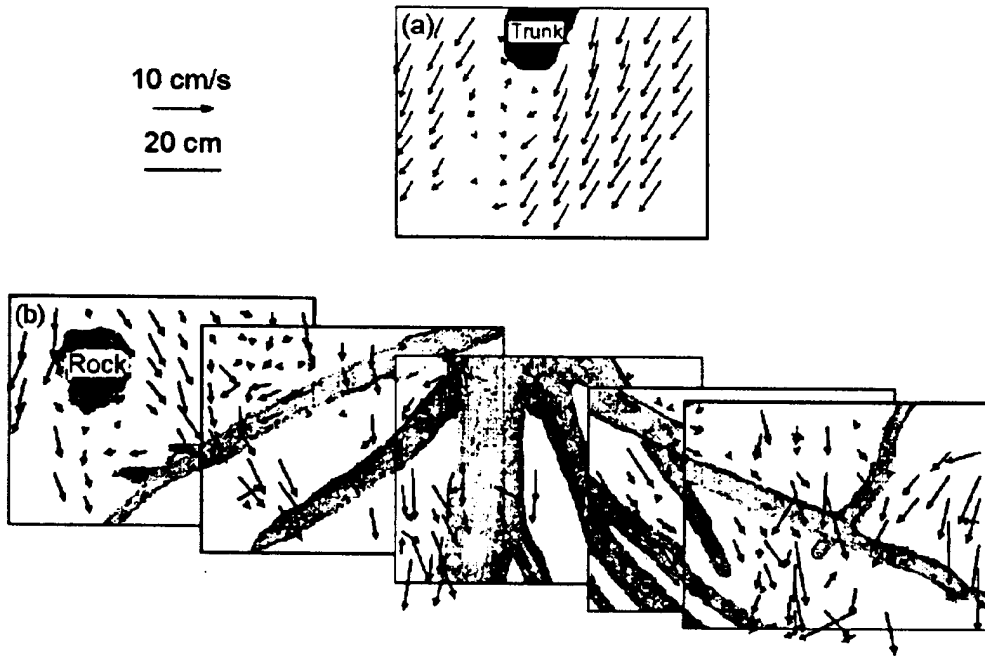


Fig. 7. Observed 1-min mean water velocities around mangroves for (a) *Ceriops* sp. and (b) *Rhizophora* sp. on December 3, 1994.

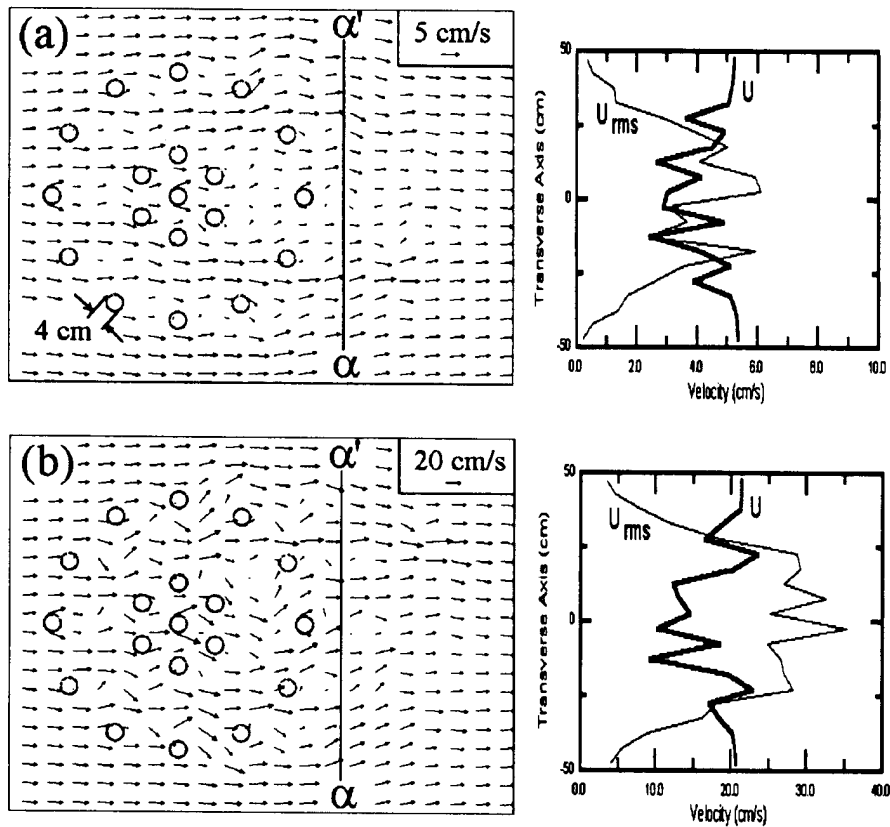


Fig. 8. (Left) Predicted horizontal velocities around a *Rhizophora* root matrix for an approach velocity of (a) 0.05 and (b) 0.2 m s^{-1} . (Right) Mean velocity U and root mean squared velocity U_{rms} along the transect $\alpha\text{-}\alpha'$ shown in the left figure. Note the stagnation zones and the jets interacting one with the other.

dimensional and is more than sufficient to keep the 100 μm flocs in suspension.

Conclusion

Mangrove forests are an important buffer between the sea and the land. They are not just passive colonisers of mud banks, but actively capture mud to create their own environments. The way they do this is to maintain high turbulence in the water flow through the forest; this high level of turbulence maintains in suspension the flocs of fine cohesive sediment which enter the forests at flood tide. Turbulent intensities are the largest for trees forming a complex matrix of roots such as *Rhizophora* sp. and smallest for single trees such as *Ceriops* sp. Sedimentation occurs when turbulence vanishes near slack high tide. The settled sediment is not re-entrained at ebb tide because the high vegetation density inhibits currents which are too sluggish to erode the sediment.

Mangroves actively pump fine, cohesive sediment from the tidal creeks and the coastal ocean. Mangroves are thus an important sink for fine sediment from rivers and coastal waters. While the biological role of mangroves in the biological food chain of coastal waters has been well documented (Robertson and Alongi, 1992), mangroves appear also to have an important physical effect. The removal of mangroves may increase water turbidity and hence decrease primary productivity by planktonic algae in tidal creeks and coastal waters surrounding mangrove ecosystem.

Acknowledgments

This study was supported by the Research Development Corporation of Japan, the Port and Harbour Research Institute of Japan, the Australian Institute of Marine Science and the IBM International Foundation. This is contribution number 790 from Australian Institute of Marine Science.

References

- Ayukai, T. & Wolanski, E. 1996. Importance of biologically mediated removal of fine sediments from the Fly River plume, Papua New Guinea, Estuarine, Coastal and Shelf Science, in press.
- Burke, R.W. & Stolzenbach, K.H. 1983. Free surface flow through salt marsh. Massachusetts Institute of Technology Sea Grant College Program, Publication No. MITSG 83-16, Cambridge, MA.
- Chow, Ven Te. 1959. Open channel hydraulics, Macgraw-Hill, New York.
- Dyer, K.R. 1986. Coastal and Estuarine Dynamics. John Wiley, New York
- Eisma, D., Schumacher, T., Boekel, H., van Herwaarden, J., Franken, H., Laan, M., Vaars, A., Eugenraam, F. & Kalf, J. 1990. A camera and image-analysis system for in-situ observations of flocs in natural waters. Netherlands Journal of Sea Research, 27:43–56.
- Furukawa, K. & Wolanski, E. 1996. Shallow water frictional effects in island wakes. Continental Shelf Research, in press.
- Furukawa, K., Wolanski, E. & Mueller, H. 1996. Currents and sediment transport in mangrove forests. Estuarine, Coastal and Shelf Science, in press.
- Gibbs, R.J. 1985. Estuarine flocs: their size, settling velocity and density. Journal of Geophysical Research, 90:3249–3251.
- Gibbs, R.J. & Konwar, L. 1986. Coagulation and settling of Amazon River suspended sediment. Continental Shelf Research, 6:127–149.
- Holeman, J.M. 1968. The sediment yield of major rivers of the world. Water Resources Research, 4:737–747.
- Hosokawa, Y. & Furukawa, K. 1994. Surface flows and particle settling in a coastal reed field. Water Science and Technology, 29(4):43–53.
- King, B. & Wolanski, E. 1995. Friction reduction in turbid estuaries. In: Pattiaratchi, C. (ed) Coastal and estuarine studies, American Geophysical Union, Washington D.C., in press.
- Kjerfve, B.J., Miranda, L.J. & Wolanski, E. 1991. Modeling water circulation in an estuary and inter-tidal salt marsh system. Netherlands Journal of Sea Research, 28:141–147.
- Larone, J.B. & Mosley, M.P. (eds). 1982. Erosion and sediment yield. Hutchinson Ross Publish Co., Stoudsburg.
- Lixian, D. & Wolanski, E. 1996. Link between mixing processes and suspended sediment dynamics in the Jiaojiang River estuary, China. Estuarine, Coastal and Shelf Science, in press.
- Mazda, Y., Kanazawa, N. & Wolanski, E. 1995. Tidal asymmetry in mangrove creeks. Hydrobiologia, 295:51–58.
- Mazda, Y., Wolanski, E., Sase, A., Ohtsuka, D. & King, B. 1996. Drag force due to vegetation in mangrove swamps. Estuarine, Coastal and Shelf Science, in press.
- Robertson, A.I. & Alongi, D.M. (eds). 1992. Tropical mangrove ecosystems. American Geophysical Union, Washington D.C.
- Shi, Z., Pethick, J.S. & Pye, K. 1995. Flow structure in and above the various heights of a saltmarsh canopy: A laboratory flume study. Journal of Coastal Research, 11(4):1204–1209.
- Wells, J.T. 1989. In-situ measurements of large aggregates

- over a fluid mud bed. *Journal of Coastal Research*, 5:75-86.
- Wolanski, E. 1994. *Physical oceanography processes of the Great Barrier Reef*. CRC Press, Boca Raton, Florida.
- Wolanski, E. 1995. Transport of sediment in mangrove swamps. *Hydrobiologia*, 295:31-42.
- Wolanski, E. & Gibbs, R.J. 1995. Flocculation of suspended sediment in the Fly River estuary, Papua New Guinea. *Journal of Coastal Research*, 40:321-337.
- Wolanski, E., Jones, M. & Bunt, J.S. 1980. Hydrodynamics of a tidal creek - mangrove swamp system. *Australian Journal of Marine Freshwater Research*, 31:431-450.
- Wolanski, E., Chappell, J., Ridd, P. Vertessy, R. 1988. Fluidisation of mud in estuaries. *Journal of Geophysical Research*, 93:2351-2361.
- Wolanski, E., Mazda, Y. & Ridd, P. 1992. Mangrove hydrodynamics. pp. 436-462. In: Robertson, A.I. & Alongi, D.M. (eds), *Tropical mangrove ecosystems*, American Geophysical Union, Washington D.C.
- Wolanski, E., King, B. & Galloway, D. 1995. Dynamics of the turbidity maximum in the Fly River estuary, Papua New Guinea. *Estuarine, Coastal and Shelf Science*, 40:321-337.
- Woodroffe, C.D. 1985. Studies of mangrove basin, Tuff Crater, New Zealand: II. Comparison of volumetric and velocity-area methods of estimating tidal flux. *Estuarine, Coastal and Shelf Science*. 20:431-445.
- Woodroffe, C. 1992. Mangrove sediments and geomorphology. pp.7-41 in Robertson, A.I. & D.M. Alongi (eds), *Tropical mangrove ecosystems*, American Geophysical Union, Washington D.C.
- Woolnough, S.J., Allen, J.R.L. & Wood, W.L. 1995. An exploratory numerical model of sediment deposition over tidal salt marshes. *Estuarine, Coastal and Shelf Science*, 41:515-543.

Annex RJ-6

Y. Mazda, M. Magi, M. Kogo, P.N. Hong, “Mangrove as Coastal Protection from Waves in the Tong King Delta, Vietnam”, *Mangroves and Salt Marshes*, Vol. 1, 1997, pp. 127-135.

Mangroves as a coastal protection from waves in the Tong King delta, Vietnam

Yoshihiro Mazda¹, Michimasa Magi¹, Motohiko Kogo² and Phan Nguyen Hong³

¹Department of Marine Science, School of Marine Science and Technology, Tokai University, 3-20-1, Orido, Shimizu, Shizuoka, 424 Japan; ²Action for Mangrove Reforestation, 3-29-14, Honcho, Nakano, Tokyo, 164 Japan; ³Mangrove Ecosystem Research Centre, Vietnam National University, 91 Nguyen Khuyen Street, Hanoi, Vietnam

Keywords: mangroves, reforestation, wave reduction, flow resistance, Tong King delta, coastal protection

Abstract

The wave reduction (wave period; 5–8 sec.) was investigated in a mangrove reforestation area (*Kandelia candel*) close to aquaculture ponds in the Tong King delta, Vietnam.

On one site where only young mangrove trees grew, the wave reduction due to the drag force on the trees was hardly effective. On the other site where mangrove trees were sufficiently tall, the rate of wave reduction per 100 m was as large as 20%. Due to the high density of vegetation distributed throughout the whole water depth, the effect of wave reduction was large even when the water depth increased. These results demonstrate the usefulness of mangrove reforestation for coastal protection.

Introduction

Along the coast of Vietnam, earnest and sober efforts for planting mangroves have been executed on an extensive scale. In order to promote the effective plantation, to preserve the environment of the planted forests and to utilize the ecosystem developed in the environment, physical, especially hydrodynamic processes such as tides, sea waves and water flows in and around the forests need to be understood, because these areas which belong to the fringe forest type (F-type mangal; Lugo and Snedaker, 1974) face to the open sea and are directly exposed to the action of tropical depressions, storms and typhoons (Hong and San, 1993).

As stated by Kjerfve (1990) and Mazda (1993), it is only a short time since studies of the physical processes in mangrove areas have been initiated. Ridd et al. (1990), Wolanski et al. (1990), Mazda et al. (1990), Wolanski et al. (1992), and Mazda et al. (1995) have studied some tidal periodic phenomena in mangrove areas along rivers or estuaries protected from the open sea. However, quanti-

tative studies about the physical processes in F-type mangal are very few.

We observed the physical processes in F-type mangals at coastal areas of Thuy Hai and Thuy Truong in the Thai Thuy dist., Thai Binh prov., Vietnam, in a delta of the Gulf of Tong King from 17th to 21st November, 1994. In this paper, we describe the characteristics of water elevation and water flow in these areas, and demonstrate the wave reduction by mangroves mainly at the coast of Thuy Hai, where *Kandelia candel* has been planted for several years.

Study sites and measurements

The coast along Thuy Hai and Thuy Truong has an extremely flat tidal area about 8km wide (the slope of the bottom floor is 0.5/1000) due to alluvium discharged from the Hong River (Figure 1). In the coastal area of Thuy Hai the seedlings of *Kandelia candel* have been artificially planted in a strip 1.5 km wide (toward offshore) and 3 km long. The

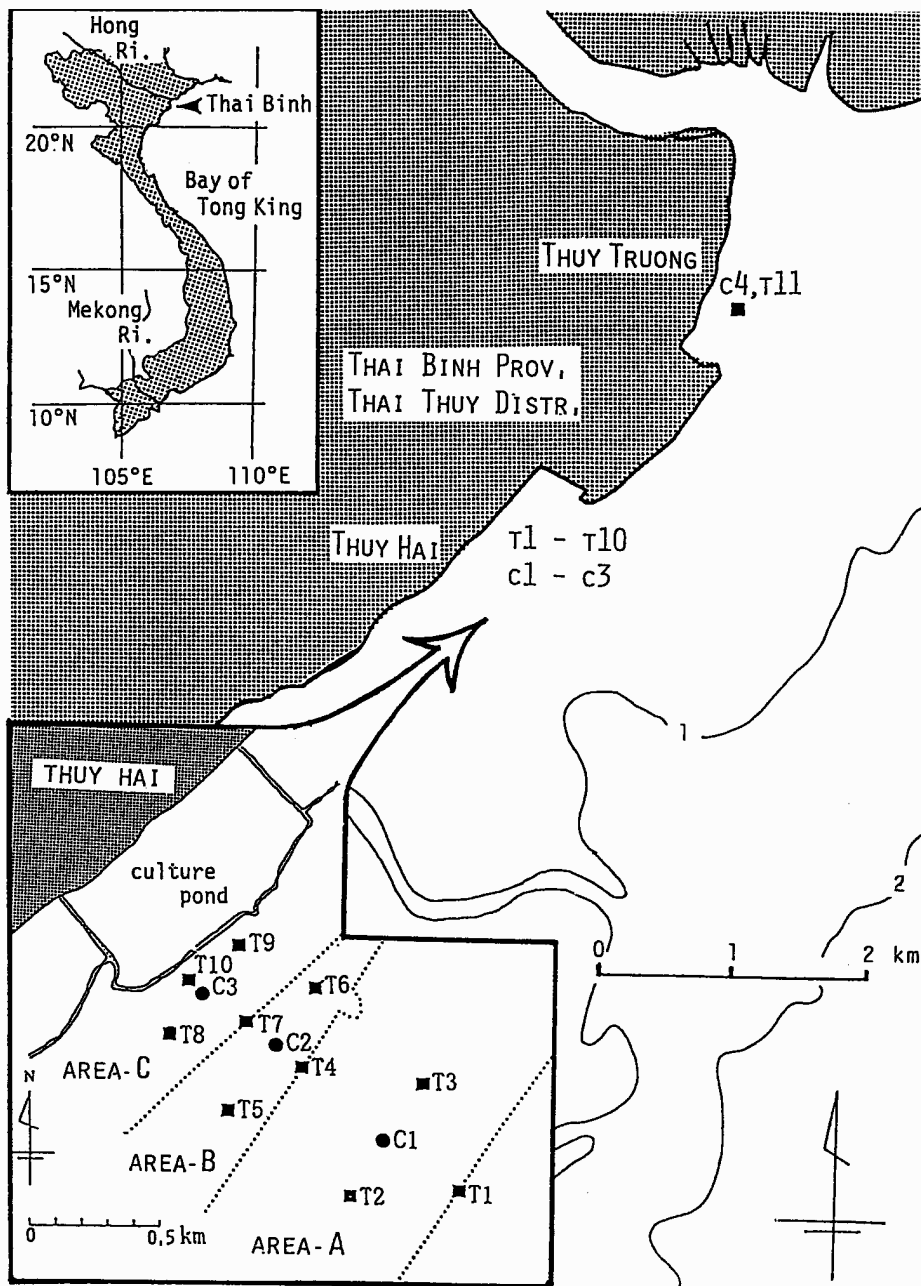


Figure 1. Location map and field sites.

area is composed of 3 parts, that is, Area-A of a ½-year-old trees (seedlings), Area-B of 2–3-year-old trees and Area-C of 5–6-year-old trees. These three areas touch each other and are continuous from offshore to an artificial sea dyke which protects shrimp and crab culture ponds. On the other hand,

in the coast of Thuy Truong, seeds of *Sonneratia caseolaris* were planted only 2 months before our studies.

Water levels were measured at 11 stations (Stns T1 to T11; see Figure 1) together with current velocities 2 cm above the sea floor at 4 stations

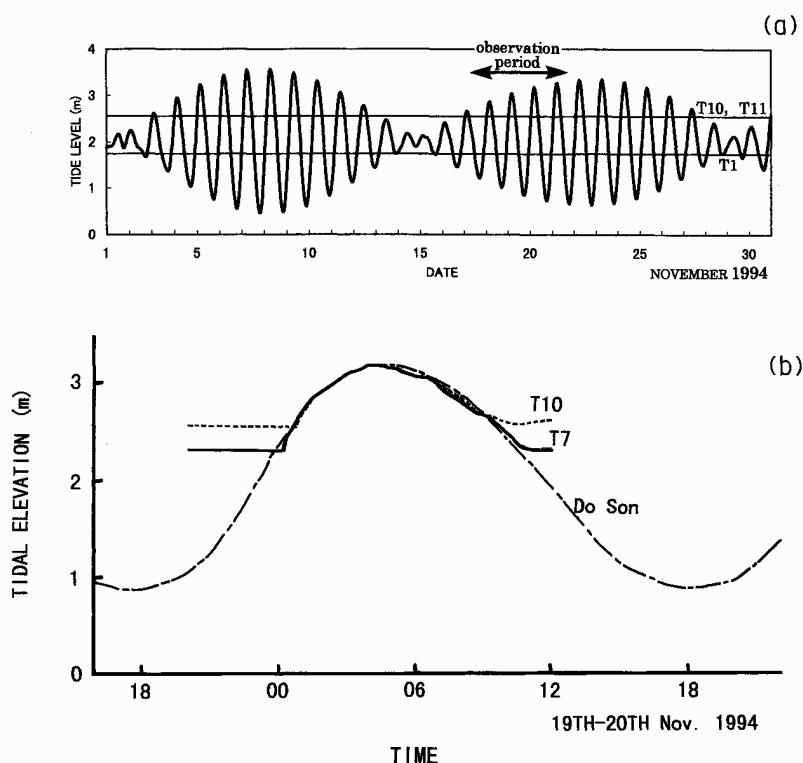


Figure 2. (a) Time series of predicted tidal height at Do Son, and sea floor elevations at Stns T1, T10 and T11. (b) Low-pass filtered tidal elevations at Do Son and Stns T7 and T10.

(Stns C1 to C4 in Figure 1). RMD-type water level gauges (Rigoshia & Co., Ltd.) and ACM-8M electro-magnetic current meters (Alec Electronics Co., Ltd.) were used with 2-sec sampling period.

Analyses and discussion

Tidal variation of water level

Figure 2a shows the predicted tide level at Do Son 20km far north of Thuy Hai as well as the levels of the sea floors at Stns T1, T10 and T11. Station T1 is submerged 2/3 of a day throughout the year, and at neap tide remains submerged for a few days. On the other hand, at Stns T10 and T11 the bottom mud emerges 2/3 of a day throughout the year, and at neap tide it can remain exposed for a few days.

Figure 2b shows the tidal elevations at Stns T7 and T10 after filtering out high-frequency from the raw data, together with the tide at Do Son. The

tides at Stns T7 and T10 rise faster at the early stage of flood tide and fall slower at the latter stage of ebb tide than at Do Son. This finding may be explained by the effect of flow resistance due to the mangrove vegetation and the bottom mud. However, these changes are considerably smaller than those in mangrove swamps dominated by *Rhizophora* spp. or *Bruguiera* spp. (Wolanski et al., 1992; Mazda et al., unpubl. data), probably because *Rhizophora* spp. and *Bruguiera* spp. have intricate and large prop roots or numerous pneumatophores, compared to *Kandelia candel*.

High-frequency sea level fluctuations

The high-frequency sea level fluctuations (Figure 3) are due to the swell (period: 5–8 sec) with the characteristics of the long wave in shallow waters. The wave height of the swell at all stations increases with increasing tidal level or water depth, and

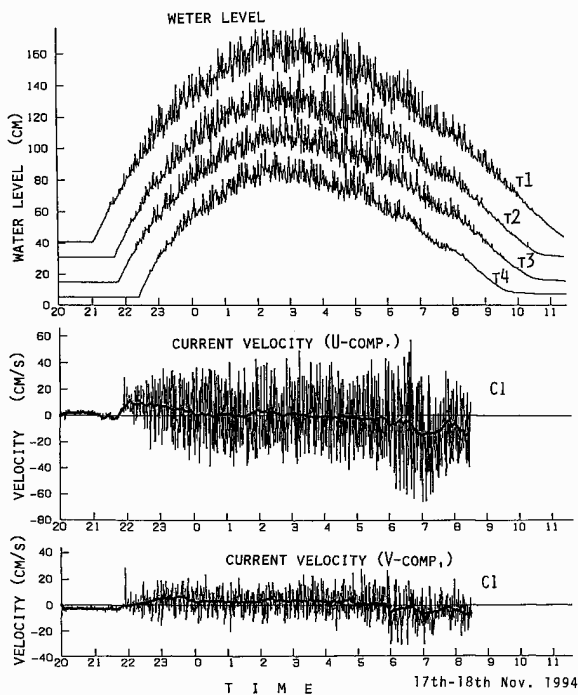


Figure 3. Time series of water elevations at Stns T1 to T4 and current velocity at Stn. C1 (shifted vertically for visualization). U- and V-components of currents are respectively perpendicular and parallel to the coast. The thick lines in the velocity time series are the low-pass filtered velocity.

decreases with increasing proximity to the coast. These findings suggest wave energy loss caused by bottom friction and resistance to flow due to mangrove vegetation.

Characteristics of current velocity

The high-frequency current velocity (Figure 3) are due to the swell. The amplitude of current velocity is as large as 0.4 ms^{-1} offshore (Stn. C1), and it is much smaller (0.1 ms^{-1}) inshore (Stn. C3; not shown). The velocity vector is essentially perpendicular to the coast.

The low-frequency velocities (the thick lines in Figure 3) vary somewhat tidally. At all stations the magnitude of low-frequency velocity is small compared to that of high-frequency. The high-frequency velocity fluctuations, i.e. the turbulent flow, have an effect to disperse materials such as seeds of mangroves, fish larvae, nutrients in water and

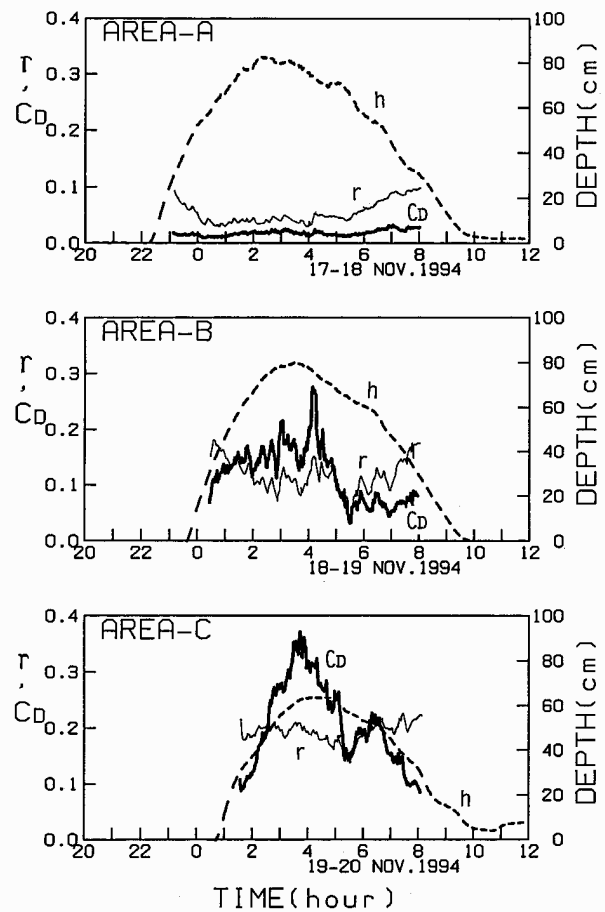


Figure 4. Time series plot of the rate of wave reduction r , the resistance coefficient C_D and the water depth h . r and C_D are calculated by using the significant wave heights (top) at Stns T1 and T2 in Area-A, (middle) at Stns T4 and T7 in Area-B, and (bottom) at Stns T7 and T10 in Area-C.

bottom sediments. On the other hand, even if the magnitude of low-frequency velocity is small, it plays an important role to transport materials far distance during a long time.

Wave reduction due to mangrove vegetation

The rate of wave reduction per 100 m in the direction of wave propagation is defined as

$$r = \frac{H_S - H_L}{H_S} \quad (1)$$

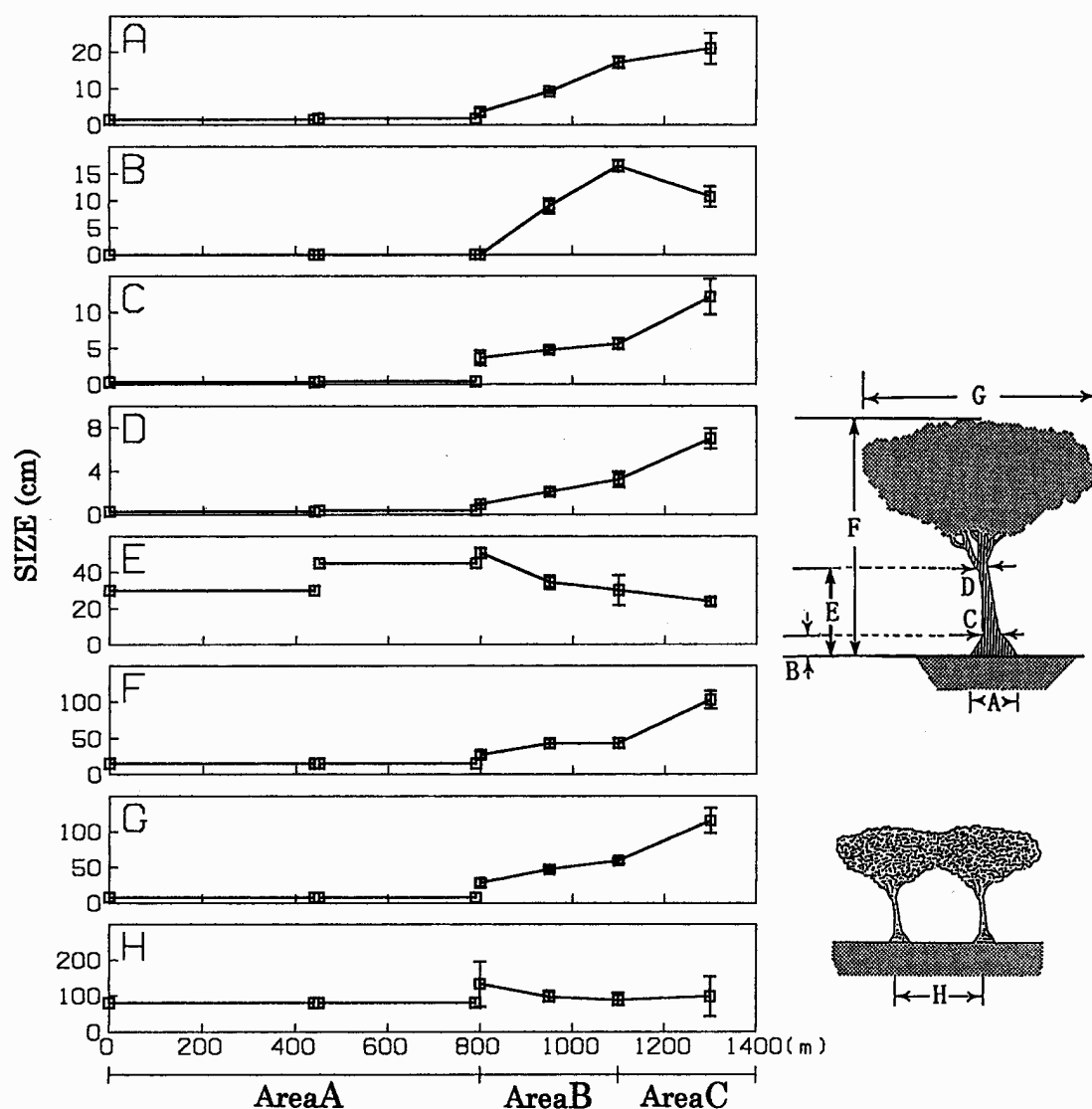


Figure 5. Cross-shelf changes in mangrove vegetation. Vertical bars mean the standard deviation.

where H_S is the wave height at a sea side station and H_L is the wave height at a station 100m further inshore. The variations of r in Areas-A, B and C, individually, are shown in Figure 4. The value of r varies little in a tidal cycle and is the greatest in Area-C, smaller in Area-B and the smallest in Area-A. As shown in Figure 5, the sizes of the trees increase with the number of years after planting. The differences in the value of r between Areas-A, B and C (Figure 4) correspond to the differences in the degree of growth of the vegetation

between those areas, demonstrating the effect of the drag force due to the trees.

Variation of the resistance coefficient

The drag force for the water flowing between the trees occurs throughout the whole water depth from the sea floor to the water surface. For tidal currents, Wolanski et al. (1992), Furukawa and Wolanski (1996) and Mazda et al. (unpubl. data)

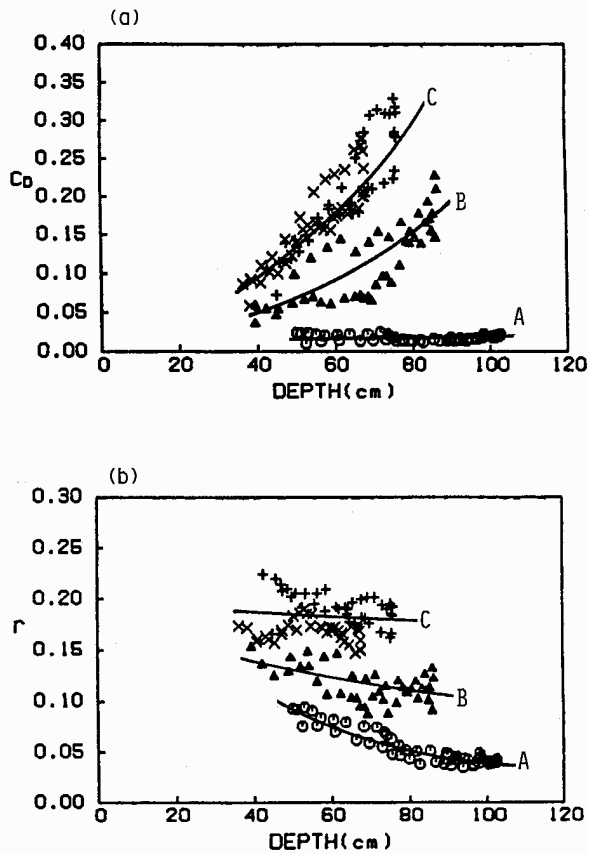


Figure 6. (a) Variation of the resistance coefficient C_D with the water depth h . (b) Variation of the rate of wave reduction r with the water depth h . The smooth lines are the suggested best-fit.

have studied the drag force on pneumatophores, prop roots, trunks and canopies. These processes occur also at high frequencies, but until this study none of quantitative information was available.

The wave reduction caused by the bottom friction in shallow, vegetation-free coastal waters has been discussed since Bretschneider and Reid (1954). Here, we provisionally calculate the effect of the flow resistance due to mangrove vegetation distributed throughout the whole water depth as a bottom friction. In shallow waters the wave reduction caused by the bottom friction is obtained as

$$\frac{H_2}{H_1} = \frac{1}{1 + \frac{\pi^5 K_s^2}{\sqrt{2} g^2 T^4} C_D H_1 \Delta x \left(\sinh \frac{2\pi h}{L} \right)^{-3}} \quad (2)$$

In Eq. (2), H_1 and H_2 are the wave heights respectively at an offshore station and an inshore station, Δx is the distance between these two stations, h is the mean depth between these two stations, T is the wave period, L is the wave length, g is the acceleration due to gravity, K_s is the shoaling coefficient and C_D is the resistance coefficient due to the bottom stress which is defined by

$$\tau = \frac{1}{2} C_D \rho u^2, \quad (3)$$

where ρ is the density of sea water and u is the current velocity in the direction of wave propagation (Bretschneider and Reid, 1954).

For the long wave such as the swell in shallow waters, Eq. (2) is approximated as

$$\frac{H_2}{H_1} = \frac{1}{1 + \frac{C_D \pi H_1 \Delta x}{32 \sqrt{2} h^2}} \quad (4)$$

From Eq. (4), the resistance coefficient C_D is calculated as

$$C_D = \frac{32 \sqrt{2}}{\pi} = \frac{h^2}{H_1 \Delta x} \left(\frac{H_1}{H_2} - 1 \right) \quad (5)$$

The variations of C_D in Areas-A, B and C, individually, are shown in Figure 4. Values of C_D vary significantly between Areas-A, B and C. In Area-A, the tidal change in C_D is not apparent. C_D in Area-C is the largest and varies greatly between 0.1 and 0.4.

The dependence of C_D on the water depth varies between Areas-A, B and C (Figure 6a). The magnitude of C_D in Area-A is the same order of that (0.01) calculated from the wave energy loss due to the bottom friction by Bretschneider (1954). This finding means that the wave reduction in Area-A is caused by the bottom friction, and the drag force on the plants is insignificant. On the other hand, in Area-C, C_D increases considerably with increasing water depth. Since soil conditions are similar in all areas and since mangrove trees are much more developed in Area-C than in Areas-A and B, the

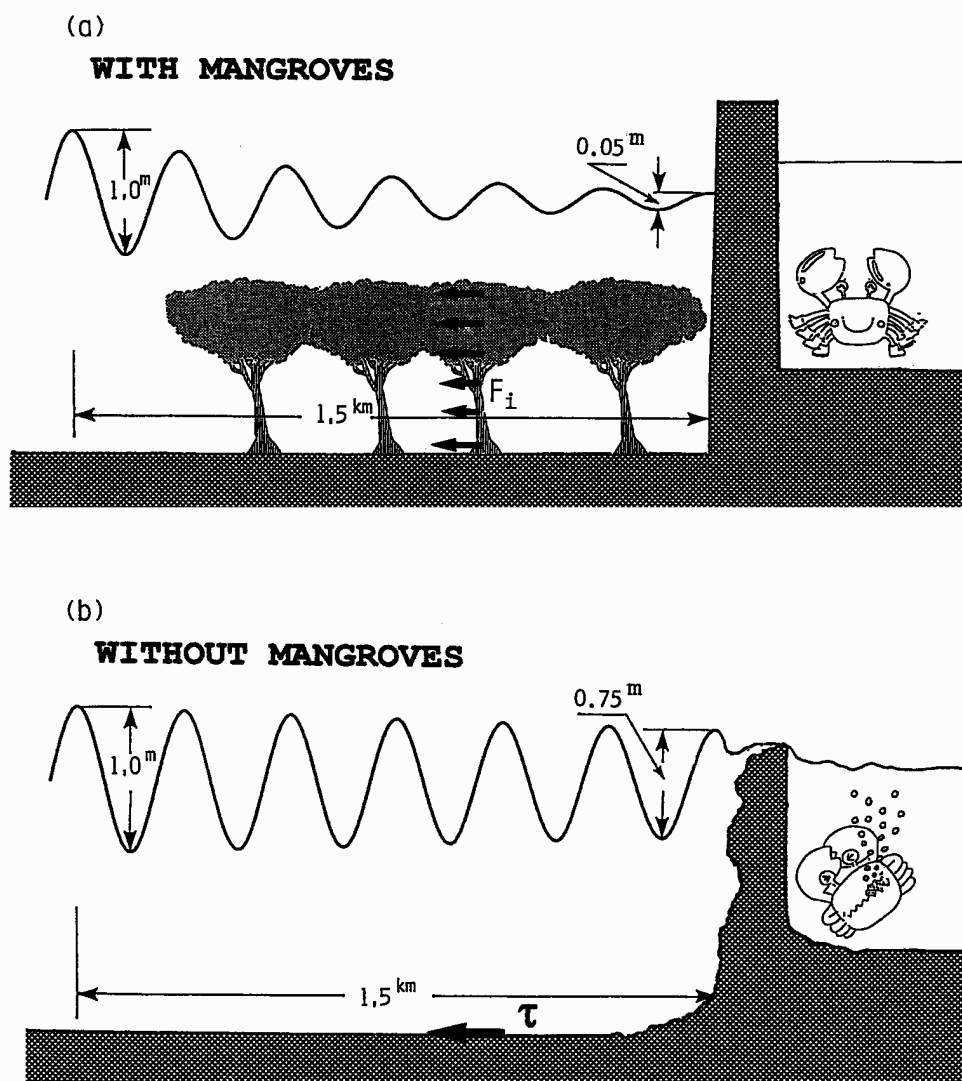


Figure 7. Differences in the effect of wave reduction (a) with and (b) without mangroves. In (a) the drag force on the plants ΣF_i occurs throughout the water depth. In (b) the bottom friction τ occurs only at the sea floor.

dependence of C_D on the water depth in Area-C implies that the wave reduction is strongly caused by the vegetation density (submerged trunks, branches and leaves). In Area-B, the magnitude of C_D lies between those of Areas-A and C, because the vegetation density lies between those of Areas-A and C.

The bottom friction coefficient depends on the wave period (Iwagaki and Kakinuma, 1967). The scattering of the data in each area in Figure 6(a) may be due to the variation of wave period from 5 to 8 seconds during the observation.

Effect of mangrove vegetation density on wave reduction

In Area-A, the value of r decreases with increasing water depth (Figure 6b), because, with little vegetation, the wave energy loss is caused by bottom friction only. On the other hand, in Area-C, r is about constant, or independent of water depth because the wave energy loss in Area-C is caused by the drag force on the submerged plants which increase with increasing water depth.

Our finding that in a well grown mangrove area

the effect of wave reduction does not decrease with increasing water depth, has important practical implications. Indeed, tropical depressions, storms and typhoons often occur in the central and northern coasts of Vietnam, and induce the mean sea level rise (Hong and San, 1993). Furthermore, the sea level may rise by 0.6 m within the next century due to global warming. In such larger water depths, the high density of vegetation distributed throughout the whole water depth will still work effectively to reduce wave and protect the coast from wave erosion.

At present, in Area-A the rate of wave reduction r is small (0.01–0.03) when the water depth is larger than 1 m, because the vegetation is still young and sparse. However, in Area-C where mangrove trees of 5–6-years-old are well established, r is as large as 0.20. Within six years all the trees in Area-B and also in Area-A will have grown sufficiently so that the wave height of 1 m at the open sea will reduce to 0.05 m at the coast (Figure 7a), while without mangroves in this coastal area the waves would arrive at the coast with wave height of 0.75 m (Figure 7b).

The distortion of the tidal curve in this area is considerably smaller (Figure 2b) than that in swamps vegetated by *Bruguiera* spp. or *Rhizophora* spp.. This fact suggests that the effect of the drag force on *Kandelia candel* on the long period waves such as tidal waves is weak compared to those of *Bruguiera* spp. and *Rhizophora* spp., because *Kandelia candel* has no pneumatophore. It is necessary to assess the dependences of the drag force on various mangrove species on the wave period within a wide range of waves including wind waves, storm surges, tsunamis and tides. The wave reduction results from the integrated energy loss through the whole width of the vegetated area. The vegetation density and the width of the area to be planted are also important factors for protecting the coast from wave erosion.

Conclusion

The plantation of *Kandelia candel* at the coastal area of Thuy Hai has the effect of significantly reducing swell with the periods of 5–8 sec. and protecting the coast. A six-year-old mangrove trees

strip 1.5 km wide will reduce 1 m high waves at the open sea to 0.05 m at the coast. Due to the high density of vegetation distributed throughout the whole water depth, the effect of wave reduction is constant even when the water depth increases. Further investigations are necessary to quantify the dependences of the wave reduction on the water depth, the wave period, the wave height, the species of mangrove trees and the distance between trees.

Acknowledgments

This study was carried out by the Action for Mangrove Reforestation (ACTMANG) supported by a grant of Postal Savings for International Voluntary Aid, Japan. We thank Mr Koichi Tsuruda and Mr Tetsumi Asano of ACTMANG, Mr Shinji Hatori at Gunma University, Mr Tran Toung Truc at Hanoi National University, the People's Committees of Thai Binh province, of Thai Thuy district, of Thuy Hai village, of Thuy Truong village, the coastal people for their help and Dr Tran Duc Thanh of Haiphong Institute of Oceanology provided data on the sea level at Do Son. Finally, we thank Dr Eric Wolanski at the Australian Institute of Marine Science for reviewing the manuscript.

References

- Bretschneider, C.L. and Reid, R.O. 1954. Modification of wave-height due to bottom friction, percolation and refraction. B.E.B. Tech. Memo., No. 45, 1–36.
- Bretschneider, C.L. 1954. Generation of wind waves over a shallow bottom. B.E.B. Tech. Memo., No. 51, 1–24.
- Furukawa, K. and Wolanski, E. 1996. Sedimentation in mangrove forests. *Mangroves and Salt Marshes*, 1, 3–10.
- Hong, P.N. and San, H.T. 1993. *Mangroves of Vietnam*. IUCN, Bangkok, Thailand, 173 pp.
- Iwagaki, I. and Kakinuma, T. 1967. On the bottom friction factors off five Japanese coasts. *Coast. Eng. Japan*. Vol.X, 13–22.
- Kjerfve, B. 1990. Manual for investigation of hydrological processes in mangrove ecosystems. UNESCO/UNDP, Tompson Press, 79 pp.
- Lugo, A.E. and Snedaker, S.C. 1974. The ecology of mangroves. *Annual Review of Ecology and Systematics* 5: 39–64.
- Mazda, Y., Yokochi, H. and Sato, Y. 1990. Groundwater flow in the Bashita- Minato mangrove area, and its influence on

- water and bottom mud properties. *Estuar., Coast. and Shelf Sci.* 31: 621–638.
- Mazda, Y. 1993. Present situation of physical study in mangrove regions. *J. Fac. Marine Sci. and Tech., Tokai Univ.* 35: 169–184.
- Mazda, Y., Kanazawa, N. and Wolanski, E. 1995. Tidal asymmetry in mangrove creeks. *Hydrobiologia* 295: 51–58.
- Ridd, P.V., Wolanski, E. and Mazda, Y. 1990. Longitudinal diffusion in mangrove-fringed tidal creeks. *Estuar., Coast. and Shelf Sci.* 31: 541–554.
- Wolanski, E., Mazda, Y., King, B. and Gay, S. 1990. Dynamics, flashing and trapping in Hinchinbrook Channel, a giant mangrove swamp, Australia. *Estuar., Coast. And Shelf Sci.* 31: 555–579.
- Wolanski, E., Mazda, Y. and Ridd, P.V. 1992. Mangrove hydrodynamics. In: Robertson, A.I. and Alongi, D.M. (eds), *Tropical Mangrove Ecosystems. Coastal and Estuarine Studies 41*. American Geophysical Union, Washington, DC, 43–62.

Annex RJ-7

J.M. Smoak, S.R. Patchneelam, "Sediment Mixing and Accumulation in a Mangrove Ecosystem: Evidence from ^{210}Pb , ^{234}Th and ^7Be ", *Mangroves and Salt Marshes*, Vol. 3, 1999, pp. 17-27.

Sediment mixing and accumulation in a mangrove ecosystem: evidence from ^{210}Pb , ^{234}Th and ^7Be

Joseph M. Smoak^{1,*} & Sambasiva R. Patchineelam²

¹*Department of Geological Sciences, University of South Carolina, Columbia, SC 29208, USA*

²*Departamento de Geoquímica, Universidade Federal Fluminense, Niterói, Brazil*

(Received: 30 December 1997; accepted in revised form: 12 August 1998)

Key words: lead, thorium, beryllium, Brazil

Abstract

^{210}Pb , ^{234}Th and ^7Be activities were measured to establish sediment accumulation rates, estimate sediment mixing rates, and determine the depth of the sediment mixed layer in the Sepetiba Bay mangrove ecosystem near Rio de Janeiro City, Brazil. Three sediment cores were collected from Enseada das Garças, a typical exposed tidal flat region with a sequence of sedimentary features. The seaward edge of this sequence is a mud flat with the landward portion covered with *Spartina alterniflora* followed by mangrove vegetation. An additional core was collected on an overwash island near Barra de Guaratiba, which is covered with mangroves without a mud flat or *Spartina alterniflora* sequence. Sediment accumulation rates were determined to range up to 1.8 cm/yr with the *Spartina alterniflora* having the maximum rate. Mixing rates were estimated for the *Spartina alterniflora* core at 40 cm²/yr based on ^{210}Pb and ^7Be from the upper mixed region of the core. The ^{234}Th activity in this core suggested that either mixing or the input of ^{234}Th were not in steady state. The sediment mixed region depth ranged from 4 cm to greater than 30 cm. At the Enseada das Garças site the mixing depth decreased in the landward direction (i.e. mud flats > 30 cm, *Spartina alterniflora* 11 cm, mangroves 4 cm). Along with this decrease in sediment mixing depth was a shift from physical to biological mixing. The Barra de Guaratiba core had a sediment mixed layer of 13 cm as a result of physical and intense biological activity.

Introduction

Recently, reclamation of mangrove ecosystems for agricultural, industrial, urban and other forms of development has been increasing and causing irreversible damage in coastal regions throughout the tropics (Hatcher et al., 1989). Along with the destruction of the mangroves comes the anthropogenic effects associated with the new developments. The mangrove sediments contain a historical record of information on the temporal changes that have been brought about as a result of these actions. This record is altered or smeared by the effects of sediment mixing (i.e. physical and/or biological mixing), which influences the preservation of the physical sedimentary structures (Nittrouer and Sternberg, 1981). The alteration

of the record depends on the intensity, depth and nature of the sediment mixing as well as the sediment accumulation rate. Sediment mixing also affects the alteration of biogenic components and pore-water concentrations of dissolved chemical species within the sediment mixed layer (Schink and Guinasso, 1977; Berner, 1980; Aller, 1982). In addition, Yingst and Rhoads (1980) documented that microbial activity is influenced by sediment mixing rates.

Mangroves dominate approximately 75% of the world's coastline between latitudes 25° N and 25° S (McGill, 1959). These tropical coastal areas are responsible for about 75% of the sediment discharged from land to sea. Often mangroves are considered to be equivalent to salt marshes that develop on extensive suitable intertidal zones with great supply of fine-grained sediment and abundant rainfall or fresh water supply (Walsh, 1974). Geologists view mangrove shorelines as sediment sinks and mangroves

* Present Address: Department of Fisheries and Aquatic Sciences, University of Florida, 7922 NW 71st Street, Gainesville, FL 32653, USA

are thought to accelerate the rate of mud accretion (Woodroffe, 1992). Young intertidal deposits that are covered by vegetation are protected against erosion by the dense network of trunks and pneumatophores that act as efficient sediment trappers (Scoffin, 1970). The underground root systems also play an important role as sediment binders (Scoffin, 1970). The sediments accumulate at the slack of high tide and after floods bringing material from the sea and land. The accumulating sediments are a mixture of clastic sediment and organic materials produced by the plants and their associated fauna (Bird, 1971).

While many human communities have a traditional dependence on mangroves, understanding mangrove ecosystems lags behind that of many other ecosystems (Bunt, 1992). Despite the acceptance that mangrove ecosystems are important sinks for sediments, few studies have addressed sediment mixing and accumulation in this environment. Simple accumulation measurements have been made by simulating pneumatophores using rods or stakes. In Australia, sedimentation rates determined by this method have shown varying rates from -11 to $+4.6$ mm/yr (Spenceley, 1977, 1982). The pattern of sedimentation or erosion determined by the stake method has been questioned as the stakes themselves may alter these processes. Long-term accumulation rates have been determined using radiocarbon (Woodroffe, 1990). However, only one study examining sedimentation rates over the past 100 years has been conducted in which Lynch et al. (1989) determined accumulation rates of up to 1.7 and 4.4 mm/yr in mangroves of Florida and Mexico, respectively, using ^{210}Pb and ^{137}Cs . ^{210}Pb has proved to be a valuable tracer of sediment mixing and accumulation in a variety of environments (Koide et al., 1972; Benninger et al., 1979; Nittrouer and Sternberg, 1981; Nittrouer et al., 1984; Carpenter et al., 1984; Davis et al., 1984; Sharma et al., 1987; Lynch et al., 1989; Crusius and Anderson, 1991; and many others). However, with the exception of Lynch et al. (1989), this approach has been neglected in mangrove ecosystems. Short-lived radionuclides ^{234}Th and ^7Be have been examined to determine sediment mixing rates in a variety of environments (Aller and Cochran, 1976; Aller et al., 1980; Krishnaswami et al., 1980; Aller and DeMaster, 1984; DeMaster et al., 1985; Cacey et al., 1986; Rice, 1986) but have not been applied to mangrove ecosystems.

^{210}Pb and ^{234}Th are naturally occurring radionuclides of the ^{238}U decay series with a 22.3 year and 24.1 day half life, respectively. ^{210}Pb is used to examine sediment processes on a 100 year time scale. ^{210}Pb is supplied by its effective parent ^{226}Ra

in seawater and from ^{222}Rn in the atmosphere. The atmospheric source is produced as ^{222}Rn , a short-lived ($t_{1/2} = 3.8$ days) intermediate daughter of ^{226}Ra , escapes from the earth's crust, decays to ^{210}Pb , and is deposited back to the ground. In most shallow water environments, atmospheric input is the major source. ^{234}Th is used to examine mixing processes on a 100 day time scale and is produced in seawater from ^{238}U . The cosmogenically produced radionuclide ^7Be also is a useful tracer with a 53 day half life that can be used to examine short-time scale (i.e. 250 days) mixing events. ^7Be is produced in the atmosphere by spallation reactions of cosmic rays. These three tracers have the very advantageous property of being particle reactive and therefore, particle bound in the marine environment. This property combined with a known decay rate allows the tracers to be used in the investigation of sediment mixing and accumulation on the respective time scales of the individual radionuclides. In the present study we use these radionuclides to establish sediment accumulation rates, estimate sediment mixing rates and determine the depth of the sediment mixed layer in the Sepetiba Bay mangrove ecosystem near Rio de Janeiro City, Brazil.

Study area

Brazil has 10% of the world's mangrove ecosystems most of which form a strip along a large portion of the coast of Brazil from Amapá in the north to Santa Catarina in the south. In the northern states, the mangrove systems are well preserved, due to a low population density and limited industrial development. However, the southeastern coast has been highly influenced by urban and industrial development (Kjerfve and Lacerda, 1993).

Sepetiba Bay is a highly industrialized area located 60 km west of the city of Rio de Janeiro (Figure 1). Its first industry was a zinc smelter, which started around 1963 (FEEMA, 1980). Since then almost 400 industries, mainly pyro-metallurgical plants, have been established in the drainage basins of the São Francisco canal and Rio Guandu, which are the fresh water inputs into the bay. Water circulation in the bay is controlled by the tides and winds. Almost 50% of the inner bay area is characterized by tidal flats exposed during low tide. Borges et al. (1989) studied sediments in the bay and compared bathymetric charts of 1868 and 1981. They determined that the north and northeastern parts of the bay are areas of sediment accumulation whereas the southern inner bay along the Marambaia barrier island is an erosional area.

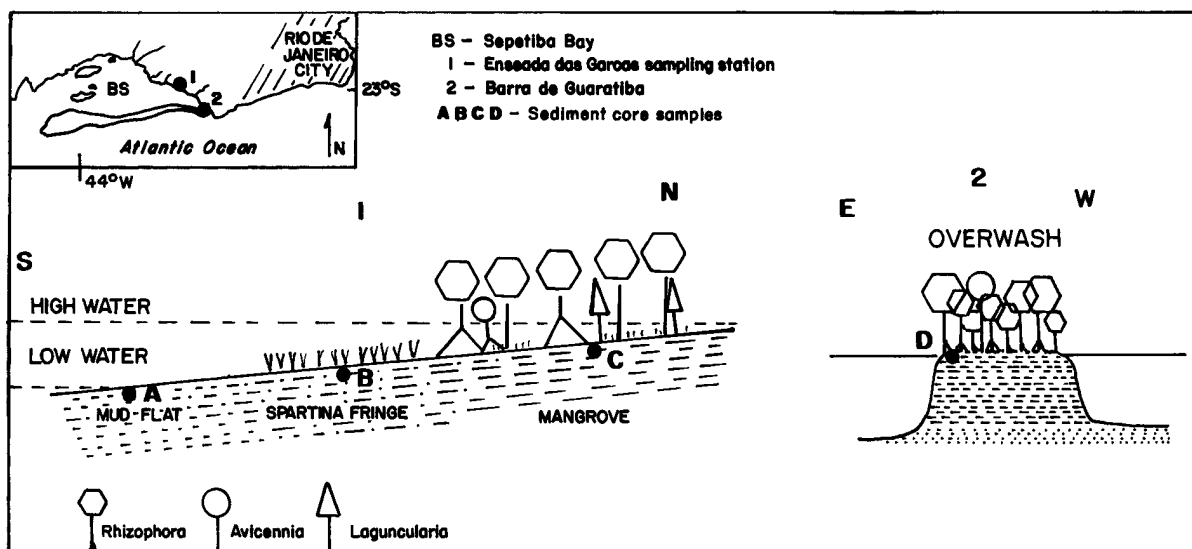


Figure 1. Map of Sepetiba Bay and location of sampling sites.

Two sampling locations within the bay were selected for this study: (1) Enseada das Garças and (2) Barra de Guaratiba (Figure 1). Enseada das Garças has typical tidal flats of the northeastern part of the bay, exposed during low tide with a sequence of sedimentary features. At the seaward edge a 30 m mud flat swath along the coastline with half of the area covered by the sea grass *Spartina alterniflora* Loisel followed by 70 m of mangrove vegetation. The mud flat sediments consist of 95% silt and clay sized particles. At the spartina fringe location grain size ranges from 70–90% silt and clay with roots penetrating to 20 cm. The mangrove sediment grain size is 65–75% silt and clay with roots down to 14 cm. Three characteristic species compose the mangrove community: *Rhizophora mangle* L., *Avicennia schaueriana* Stapf. et Leechman and *Laguncularia racemosa* (L.) Gaertn.

The sediment dwelling fauna in the mangroves includes the largest number of species, in particular crustaceans and mollusks. Typical representatives are the crabs *Cardiswa guanhumi*, *Ucides cordatus*, the mussels *Mytella guyanensis* and *M. falcata*; the cockles *Anomalocardia brasiliensis* and *Iphigenia brasiliensis* and the snail *Mellanpus coffeus* (Kjerfve and Lacerda, 1990).

At the Barra de Guaratiba station the mangroves are on an overwash island without a mud flat sequence. The island is located in front of the canal, which separates the continent from the Marauibia barrier island. The mangrove vegetation is similar to the Enseada das Garças site in composition, and the fauna in the sediment is the same except the crabs, *Cardisouina*

guanhumi, are in large number and are responsible for intensive bio-mixing compared to the other site. The sediment grain size is 65–75% clay and silt with roots down to 13 cm.

Sediment mixing and accumulation model

Sediment mixing, sediment accumulation, radioactive decay, and parent radionuclide supported production affect radiochemical profiles in the sediments. These processes are included in the following steady-state equation (Guinasso and Schink, 1975):

$$D \frac{\partial^2 A}{\partial z^2} - S \frac{\partial A}{\partial z} - \lambda A + P = 0, \quad (1)$$

A is the total activity of the radionuclide (dpm/g), D is a coefficient characterizing the sediment mixing rate (cm^2/y), z is depth below the sediment–water interface (cm), S is sediment accumulation (cm/yr), λ is the decay constant (1/yr), and P is the production from parent radionuclide (dpm/g/y). By using the excess activity the production term may be omitted. The solution to this equation can be rearranged to calculate accumulation rates.

$$S = \frac{\lambda z}{\ln(A_0/A_z)} - \frac{D}{z} \left[\ln \left(\frac{A_0}{A_z} \right) \right]. \quad (2)$$

Sediment mixing by biological and physical processes is modeled as a diffusive process. While sediment mixing is not truly a diffusive process, it may appear like a diffusive process if non-diffusive individual events

Table 1. Excess ^{210}Pb , excess ^{234}Th and ^7Be activities (dpm/g)

Spartina fringe (B)	ex ^{210}Pb dpm/g	ex ^{234}Th dpm/g	^7Be dpm/g
0-1	5.98	1.17	nd
1-2	6.02	nd	7.05
2-3	5.47	nd	3.53
3-4	4.91	nd	3.55
4-5	3.39		
5-7	5.25		
7-9	2.66		
9-11	4.87		
11-13	5.39		
13-15	4.21		
20-25	2.84		
25-30	1.20		
30-35	0.63		
30-35	0.16		
Mud flat (A)			
0-1	2.79		
1-2	3.45		
2-3	3.73		
3-4	2.95		
4-5	3.40		
6-7	3.97		
7-8	3.65		
9-10	3.08		
13-16	3.24		
25-30	3.18		
Mangrove (C)			
0-1	4.00		
1-2	3.52		
2-3	3.72		
3-4	4.55		
4-5	4.27		
6-7	2.85		
7-8	3.62		
9-10	0.86		
25-30	0.03		
Overwash (D)			
0-1	2.00		
1-2	1.71		
2-3	1.61		
3-4	1.54		
4-5	1.37		
6-7	1.57		
7-8	1.73		
9-10	1.91		
10-13	2.10		
16-19	0.50		

are integrated over many events occurring rapidly as compared to the tracer time scale. Equation 2 can be further simplified to equation (3) if mixing is rapid and accumulation slow.

$$D = \lambda \left[\frac{z}{\ln(A_0/A_z)} \right]^2. \quad (3)$$

Eventually sediment reaches a depth where it is no longer affected by sediment mixing. Below the region affected by sediment mixing the sediment accumulation rate can be calculated ignoring the mixing term using the following equation:

$$S = \frac{\lambda z}{\ln(A_0/A_z)}. \quad (4)$$

As stated above, sediment mixing is not truly diffusive and sediments are moved advectively by biological and physical processes. If these advective processes occur on a time scale similar to the tracer time scale the tracer profile may not appear as diffusive. In order for a diffusion model to accurately represent the physical process, sediment particles must be moved in a random manner over short distances. Therefore, a large step length in the advection of sediment may violate the diffusion model assumptions. Selective feeding by benthic fauna due to size, shape, texture or composition also would violate the assumption of diffusive mixing by creating non-random movement. Therefore, not all mixing will appear as a diffusive process as revealed by some or all tracers.

Methods

Four sediment cores were collected by inserting a core tube with a 7 cm diameter into the sediment during low tide in October 1995. The core locations are shown in Figure 1. Three of these cores are from the Enseada das Garças station (1): (A) mud flat, (B) Spartina fringe and (C) mangrove. The fourth core was taken from the Barra de Guaratiba station (2) on a overwash island (D). The cores were immediately transferred to the laboratory and subsampled as indicated in Table 1.

^{210}Pb , ^{226}Ra , ^7Be and ^{234}Th measurements were made using a semi-planar intrinsic germanium detector coupled to a multichannel analyzer. Wet, homogenized sediment was placed into preweighed 70 ml plastic petri dishes. Activity was calculated by multiplying the counts per minute by a factor that includes the gamma-ray intensity and detector efficiency. This factor was determined from standard calibrations. Identical geometry was used for all samples. ^{210}Pb activity was determined by the direct measurement of 46.5 KeV

gamma peak. ^{226}Ra activity was determined by a weighted average from two ^{214}Pb energies, 295.2 and 351.9, and a ^{214}Bi gamma peak at 609.3 KeV (Moore, 1984). For ^{226}Ra measurements, the packed samples were set aside for at least 21 days to allow for ^{222}Rn to ingrow and secular equilibrium to be established between ^{226}Ra and its granddaughters ^{214}Pb and ^{214}Bi . Excess ^{210}Pb activity was calculated by subtracting the supported ^{210}Pb (i.e. ^{226}Ra activity). ^7Be was determined directly from its gamma peak at 477.6 KeV. ^{234}Th activity was determined from the direct measurement of its 63.3 KeV gamma peak. ^{234}Th supported by ^{238}U was determined by recounting the samples after allowing for the decay of the excess ^{234}Th . The activity measured in the second counting was subtracted from the first giving excess ^{234}Th (activity not supported by ^{238}U). ^7Be and excess ^{234}Th were corrected for the decay since the time of collection. For gamma energies below about 295 KeV self-absorption is significant, and the corrections were made using the approach of Cutshall et al. (1983). After gamma counting, samples were dried to determine dry weight.

The above gamma method was used for the Spartina fringe (B) core while for the mud flat (A), mangrove (C) and the overwash (D) cores only ^{210}Pb was determined. For the latter cores ^{210}Pb activity was measured by alpha counting its granddaughter, ^{210}Po , using a technique similar to DeMaster et al. (1985). A ^{209}Po spike (used as a yield determinant) was added to 3 g of dried sediment prior to total dissolution with HF, HClO_4 , HNO_3 and HCl. After the sediment was dissolved, the sample was taken to dryness and then picked up in 6 N HCl. The 6 N HCl solution was diluted to 1.5 N HCl and several milligrams of ascorbic acid were added to the solution in order to complex iron. The polonium isotopes were removed from the solution by spontaneous electrodeposition onto a silver planchet and measured by alpha spectroscopy. ^{210}Pb activity from the deepest samples was used to determine the supported ^{210}Pb activity.

Results

Sample intervals, excess ^{210}Pb , excess ^{234}Th and ^7Be are all shown in the Table 1. Errors for ^{210}Pb , ^{234}Th and ^7Be are approximately $\pm 5\%$, 10% and 20% , respectively, based on one sigma counting statistics. Activity profiles for each core are shown in Figures 2–5. Diffusive mixing coefficients from near vertical profiles were calculated using equation (3). Since the profiles are nearly vertical, only a minimum estimate of the sediment mixing coefficient can be calculated. Sedi-

ment accumulation was determined from the slope of the least-squares regression line from the excess ^{210}Pb activity with depth below the sediment mixed layer using equation (4). This assumes no mixing below the sediment mixed layer. Mixing within this accumulation region would cause an over estimation of the accumulation rates. However, there is no evidence of deep mixing observed in these cores.

The mud flat core has an excess ^{210}Pb mixed region down to at least 30 cm, which is the entire length of the core. The excess ^{210}Pb activity within this deep mixed region increases slightly, therefore a sediment mixing rate was not calculated. Since the core did not penetrate the mixed layer it is impossible to calculate a sediment accumulation rate in this core.

The excess ^{210}Pb profile for the Spartina fringe core has a mixed region down to 11 cm. The minimum sediment mixing rate within this region is $40\text{ cm}^2/\text{yr}$ based on excess ^{210}Pb activity. This calculation ignores two points with somewhat lower activities caused by large shells in the samples. Below the mixed region the excess ^{210}Pb profile exhibits exponential decay. The least-squares line yields an accumulation rate of $1.8\text{ mm}/\text{yr}$. ^7Be penetrates to 4 cm depth while ^{234}Th is only detected in the surface interval. For this core it also was possible to calculate a mixing rate based on ^7Be . The ^7Be activity least-square line yields a mixing rate of $15\text{ cm}^2/\text{yr}$. In addition, the upper (1–2 cm) and lower (3–4 cm) ^7Be intervals were used and a $40\text{ cm}^2/\text{yr}$ mixing rate was calculated.

The mangrove core has an excess ^{210}Pb profile exhibiting mixing down to 4 cm. The excess ^{210}Pb activity increases within this region, therefore a sediment mixing rate was not calculated. Below the mixed region an accumulation rate of $1.2\text{ mm}/\text{yr}$ was calculated. This accumulation rate is only an estimate due to the few data points within the accumulation region.

The excess ^{210}Pb profile from the overwash core shows a mixed region down to 13 cm. The excess ^{210}Pb activity in this core increases slightly with depth, therefore it is not possible to calculate a sediment mixing rate. There is only one data point below this region. Using the last data point in the mixed region and the single point below we calculate an accumulation rate of $1.3\text{ mm}/\text{yr}$. This is only an approximation based on these two data points.

Discussion

Sediment mixing

The mixed layer depths range from 4 cm in the mangroves at the Enseada das Garças station to 13 cm on

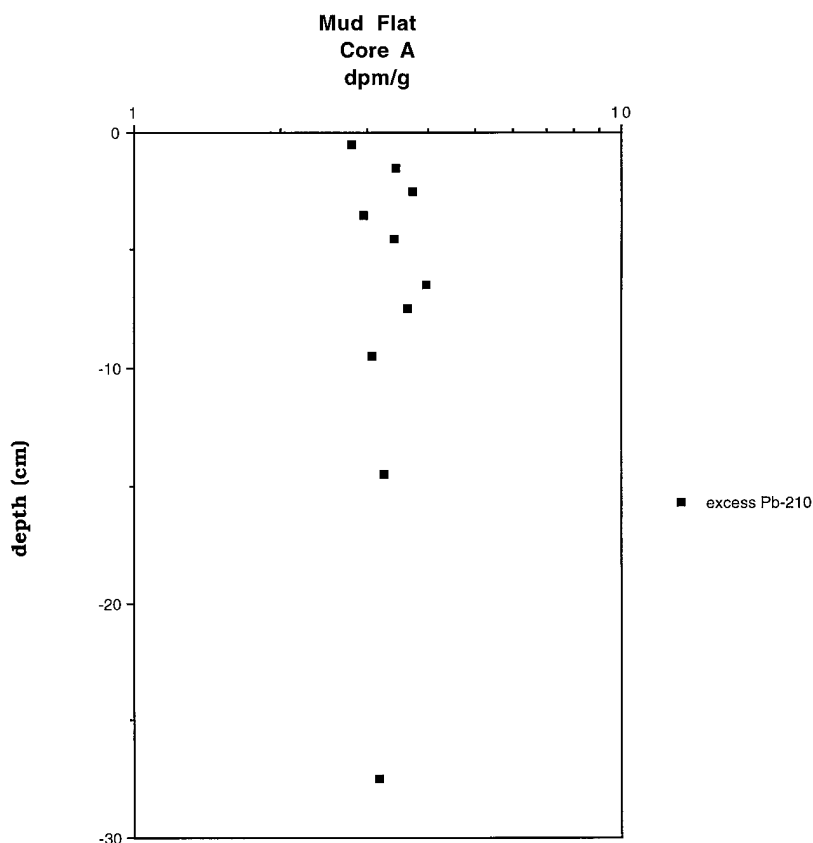


Figure 2. Excess ^{210}Pb activity profile.

the overwash at the Barra de Guaratiba station. However, the mud flat region at the Enseada das Garças station is an exception where mixing is at least to 30 cm depth, which was the maximum depth of penetration for this core. This deep mixing is the result of intensive physical mixing as benthic fauna are absent. As the tide rises sediment is resuspended, and at high tide the mud flat sediment is highly disturbed with much sediment in suspension (direct observation). During cold front events, this physical disturbance is very intensive, which happens almost 50 times a year and mainly in the spring season.

In the *Spartina* fringe core, the excess ^{210}Pb shows a mixed layer down to 11 cm. Due to the presence of the *Spartina*, this region is influenced less by physical mixing than the mud flat and more by the many species of sediment fauna mentioned in the study site description. From the ^{210}Pb profile in this mixed region, a minimum sediment mixing rate can be calculated based on the mixing required to produce the vertical profile. However, the profile exhibits some non-diffusive traits (i.e. not truly uniform profiles) even on the longer time

scale of ^{210}Pb , as do the other cores. Therefore, this is a crude estimate of sediment mixing. Most likely this is not an appropriate manner in which to calculate sediment mixing rates from this profile. Having stated this we will proceed with a discussion based on this estimated mixing rate in order to compare with the work of other investigators who also applied this method. The minimum mixing estimate calculated was $40 \text{ cm}^2/\text{yr}$ for the *Spartina* fringe. This was the only core that had a decrease in excess ^{210}Pb activity with depth in the mixed layer. Typical continental shelf margin environments have mixing rates ranging from $1\text{--}30 \text{ cm}^2/\text{yr}$ (Carpenter et al., 1982; DeMaster et al., 1985). Carpenter et al. (1984) observed mixing rates in Puget Sound ranging from 1.5 to greater than $370 \text{ cm}^2/\text{yr}$ based on ^{210}Pb . Therefore, the mixing rate in the *Spartina* fringe core is in the high range or greater than typical values for margin environments, but most likely not as extreme as those observed in Puget Sound.

Short-lived radionuclides are often used to examine mixing because the same rates that produce vertical profiles in ^{210}Pb will yield decreasing profiles in the

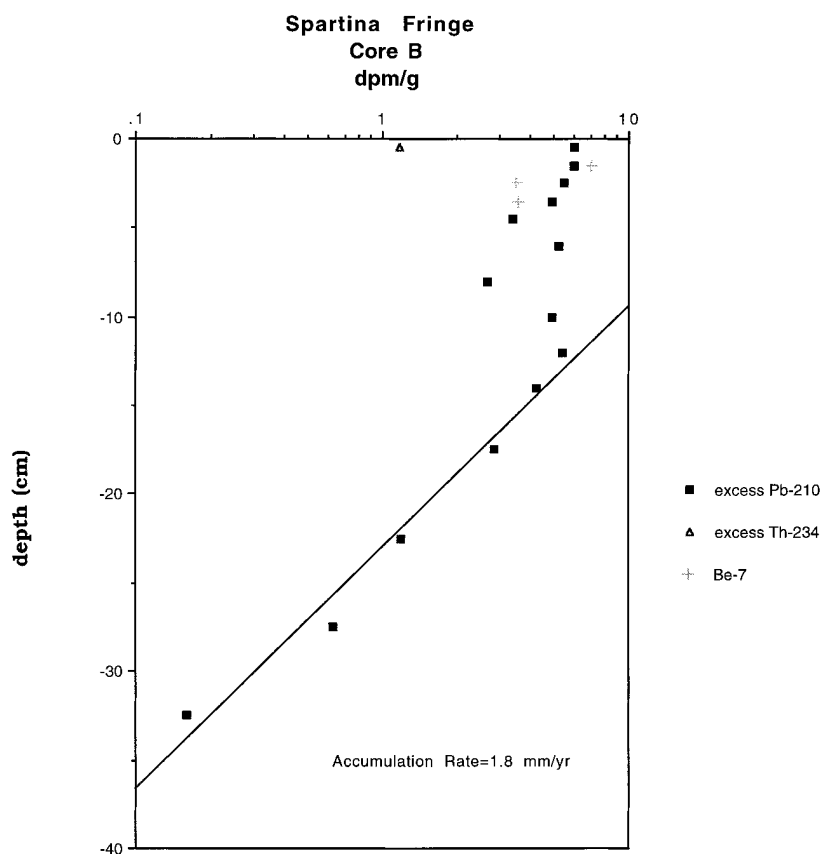


Figure 3. Excess ^{210}Pb , excess ^{234}Th and ^7Be activity profiles.

shorter-lived species due to the time scale. However, the shorter-lived species often record a different and most often higher mixing rates perhaps as a result of seasonal and/or age dependent mixing (Smith et al., 1993). In the Spartina fringe core, ^7Be penetrates to a depth of 4 cm with the maximum activity measured at the 1–2 cm interval. ^7Be was not detected in the surface layer possibly due to the low mass of the sample and this should not be interpreted as a zero activity. An estimate of the sediment mixing rate was determined from ^7Be using two methods. A mixing rate of $15\text{ cm}^2/\text{yr}$ was calculated using a least-squares line and a $40\text{ cm}^2/\text{yr}$ rate was calculated using the upper and lower data points only. The later method was used because the 2–3 and 3–4 cm interval activities were identical and the $40\text{ cm}^2/\text{yr}$ mixing rate is required to produce the measured activity in the 3–4 cm interval. This rate was the same magnitude as the mixing rate determined using excess ^{210}Pb ($40\text{ cm}^2/\text{yr}$). Therefore, the sediment mixing rate over the past 250 days is similar to the long term rate. This does not necessarily mean the rate has remained constant. If the mixing rate was the same

over the last 100 days, ^{234}Th should be detected in the 1–2 cm interval, which is not the case. ^{234}Th is only detected in the 0–1 cm surface interval. There are two explanations that could account for this observation. The first is that the mixing rate varied over the last 250 days and was slower in the last 100 days. This could be the result of a temporal change or a migration of the biological and/or physical mixing. An alternative explanation would be that mixing has not decreased, but that the addition of excess ^{234}Th is not a steady-state process. Excess ^{210}Pb and ^7Be are deposited from the atmosphere while ^{234}Th is dependent on the addition of sediment or the removal of ^{234}Th from seawater passing over the sediment surface. Addition of excess ^{210}Pb and ^7Be also may vary with time, but the longer time scales would dampen the effects. Therefore, the differences observed could be the result of the tracer source and not the sediment mixing rate.

The mangrove area at the Enseada das Garças station has a mixed layer 4 cm deep. This area is thought to be influenced even less by physical mixing than the Spartina fringe because the physical forces should

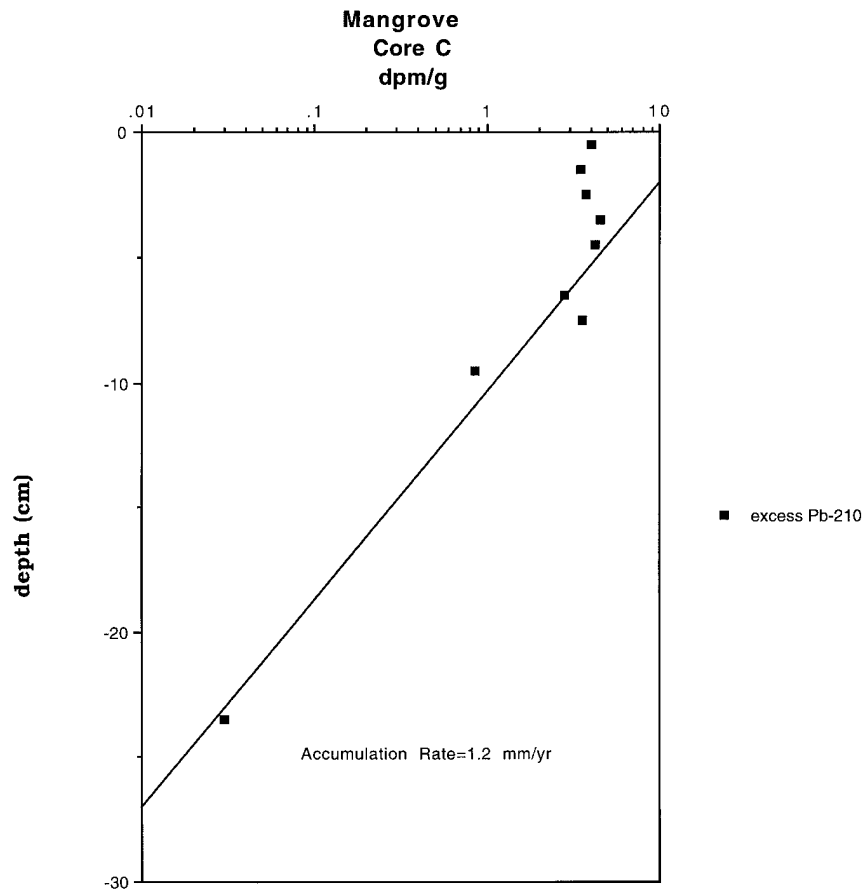


Figure 4. Excess ^{210}Pb activity profile.

be dampened as the mangroves are protected by the *Spartina*. Also this core was not taken from the edge of the mangroves but further within the mangroves, which provides additional protection from physical disturbance. The overwash core at the Barra de Guaratiba station while also from a mangrove region does not have the protection of the *Spartina* fringe and is on the edge of the mangroves. This results in a deeper mixed layer of 13 cm. The overwash also has a higher occurrence of the crabs as mentioned in the study site description, which are responsible for increased biological mixing.

The mixed layer depths in these cores are similar to those observed in Long Island Sound (Benniger et al., 1979), a South Carolina salt marsh (Sharma et al., 1987) and the Washington continental shelf (Nittrouer et al., 1984). However, the previous investigation in a mangrove ecosystem revealed a shallow mixed region down to 2.9 cm in only one core from Boca Chica, Mexico, of the seven other cores from Mexico and Florida no other evidence of mixing was observed (Lynch et al.,

1989). The difference between Lynch et al. (1989) and the present study may be due to the differences in the regions or heterogeneity within the mangrove ecosystems examined.

Sediment accumulation

Based on the profiles below the mixed layer and assuming negligible mixing in this region, the sediment accumulation rates calculated range from 1.2 to 1.8 mm/yr. The highest accumulation rate measured was for the *Spartina* fringe, which is most likely due to the high sediment trapping ability of the *Spartina*. The higher accumulation rate may also be influenced by the close proximity to the mud flat, which during disturbance events could be a major source of sediment. Other studies in mangroves (Lynch et al., 1989) and salt marsh ecosystems (Hatton et al., 1983; DeLaune et al., 1983; Feijtel et al., 1985; Stevenson et al., 1985) have documented similar higher accumulation rates on fringes as opposed to backmarsh areas. While

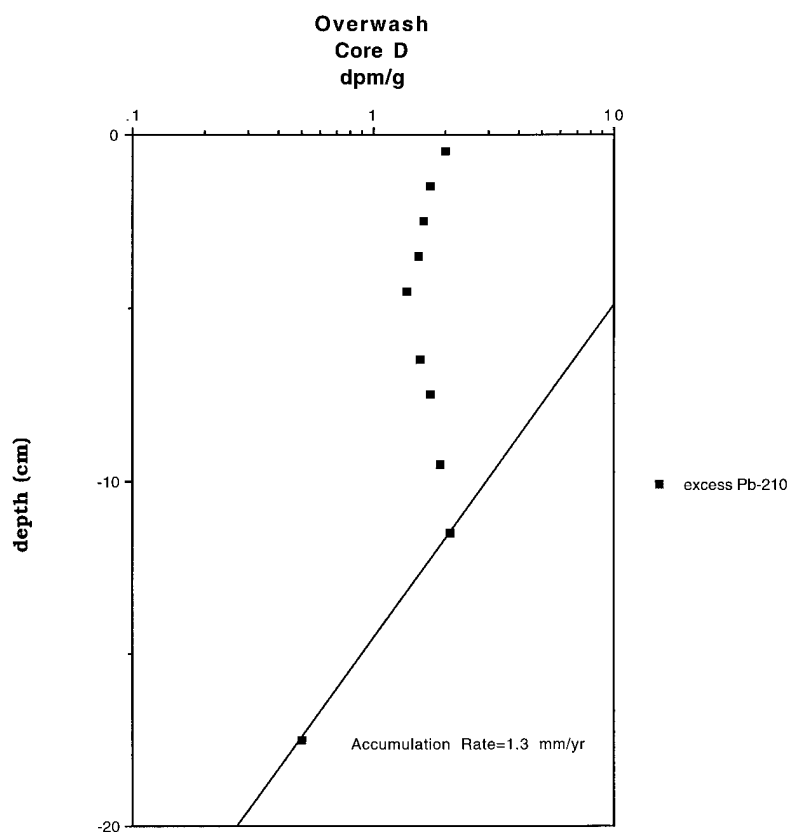


Figure 5. Excess ^{210}Pb activity profile.

the physical environments of the two mangrove sites are somewhat different the balance between trapping of sediment and the supply of sediment appear similar. This produces nearly identical accumulation rates of 1.2 mm/yr in the Enseada das Garças mangroves and 1.3 mm/yr from the overwash mangrove site. Both cores from the mangroves appear to have similar accumulation rates although the data used to calculate these rates are sparse. Because of the sparse data within the accumulation region, these rates are estimates.

Lynch et al. (1989) determined accumulation rates using excess ^{210}Pb in mangroves of Florida and Mexico to range from 1.0 to 4.4 mm/yr. Salt marsh sediment accumulation rates along the east coast of North America range from 1.4 to 5.0 mm/yr (Sharma et al., 1987). Therefore, the sediment accumulation rates calculated in the present study fall within the same range as salt marshes and other mangrove ecosystems.

For mangrove vegetation to persist, the sediment accumulation rate must follow the rise and fall of sea level. Because of this dependence, mangrove peat deposits have been used to record sea level over time (Scholl and Stuiver, 1967; Scholl et al.,

1969; Woodroffe, 1981). In the salt marshes of North America, vertical accretion and sea level rise are in good agreement. Lynch et al. (1989) show that the mangrove systems in Florida and Mexico are following the rate of sea level rise as well. While practically no work on the modern rate of sea level change has been conducted in this region, the change is thought to be approximately zero. Therefore, the rate of mangrove sediment accretion is outpacing the sea level change. This means the mangroves will continue to grow and possibly move seaward. Another possibility is that approximately a 1 mm/yr sea level rise has gone undetected. Based on the past use of mangrove peat deposits to record sea level and the recent studies documenting salt marsh and mangrove accretion following sea level, approximately a 1 mm/yr sea level rise in this area seems very likely.

Conclusion

Sediment mixing depth decreases from the mud flat through the *Spartina* fringe to the mangrove area at

Enseada das Garças. The mixed layer in the mud flat is at least 30 cm and due to physical mixing. The mixed layer in the *Spartina* fringe is 11 cm and caused by a combination of physical and biological mixing. The mangroves are well protected from physical mixing and have a mixed layer of 4 cm created by biological mixing. Therefore, as we move inland from the mud flat the depth of mixing decreases and the cause of the mixing shifts from physical to biological. The mixed layer at the overwash is 13 cm deep and has the potential to be caused by physical and biological mixing. The ^7Be and ^{234}Th data from a single core suggests future studies in mangrove ecosystems would benefit from examining these shorter-lived radionuclides in the investigation of sediment mixing. These radionuclides could provide better estimates of rapid diffusive mixing and identify areas of advective mixing.

The *Spartina* fringe has a sediment accumulation rate of 1.8 mm/yr and is the fastest rate observed in this study. The high accumulation rate is the result of the trapping efficiency of the *Spartina* and the close proximity of the mud flat. The mud flat is physically disturbed often and therefore can supply sediment to the *Spartina* fringe. The mangrove site at Enseada das Garças and the overwash at Barra de Guaratiba have an estimated sediment accumulation rate of 1.2 and 1.3 mm/yr, respectively. It is typical for areas farther inland to have lower accumulation rates. For the mangroves to persist it is necessary for the accumulation rate to follow sea level, therefore these accumulation rates suggest a sea level rise in the range of 1 mm/yr in this area. This estimate is the only hint at the sea level change in the area and additional investigation is needed to confirm this possibility.

Acknowledgements

The authors are grateful to Dr. Willard Moore for helpful discussions, constructive criticism and the use of his laboratory for gamma measurements. We also are grateful to Dr. David DeMaster for the use of his laboratory for alpha measurements. Jim Krest and Eron Higgins are thanked for their laboratory assistance. The second author is supported by Conselho Nacional de Desenvolvimento Científico e Tecnológico (CNPq) and Financiadora de Estudos e Projetos (FINEP).

References

Aller, R.C. and Cochran, J.K. 1976. $^{234}\text{Th}/^{238}\text{U}$ disequilibrium in nearshore sediments: particle reworking and diagenetic time scales. *Earth and Planetary Science Letters* 29: 37–50.

- Aller, R.C., Benninger, L.K. and Cochran, J.K. 1980. Tracking particle-associated processes in nearshore environments by use of $^{234}\text{Th}/^{238}\text{U}$ disequilibrium. *Earth and Planetary Science Letters*, 47: 161–170.
- Aller, R.C. 1982. The effects of macrobenthos on chemical properties of marine sediment and overlying water, pp. 53–102. In: McCall, P.L. and Tevesz, M.S.J. (eds), *Animal-Sediment Relations*. Plenum Press, New York.
- Aller, R.C. and DeMaster, D.J. 1984. Estimates of particle flux and reworking at the deep-sea floor using $^{234}\text{Th}/^{238}\text{U}$ disequilibrium. *Earth and Planetary Science Letters* 67: 308–318.
- Benninger, L.K., Aller, R.C., Cochran, J.K. and Turekian, K.K. 1979. Effects of biological sediment mixing on the ^{210}Pb chronology and trace metal distribution in a long island sound sediment core. *Earth and Planetary Science Letters* 43: 241–259.
- Berner, R.A. 1980. *Early Diagenesis: A Theoretical Approach*. Princeton University Press, Princeton, NJ, 241 pp.
- Bird, E.C.F. 1971. Mangroves as land-builders. *Victorian Naturalist* 88: 189–197.
- Borges, H.V., Figueiredo, Jr., A.G. and Beisl, C.H. 1989. Baía de Sepetiba-evolução geomorfológica nos últimos 100 anos. In: *1º Simposio de Geologia do Sudeste*, Rio de Janeiro, Brazil, pp. 59–60.
- Bunt, J.S. 1992. Introduction. In: Robertson, A.I. and Alongi, D.M. (eds), *Coastal and Estuarine Studies*, Vol. 41, *Tropical Mangrove Ecosystems*. American Geophysical Union, Washington, DC, pp.1–6.
- Carpenter, R., Peterson, M.L., Bennett, J.T. and Somayajulu, B.L.K. 1984. Mixing and cycling of uranium, thorium and ^{210}Pb in Puget Sound sediments. *Geochimica et Cosmochimica Acta* 48: 1949–1963.
- Casey, W.H., Larsen, I.L. and Olsen, C.R. 1986. The distribution of cosmogenic ^7Be in salt marsh sediments. *Geophysical Research Letters* 13: 322–325.
- Crusius, J. and Anderson, R.F. 1991. Immobility of ^{210}Pb in Black Sea sediments. *Geochimica et Cosmochimica Acta*, 55: 327–333.
- Cutshall, N.H., Larsen, I.L. and Olsen, C.R. 1983. Direct analysis of ^{210}Pb in sediment samples: self-absorption corrections. *Nuclear Instruments and Methods* 206: 309–312.
- Davis, R.B., Hess, C.T., Norton, S.A., Hanson, D.W., Hoagland, K.D. and Anderson, D.S. 1984. ^{137}Cs and ^{210}Pb dating of sediments from soft-water lakes in New England and Scandinavia, a failure of ^{137}Cs dating. *Chemical Geology* 44: 151–185.
- DeLaune, R.D., Baumann, R.H. and Gosselink, J.G. 1983. Relationships among vertical accretion, coastal submergence, and erosion in a Louisiana Gulf Coast marsh. *Journal of Sedimentary Petrology* 53: 147–157.
- DeMaster, D.J., McKee, B.A., Nittrouer, C.A., Jiangchu, Q. and Guodong, C. 1985. Rates of sediment accumulation and particle reworking based on radiochemical measurements from continental shelf deposits in the East China Sea. *Continental Shelf Research* 4: 143–158.
- FEEMA, 1980. Levantamento de metais pesados do Estado do Rio de Janeiro: Relatório preliminar-out. Rio de Janeiro, 72 pp.
- Feijtel, T.C., DeLaune, R.D. and Patrick, Jr., W.H. 1985. Carbon flow in coastal Louisiana. *Marine Ecology Prog. Series* 24: 255–260.
- Hatcher, B.G., Johannes, R.E., and Robertson, A.I. 1989. Review of research relevant to conservation of shallow tropical marine ecosystems. *Oceanography and Marine Biology: An Annual Review* 27: 337–414.

- Hatton, R.S., DeLaune, R.D. and Patrick, Jr., W.H. 1983. Sedimentation, accretion and subsidence in marshes of Barataria Basin, Louisiana. *Limnology and Oceanography* 28: 494–502.
- Kjerfve and Lacerda, 1993. Mangroves of Brazil. In: Lacerda, L.D. (ed.), *Conservation and sustainable utilization of mangrove forest in Latin America and Africa regions. Part I Latin America*. ITTO/ International Society for Mangrove Ecosystems. Okinawa, Japan, 272 pp.
- Koide, M., Soutar, A. and Goldberg, E.D. 1972. Marine geochronology with ^{210}Pb . *Earth and Planetary Science Letters* 14: 442–446.
- Krishnaswami, S., Benninger, L.K., Aller, R.C. and Von Damm, K.L. 1980. Atmospherically-derived radionuclides as tracers of sediment mixing and accumulation in near-shore marine and lake sediments: evidence from ^7Be , ^{210}Pb and $^{239,240}\text{Pu}$. *Earth and Planetary Science Letters* 47: 307–318.
- Lynch, J.C., Meriwether, J.R., McKee, B.A., Vera-Herrera, F. and Twilley, R.R. 1989. Recent accretion in mangrove ecosystems based on ^{137}Cs and ^{210}Pb . *Estuaries* 4: 284–299.
- McGill, J.T. 1959. Coastal classification maps, pp. 1–22. In: Russell, R.J. (ed.), *Second Coastal Geography Conference*, Coastal Studies Institute. Louisiana State University, Baton Rouge.
- Moore, W.S. 1984. Radium isotope measurements using germanium detectors. *Nuclear Instruments and Methods* 223: 407–411.
- Nittrouer, C.A., Sternberg, R.W., Carpenter, R. and Bennett, J.T. 1979. The use of ^{210}Pb geochronology as a sedimentological tool: application to the Washington continental shelf. *Marine Geology*, 31: 297–316.
- Nittrouer, C.A. and Sternberg, R.W. 1981. The formation of sedimentary strata in an allochthonous shelf environment: the Washington continental shelf. *Marine Geology* 42: 201–232.
- Nittrouer, C.A., DeMaster, D.J., McKee, B.A., Cutshall, N.H. and Larsen, I.L. 1984. The effect of sediment mixing on ^{210}Pb accumulation rates from the Washington continental shelf. *Marine Geology* 54: 201–221.
- Rice, D.L. 1986. Early diagenesis in bioadvective sediments: relationships between the diagenesis of ^7Be , sediment reworking rates, and the abundance of conveyor-belt deposit feeders. *Journal of Marine Research* 44: 149–184.
- Schink, D.R. and Guinasso, N.L. 1977. Effects of bioturbation on sediment-seawater interaction. *Marine Geology* 23: 133–154.
- Scholl, D.W., and Stuiver, M. 1967. Recent submergence of southern Florida: A comparison with adjacent coast and other eustatic data. *Ecology Society of America Bulletin*, 78: 437–454.
- Scholl, D.W., Craighead, F.C. and Stuiver, M. 1969. Florida submergence curve revised: Its relation to coastal sedimentation rates. *Science* 163: 562–564.
- Scoffin, T.P. 1970. The trapping and binding of subtidal carbonate sediments by marine vegetation in Bimini Lagoon, Bahamas. *Journal of Sedimentary Petrology* 40: 249–273.
- Sharma, R., Gardner, L.R., Moore, W.S. and Bollinger, M.S. 1987. Sedimentation and bioturbation in a salt marsh as revealed by ^{210}Pb , ^{137}Cs and ^7Be studies. *Limnology and Oceanography* 32: 313–326.
- Smith, C.R., Pope, R.H., DeMaster, D.J. and Magaard, L. 1993. Age-dependent mixing of deep-sea sediments. *Geochimica et Cosmochimica Acta* 57: 1473–1488.
- Spenceley, A.P. 1977. The role of pneumatophores in sedimentary processes. *Marine Geology* 24: M31–M37.
- Spenceley, A.P. 1982. Sedimentation patterns in a mangal on Magnetic Island near Townville, North Queensland, Australia. *Singapore Journal of Tropical Geography* 3: 100–107.
- Stevenson, J.C., Kearney, M.S. and Pendleton, E.C. 1985. Sedimentation and erosion in a Chesapeake Bay brackish marsh system. *Marine Geology* 67: 213–235.
- Walsh, G.E. 1974. Mangroves: a review, pp. 51–174. In: Reimold, R.J. and Queen, W.H. (eds), *Ecology of Halophytes*. Academic Press, New York.
- Woodroffe, C.D. 1981. Mangrove swamp stratigraphy and Holocene transgression, Grand Cayman Island, West Indies. *Marine Geology* 41: 271–294.
- Woodroffe, C.D. 1990. The impact of sea-level rise on mangrove shorelines. *Progress in Physical Geography* 14: 483–520.
- Woodroffe, C. 1992. Mangrove sediment and geomorphology, pp. 7–41. In: Robertson, A.I. and Alongi, D.M. (eds), *Coastal and Estuarine Studies*, Vol. 41, *Tropical Mangrove Ecosystems*. American Geophysical Union, Washington, DC.
- Yingst, J.Y. and Rhoads, D.C. 1980. The role of bioturbation in the enhancement of microbial turnover rates in marine sediments, pp. 407–422. In: Tenore, K.R. and Coull, B.C. (eds), *Marine Benthic Dynamics*. University of South Carolina Press, Columbia, SC.

Annex RJ-8

K. Harada, F. Imamura, T. Hiraishi, “Experimental Study on the Effect in Reducing Tsunami by the Coastal Permeable Structures”, *Proceedings of the Twelfth International Offshore and Polar Engineering Conference*, 2002, pp. 652-658.

Experimental Study on the Effect in Reducing Tsunami by the Coastal Permeable Structures

Kenji HARADA and Fumihiko IMAMURA

Disaster Control Research Center, Graduate School of Engineering, Tohoku University
Sendai, Miyagi, JAPAN

Tetsuya HIRAISHI

Port and Airport Research Institute, Independent Administrative Institution
Yokosuka, Kanagawa, JAPAN

ABSTRACT

In order to understand the tsunami reduction effect of the coastal permeable structures as the coastal forest and the artificial wave dissipating structure, the hydraulic experiment is carried out. The hydraulic experiment for the tsunami of two different amplitudes with five kinds of models; mangrove, coastal forest, wave dissipating block, rock breakwater, houses, with different structure and porosity was carried out in order to measure an effectiveness in reducing tsunami disaster. Wave height, the horizontal velocity, and wave pressure were measured for each model case. The measuring points are arranged by considering the impact of the tsunami due to the existence of permeable structure, and the change of tsunami at the front and rear side of a model, and the reduction effect by model conditions was compared. Comparing with the forest case and the artificial structure case, the quantity of reduction on the forest case is smaller than the artificial structure. Although there is the reduction effect by the forest existence and the coastal forest is effective in the damage mitigation by tsunami. Experimental results suggest that the tsunami reduction effect in the water level, the flow velocity and fluid force in the structure back by the permeable structures was fully expectable.

KEY WORDS: Tsunami; coastal permeable structure; coastal forest; artificial wave dissipating structure; fluid force; tsunami reduction

INTRODUCTION

Appropriate Utilization of Natural and Artificial Barriers

The countries along the Pacific coast have been much damaged and caused human and economical loss by earthquakes and tsunamis. In Japan, the artificial coastal barriers such as seawalls and breakwaters have been constructed and have played an important role in protecting the coastal area from natural hazards (tsunami, tidal wave, high wave). Now we have faced serious problem in environment and maintenance of the artificial coastal barriers for long term. Although the frequency of these disasters is high in other countries in Southeast Asian, the prevention countermeasures to the damage by tsunami are not taken fully. There are also reasons of environmental problem and high costs of the construction and long time maintenance of the artificial coastal

barriers. Under such condition, it has recently been recognized that mangroves and other coastal vegetation forming important marine-coastal ecosystem can be utilized as a natural and effective buffer against the impact of large waves.

It is time to provide with technical information and guideline for coastal barrier by using natural and artificial functions for more appropriate management for natural disaster reduction and keeping environment.

Previous Study

The action of waves and currents through vegetation in an attempt to understand the flow field in a mangrove forest has been numerically investigated. Especially tide, wind-waves and storm-surges are concerned for an ecosystem in ordinary conditions. Petryk and Bosmajian (1976) introduced a method of force balance to estimate the Manning friction coefficient due to vegetation and boundary roughness, and suggested that a flow is resisted mainly due to the drag force of vegetation. Wolanski et al. (1980), Wolanski et al. (1992), and Kanazawa and Mazda (1994) also studied the flow field of tide on mangrove and simulated the flow field in a mangrove swamp and creek by using the Manning roughness coefficient, n , in their computer model. These suggested that n is on the order of 0.2-0.4 in a swamp and 0.02-0.04 in a creek.

As for a tsunami passing through an obstacle, Goto and Shuto (1983) experimentally studied the energy head loss to evaluate the effect of large obstacles on tsunami inundation. They numerically simulated tsunami behavior on land with large-scale obstacles. The obstacles, however, were limited to simple type of rectangular in one-dimensional and steady flow. Noji et al. (1993) carried out experimental and numerical analysis of the movement of rocks transported by a tsunami and modeled the impact force as inertia due to tsunami attack, in which the drag coefficient, C_D ranges from 2-6 and the virtual mass coefficient, C_M , is approximately 2 when the rocky model is completely submerged. The drag coefficient is significant and not negligible in the case of a tsunami attacking to coastal vegetation. Harada et al. (2000) proposed the tsunami numerical simulation including the effect of coastal forest resistances. However, they have not formulated thoroughly

forest resistance coefficients. Harada and Imamura (2001) proposed the resistance coefficients due to mangrove under the unsteady flow from the hydraulic experiment analysis. They suggested that C_D is related to the volume occupation rate. However the quantitative and concrete role of coastal forests in reducing the impact of attacking waves has not been established.

The effect to reduce tsunami by the coastal forests and the artificial coastal barriers is effective and is expected as a coastal prevention countermeasure. However, the concrete effectiveness of these coastal forest and artificial structures in reducing tsunami has not been understood clearly. Then, the hydraulic experiment was carried about the coastal forests and the permeable structures, and the effectiveness in reducing tsunami disaster was examined. For the understanding mechanism of the tsunami reduction by the coastal forests and the permeable structures in the coast, the purpose of this study is examining the effect of reducing tsunami by the hydraulic experiment.

HYDRAULIC EXPERIMENT

Permeable Models for Tsunami Reduction

To compare the effects of different permeable model with types, five type permeable structures with different porosity and design are selected in the hydraulic experiment. Two kinds of coastal forest models were designed to compare with porosity distribution. One is the mangrove model which porosity is changed in the vertical direction by consisting of root, trunk and leaf. The other is a model, which have no change of porosity in the vertical direction. Two kinds of penetrable structure models were made for compare to the tsunami reducing effect with forest model. One is a piled up the wave-dissipating block and the other is the rock breakwater which is a basket containing the gravel. As a model of a house group, the square pillar was arranged in the channel. The case without permeable structure was also carried out to compare the result with models. The experimental models and conditions are summarized in Table 1.

Table 1. Experimental conditions

No.	Model	Condition	Porosity	Valves
Case-1	Without	---	1	2
Case-2				5
Case-3	Forest	Mangrove (72 cylinders)	0.964 - 0.973	2
Case-4				5
Case-5				2
Case-6		Leaf and Branch (5cm x 4 sheets)	0.97	5
Case-7	Permeable structure	Wave Dissipating Block	0.75	2
Case-8				5
Case-9				2
Case-10		Rock Breakwater (Gravel)	0.38	5
Case-11	Houses	10 x 10 x 30cm Square pillar 16	0.36	2
Case-12				5

The sketch of mangrove model is shown in Fig.1. The mangrove model is consists of three parts; root, trunk and leaf. The root in the model is made of the porous sheet with a thickness of 0.05m and it was put on the bottom of the channel. The leaf in the model is also made of porous sheet and it was put at the height of 0.15-0.20m from the bottom. The trunk is composed of the plastic pillar with a diameter of 0.01 m. The plastic pillar was arranged to 0.08 m in interval and the total of 72 pillars (6 x 12) was put with a staggered pattern. The porosity of a mangrove model is varies with water depth, which value is between

0.964-0.973.

The sketch of the leaf and branch forest model is shown in Fig.2. The leaf and branch forest model is made of the porous sheets consisting of thin plastic. A porous sheet has the thickness of 0.05m and the size of 0.5 x 0.5m. The model is composed of four porous sheets and became 0.20 m in height. This model has no change of porosity in the vertical direction, because it is assumed that the forest where branch and leaf have grown is thick uniformly in the vertical direction. The porosity of the leaf and branch forest model became 0.97.

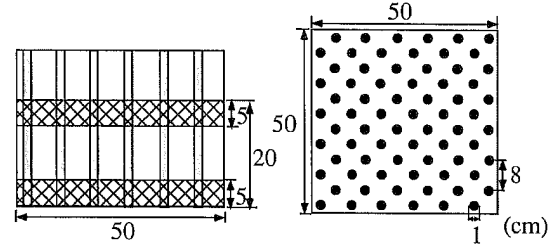


Fig.1 Sketch of Mangrove Model (side view and over view)

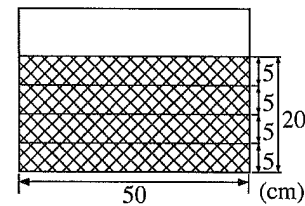


Fig.2 Sketch of leaf and branch forest model (side view)

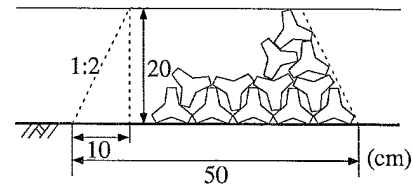


Fig.3 Sketch of wave dissipating block model (side view)

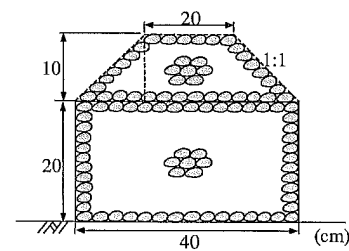


Fig.4 Sketch of rock breakwater model (side view)

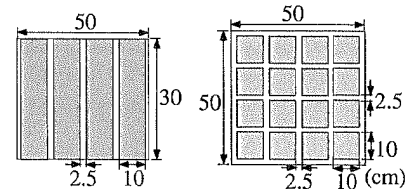


Fig.5 Sketch of house group model (side view and over view)

The sketch of wave dissipating block models is shown in Fig.3. The wave dissipating block models is piled on the experimental channel. One block model is made of concrete, which are 0.073 kg in weight and $1.78 \times 10^{-7} \text{ m}^3$ in volume. 546 block models were totally piled to 0.20m in height, 0.3m in top width, 0.5m in bottom with, and 2:1 in slopes in both side. The porosity of the model became 0.75.

The sketch of rock breakwater model is shown in Fig.4. The rock breakwater model is made of two baskets containing the gravel. One is the trapezoid section model and the other is the rectangular one. The trapezoid section model is 0.1m in height, 0.2m in top width, 0.4m in bottom width, and 1:1 in both side slopes. The rectangular model is 0.2m in height, and 0.4m in width. The trapezoid side model was put on the rectangular side model. The size of the used gravel is 0.02m or less in particle diameter. The porosity of the model is 0.38.

The sketch of house group model is shown in Fig.5. We designed the house group model making of the square pillars, which are plastic board of 0.1m widths and length, and 0.3 m height. A total of 16 square pillars (4 x 4) have been arranged in the channel. The distance between each square pillar is 0.025m and the porosity of the model became 0.36.

Experimental Set - up

The hydraulic experiment for unsteady flow modeling transient wave of tsunami was carried out in an open channel of 20.7 m in length, 1.0 m in height, 1.0 m in width as shown in Fig.6. From the one end of the channel, a flat bottom of 0.7 m in depth is connected by a steep slope of 1:3 to a shallow flat bottom of 0.16 m in depth. The slope of 1:30 continues to the other end of the channel, which can reduce the reflected wave after passing the mangrove model. The wave generator was installed in the end of channel at the deeper side. This wave generator has five electromagnetic valves for control wave height. Discharging the water from tank generates a long wave with bore front. The generated wave is controlled by the opening and the closing the five valves. The channel width in the slope is narrowed to 0.5 m to amplify wave enough to be measured.

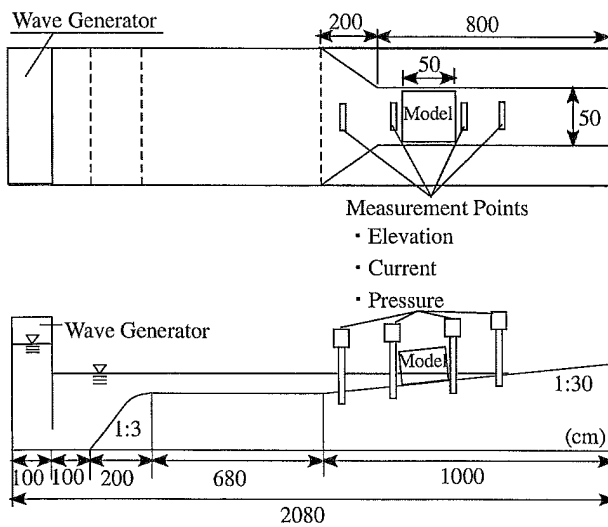


Fig.6 Experimental Set-up (over view and side view)

The permeable models were placed on the slope of 1:30 in shallow water, the 3.35 m distance from the slope beginning (see Fig.7). Fig.7

shows the measurement points (M.P.1: Incident point, M.P.2: Front side of model, M.P.3: Rear side of model, M.P.4: Transmitted point) in the hydraulic experiment. Water elevation and current at each measurement points were measured for further understanding of wave transformation due to permeable structures. Additionally, the wave pressure gauges were installed, and the pressure due to the unsteady flow at each measurement points were measured. The pressure gauges were fixed at measuring points on the model.

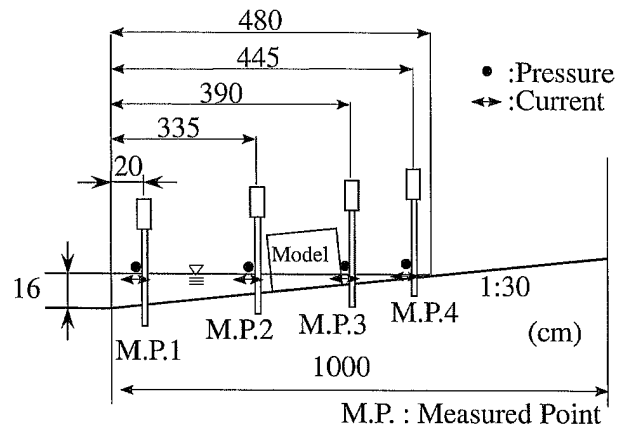


Fig.7 Measurement points

In this study, two case of different wave height are carried out for examining with tsunami height. For the case of large and small wave height, five and two electro magnetic valves are opened. In the condition without model, the maximum value of wave height at the measuring point 1 is 0.142m at the case of five valves opened and 0.129 m at the case of two valves opened.

Some of wave dissipating blocks were flowed out by the wave action at the case of five valves opened generating large wave height. This is why the data of this case could not be measured and not used.

EXPERIMENTAL RESULTS

Hydraulic Properties with and without permeable models

In this subsection, the variations of measured data by the case with and without the models are explained. As an example of experimental data, Fig.8, 9 and 10 show time series of the water elevation, current and pressure at M.P.2, M.P.3 and M.P.4. The conditions are the leaf and branch forest model at small wave height (Case-5) and the case without model at small wave height (Case-1).

By the reflection of forest model, the water elevation increased to 0.055m (+63%) in the maximum at the front of the model (M.P.2). At the rear of model (M.P.3), the water elevation decreased to 0.053m (-58%) in the maximum. This is the tsunami reduction effect in height at the rear of permeable structure. In the same way, the current decreased at front of model by reflection, and at rear of the model by energy dissipation. Especially, the maximum value of current at the rear of the model decreased to 0.32 m/sec, indicating current reduction effect of 35%. At the front of the model, pressure became large by the increasing water elevation. The pressure decreased by the decrease of water elevation at the model back.

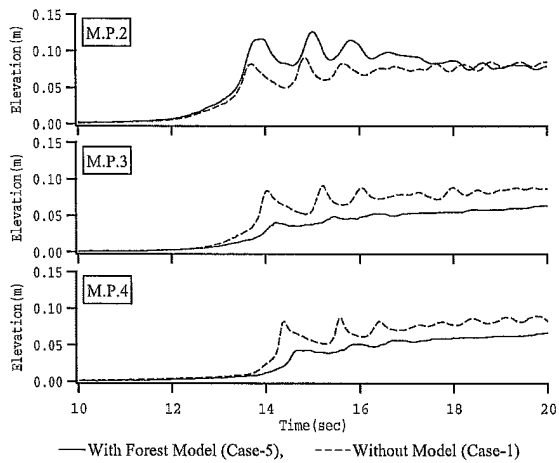


Fig.8 Elevation data (Case-5 and Case-1)

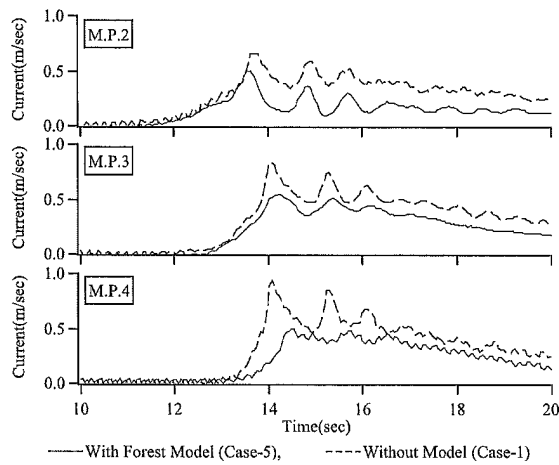


Fig.9 Current data (Case-5 and Case-1)

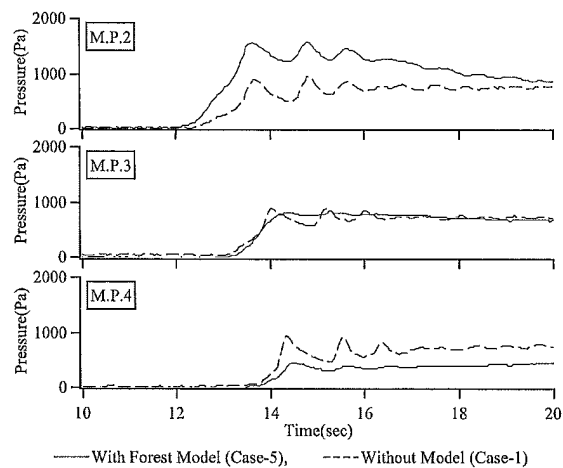


Fig.10 Pressure data (Case-5 and Case-1)

Variation Rate of Maximum Values

In order to examine the effect of the model, the variation rate of maximum values of elevation, current and pressure by using the data with and without the models are examined at every measurement points. Elevation is important parameter to discuss the inundation causing human house damage. Current and pressure are also important items to estimate house damage by tsunami wave force including inertia and drag forces. The value of variation rate can be calculated by dividing with the data with permeable model and without model. The values of variation rate become less than 1.0 means the decrease of the data with the models, including the effect due to the model. The changes of the measurement in the case of a small wave height by the existence of a model are shown to Fig.11, 12, and 13.

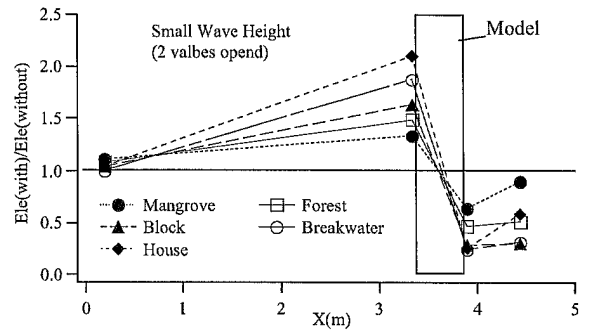


Fig.11 Variation Rate of Maximum Elevation on Small Wave Height

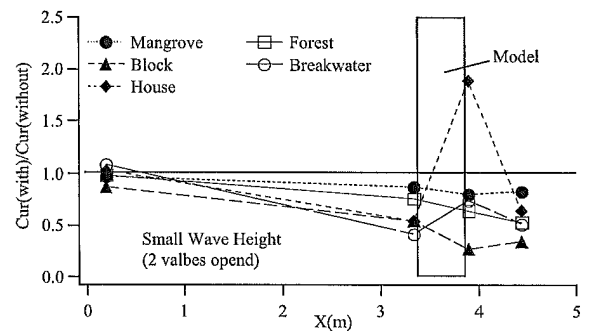


Fig.12 Variation Rate of Maximum Current on Small Wave Height

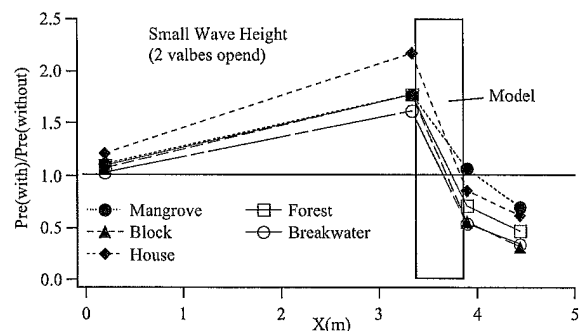


Fig.13 Variation Rate of Maximum Pressure on Small Wave Height
As the first of three items to study, the variation rate of the maximum

value of elevation at each measuring point is shown in Fig.11. Increasing at the front and decrease at the back of the models are observed, suggesting that the area of the front become more dangerous and one at the back safer. The transmitted wave became large at the front and small at the back by reflection of the models, which is common for the all models. Additionally, the reduction effect of the coastal forest models of mangrove and forest is almost as same as that by artificial barriers.

The next, Fig.12 shows the variation rate of the maximum value of current which decreased at all measurement points for the models except for house group model due to the reflection at front of models. Passing through the models could dissipate the wave dynamics energy at any point. Largest reduction effect of current is observed at the back of model. The reduction effect of current at back is different among the models. The effect of costal forest models with large porosity is smallest. But there is one cases in which increased the rear of model. In house model case, current in the rear increases by passing through the narrow space between the square pillars as house models. After passing through the model, the maximum change of current at M.P.4 is reduced.

Finally, the variation rate of the maximum value of measured pressure is shown in Fig.13. Measured pressure increase at the front of model (M.P.2). From Fig.11 and Fig.13, it is considered that the increase of pressure at the front is influenced by the increase of elevation. At the behind of the models (M.P.3), the variation rate of measured pressure for the case of artificial barriers models with small porosity become under 1.0 but those for the case of coastal forest models with large porosity are still over 1.0. The flow patters at the behind of coastal forest models might be complicated and influence the pressure. On the other hand, at the back of the all models (M.P.4), the variation rate of the measured pressure for the all model cases becomes less than 1.0. The measurement pressure at the back is decreased in all cases.

Through the data at the transmitted point (M.P.4) in Figs 11, 12 and 13, it is shown that there are the obvious reduction effects of elevation and pressure for the all models, however that of current for the house model is different. Additionally, we can expect that the reduction effect of tsunami for the forest is almost same as those as artificial barriers.

Fig.14, 15 and 16 show the variation rate of the maximum values on elevation, current and pressure at the case of large wave height. Since the model conditions are same as the case of small wave height, the tendency of the variation rate of value become almost same. Each value (elevation, current and pressure) is reduced at the rear side by the permeable models.

Hydraulic Forces in Reducing Tsunami Impact

When we discuss the tsunami reduction effect behind the permeable structures, house damage due to tsunami is one of major items. Generally, the main force causing house damage in the case of steady flow is drag force. Hatori (1984) proposed relationship between the hydraulic force and the house damage due to tsunami. The hydraulic force is expressed by Eq.1, product of water density: ρ , the inundation depth: η and the square of flow current: u^2 meaning that the hydraulic force is corresponding to drag force. Hiraishi et al. (2000) also discussed the house damage due to tidal wave with the hydraulic force. In the case of the wooden house, those would be destroyed when the hydraulic force factor exceed 5×10^3 N/m.

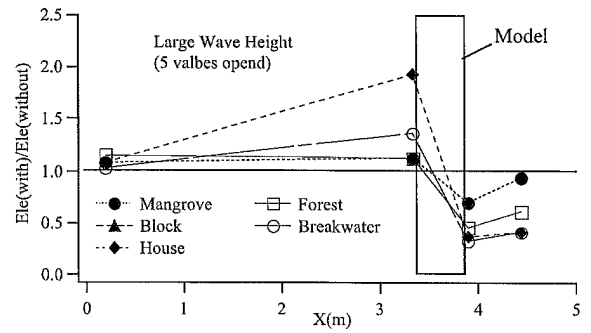


Fig.14 Variation Rate of Maximum Elevation on Large Wave Height

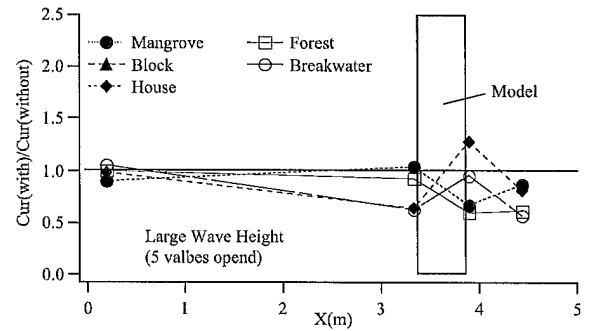


Fig.15 Variation Rate of Maximum Current on Large Wave Height

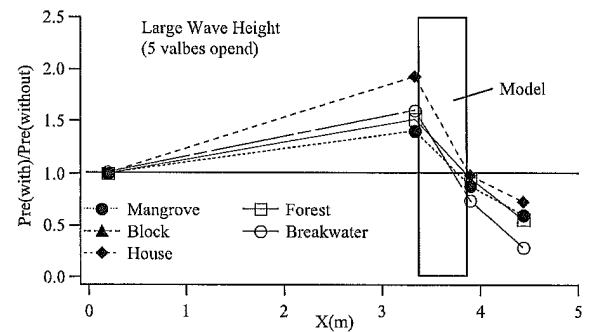


Fig.16 Variation Rate of Maximum Pressure on Large Wave Height

$$(Hydraulic\ Force) = \rho \cdot \eta \cdot u^2 \quad (1)$$

Fig.17 shows the time histories of hydraulic force from experimental data. The conditions are the case of leaf and branch forest model at small wave height (Case-5) and the case without model at small wave height (Case-1). This figure clearly shows that the hydraulic force is reduced at M.P.2 (front), M.P.3 (rear) and M.P.4 (transmitted point). The hydraulic force is decreased by the reduction of current due to the reflection at front of model (M.P.2). And the hydraulic force factor is decreased caused by the reduction of elevation and current due to the energy dissipation at M.P.3 and M.P.4. These mean that the effect of tsunami reduction on house damage behind the forest is fully expectable. There are the same tendencies to the other experimental cases.

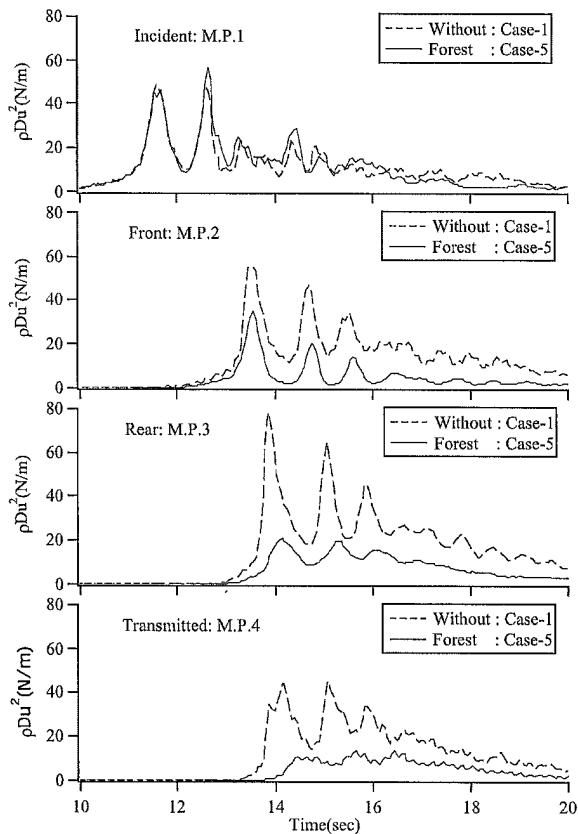


Fig.17 Time Series Data on Hydraulic Force Factor, Comparison of The Case Without Model and With Forest Model

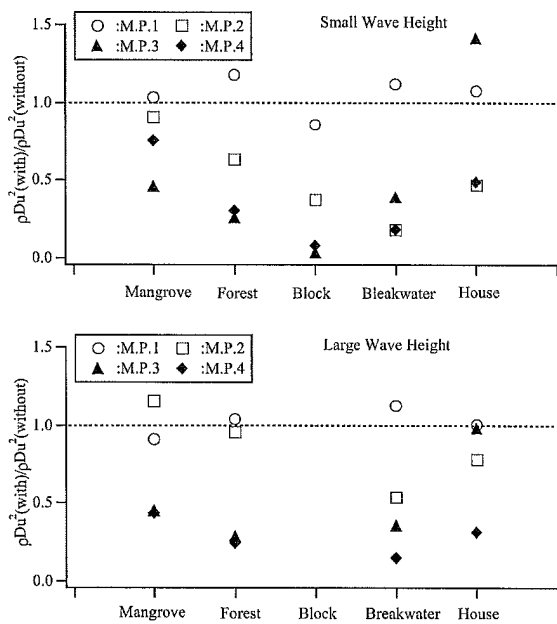


Fig.18 The rate of maximum hydraulic force factor with and without model (Small and Large wave height).

For further understanding of the reduction effect by the permeable structures, the rates of maximum hydraulic force with and without model case are shown in Fig.18. The open circles and open squares mean the variation rate of the maximum values of hydraulic force $[\rho \cdot \eta \cdot u^2(\text{with}) / \rho \cdot \eta \cdot u^2(\text{without})]$ at the front side of model (M.P.1 and M.P.2). The solid triangles and solid lozenge mean the variation rate of the maximum value of hydraulic force at the behind of model (M.P.3 and M.P.4). The rate at the M.P.4 (transmitted point) is less than 1.0 in all cases. This means that the hydraulic forces are reduced due to the permeable structures at the behind of model. Especially there is the tsunami reduction effect in hydraulic force not only the artificial permeable structure models but also the forest type model (Mangrove and Forest).

CONCLUSIONS

For the understanding of the tsunami reduction effect by the coastal forests and the permeable structures in the coast, the hydraulic experiment was carried out. The obtained result is as follows.

1. From the comparison between the two cases with and without the permeable model, the variation rate of the maximum of elevation, current and pressure are reduced at behind of model in almost all cases. And this experimental analysis means the effectiveness of tsunami reduction at behind of model by all permeable structures; mangrove, forest, wave dissipating block, rock breakwater, houses.
2. The hydraulic force can be reduced at behind of model in all cases, suggesting the tsunami reduction effect in hydraulic force for not only the artificial permeable structure models but also the forest type models; Mangrove and Forest.

By taking in tsunami reduction effects to numerical simulation, it becomes possible to acquire the useful information about tsunami disaster prevention countermeasures.

ACKNOWLEDGEMENTS

The research presented herein is, in part, supported by JSPS Research Fellowships for Young Scientists. The hydraulic experiment was carried out in cooperated with Port and Harbor Research Institute; PHRI (present Port and Airport Research Institute; PARI), Japan. We thank to PHRI for the cooperation in the hydraulic experiment.

REFERENCES

- Goto, C. and N. Shuto (1983). "Effect of Large Obstacles on Tsunami Inundation," *Tsunamis Their Science and Engineering*, ed. by K. Iida and T. Iwasaki, Terra Sc. Pubs. Comp., Tokyo, pp. 511-525.
- Harada K., T. Aburaya, L. Hamzah and F. Imamura (2000). "Examination on the Effect of Control Forest to Reduce a Tsunami Energy," *Proceedings of Coastal Engineering*, JSCE, Vol.47 (1), pp. 366-370 (In Japanese).
- Harada K. and F. Imamura (2001). "Experimental study on the resistance by mangrove under the unsteady flow," *Proceedings of the first Asian and Pacific Coastal Engineering Conference*, Dalian, China, Vol.2, pp. 975-984.
- Hatori T. (1984). "On the damage to houses due to Tsunamis," *Bull. Earthq. Res. Inst. Univ. Tokyo*, Vol.59, pp.433-439 (In Japanese).
- Hiraishi T., K. Hirayama, H. Kawai, I. Uehara (2000). "Wave overtopping and storm surge by typhoon 9918 at Ryugatake Town in West Japan," *Proceedings of Coastal Engineering*, JSCE, Vol.47 (1),

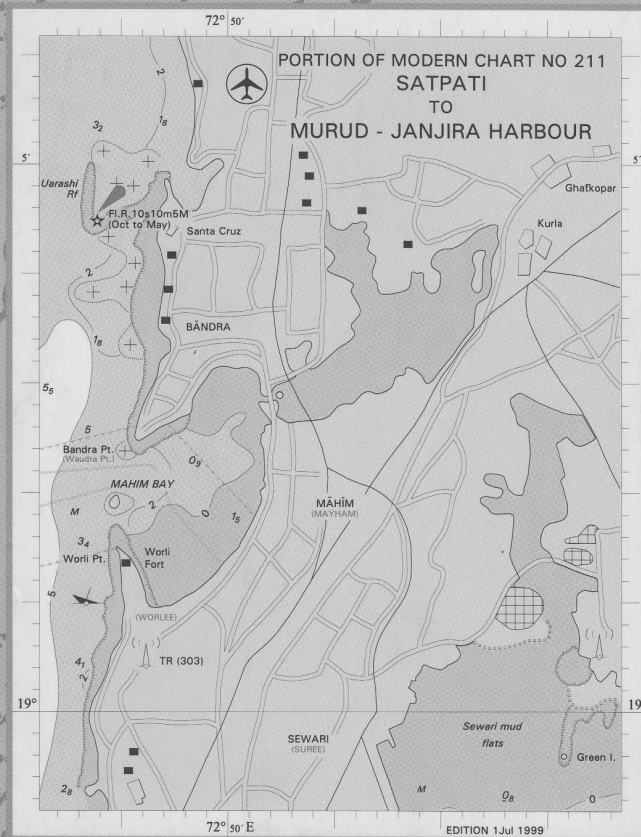
- pp. 306-310 (In Japanese).
- Kanazawa, N. and Y. Mazda (1994). "Tidal flow asymmetry in mangroves estuaries," *Ocean Research*, vol. 3, No.1, pp.1-11 (in Japanese).
- Noji, M. F. Imamura, N. Shuto (1993). "Numerical simulation of movement of large rocks transported by Tsunamis," *Proc. Of IUGG/IOC Intrenational Symposium*, Wakayama, Japan, pp. 189-197.
- Petryk, S., G. Bosmijian (1975). "Analysis of Flow Through Vegetation," *Journal of Hydraulics Div.*, ASCE, 1975, pp. 871-884.
- Wolanski, E, Jones, M., and Bunt, J.S. (1980). "Hydrodynamics of a tidal creek-mangrove swamp system." *Australian Journal of Marine and Freshwater Research* 31: pp. 431-450.
- Wolanski, E., Y. Mazda, and P. Ridd (1992). "Mangrove hydrodynamics". In Robertson, A.I. Alongi, D.M. (Eds.), *Tropical mangrove Ecosystems*, American Geophysical Union, pp. 43-62.

Annex RJ-9

M. Bhattacharya, *Charting the Deep, A History of the Indian Naval Hydrographic Department*, National Hydrographic Office, 2004, pp. 130-131.

Charting the Deep

A History of the Indian Naval Hydrographic Department



Keep the Portuguese Church at C, on with the round guese Church at 1, on with the above marks, untill you see Fort; you may then steer of guese Church in 2 1/2 fathoms

Another good mark for going over the BAR is the Point of the Hill, at D, on with the N. Part of MAXIMAN Fort, untill you have the mark as before directed; To go clear of the Shoal, at E, you must open the Writing Office, at F, clear to the Northward of MAXIMAN Fort.



Dr. Manoshi Bhattacharya

© The Chief Hydrographer to the Government of India

All rights reserved. No part of this publication may be reproduced, stored in a retrieval system or transmitted, in any form or by any means, electronic, mechanical, photocopying, recording, or otherwise, without the prior permission of the publisher.

Published by
National Hydrographic Office,
107A, Rajpur Road,
Dehradun - 248 001, India

First Published 2004

Distributed by
Himalayan Books
17-L, Connaught Circus,
New Delhi - 110 013
☎: 2341-7126 Fax: 091-11-2341-7731
E-mail: ebs@vsnl.com

ISBN
81-7002-083-2

Typeset, Processed and Printed at
Ajanta Offset & Packagings Ltd.
1, Bahadurshah Zafar Marg, New Delhi-110 002

Sponsored by
Indian Ports Association, New Delhi

Portuguese Hydrography

The Goan Naval services supervised the survey and publication of the plan of the Aguada Bay and the bar of the Mandovi River in 1926. A report was published in 1930, about their activities since 1898. The first radiotelegraph station was set up in 1931 to provide improved hydrographic services to the increasing river traffic.

International Cooperation

Lieutenant Commander TMS Milnes Henderson attended the International Hydrographic Conference in Monaco in October 1926.

Commander Melhuish attended the Empire Conference of Surveyors and the International Geographic Congress in 1928.

Lieutenant Ryland attended the International Oceanographic Conference at Seville in 1929.

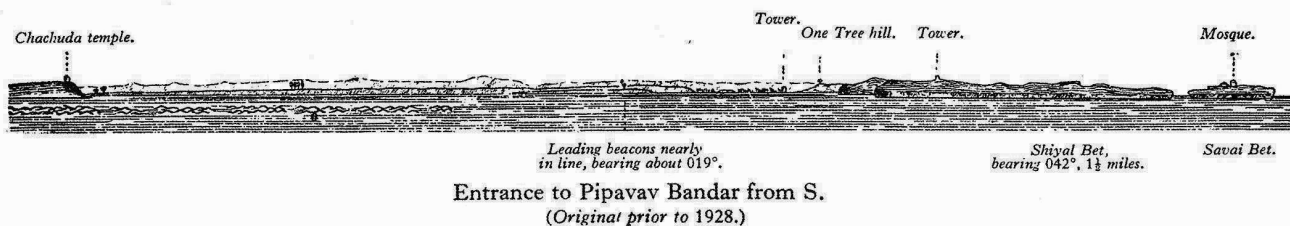
difficult due to the thick mud and mangroves. The first lieutenant, a midshipman and one rating were washed off Blemish Rock in Mandwa Bay. Though badly injured, they were all recovered. In all, 14 surveys covering 400 miles of coastline and 1250 square miles of sounding including a search for the Wadge Bank and shoals were carried out. "Investigator", assisted by "Palinurus", carried out a survey from Gogha to the Bhavnagar lighthouse on a scale of 1:25000. The "Investigator" went on to survey Port Albert Victor on a scale of 1:12500. On February 8, 1927, the survey of the Kathiawar Coast from Diu Head to Chanch was started on a scale of 1:75000. This was carried upto Rajpur and included a survey of the Simbor Anchorage. "Palinurus" did an independent survey of the Kathiawar Coast from Patwa Bay to Gopnath Point finishing in time for the refit season and the annual survey of the government dockyard.

The months of October and November 1927 were spent with both ships surveying the area between Gopnath Point and Gogha, on a scale of 1:75000. Having verified the shoals off Gwadar the "Investigator" proceeded to conduct a preliminary survey of the northern portion of the South Patches in the Bay of Bengal and a sketch survey of the North Patches including that of the Dolphin Shoals. The study of the approaches to the Karnaphuli River occupied the rest of the season.

The R.I.M.S. "Palinurus" conducted an independent survey of the Kathiawar Coast from Rajpur to Diu Head and then spent the rest of her time in intensive gunnery training as the proposed, Jaffnapatnam, survey was abandoned by the government of Ceylon.

In October 1928, H.M.I.S. "Palinurus" surveyed the West Coast, southwards from Mangalore. This survey was carried out over four seasons, all the way down to the Tellicherry Anchorage. By January 23, 1929, she left to investigate the shoals on the Wadge Bank, southwest of Cape Comorin. The shoals northeast of Trincomali were examined next. A survey of the roadstead at Cuddalore was completed before she returned to Bombay.

The next year saw a continuation of the West Coast survey. H. M. I.S. "Investigator" surveyed the approaches to the Karnaphuli River, Chittagong followed by a survey of the approaches to the Rangoon River. Tide parties





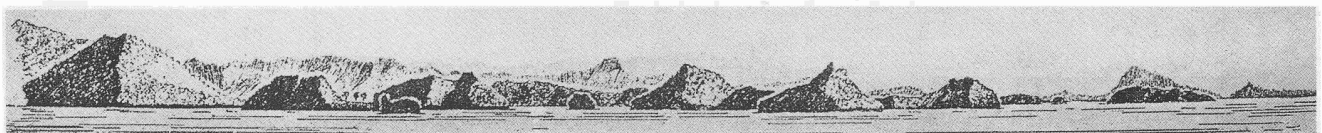
(Left to right standing)
 Jefford, Hunt, Thomson,
 Caws, Paine
 (Left to right sitting)
 Sanderson, Melhuish,
 Ryland

were established on the Krishna and China Bakir Light Vessels, the Bumliton Creek was examined and soundings were taken around Alguada. The Rangoon River survey and the survey of the approaches to the Pakchan River occupied the rest of the season. The "Investigator" remained deployed in this region for three consecutive seasons.

On October 4, 1930, H.M.I.S. "Investigator" inspected the meteorological station, at the request of the director Meteorological Department, India, and erected new instruments at Car Nicobar en route to Victoria Point. The survey of the Mergui Peninsula was continued and a resurvey of the southern approaches to the Pakchan River completed.

H.M.I.S. "Palinurus", commanded by Lieutenant Commander J Ryland, undertook a small survey for Bhavnagar followed by a survey of Port Navlakhi and an examination of the Cochin Roadstead. The early days of March were spent in the survey of the Alleppey roads and the vessel then sailed to Cannanore to continue with the West Coast survey. In the course of the year, the "Palinurus" had sailed 4176 miles with 1701 miles of sounding covering 178 square miles of water and 38 miles of coastline.

In 1930, the first Indian to join the Hooghly River Survey was Mr. Ramdass Katari, a graduate of the first batch trained on board the Training Ship "Dufferin". Having served till 1939, he went on to join the Royal Indian Navy Reserve and eventually became the first Indian chief of Naval Staff of the Indian Navy.



Pulau Tonton. Conspicuous double peak in line with E. tangent of Thane islet, bearing 149°, 4 miles. Sims reef beacon Akha Barit. Pulau Besin. Pulau Jungis. Goli Chang.

Leading Mark for the northern approach to Pakchan River.
 (Original dated 1930.)

Annex RJ-10

U. Thampanya, J.E. Vermaat, S. Sinsakul, N. Panapitukkul, "Coastal Erosion and Mangrove Progradation of Southern Thailand", *Estuarine, Coastal and Shelf Science*, Vol. 68, 2006, pp. 75-85.

Coastal erosion and mangrove progradation of Southern Thailand

U. Thampanya^a, J.E. Vermaat^{b,*}, S. Sinsakul^c, N. Panapitukkul^d

^a Coastal Resources Institute, Prince of Songkla University, Hat Yai, Songkhla 90110, Thailand

^b Institute for Environmental Studies, Vrije Universiteit, De Boelelaan 1087, 1081 HV Amsterdam, The Netherlands

^c Department of Mineral Resources, Rama VI Road, Bangkok, Thailand

^d Department of Natural Resources, Prince of Songkla University, Hat Yai, Songkhla 90110, Thailand

Received 3 November 2005; accepted 13 January 2006

Available online 30 March 2006

Abstract

Approximately 60% of the southern Thai coastline used to be occupied by mangroves according to the first mangrove forest assessment in 1961. During the past three decades, these mangrove areas have been reduced to about 50% with less than 10% left on the east coast. Coastal erosion and accretion occur irregularly along the coast but an intensification of erosion has been noticed during the past decade. This study assessed the relationship between mangrove presence and changes in coastal area. Mangrove colonization rates were assessed using in situ transects and remote sensing time series. Both methods led to comparable estimates ranging between 5 and 40 m y⁻¹. Quantitative data on changes of coastal segments along southern Thai coastlines as well as available possible factors responsible for these changes were compiled. Overall, net erosion prevailed (1.3 ± 0.4 m y⁻¹). The Gulf of Thailand coastline in the East of the country was found to be most dynamic: change occurred along more coastal segments than in the West (43% vs. 16%). Rates of erosion and accretion were also higher, 3.6 versus 2.9 m y⁻¹ and 2.6 versus 1.5 m y⁻¹, respectively. Total area losses accounted for 0.91 km² y⁻¹ for the Gulf coast and 0.25 km² y⁻¹ for the West. Coasts with and without mangroves behaved differently: in the presence of mangroves less erosion was observed whilst expansion occurred at particular coastal types with mangrove existence, i.e. river mouths and sheltered bays. Possible underlying causes were examined using multivariate analysis. Eroded areas were found to increase with increased area of shrimp farms, increased fetch to the prevailing monsoon, and when dams reduced riverine inputs. Notably, however, in areas where erosion prevailed, the presence of mangroves reduced these erosion rates. Mangrove loss was found to be higher in the presence of shrimp farms and in areas where mangrove forests used to be extensive in the past.

© 2006 Elsevier Ltd. All rights reserved.

Keywords: mangrove; progradation; erosion; sedimentation; Thailand; Asia

1. Introduction

Historically, large tracts of the coastal zone of SE Asia have been occupied by mangroves (Rao, 1986; Aksornkoae, 1993). During the past decades, these mangroves have been cleared over vast areas to accommodate increasingly intensive forms of land-use for human benefit such as settlement, transport infrastructure, agriculture and aquaculture, especially shrimp farming. Traditionally, mangrove forests provide the coastal human population with a variety of goods and services on which poorer strata of society depend strongly (Aksornkoae,

1993; Ruitenbeek, 1994; Plathong and Sitthirach, 1998; Gilbert and Janssen, 1998; Semesi, 1998; Janssen and Padilla, 1999).

The notion of the importance of mangrove forests has urged widespread reforestation schemes to cope with this decline (FAO, 1994; Havanond, 1995; Field, 1999). The success of reforestation has been variable, however, amongst others due to the neglect of the ecology of sites and species (Khemnark, 1995; Havanond, 1995; Elster, 2000; Thampanya et al., 2002a,b). Mangroves have their widest extent in lowland deltas (Woodroffe, 1992; Robertson and Alongi, 1992), i.e. where sediment delivery allows a net progression of a soft-bottom coastline. Deltaic coasts are affected by changes both on the land and in the sea. Anthropogenic activities in upland catchments such as deforestation, cultivation, dam constructions as well as coastal activities such as construction of ports,

* Corresponding author.

E-mail address: jan.vermaat@ivm.falw.vu.nl (J.E. Vermaat).

sand barriers, break-waters and jetties, all may have adverse impacts on the sediment delivery and thus on the availability of mangrove habitats (FAO, 1994; Saito, 2001; Hogarth, 2001). An important question is whether mangroves simply follow the geologically changing coastlines or also protect the coastlines from erosion, hence accelerate the entrapment of suspended particulate matter from land and sea (Thom, 1982; Field, 1995; Blasco et al., 1996; Furukawa and Wolanski, 1996). The latter would provide a potentially powerful feedback enabling the continued existence of mangrove stands at reduced terrestrial sediment delivery and, possibly, foreseen sea level rise (Ellison, 1993; Blasco et al., 1996; Hogarth, 2001). However, it is difficult to establish experimentally, because of the vast spatial scale of the system invaded. We therefore attempted a multivariate approach, using provinces and coastal segments in Southern Thailand as replicates.

In this paper we provide a regional overview of coastal progradation and erosion along the coasts of Southern Thailand and specifically focus on long-term development in a number of areas with comparatively large mangrove stands. We combine detailed longer time coastal development assessment for these sites using remote sensing in combination with in situ studies and compare the results with overall patterns synthesized from coastal surveys for all coastal provinces of Southern Thailand (from Sinsakul et al., 1999, 2002). Our aims were: (1) to assess whether natural coastal development of mangrove-dominated coastlines is different from that of others; and (2) to identify factors responsible for the expansion or recession of mangrove-dominated coastlines. In addition, we address a methodology issue and verify whether remote sensing and in situ tree-age size distributions (Panapitukkul et al., 1998) provide comparable estimates of coastline progradation.

2. Materials and methods

2.1. Study area

Southern Thailand is approximately situated between 6° to 11° Northern latitude and 98° to 103° Western longitude. Its coastlines faces two different seas: the eastern is exposed to the Gulf of Thailand and the western to the Andaman Sea. The Gulf of Thailand, an inlet of the South China Sea, has a coastline along the southern region stretching for approximately 930 km. Many rivers discharge water and sediment into the gulf. The Andaman Sea, which connected to the Indian Ocean, has a 937 km long coastline.

The geomorphology of the gulf coast is characterized by a long and wide mainland beach of sand and dunes, with lagoons, bays and spits. Pocket beaches, extensive and well-preserved tidal flats, cliff coasts and numerous islands dominate the Andaman coast. Extensive mangroves along the Andaman coast accounted for approximately 80% of total mangrove area (1675 km²) of the country in 1998 (Royal Forest Department, 2004). On the gulf coast, the remaining mangroves are present at sheltered coastlines (Fig. 1). Tidal range on the east coast varies slightly between 0.3 and 1.1 m, with two types of tide: mixed but predominantly diurnal in the upper part and

mixed but predominantly semidiurnal in the lower part. Along the western coast, the tide is mixed semidiurnal with a relatively high tidal range between 1.1 and 3.6 m (Siripong, 1985).

The area has a tropical climate with two monsoonal winds: the northeast (NE) during mid October to March and the southwest (SW) during May to September. The NE wind has a longer fetch and mainly generates waves along the Gulf coast. Highest waves along the Andaman coast are generated by the SW monsoonal wind. Peaks in wind and wave intensity caused by the passing cyclones frequently accompany the retreat of the monsoon during October to November (Vongvisessomjai et al., 1996). The annual rainfall of the Southern region is higher than in other parts of Thailand and highest precipitation occurs on the Andaman coast (2100–4000 mm y⁻¹) whilst it ranges between 1600 and 2400 mm y⁻¹ on the Gulf coast.

There are six coastal provinces along the east coast and another six along the west coast. In this study, we selected four provinces with extensive mangrove areas as the sites for our detailed surveys of mangrove progression: Ranong and Satun on the Andaman coast and Nakhon Si Thammarat (i.e. Pak Phanang Bay) and Pattani on the Gulf coast (Fig. 1). Different mangrove taxa prevail in these four sites (Table 1).

2.2. Remote sensing method

To distinguish changes in mangrove forest expansion and cover longer-time development, we use a 30-year time period for assessment. Therefore, black and white aerial photographs and Landsat-TM satellite data of the four study sites were used. The aerial photographs of 6 and 7 September 1966 (resolution of 1:50,000, analog format, dimension: 23 cm × 23 cm) were available for Satun and Nakhon Si Thammarat, respectively, while black and white aerial photographs of 23 March 1967 were obtained for Ranong and 1 April 1967 for Pattani. Available cloud free Landsat-TM imagery (pixel size of 25 m, band 1–7, digital format) of Satun and Pak Phanang areas were acquired on 7 March 1997 and 1 October 1997, while those of Pattani and Ranong were acquired on 20 April 1998 and 24 August 1998, respectively. In addition, a topographic map of each area, with resolution of 1:50,000 in analog format produced by the Royal Thai Survey Department in 1973, was used as reference material.

Table 1
Abundance of main mangrove species present along the mangrove forest edges in the selected sites (based on field observations and Plathong and Sitthirach, 1998). a, abundant; f, frequent; o, occasionally; n, not present

Species	Sites			
	Nakhon Si Thammarat	Pattani	Ranong	Satun
<i>Avicennia alba</i>	a	a	f	f
<i>Avicennia officinalis</i>	f	o	o	o
<i>Avicennia marina</i>	f	a	n	n
<i>Rhizophora apiculata</i>	a	a	a	a
<i>Rhizophora mucronata</i>	f	f	o	f
<i>Sonneratia alba</i>	o	o	f	f
<i>Sonneratia caseolaris</i>	a	o	o	o

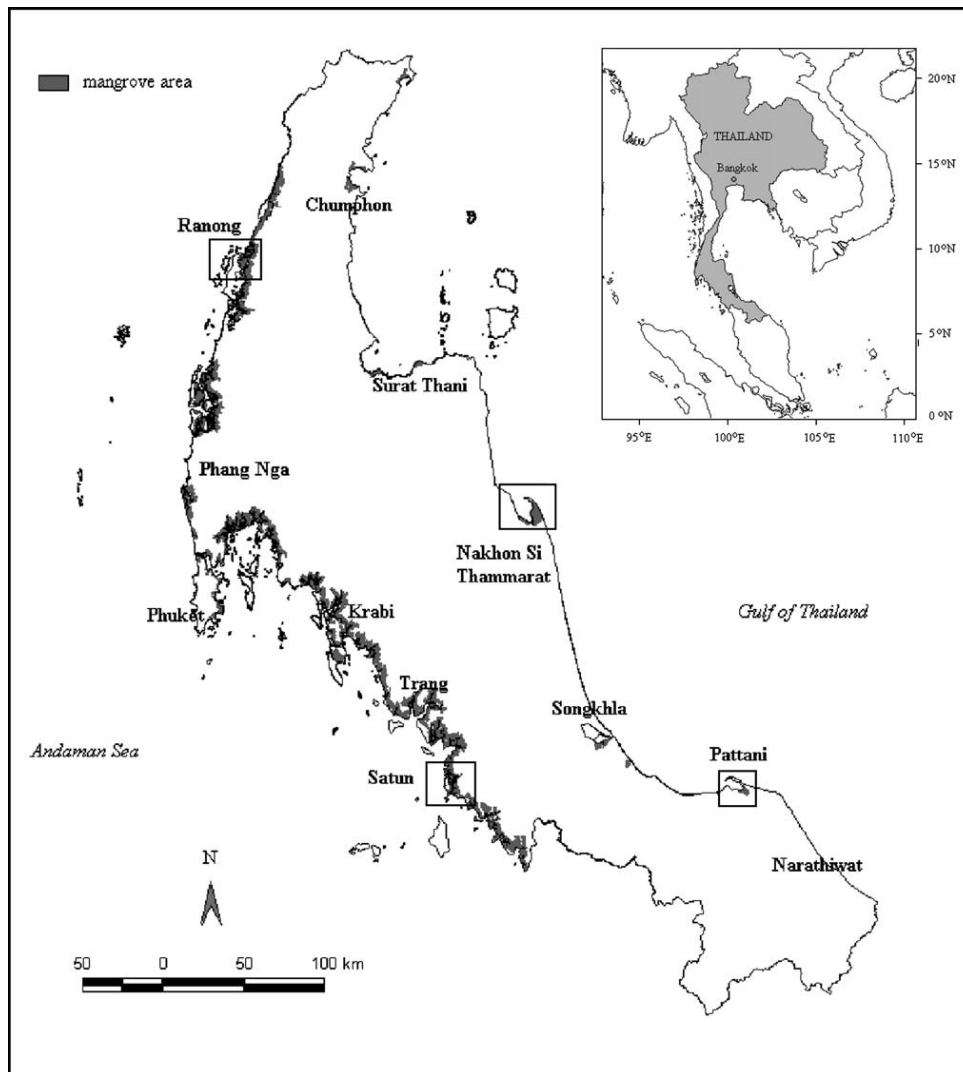


Fig. 1. Map of Southern Thailand showing mangrove areas and four selected study sites, and geographic names use in the text.

All analog data were transformed into digital data using scanners. Data preparation and image processing were carried out using the ERDAS Imagine software version 8.5. The aerial photo image of each study area was geo-referenced with the topographic map considering the UTM-Everest co-ordinates system and thus registered with the satellite image. In addition, it is necessary for aerial photographs to be joined together under mosaic operation to cover the area of study while satellite images were subset. Since this study emphasizes mangrove forest edges, areas in the vicinity of the shoreline have been examined.

The visible bands of satellite data (RGB 3,2,1: true color composite) were used for a first reconnaissance. Due to a relatively low image quality, image enhancement technique was employed to the aerial photograph of Ranong. Thereafter, both aerial photographs and satellite images were classified using unsupervised classification with 10 classes. Subsequently, the subclasses were merged and recoded to three classes: water, mangroves and mud. Finally, the classified aerial photo image and satellite image were added (Panapitukkul et al., 1998) by operation utility.

Mangrove expansion is interpreted from the resulting pictures as differences in mangrove forest edge and area between the two successive dates. Between 40 and 80 perpendicular lines were drawn between the two edges and progression was measured from these lines as distances between 1966 and 1997 for Satun and Nakhon Si Thammarat and from 1967 to 1998 for Pattani and Ranong.

2.3. Ground truthing

The reconnaissance surveys of the study areas have been made within the Coastal Ecosystems Response to Deforestation-derived Siltation in Southeast Asia (CERDS) Project during 1996–1997 (Panapitukkul et al., 1998; Kamp-Nielsen et al., 2002). The results of image classification from the remote sensing (RS) methodology were verified based on these surveys as well as from later in situ fieldwork by the first author. The in situ studies were carried out at all sites (Pattani in September 1999, Ranong and Satun in August 2000, and Nakhon Si Thammarat in September 2000) in order to quantify mangrove

expansion rates and validate the progression rates obtained from the remote sensing technique. Temporal line transects were set up in the areas where mangrove progression was apparent according to the remote sensing results. A Global Positioning System (GPS) was used to locate the transects.

Transect lines started from the edge of the present closed forest characterized with mature trees perpendicular to the waterway or to the furthest individual. Then 10 × 10-m plots were set up evenly along each transect to examine the age of mangrove trees. Number of line transects and number of plots varied among the four sites depending on their mangrove characteristics and accessibility. In Pak Phanang Bay, Nakhon Si Thammarat, three line transects were set up in bay features and another four in cape features with 8–10 plots on each transect. For the other study sites, mangrove progression areas are small, therefore, five transects with 5–10 plots each were located for Ranong and Pattani Bay and eight transects with the same number of plots were located for Satun area.

In each plot, we measured height and circumference at breast height (1.3 m from substrate) of the three largest specimens. Subsequently, data on girth at breast height were converted to diameter at breast height (DBH) using circumference = $\pi \times \text{DBH}$, where $\pi = 3.14$. For young trees with height less than 2 m, we also counted the number of internodes present along the main stem as in Panapitukkul et al. (1998). Age of the oldest tree was estimated using fitted allometric height-age or DBH-age curves (Thampanya and Vermaat, in preparation). For young trees, age was calculated from the ratio of total number of internodes and the average annual number of internodes produced for each species i.e. 16.0 ± 0.8 internodes for *Avicennia*, 25.0 ± 1.2 for *Sonneratia caseolaris* and 8.3 ± 0.4 for *Rhizophora apiculata* (Duarte et al., 1999).

The maximum age of the oldest individual along the transect represents an estimated time since that tree colonized the plot (Panapitukkul et al., 1998) and also of the time that the mudflat emerged sufficiently high above the low water line to be colonized. Hence, the progression rate of mangrove colonization was estimated from the fitted regression equation derived from the increase distance from the present forest edge in time, as follows:

$$\text{Distance from forest edge (m)} = A + B \\ \times \text{Maximum age (days)}$$

where: A = intercept of the regression equation; B = slope or progression rate (m day^{-1}).

2.4. Compilation of datasets

To obtain an overview of coastal change patterns in Southern Thailand and assess underlying factors, datasets on natural coastal development of this region and possible causal factors were compiled. The results of coastal surveys by the Geological Survey Division, Department of Mineral Resources, Thailand (Sinsakul et al., 1999, 2002), were taken into consideration. These surveys aimed to assess the current status of the coastal geo-environment, coastal problems and their causes. The

Andaman Sea coast was surveyed in the year 1997. For the Gulf of Thailand, the survey was carried out during 1998–2000.

We synthesized relevant quantitative data from these surveys into a dataset of coastal development for all coastal provinces of Southern Thailand. This set contains data on coastal change during 1967–1998 in terms of erosion and accretion for coastal segments of 0.5–30 km long ($n = 142$), magnitude (rate in m y^{-1}), cause of change, coastal type and, presence and condition of mangroves in the areas. We used six categories of coastal type: rocky, rocky sand, sandy, sandy mud, muddy, and river/canal mouth. Similarly, four categories were assigned to the presence and condition of mangroves: dense or intact, scattered or degraded former mangrove area and not present.

Comprehensive long-term baseline oceanographic data such as wave, wind and current of this region are limited. This study, therefore, attempted to compile quantitative data of other direct or indirect possible causal factors for coastal change from various sources. Some important possible factors were also calculated to accomplish the dataset. This set consists of southern Thai data on a province basis including precipitation, hydrological, land use and important coastal data such as coastal length and fetch.

2.5. Data analysis

The data on mangrove expansion and coastal change were subsequently analyzed using standard statistical software (SPSS and Microsoft Excel). Analysis of variance was applied to examine the difference of mangrove progression rate resulting from the RS method and ground truthing as well as to examine the effect of coastal factors such as locality, coastal type and mangrove presence, on rate of coastal change.

Possible factors responsible for coastal change were assessed using stepwise multiple regressions. We examined these for net coastal change, coastal erosion and accretion subsequently. In addition, mangrove area loss was also examined for its causal factors. Since no mangroves have been reported for Narathiwat province, this province was not selected in the data analysis concerning mangrove aspects.

3. Results

3.1. Mangrove progression in selected sites

Remote sensing imagery suggested that mangrove progression differed strongly between eastern and western sites: in the east, mangrove progress in the selected river mouths has been in the order of 140–1200 m over the period of about 31 years, or approximately $5\text{--}38 \text{ m y}^{-1}$. In the west, however, equally large mangrove forests increased only little in the seaward direction: 10–90 m over 31 years or less than 3 m y^{-1} . Mean annual progression rate was significantly higher in Pak Phanang Bay, Nakhon Si Thammarat than in the other three sites (Fig. 2).

Progress measured from remote sensing imagery and ground truth transects were compared. No significant difference was found in overall progression rate estimates by the

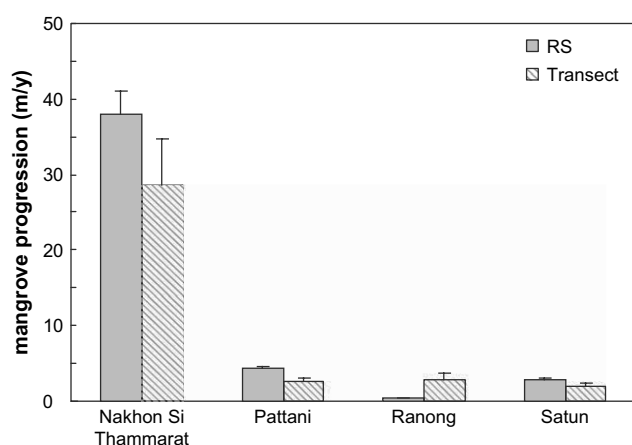


Fig. 2. Mangrove progression rates obtained from the two methods: RS (remote sensing) and transect (ground truthing), and the Tukey comparison of the four study sites.

two methods ($p = 0.125$), but the method and site interaction was significant ($p = 0.038$). This can probably be explained by the fact that the difference between the two methods was relatively large at one site, Ranong, where the in situ transects still suggest some progress ($3 \pm 1 \text{ m y}^{-1}$) but the remote sensing method showed little progress ($0.3 \pm 0.03 \text{ m y}^{-1}$, Fig. 2). In the other sites both methods yielded rather comparable estimates of mangrove progression.

3.2. Erosion and accretion along southern Thai coastlines

It was found that all coastal provinces of Southern Thailand, in the east as well as the west, have been experiencing coastline change. Retreats of marginal shoreline occurred

irregularly. Erosion was more prevalent on the Gulf coast than the Andaman coast. For instance, large lengths of the eastern coastline were found to be subject to erosion, particularly in Nakhon Si Thammarat and Narathiwat, whilst on the western coast this is less pronounced. On the other hand, tidal flats and sand bars in the East have also been prograding continuously with substantial rates in sheltered areas such as Pak Phanang Bay and Pattani Bay. In general, however, coastal areas of Southern Thailand are diminishing. Area losses amount from approximately 0.01 to $0.32 \text{ km}^2 \text{ y}^{-1}$ per province (Table 2).

Different provinces along southern Thai coastlines displayed great contrasts in terms of percent coastline change (Table 2). Overall, eroded distances for the east and the west coasts accounted for 29% and 11% of their total length, respectively. Narathiwat, the southernmost province, exhibited the highest proportion of eroding coastline (82% of its 50 km) followed by 59% for Nakhon Si Thammarat, while a maximum of only 19% was found on the west coast (Ranong and Trang). Percent accretion had a similar pattern, ranging from 2% to 9% for the west and from 3% to 21% for the east coast.

Although the west and east coasts they appear to show different patterns in percentage of coastal change among provinces, in an overall analysis of variance considering rate of change (both erosion and progradation) among segments, we found no significant difference between the two coasts as well as among the six different types of coastline distinguished (Table 3), probably due to the large variability observed. In contrast, the degree of mangrove presence did matter since it was highly significant explaining about 11% of the variance ($p < 0.001$, Table 3). Additionally, the interaction between degree of mangrove presence with coast and with coastal type showed significant differences ($p < 0.005$ and $p < 0.003$,

Table 2

Coastal change in the coastal provinces of Southern Thailand, area of mangroves, number of coastal segments^a with changed area (N), length of changed coastline (L, km), mean rate (SE) of change (R, m y^{-1}) and estimated net change over the period of 1967–1998

Province	Length of coastline (km)	Mangrove area in 2000 (km^2)	Erosion			Accretion			Estimated net change ($\text{km}^2 \text{ y}^{-1}$)
			N	L	R	N	L	R	
<i>East coast</i>									
Chumphon	185	79	11	16	1.6 (0.1)	8	10	1.6 (0.2)	-0.01
Surat Thani	135	35	8	24	3.5 (1.8)	9	11	1.6 (0.2)	-0.14
Nakhon Si Thammarat	190	99	9	112	4.0 (0.9)	4	21	8.9 (7.0)	-0.32
Songkhla	150	47	11	41	2.3 (0.4)	4	32	2.5 (0.3)	-0.02
Pattani	170	35	8	24	6.7 (1.7)	3	6	2.8 (0.7)	-0.12
Narathiwat	50	0	6	41	5.0 (1.6)	1	2	4.0 (0.0)	-0.29
Total	880	296	53	258	3.6 (0.5) ^b	29	82	2.9 (1.0) ^b	-0.13 ^b
<i>West coast</i>									
Ranong	135	253	7	25	2.6 (0.6)	1	4	2.0 (0.0)	-0.06
Phang Nga	216	454	9	28	1.8 (0.2)	5	10	1.5 (0.3)	-0.04
Phuket	185	22	2	5	5.8 (4.3)	0	—	—	-0.03
Krabi	160	349	9	17	2.7 (0.6)	5	6	1.6 (0.4)	-0.03
Trang	119	335	7	23	2.2 (0.5)	5	11	1.0 (0.0)	-0.05
Satun	168	353	9	15	3.0 (0.8)	1	4	2.5 (0.0)	-0.03
Total	983	1766	43	113	2.6 (0.3) ^b	17	35	1.5 (0.2) ^b	-0.04 ^b

^a Segment is a portion of coastline in a province which was observed to be eroded or accreted.

^b Average rate

Table 3

Analysis of variance examining the effects of coastal side (eastern, western), coastal type and presence of mangroves on rate of coastal change (both negative erosion and positive accretion) in 142 coastal segments. Presented are the degree of freedom (df), SS, percentage of variance explained (factor SS/total SS \times 100), and level of significance (p)

Factors	df	SS	% variance	p
Coast (west vs. east)	1	2	<1	0.709
Coastal types ^a	5	49	2	0.625
Degree of mangrove presence	3	327	11	0.001
Coast \times Coastal type	3	98	3	0.078
Mangrove presence \times Coast	3	191	7	0.005
Mangrove presence \times Coastal type	5	270	9	0.003
Residual	121	1690	59	
Total	142	2868		

^a Coastal types distinguished; see Fig. 3.

respectively, Table 3). This suggests that coastlines with mangroves behave differently on the Andaman and on the Gulf coasts, as well as on different coastal types.

Remarkably, in the overall ANOVA we found no significant difference in rate of coastal change among the six coastal types despite the apparent pattern in the means (Fig. 3a). We must conclude that variability within these types is substantial along southern Thai coastlines. Probably, sandy and sandy-mud coasts are more fragile than the others whilst mudflats experienced less erosion (less than 1 m y^{-1}). This is also in accordance with the presence of mangroves (Fig. 3d), which usually dominate mudflat shorelines and river mouths. Here

too significant interactions between mangrove presence and coast (east-west) as well as mangrove presence and coast type (Table 3) suggest the importance of mangrove presence: only where mangroves are present, accretion is positive (Fig. 3c) and accretion occurs only where dense mangroves occur along the east coast (Fig. 3f). In addition, the erosion rate was found to be higher in coastal segments without mangroves than those with mangroves (Fig. 4): indeed several segments without mangroves witnessed quite high erosion ($>10 \text{ m y}^{-1}$).

3.3. Possible factors responsible for coastal changes

Generally, there are many inter-related causes of coastal change, which can be long-term and short-term, natural and man-induced. In this study, we collected relevant data on possible factors responsible for coastal changes from several sources as summarized in Table 4 where we used province as unit of comparison. Available long-term data were averaged to get representative values. Data on rainfall were available for the period of 1971–2000 and sediment yield for 1979–2000. The examined coastal change data covered the period between 1967 and 1998.

In stepwise multiple regressions assessing possible causes of coastal change, we have tested a number of models. Two initial models were selected for examining causal factors of net coastal area loss: model (a) examined variables 1–14 and model (b) examined variables 1–16 (Table 5). Stepwise

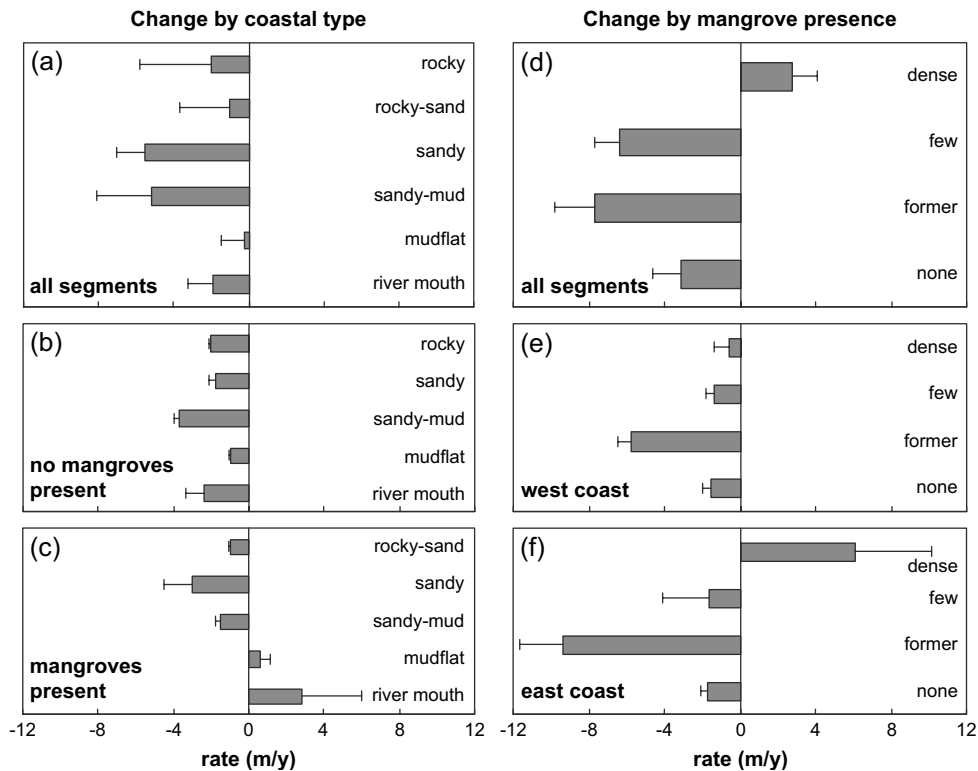


Fig. 3. Magnitude of coastal change categorized by coastal type of: (a) all segments, (b) segments with no mangrove presence, (c) segments with mangrove presence; and degree of mangrove presence of: (d) all segments, (e) segments of the west coast, and (f) segments of the east coast.

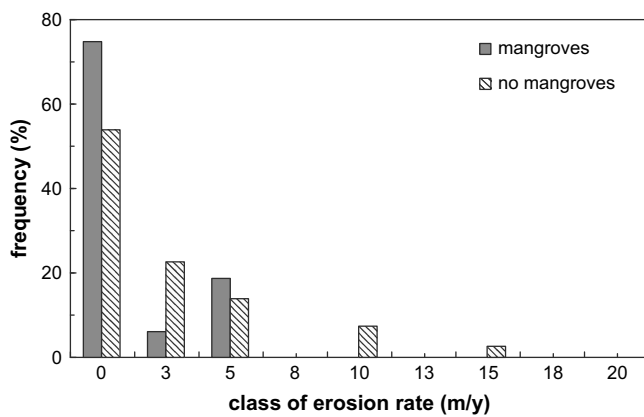


Fig. 4. Class of erosion rate and frequency of coastal segments with and without mangroves. Mean erosion rates are $2.3 \pm 0.4 \text{ m y}^{-1}$ for segments with mangroves and $3.3 \pm 0.4 \text{ m y}^{-1}$ for segments without mangroves. The *t*-test statistics shows significant different erosion rate between these two coastal types (*t*-test, $p = 0.048$).

regression then iteratively selected the best (in terms of explained variance) combination of independent variables. Apart from the two obvious factors that add up to net change, i.e. erosion and accretion, the models suggest that fetch, catchment area, coastal length and the presence of dams affected net coastal change significantly. For example, an increase of 100 km fetch enhanced net area loss in the order of 4580 m^2 (or approximately 0.05 ha), the presence of dams across inflow rivers caused considerable net area loss of about $91,510 \text{ m}^2$ (or 0.92 ha) and loss increased by 10 m^2 for 1 km^2 increase in catchment area (Fig. 5).

Models (c), (d) and (e) determined correlations of eroded area. In model (c), variables 1–11 were included and model (d) examined the same set of variables with the addition of shrimp farms. These two models show that mangrove loss, mangrove area in 1996, fetch and shrimp farm area were factors correlating with coastal erosion. One km^2 of mangrove area loss contributed to 830 m^2 of eroded area and 1 km^2

increment in shrimp farm area increased the eroded area in the order of 2170 m^2 (or 0.02 ha). On the contrary, 1 km^2 of mangrove area in 1996 reduced the eroded area by 430 m^2 . In model (e), the same set of variables was examined but included data of Narathiwat. Here it was found that on top of the mangrove area loss and fetch factors, the presence of dams was significant (a slope of $114 \times 1000 \text{ m}^2$, Table 5).

Similarly, shrimp farm area and fetch were significant positive factors of coastal accretion determining in model (f) that examined variables 1 to 12. Here, exposed provinces with more shrimp farming were probably subject to both more erosion (model (d)) and accretion (model (f)). This model also indicates that accreted area may be reduced by 10 m^2 with 1 km^2 increment of catchment size, or larger catchments witnessed less accretion. In addition, when the eroded area variable was included in model (g), it was found that the presence of dams and amount of rainfall had negative correlation to accreted area (Table 5). Model (h) examined the same set of variables with the inclusion of Narathiwat data. This model reveals that apart from the eroded area and the presence of dams, coastal length was another causal factor. An increase of 1 km coastal length led to 470 m^2 of accreted area (Table 5).

Factors responsible for mangrove area loss were assessed in models (i) and (j). In model (i), variables 1–8 and 11–13 were examined. The model suggests that besides the mangrove area in 1961, shrimp farm area and eroded led to mangrove area loss during 1961 to 1996. The shrimp farms was the most severe factor; increases in 1 km^2 of shrimp farm area caused 1.44 km^2 of mangrove area loss, whilst 1000 m^2 of eroded area related to mangrove area loss of about 0.25 km^2 (Table 5). The presence of dams was explicit as one of a possible causal factor of mangrove area loss in model (j) when shrimp farm area and eroded area were excluded from the examined variables. This model suggests that the presence of dams intensified mangrove area loss (Table 5, see also Fig. 5).

Table 4
Ranges across provinces in quantified possible causal factors of southern Thai coastal change used in multiple regression analysis

Variable no./name	Median	Min	Max	Sources
1. Coastal length (km)	164	50	216	Sinsakul et al., 1999, 2002
2. Catchment area (km^2)	2838	159	8969	Royal Irrigation Department, 2004
3. Rainfall (mm y^{-1})	2197	1816	4021	Meteorological Department, 2004
4. Sediment yield (ton km^{-2})	160	85	339	Royal Irrigation Department, 2004
5. Presence of dams in major rivers' draining a province (yes/no)	—	—	—	Royal Irrigation Department, 2004
6. Coastal water suspended solids in 2003 (mg l^{-1})	17	7	46	Pollution Control Department, 2003
7. River plume (km^2)	102	24	477	Estimated from 2000 and 2001 Landsat Satellite images
8. Mangrove area in 1961 (km^2)	281	13	612	Royal Forest Department, 2004
9. Mangrove area in 1996 (km^2)	58	6	304	Royal Forest Department, 2004
10. Mangrove area loss (km^2)	131	7	528	Royal Forest Department, 2004
11. Fetch ($\times 100 \text{ km}$)	6	4	19	Calculated from world atlas map
12. Shrimp farm area in 1996 (km^2)	11	2	105	Charupatt and Charupatt, 1997
13. Eroded area ($\times 1000 \text{ m}^2$)	64	26	560	Sinsakul et al., 1999, 2002
14. Accreted area ($\times 1000 \text{ m}^2$)	12	0.0	240	Sinsakul et al., 1999, 2002
15. Eroded distance ($\times 1000 \text{ m}^2$)	24	5	112	Sinsakul et al., 1999, 2002
16. Accreted distance ($\times 1000 \text{ m}^2$)	8	0	32	Sinsakul et al., 1999, 2002
17. Net area loss (ha) for the period of 1967–1998	36	0.3	290	Calculated from Sinsakul et al., 1999, 2002

Table 5

Stepwise multiple regressions relating coastal changes to possible causal factors across southern Thai provinces. Different runs (a–j) involved the correlate combination of net loss, eroded area, accreted area and mangrove loss with different sets of independent variables. All models were highly significant. Presented are dependent variables, selected variables, slope and significant level of each selected variable, model intercept, coefficient of determination (r^2) and excluded variables. Examined variable codes: 1, coastal length; 2, catchment area; 3, rainfall; 4, sediment yield; 5, presence of dams; 6, suspended solid; 7, river plume; 8, mangrove area 1961; 9, mangrove area 1996; 10, mangrove area loss; 11, fetch; 12, shrimp farm area; 13, eroded area; 14, accreted area; 15, eroded distance; 16, accreted distance. Narathiwat province was not included in runs (c), (d), (f) and (g). In runs (i) and (j), presence of dams and shrimp farms could not be included together as that led to over parameterization

Model no./dependent variable	Selected variables					Excluded variable
	Variable	Slope (SE)	<i>p</i>	Intercept (SE)	Overall r^2	
<i>Determination of net coastal area loss</i>						
(a) Net area loss	Accreted area (14)	−1.96 (0.13)	0.00	−7.75 (9.36)	0.98	1,3,4,5,6,7,8,9,10,12
	Eroded area (13)	0.67 (0.06)	0.00			
	Fetch (11)	4.58 (1.01)	0.00			
(b) Net area loss	Catchment area (2)	0.01 (0.002)	0.03	103.58 (45.31)	0.95	2,3,4,6,7,8,9,10,11,12,13,16
	Coastal length (1)	−0.58 (0.22)	0.03			
	Dam (5)	91.51 (17.41)	0.00			
	Accreted area (14)	−1.58 (0.43)	0.01			
(c) Eroded area	Eroded distance (15)	2.68 (1.05)	0.04			
	Mangrove loss (10)	0.83 (0.09)	0.01	−39.08 (32.37)	0.95	1,2,3,4,5,6,7,8
	Fetch (11)	9.06 (2.51)	0.01			
Mangrove 96 (9)	−0.43 (0.13)	0.01				
(d) Eroded area	Shrimp farm (12)	2.17 (0.65)	0.01	−90.67 (25.12)	0.95	1,2,3,4,5,6,7,8,9
	Fetch (11)	11.56 (2.21)	0.00			
	Mangrove loss (10)	0.33 (0.13)	0.04			
(e) Eroded area	Dam (5)	113.66 (48.91)	0.04	−89.72 (38.89)	0.88	1,2,3,4,6,7,8,9,12
	Mangrove loss (10)	0.48 (0.13)	0.01			
	Fetch (11)	12.07 (3.74)	0.01			
<i>Determination of coastal accretion</i>						
(f) Accreted area	Shrimp farm (12)	1.84 (0.15)	0.00	−21.64 (7.78)	0.98	1,3,4,5,6,7,8,9,10
	Fetch (11)	5.48 (0.67)	0.00			
	Catchment area (2)	−0.01 (0.002)	0.00			
(g) Accreted area	Eroded area (13)	0.37 (0.02)	0.00	−15.02 (5.43)	0.99	1,2,4,6,7,8,9,10
	Dam (5)	−64.83 (3.21)	0.00			
	Fetch (11)	3.43 (0.31)	0.03			
	Shrimp farm (12)	0.57 (0.09)	0.00			
	Rainfall (3)	−0.01 (0.002)	0.01			
(h) Accreted area	Eroded area (13)	0.51 (0.07)	0.00	−86.68 (29.70)	0.91	2,3,4,6,7,8,9,10,11,12
	Coastal length (1)	0.47 (0.18)	0.03			
	Dam (5)	−54.79 (22.71)	0.04			
<i>Determination of mangrove area loss</i>						
(i) Mangrove loss	Mangrove 61 (8)	0.43 (0.04)	0.00	−28.50 (12.58)	0.98	1,2,3,4,5,6,7,11
	Shrimp farm (12)	1.44 (0.47)	0.02			
	Eroded area (13)	0.25 (0.10)	0.04			
(j) Mangrove loss	Mangrove 61 (8)	0.56 (0.08)	0.00	−38.73 (30.15)	0.89	1,2,3,4,6,7,11
	Dam (5)	131.71 (37.31)	0.01			

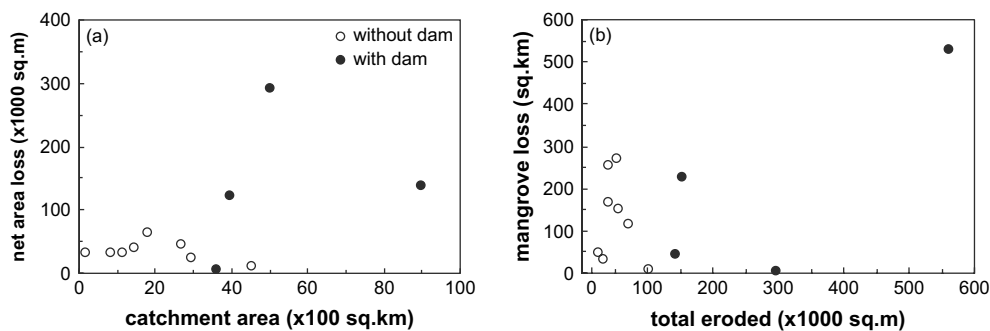


Fig. 5. (a) Net area loss versus size of catchment with and without the presence of dams; (b) total eroded area versus mangrove area loss with and without the presence of dams.

4. Discussion

Generally, mangrove progress estimated in the remotely sensed data and in ground truth transects was quite similar. Only one site (Ranong), where the steep geomorphology prevented the formation of extensive mudflats, showed a significant difference between these two methods. Mangrove expansion rates were in the order of $2\text{--}4\text{ m y}^{-1}$, with the exception of the more rapidly expanding forest in an infilling sheltered bay of Pak Phanang ($25\text{--}40\text{ m y}^{-1}$ or approximately $0.35\text{ km}^2\text{ y}^{-1}$). This progress rate is, however, considerably less than that reported for the Segara Anakan area in Indonesia ($2\text{ km}^2\text{ y}^{-1}$, Purba, 1991). The significant difference in progress rate between the two methods at Ranong is probably caused by progress being less than the resolution of the Landsat satellite imagery (pixel size of $25\text{ m} \times 25\text{ m}$) since the majority of measured distances were within 1–2 pixels. Here, the remote sensing method encountered an obvious technical limitation compared to in situ transects. A similar limitation was found by Maged et al. (1998).

On the larger spatial scale of coastal segments ($0.5\text{--}30\text{ km}$) grouped within 12 coastal provinces, we found overall net coastal erosion. This erosion was significantly higher along the eastern coast than in the west. Presence of mangroves was associated with the remaining areas of positive accretion. Notably, river mouths with mangroves and dense mangrove sites of the east coast were these areas of positive coastal accretion. Elsewhere, irrespective of coastal type, erosion predominated. Erosion rate varied locally between 1.6 and 6.7 m y^{-1} whilst accretion ranged from 1.0 to 8.9 m y^{-1} . Along the east coast, total eroded area amounted to $0.91\text{ km}^2\text{ y}^{-1}$ and an average per province was 0.13 m y^{-1} , whilst corresponding estimates in the west were 0.25 and 0.04 m y^{-1} , respectively. The overall erosion rate on the east coast is 3.6 m y^{-1} , which is comparable to that of Kuala Terengganu on eastern peninsular Malaysia ($0.2\text{--}4.0\text{ m y}^{-1}$, Maged et al., 1999). The net area loss found here was higher than that reported for the Bay of Bengal ($0.65\text{ km}^2\text{ y}^{-1}$, Ghosh et al., 2001) but slightly less than that of the Camau Peninsula in Vietnam ($1.1\text{ km}^2\text{ y}^{-1}$, Saito, 2001). Hence, comparable net erosion rates have been observed elsewhere in Asian coastal areas, suggesting that such erosion is widespread.

Our multivariate analysis examining possible factors underlying observed coastal changes was limited by a lack of long-term oceanographic data and the spatial resolution of available quantitative data (province as a basis). Nonetheless, we were able to quantify aspects of terrestrial hydrology, coastal morphology, coastal land use, and mangrove dynamics. It was found that net coastal area loss, i.e. accretion minus erosion, was governed by fetch, coastal length, catchment area and the presence of dams. Coasts with longer fetch are more strongly attacked by waves during monsoonal periods and thus are probably more vulnerable to loose coastal land. A larger catchment area probably also increased exposure to the monsoons. More importantly, the presence of dams in the river appeared to aggravate this pattern (Fig. 5a), probably because it reduced fluvial sediment supply to the littoral zone

(Milliman, 2001; Lacerda and Marins, 2002; Bonora et al., 2002; Batalla, 2003; Bird et al., 2004). Gross erosion was correlated not only to fetch, but also to the increase of shrimp farm area and associated loss in mangrove area. Likewise, this pattern was found to be enhanced by the presence of dams (Fig. 5b). Unexpectedly, positive accretion also occurred in areas with more shrimp farms and higher fetch to the monsoons. This is probably related to the coincidence of concentrated shrimp farm developments on the wide gradual slope of the eastern coastal plains that have sandbar-dominated coastlines. Discontinued occurrence of erosion and accretion coupled with sand movement may also account for this pattern. The eroded sediment is transported from higher energy segments by littoral drift to lower energy segments and accumulates there. The eastern coast therefore clearly features as more dynamic than the western coast: substantial proportions of the coast are subject to both erosion and accretion.

This study revealed that southern Thai coastlines with and without mangroves behave differently. Mangrove-dominated coastal segments exhibited less erosion while non-vegetated segments or former mangrove areas incurred substantial erosion. The dense structure of mangrove root systems possibly helps consolidate the coastal soil, hence the shoreline is more resistant to erosion (Mazda et al., 1997). Furthermore, mangrove roots reduce flow and promote flocculation and sedimentation upon the soil surface, eventually allowing positive accretion (Furukawa and Wolanski, 1996; Smoak and Patchneelam, 1999), particularly at river mouths or bays on the eastern coast. On the contrary, exposed and unconsolidated soils of non-vegetated and former mangrove land are more prone to erode. Our multivariate dataset provided correlative patterns supporting the significance of mangroves (e.g. Fig. 3). Clearly, reduced sediment delivery to the coast has reduced the amount of mangrove habitat. These data also support the quantitative contention made elsewhere (Mazda et al., 1997) that mangroves reduce erosion (Figs. 3b,c and 4).

Our study suggests that apart from natural phenomena such as exposure to wave attack during the monsoons, anthropogenic activities have had severe impacts on changes of southern Thai coastlines, particularly in relation to conversion of mangrove area to shrimp ponds and the damming of major rivers. Therefore, the existence of mangroves and a continued riverine sediment flux are crucial to maintain coastal stability in the region. Indeed, presently due to extensive coastal development and inland damming, erosion prevails at rates around 1.3 m y^{-1} . This situation is likely to intensify due to global climate change in the next decades. Therefore, its consequences and possible remedial measures should urgently be taken into account in coastal management schemes. Consideration of range possible management strategies for specific coastal segments would require a careful balancing of local coastline and sediment dynamics. A possible, inexpensive and natural-friendly strategy is mangrove plantation. Although mangroves may not prevent coastal erosion ultimately, the existence of a $300\text{--}500\text{ m}$ belt of mangroves may help reducing erosion rate (Winterwerp et al., 2005). Another possible strategy to sustain the coastal zone area is to enhance the total area

covered by mangroves. The easiest and least expensive way to achieve this goal is to assist natural mangrove colonization in sheltered coastal segments by providing or enhancing seedling fluxes to the area, protecting seedlings from herbivory and increasing propagule retention time with artificial shelters. Introduction and maintenance of mangrove plantations in vulnerable areas is probably beneficial for long-term coastal protection to gradual, continuous erosion or also more severe events such as a tsunami. More importantly, governments should issue and enforce legislation to control aquaculture industry in the coastal zone. For instance, the cultivation ponds must be located at the certain minimum distance from the coastline or located at least behind 300–500 mangrove or beach forests and some mitigation measures for coastal erosion must be prepared. Such legislation would profitably be accompanied by monitoring and should be enforced by authorized government agencies.

Acknowledgments

The authors are grateful to the Netherlands Foundation for the Advancement of Tropical Research: WOTRO (project WB 84-412) for financially supporting this study. We would like to thank The Marine Section of The Pollution Control Department for providing provincial sediment data and C. Worachina, W. Rattananond and the forestry staff at Ao Phangnga National Park for their assistance in the field. We are also grateful to Professor Patrick Denny for his suggestions and critical reading of the manuscript.

References

- Aksornkoae, S., 1993. Ecology and Management of Mangroves. IUCN, Bangkok, Thailand, 176 pp.
- Batalla, R.J., 2003. Sediment deficit in rivers caused by dams and in stream gravel mining. A review with examples from NE Spain. *Cuaternario y Geomorfología* 17, 79–91.
- Bird, M., Chua, S., Fifield, L.K., Teh, T.S., Lai, J., 2004. Evolution of the Sungei Buloh-Kranji mangrove coast, Singapore. *Applied Geography* 24, 181–198.
- Blasco, F., Saenger, P., Janodet, E., 1996. Mangroves as indicators of coastal change. *Catena* 27, 167–178.
- Bonora, N., Immordino, F., Schiavi, C., Simeoni, U., Valpreda, E., 2002. Interaction between catchment basin management and coastal evolution (Southern Italy). *Journal of Coastal Research* 36, 81–88.
- Charupatt, T., Charupatt, J., 1997. Application of Landsat 5-TM for monitoring the changes of mangrove forest area in Thailand. In: Proceedings of the 10th National Seminar on Mangrove Ecology. National Research Council of Thailand, pp. V9, 1–8 (in Thai).
- Duarte, C.M., Thampanya, U., Terrados, J., Geertz-Hansen, O., Fortes, M.D., 1999. The determination of the age and growth of SE Asian mangrove seedlings from internodal counts. *Mangroves and Salt Marshes* 3, 251–257.
- Ellison, J.C., 1993. Mangrove retreat with rising sea level, Bermuda. *Estuarine, Coastal and Shelf Science* 37, 75–87.
- Elster, C., 2000. Reason for reforestation success and failure with three mangrove species in Colombia. *Forest Ecology and Management* 131, 201–214.
- FAO, 1994. Mangrove Forest Management Guidelines. FAO Forestry Paper No. 117. FAO, Rome, Italy, 319 pp.
- Field, C.D., 1995. Impact of expected climate change on mangroves. *Hydrobiologia* 295, 75–81.
- Field, C.D., 1999. Mangrove rehabilitation: choice and necessity. *Hydrobiologia* 413, 47–52.
- Furukawa, K., Wolanski, E., 1996. Sedimentation in mangrove forests. *Mangroves and Salt Marshes* 1, 3–10.
- Ghosh, T., Bhandari, G., Hazra, S., 2001. Assessment of land use/land cover dynamics and shoreline changes of Sagar Island through remote sensing. In: Proceedings of the 22nd Asian Conference on Remote Sensing. Singapore National University, Singapore Institute of Surveyors and Values and Asian Association on Remote Sensing.
- Gilbert, A.J., Janssen, R., 1998. Use of environmental functions to communicate the values of a mangrove ecosystem under different management regimes. *Ecological Economics* 25, 323–346.
- Havanond, S., 1995. Re-afforestation of mangrove forests in Thailand. In: Khemnar, C. (Ed.), Ecology and Management of Mangrove Restoration and Regeneration in East and Southeast Asia, Proceeding of the ECOTONE IV. Kasetsart University, Bangkok, Thailand, pp. 203–216.
- Hogarth, P.J., 2001. Mangroves and global climate change. In: Borgese, E.M., Chircop, A., McConnell, M. (Eds.), Environment and Coastal Management, Ocean Yearbook 15. The University of Chicago Press, pp. 331–349.
- Janssen, R., Padilla, J.E., 1999. Preservation or conservation? Valuation and evaluation of a mangrove forest in the Philippines. *Environmental and Resource Economics* 14, 297–331.
- Kamp-Nielsen, L., Vermaat, J.E., Wesseling, I., Borum, J., Geertz-Hansen, O., 2002. Sediment properties along gradients of siltation in South-east Asia. *Estuarine, Coastal and Shelf Science* 54, 127–137.
- Khemnar, C. (Ed.), 1995. Ecology and management of mangrove restoration and regeneration in East and Southeast Asia. Proceeding of the ECOTONE IV. Amarin Co Ltd., Bangkok, Thailand, 339 pp.
- Lacerda, L.D., Marins, R.V., 2002. River damming and changes in mangrove distribution. *ISME/GLOMIS Electronic Journal* 2 (1), 1–4. <http://www.glomis.com/ej/pdf/ej03.pdf>.
- Maged, M.M., Mansor, S.B., Mohamed, M.I.H., 1998. Shoreline change detection using TOPSAR/AIRSAR data. Proceeding of the 19th Asian Conference on Remote Sensing. Asian Association of Remote Sensing, Tokyo, Japan, J4-1–J4-6.
- Maged, M.M., Mohamed, M.I.H., Mansor, S., 1999. Modeling of shoreline erosion by using TOPSAR Data. 2nd International Symposium on Operationalization of Remote Sensing. ITC, Enschede, The Netherlands.
- Mazda, Y., Magi, M., Kogo, M., Hong, P.N., 1997. Mangroves as a coastal protection from waves in the Tong King delta Vietnam. *Mangroves and Salt Marshes* 1, 127–135.
- Meteorological Department, 2004. Rainfall data 1971–2000. The Meteorological Department 4353. Sukhumvit, Bangkok, Thailand.
- Milliman, J.D., 2001. Delivery and fate of fluvial water and sediment to the sea: a marine geologist's view of European rivers. *Scientia Marina* 65, 121–132.
- Panapitukkul, N., Duarte, C.M., Thampanya, U., Kheowvongsri, P., Srichai, N., Geertz-Hansen, O., Terrados, J., Boromthanasarath, S., 1998. Mangrove colonization: mangrove progression over the growing Pak Phanang (SE Thailand) mudflat. *Estuarine Coastal and Shelf Science* 47, 51–61.
- Plathong, J., Sitthirach, N., 1998. Traditional and current use of mangrove forest in Southern Thailand. Publication No.3, Wetlands International-Thailand Programme/PSU, 91 pp.
- Pollution Control Department, 2003. Water Quality Survey Along Southern Thai Coastline. Marine Water Division, Pollution Control Department, 92 Phahon Yothin road, Bangkok, Thailand.
- Purba, M., 1991. Impact of high sedimentation rate on the coastal resources of Segara Anakan, Indonesia. In: Chou, L.M., Chua, T.E., Khoo, H.W., Lim, P.E., Paw, J.N., Silvertre, G.T., Valencia, M.J., White, A.T., Wong, P.K. (Eds.), Towards an Integrated Management of Tropical Coastal Resources. ICLARM Conference Proceedings 22, pp. 143–152.
- Rao, A.N., 1986. Mangrove ecosystems of Asia and the Pacific. In: Mangrove of Asia and the Pacific: Status and Management, pp. 1–48. Tech. Rep.UNDP/UNESCO.
- Robertson, A.I., Alongi, D.M. (Eds.), 1992. Tropical Mangrove Ecosystems. Coastal and Estuarine Series; 41. American Geophysical Union, Washington, DC, 330 pp.

- Royal Forest Department, 2004. Forest Statistics 2002. Royal Forest Department 61 Phaholyathin, Ladyao, Bangkok, Thailand.
- Royal Irrigation Department, 2004. Thailand Hydrological Data 1979–2000. Hydrological Division, Royal Irrigation Department, Bangkok, Thailand.
- Ruitenbeek, H.J., 1994. Modelling economy-ecology linkages in mangroves: economic evidence for promoting conservation in Bintuni Bay, Indonesia. *Ecological Economics* 10, 233–247.
- Saito, Y., 2001. Deltas in Southeast and East Asia: their evolution and current problems. In: Mimura, N., Yokoki, H. (Eds.), *Global Change and Asia Pacific Coasts*. Proceeding of APN/SURVAS/LOICZ Joint Conference on Coastal Impacts of Climate Change and Adaptation in The Asia-Pacific Region. APN, Kobe, Japan, pp. 185–191. November 14–16, 2000.
- Semesi, A.K., 1998. Mangrove management and utilization in Eastern Africa. *Ambio* 27, 620–626.
- Sinsakul, S., Tiyapairach, S., Chaimanee, N., Aramprayoon, B., 1999. Coastal Change Along The Andaman Sea Coast of Thailand. Research Report. Geological Survey Division, Department of Mineral Resources, Thailand, 60 pp.
- Sinsakul, S., Tiyapairach, S., Chaimanee, N., Aramprayoon, B., 2002. Coastal Change Along The Gulf of Thailand Coast. Research Report. Geological Survey Division, Department of Mineral Resources, Thailand, 173 pp.
- Siripong, A., 1985. The characteristics of the ties in the gulf of Thailand. In: *Proceeding of the 5th National Seminar on Mangrove Ecology*. National Research Council of Thailand, pp. V1, 1–15 (in Thai).
- Smoak, J.M., Patchneelam, S.R., 1999. Sediment mixing and accumulation in a mangrove ecosystem: evidence from ^{210}Pb , ^{234}Th and ^7Be . *Mangroves and Salt Marshes* 3, 17–27.
- Thampanya, U., Vermaat, J.E. Diameter-age relationship for estimating age of common SE Asian mangrove taxa, in preparation.
- Thampanya, U., Vermaat, J.E., Duarte, C.M., 2002a. Colonization success of common Thai mangrove species as a function of shelter from water movement. *Marine Ecology Progress Series* 237, 111–120.
- Thampanya, U., Vermaat, J.E., Terrados, J., 2002b. The effect of increasing sediment accretion on the seedlings of three common Thai mangrove species. *Aquatic Botany* 74, 315–325.
- Thom, B.E., 1982. Mangrove ecology—A geomorphological perspective. In: Clough, B.F. (Ed.), *Mangrove Ecosystems in Australia*. Australian Institute of Marine Science and Australian National University Press, pp. 3–17.
- Vongvisessomjai, S., Polsi, R., Manotham, C., Srisaengthong, D., 1996. Coastal erosion in the Gulf of Thailand. In: Milliman, J.D., Haq, B.U. (Eds.), *Sea Level Rise and Coastal Subsidence*. Kluwer Academic Publishers, pp. 131–150.
- Winterwerp, J.C., Borst, W.G., De Vries, M.B., 2005. Pilot study on the erosion and rehabilitation of a mangrove mud coast. *Journal of Coastal Research* 21, 223–230.
- Woodroffe, C.D., 1992. Mangrove sediments and geomorphology. In: Alongi, D., Robertson, A. (Eds.), *Tropical Mangrove Ecosystem*. American Geophysical Union, Coastal and Estuarine Studies, pp. 7–41.

Annex RJ-11

Affidavits regarding the Custody of the Original Radcliffe Map, 15 July 2013.

Ajay Kanoujia
Deputy Secretary



गृह मंत्रालय
भारत सरकार
नार्थ ब्लॉक, नई दिल्ली - 110001
MINISTRY OF HOME AFFAIRS
GOVERNMENT OF INDIA
NORTH BLOCK, NEW DELHI - 110001

Tel: 2309 2728

DO No. 11012/42/2013-NE-IV

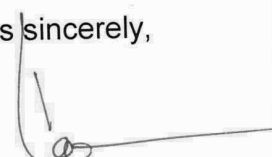
New Delhi, dated 15th July, 2013

Sub:- India-Bangladesh Maritime Delimitation Arbitration

This is to certify that SOI-IB-003/E-W Bengal East-West Bengal Original Map on Scale 1"=8 Miles signed by Sir Cyril Radcliffe was in the safe custody of the ORR of the Ministry of Home Affairs up till 12th May, 2010.

The map was handed over to National Archives of India on 13th May, 2010 vide MHA letter No. F. 1/2/2010 ORR dated 12th May, 2010.

Yours sincerely,


Ajay Kanoujia

Joint Secretary (L&T Division)
Ministry of External Affairs,
New Delhi.

F.No.8 - 4/2013 – R- I
Government of India
National Archives of India
Janpath, New Delhi 110001,

the 15 JUL 2013

To,

The Director
BSM Division
Ministry of External Affairs
Jawaharlal Nehru Bhawan
New Delhi -110011

Subject: India – Bangladesh maritime arbitration case

Sir,

This is with reference to letter no. F III/107/7/06 Boundary Cell dated 9 July 2013 on the aforesaid subject. In this regard it is being certified that original map no. SOI-IB-003/E-W Bengal on scale 1"= 8 miles, signed by Sir Cyril Radcliffe, was in the custody of the following sections of the National Archives of India since its transfer and receipt from the ORR of the Ministry of Home Affairs on 13 May 2010:

- | | |
|---|---------------------------------|
| 4. RM Division (RA section) | – 13 May 2010 – 29 March 2012 |
| 5. Records Division (A R Section) | -- 30 March 2012 - 20 June 2012 |
| 6. Records Division (Cartography section) | – 20 June 2012 - 11 June 2013 |

The map was handed over to Shri C.K.Pant, Consultant, Boundary Cell, Ministry of External Affairs on 11 June 2013 against an authorization issued by Shri Amit A Shukla, Under Secretary, Ministry of External Affairs vide letter no. I/ii/01/2010 BSM dated 10 June 2013 .

Yours faithfully,

sd/-

(Dr Ansarul Haque)
Deputy Director of Archives
Tel: 23387509

Copy to :

- ✓3. Legal Officer (L&T) Division, Ministry of External Affairs, New Delhi
4. Shri C.K.Pant, Consultant (Boundary Cell), Room No.3065, D Block, Jawaharlal Bhawan, 23-D, Janpath, New Delhi 110011

Ansarul Haque
(Dr Ansarul Haque)
Deputy Director of Archives

Annex RJ-12

Note Verbale PM/NY/443/1/2013 from the Permanent Mission of India to the United Nations
to the Secretary-General of the United Nations, 16 July 2013.



सत्यमेव जयते

संयुक्त राष्ट्र स्थित भारत का स्थायी मिशन
न्यूयॉर्क

PERMANENT MISSION OF INDIA TO THE UNITED NATIONS

235 EAST 43RD STREET • NEW YORK, N.Y. 10017

TEL: (212) 490-9660 • FAX: (212) 490-9656

EMAIL: india@un.int • indiaun@prodigy.net

PM/NY/443/1/2013

16 July 2013

The Permanent Mission of India to the United Nations presents its compliments to the Secretary General of the United Nations and has the honor to refer to the Submission made by the Republic of India on 11 May 2009, pursuant to Article 76, paragraph 8 of the United Nations Convention on the Law of the Sea (1982), to the Commission on the Limits of the Continental Shelf ("Commission") containing information on the limits of the continental shelf beyond 200 nautical miles from the baselines from which the breadth of the territorial sea is measured.

It may be noted that although India has already entered into a series of maritime boundary agreements with most of its neighbours, there are still certain outstanding maritime delimitations. Pending any agreement on the outstanding delimitation between India and a State whose coast is adjacent or opposite to that of India, India, in its partial Submission has restricted the outer limits of its continental shelf beyond 200 M to a median line, every point of which is equidistant from the nearest point from which the breadth of the territorial waters of India and of such State is measured.

In the above context, India would also like draw the attention of the Commission to the recent ITLOS judgment on Bangladesh vs. Myanmar, wherein the Tribunal has concluded that the appropriate method to be applied for delimiting the exclusive economic zone and the continental shelf between Bangladesh and Myanmar is the equidistance/relevant circumstances method. Considering the concavity of the Bangladesh coast to be a relevant circumstance for the purpose of delimiting the exclusive economic zone and the continental shelf within 200 nm, the Tribunal, in its judgment also finds that this relevant circumstance has a continuing effect beyond 200 M. The Tribunal therefore has decided that the adjusted equidistance line delimiting both the exclusive economic zone and the continental shelf within 200 M between the Parties

3/3

continues in the same direction beyond the 200 nm limit of Bangladesh until it reaches the area where the rights of third States may be affected.

Pursuant to the above decision and in the light of the ongoing Arbitration between India and Bangladesh under Annex VII of UNCLOS, the outer limits of the continental shelf of India beyond 200 M in the Bay of Bengal as provided by India in its Submission to the CLCS may have to be modified. Accordingly India would be making an amended Submission to the partial submission of 11 May 2009, following the collection and examination of additional datasets available in the region, so as to be fully consistent with the ITLOS judgment.

The Permanent Mission of India to the United Nations avails itself of this opportunity to renew to the Secretary General of the United Nations the assurances of its highest consideration.

The Secretary General of the United Nations
New York
(Attn: Division for Ocean Affairs
And the Law of the Sea)
Fax: 212 963 5847



